FATE AND MIGRATION OF DDT IN SOIL AND GROUNDWATER

THE LONG-TERM FATE AND MIGRATION OF DDT IN SOIL AND GROUNDWATER AT POINT PELEE NATIONAL PARK, ONTARIO, CANADA

By

RYAN DAVID MILLS, B.Sc.

A Thesis
Submitted to the School of Graduate Studies
In Partial Fulfillment of the Requirements
For the Degree
Master of Science

McMaster University

MASTER OF SCIENCE (2004) (Geology)	**McMaster University** **(Hamilton, Ontario)**

TITLE:	**The Long-term Fate and Migration of DDT in Soil and Groundwater at Point Pelee National Park, Ontario, Canada**
AUTHOR:	**Ryan Mills, B.Sc. (McMaster University)**
SUPERVISOR:	**Professor James E. Smith**
NUMBER OF PAGES:	**xvii, 271**

Abstract

Point Pelee National Park (PPNP), located in Leamington, Ontario, Canada experienced widespread application of DDT from 1950 until DDT was banned in Canada in 1970. While DDT has not been applied at PPNP for over 30 years, recent studies have shown that the compounds DDT, DDE and DDD are highly persistent in shallow soils at PPNP and often exceed regulatory guidelines set forth by the Ontario Ministry of the Environment and Environment Canada. Field study combined with numerical modelling was undertaken to assess the concentrations of DDT, DDE and DDD in groundwater and provide insight into the fundamental processes controlling the persistence and migration of DDT within former agricultural areas of PPNP. Results of one-dimensional pesticide fate and transport modelling from 1950 to 2003 using LEACHMP show that within former agricultural areas of PPNP, DDT is transformed primarily into DDE under aerobic conditions. Within the Camp Henry Orchard (CHO), half-lives for the production of DDE are 30 years. LEACHMP modelling showed that adsorption was the most important process limiting DDT leaching to groundwater. The depth to the water table was found to influence DDT concentrations seen at the water table throughout former agricultural areas of PPNP, and DDT is most likely leaching to the water table slowly over time. Two-dimensional saturated zone modelling using GW-WETLAND was used to test various loading scenarios based on LEACHMP simulated fluxes across the water table. Model outputs illustrated the bidirectional movement of contaminants toward both the marsh and Lake Erie, depending on the source location relative to the groundwater flow divide. Simulations showed only groundwater from deep within the aquifer would have elevated DDT concentrations in 2003 if DDT leached to groundwater between 1950 and 1970. Conversely, if DDT began to leach to groundwater in the 1990's, the model predicted that DDT was not present in deep groundwater in 2003. With continued loading, concentrations throughout the aquifer will continue to rise into the future and discharge of DDT to the marsh and Lake Erie will occur.

Acknowledgements

Many thanks go to Dr. James Smith for pointing out the many subtleties of the vadose zone and always questioning my assumptions. I am especially thankful for the guidance and mentoring provided by Dr. Allan Crowe, whose expertise was often called upon and always provided. Thank you to my thesis committee members for their time and effort spent reviewing this manuscript and providing useful feedback.

Thank you to Dr. John L. Hutson for supplying the LEACHMP model and the accompanying documentation. I am very grateful for the invaluable assistance provided by Steven G. Shikaze with the GW-WETLAND model.

Many thanks to the staff of Point Pelee National Park, especially Geordon Harvey, Tom Linke, Matthew Smith, Kelly Scott and Valerie Blazeski for their assistance in the field and the provision of data in support of this project.

Useful feedback and discussions were often provided by Karen Hodges, Rashid Bashir and Marina Mirinov, who also made the past two years much more memorable. For their support and continual offers of assistance along the way, sincere thanks are extended to my family. For her infinite understanding, never-ending encouragement and vital assistance, I am forever indebted to Vicki Thomson. Thank you so much.

Funding for this research was provided in part by CRESTech, Environment Canada and Parks Canada.

Table of Contents

Abstract iii

Acknowledgements iv

Table of Contents v

List of Figures ix

List of Tables xv

Chapter 1: Introduction.. 1

1.1 Introduction. 1
1.2 Objectives and Hypotheses...5
1.3 Geographical Setting..7
1.4 Climate...8
1.5 Geological Setting..9
1.6 PPNP Soils...12
1.7 PPNP Groundwater...12
1.8 DDT..15
  1.8.1 Properties of DDT 18
  1.8.2 Transformation of DDT 18
  1.8.3 Attenuation of DDT 21
  1.8.4 Solubility of DDT 23
  1.8.5 Volatilization of DDT 24
1.9 DDT in Soil 25
1.10 DDT in Surface Water 27
1.11 DDT in Groundwater 28

Chapter 2: Field and Laboratory Methods 36

2.1 Field Methods..37
  2.1.1 Site Selection...37
  2.1.2 Soil Sampling Techniques and Pit Excavation...................43
  2.1.3 Groundwater Sampling..46
  2.1.4 Depth to Water Table Measurements...............................48
  2.1.5 Hydraulic Conductivity Measurements..............................49
2.2 Laboratory Methods 52
  2.2.1 Groundwater Analysis for DDT, DDE and DDD.................52
  2.2.2 Soil Analyses for DDT, DDE and DDD..............................53

2.2.3 Gravimetric Soil Moisture..53
2.2.4 Volumetric Soil Moisture..54
2.2.5 Bulk Density..55
2.2.6 Organic Matter Content by Loss on Ignition..55
2.2.7 Particle Size Analysis..56
2.2.8 Porosity..58

Chapter 3: Field and Laboratory Results and Discussion 60

3.1 Soil Classification..61
3.2 Soil Texture and Structure..63
3.2.1 Grain Size..63
3.2.2 Bulk Density..65
3.2.3 Porosity..66
3.3 Soil Organic Matter..67
3.4 Soil Moisture..68
3.5 Field-saturated Hydraulic Conductivity..69
3.6 Ground Surface Elevation and Depths to Water Table..71
3.7 Statistical Analyses of Physical and Hydrological Soil Properties..75
3.8 DDT in Soil and Groundwater at PPNP..76
3.8.1 DDT in Soils – Spatial Distribution..76
3.8.2 DDT in Soils – Distribution with Depth..82
3.8.3 DDT in Groundwater – Spatial Distribution..87
3.8.4 Relationship Between DDT in Groundwater and Depth to Water Table..92
3.8.5 Relationship Between DDT in Soil and DDT in Groundwater............94

Chapter 4: Numerical Modelling of DDT Transport and Fate at Point Pelee National Park.. 112

4.1 Model Description: LEACHMP..115
4.1.1 Flow Representation..117
4.1.2 Solute Transport..119
4.1.3 Sorption..120
4.1.4 Degradation and Transformation..120
4.2 Simulation of DDT Transport to the Water Table at PPNP..122
4.2.1 Values Assigned to Model Parameters..123
4.2.2 Space and Time Discretization Parameters..124
4.2.3 Soil Hydraulic Properties..124
4.2.4 Boundary Conditions for Water Flow..127
4.2.5 Meteorological Data..127
4.2.6 Soil Physical Properties..129
4.2.7 Initial Soil Concentrations of DDT, DDE and DDD..130
4.2.8 Boundary Conditions for Solute Transport..130

- 4.2.9 Molecular Diffusion Coefficients..........130
- 4.2.10 Solubility..........132
- 4.2.11 Vapour Density..........132
- 4.2.12 Sorption-K_{oc}..........133
- 4.2.13 Isotherm Type..........133
- 4.2.14 Crop Parameters..........134
- 4.2.15 Transformation Pathways and Rate Constants..........135
- 4.2.16 Output and Summary File Parameters..........136

4.3 LEACHMP Model Calibration..........136
- 4.3.1 Flow Calibration: January 1, 1995 to September 30, 2003..........137
- 4.3.2 Flow Calibration: January 1, 1950 to September 30, 2003..........138
- 4.3.3 Solute Transport Calibration..........140
  - 4.3.3.1 Calibration of %DDT, %DDE and %DDD at CHO..........142
  - 4.3.3.2 Calibration of DDT/DDE and DDT/DDD for Shallow and Deep Soils at CHO..........143
  - 4.3.3.3 Calibration to Total DDT in the Soil Profile on May 12, 2003 at CHO..........144
  - 4.3.3.4 Comparison to Total DDT in Groundwater on May 12, 2003 at CHO..........146
  - 4.3.3.5 Assessment of Calibration Simulations..........145

4.4 Sensitivity Analysis..........150
- 4.4.1 Sensitivity Analysis for Flow Calibration..........151
- 4.4.2 Sensitivity Analysis for Solute Transport Calibration..........156

4.5 Simulation of Solute Transport at SHO..........162

4.6 Scenario Testing..........164
- 4.6.1 Removal of Organic Carbon Content from the Bm and C Horizons..........165
- 4.6.2 Application Below the Ah Horizon..........166
- 4.6.3 Ploughing of the Ah Horizon..........168
- 4.6.4 Assessment of Adsorption Behaviour at PPNP..........169
- 4.6.5 Assessment of the Historical Application Rates of DDT at PPNP..........171

4.7 Discussion of LEACHMP Modelling Results..........174

4.8 GW-WETLAND Simulations..........176
- 4.8.0 Model Description: GW-WETLAND..........176
- 4.8.1 Flow Representation..........177
- 4.8.2 Solute Transport..........180
- 4.8.3 Values Assigned to GW-WETLAND Model Parameters..........181
- 4.8.4 Space and Time Discretization Parameters..........181
- 4.8.5 Physical and Hydraulic Properties..........184
- 4.8.6 Boundary Conditions for Water Flow and Solute Transport..........185
- 4.8.7 Initial Conditions for Water Flow and Solute Transport..........188
- 4.8.8 Solute Transport Parameters..........188
- 4.8.9 GW-WETLAND Output Parameters..........189

4.9 GW-WETLAND Flow Calibration..........190

4.10 Solute Transport Simulations....................191
4.10.1 DDT Source Zones Within the Flow Domain....................192
4.10.2 DDT Loading to the Flow Domain....................193
4.11 Discussion of GW-WETLAND Modelling Results....................194
4.12 1-D and 2-D Modelling Summary....................206

Chapter 5: Conclusions and Recommendations.................... 248

5.1 Conclusions....................249
5.2 Recommendations....................254

Chapter 6: References.................... 256

Appendix 1: Model Simulations on DVD 271

List of Figures

Figure 1. Location of Point Pelee National Park including marsh overlay on aerial photograph taken in 2000. 32

Figure 2. Historical landuse at PPNP highlighting former agricultural areas (prepared by Matthew Smith, Parks Canada, 2002). 33

Figure 3. Geological cross-sections of the western barrier bar at PPNP (modified from Coakley et al., 1998). 34

Figure 4. Seasonal fluctuations of (a) Point Pelee marsh and Lake Erie, (b) the water table at NWRI's Camp Henry transect and (c) daily total precipitations measured at the PPNP weather station from 1994 to 2004. July 2002 and May 2003 sampling dates are shown as red lines. 35

Figure 5. Location of groundwater sampling locations (circles) and detailed soil sampling pits (squares) sampled during this study. 59

Figure 6. Soil profiles at CHO, SHO and AO. 96

Figure 7. Grain-size distributions with depth at CHO, SHO and AO....97

Figure 8. Soil and hydraulic properties measured with depth at CHO, SHO and AO. 98

Figure 9. Mean Total DDT concentrations (ng/g) in shallow soil (0-5 cm) at the 12 groundwater sampling sites. 99

Figure 10. %DDT : %DDE : %DDD in shallow soil (0-5 cm) collected at the 12 groundwater sampling sites. 100

Figure 11. %DDE vs. %DDT and %DDD vs. %DDT in all shallow soil analyses above the July 2002 groundwater sampling locations. Included is the 1:1 transformation line between DDT and DDE or DDD. 101

Figure 12. Distribution of ΣDDT, ΣDDE, ΣDDD and Total DDT concentrations with depth at CHO, SHO and AO soil sampling pits. 102

Figure 13. %DDT, %DDE and %DDD from 0-40 cm at CHO, SHO and AO. 103

Figure 14. Total DDT concentrations in groundwater (ng/L) at the July 2002 groundwater sampling locations. 104

Figure 15. %DDT : %DDE : %DDD in groundwater at the July 2002 groundwater sampling locations. 105

Figure 16. %DDE vs. %DDT and %DDD vs. %DDT in groundwater at the July 2002 groundwater sampling locations. Included is the 1:1 transformation line between DDT and DDE or DDD. 106

Figure 17. Relationship between (a) depth to water table and Total DDT in groundwater, (b) depth to water table and the ratio of DDT in groundwater to DDT in soil and (c) ground surface elevation and Total DDT in groundwater. 107

Figure 18. Relationship between depth to water table and %DDT, %DDE and %DDD in the July 2002 and May 2003 groundwater samples. Included are the mean %DDT and %DDE from all 68 shallow soil samples. 108

Figure 19. Relationship between (a) Log Total DDT in soil vs. log Total DDT in groundwater and (b) Log ΣDDT, ΣDDE and ΣDDD in soil vs. Log ΣDDT, ΣDDE and ΣDDD in groundwater. Values plotted at –5 represent analyses below detection limits (<IDL). 109

Figure 20. %DDT, %DDE and %DDD in soil vs. %DDT, %DDE and %DDD in groundwater. Included is the 1:1 relationship line between relative proportions in soil and groundwater. 110

Figure 21. %DDT, %DDE, and %DDD in groundwater vs. Total DDT in groundwater for samples collected in May 2002 and July 2003. 111

Figure 22. Soil moisture characteristic curves employed at 200 mm, 500 mm and 1500 mm for all LEACHMP simulations. Also presented is the best-fit soil moisture characteristic curve as measured by Marenco (2002) under drainage conditions..209

Figure 23. Modelled unsaturated hydraulic conductivity function employed in LEACHMP simulations..210

Figure 24. Measured total daily precipitation, model input precipitation, measured daily temperature and Thornthwaite estimated daily potential evapotranspiration for the calibration period from January 1, 1995 to September 30, 2003..211

Figure 25. Measured and modelled volumetric soil moisture profile from ground surface to the water table at (a) CHO and (b) SHO on May 12, 2003 as employed in LEACHMP. 212

Figure 26. Modelled volumetric soil moisture content over time from January 1, 1995 to September 30, 2003 at (a) 200, (b) 500 and (c) 1500 mm below ground surface. 213

Figure 27. Calibrated fit between modelled and measured volumetric soil moisture contents with depth at CHO on May 12, 2003. 214

Figure 28. Volumetric soil moisture profile at various times after a large infiltration event on July 17, 1989 showing the migration of water through the soil profile. 215

Figure 29. Comparison of DDT transformation and DDE formation when transformation rates are either sensitive or insensitive to moisture content and temperature variations over time. 216

Figure 30. Measured and modelled concentration profiles for simulations where relative proportions of DDT and DDE or DDD were matched for the entire profile and with depth on May 12, 2003. 217

Figure 30 (cont'd). Measured and modelled concentration profiles for simulations where relative proportions of DDT and DDE or DDD were matched for the entire profile and with depth on May 12, 2003.... 218

Figure 31. Measured and modelled concentration profiles for simulations where relative proportions of DDT and DDE or DDD were matched for the entire profile and with depth on May 12, 2003 after K_{oc} adjustments. 219

Figure 31 (cont'd). Measured and modelled concentration profiles for simulations where relative proportions of DDT and DDE or DDD were matched for the entire profile and with depth on May 12, 2003 after K_{oc} adjustments. 220

Figure 32. Measured and modelled concentration profiles for simulations where relative proportions of DDT and DDE or DDD were matched for the entire profile and with depth on May 12, 2003 after K_{oc} adjustments and concentrations with depth were matched. 221

Figure 32 (cont'd). Measured and modelled concentration profiles for simulations where relative proportions of DDT and DDE or DDD were matched for the entire profile and with depth on May 12, 2003 after K_{oc} adjustments and concentrations with depth were matched. 222

Figure 33. Sensitivity of flow calibration to values of (a) precipitation, (b) potential evapotranspiration, (c) air entry, and (d) Campbell's b parameter, (e) pore interaction parameter and (f) K_{sa}. 223

Figure 33 (cont'd). Sensitivity of flow calibration to values of (a) precipitation, (b) potential evapotranspiration, (c) air entry, and (d) Campbell's b parameter, (e) pore interaction parameter and (f) K_{sa}. 224

Figure 34. Sensitivity of solute transport calibration to values of (a) precipitation, (b) potential evapotranspiration, (c) K_{sat}, (d) K_{oc}, (e) half-life and (f) organic carbon content. 225

Figure 34 (cont'd). Sensitivity of solute transport calibration to values of (a) precipitation, (b) potential evapotranspiration, (c) K_{sat}, (d) K_{oc}, (e) half-life and (f) organic carbon content. 226

Figure 35. Solute breakthrough curves from 1950 to 2003 for simulation employing Pathway #2 and field measured organic carbon contents with depth at CHO. 227

Figure 36. Solute breakthrough curves from 1950 to 2003 for simulation employing Pathway #2 and field measured organic carbon contents with depth at SHO. 228

Figure 37. Solute breakthrough curves from 1950 to 2003 for simulation employing Pathway #2 and organic carbon contents reduced to zero below the Ah horizons (300 mm to the water table) at CHO. 229

Figure 38. Solute breakthrough curves from 1950 to 2003 for simulation employing Pathway #2 and organic carbon contents reduced to zero below the Ah horizons (300 mm to the water table) at SHO. 230

Figure 39. Solute breakthrough curves from 1950 to 2003 for simulation employing Pathway #2 where DDT was loaded below the Ah horizon in 1955, 1960, 1965 and 1970 at CHO and there was no organic carbon in the B or C horizon. 231

Figure 40. Solute breakthrough curves from 1950 to 2003 for simulation employing Pathway #2 where where surficial soils at CHO were ploughed once in 1955 at CHO and there was no organic carbon in the B or C horizon. 232

Figure 41. Solute breakthrough curves from 1950 to 2003 for simulations employing Pathway #2 where organic carbon content were reduced to zero below the Ah horizon (300 mm to the water table) and initial DDT loading was increased 10 fold at CHO. 233

Figure 42. Two-dimensional cross-section at Camp Henry including (a) conceptual model framework and DDT source zones employed in GW-WETLAND simulations of groundwater flow and solute transport and (b) hydraulic head distribution (June 1950). 234

Figure 43. Comparison of simulated and field measured elevations of the water table at selected NWRI monitoring wells located along the Camp Henry Transect from 1994 to 2004. 235

Figure 44. Comparison of simulated and modelled water table elevations at selected NWRI monitoring wells located along the Camp Henry Transect 236

Figure 45. Distribution of Total DDT in the saturated zone throughout the Camp Henry transect from 1950 to 2003 based on initial high concentration, point source pulse loading at 225, 325 and 425 m in 1950. 237

Figure 46. Distribution of Total DDT in the saturated zone throughout the Camp Henry transect from 1950 to 2003 based on initial high concentration, point source pulse loading at 225, 325 and 425 m in 1970. 238

Figure 47. Distribution of Total DDT in the saturated zone throughout the Camp Henry transect from 1950 to 2003 based on initial high concentration non-point source pulse loading from 225-430 m across the transect in 1950. 239

Figure 48. Distribution of Total DDT in the saturated zone throughout the Camp Henry transect from 1950 to 2003 based on initial high concentration non-point source pulse loading from 225-430 m across the transect in 1970. 240

Figure 49. Distribution of Total DDT in the saturated zone throughout the Camp Henry transect from 1950 to 2003 based on long-term, slowly increasing point source loading at 225, 325 and 425 m in 1950. 241

Figure 50. Distribution of Total DDT in the saturated zone throughout the Camp Henry transect from 1950 to 2003 based on long-term, slowly increasing point source loading at 225, 325 and 425 m in 1970. 242

Figure 51. Distribution of Total DDT in the saturated zone throughout the Camp Henry transect from 1950 to 2003 based on long-term, slowly increasing non-point source loading from 225-430 m across the transect in 1950. 243

Figure 52. Distribution of Total DDT in the saturated zone throughout the Camp Henry transect from 1950 to 2003 based on long-term, slowly increasing non-point source loading from 225-430 m across the transect in 1970. 244

Figure 53. Distribution of Total DDT in the saturated zone throughout the Camp Henry transect from 1950 to 2003 based on long-term (1950-present) low concentration continuous point source loading at 225 m across the transect. 245

Figure 54. Distribution of Total DDT in the saturated zone throughout the Camp Henry transect from 1950 to 2003 based on point source loading at 225, 325 and 425 m after a series of four high concentration 2-year pulse loads in 1955, 1960, 1965 and 1970. 246

Figure 55. Distribution of Total DDT in the saturated zone throughout the Camp Henry transect from 1950 to 2003 based on non-point source loading from 225-430 m after a series of four high concentration 2-year pulse loads in 1955, 1960, 1965 and 1970. 247

List of Tables

Table 1. 30-year average monthly temperatures and precipitation values for PPNP (modified from Canadian Climate Normals, 2000, Environment Canada). 9

Table 2. Examples of reported half-lives for transformation of DDT, DDE and DDD. 20

Table 3. Examples of log K_{ow}, log K_{om} and log K_{oc} values for DDT, DDE, and DDD. 23

Table 4. Examples of solubility values reported in the literature for DDT, DDE and DDD. 24

Table 5. Examples of reported values of vapour pressure (V_p), vapour density (V_d), and Henry's Law partition coefficient (K_H) for DDT, DDE and DDD. 25

Table 6: Parameters measured in the field and laboratory during 2002/2003..........37

Table 7. Groundwater samples and replicates collected during July 2002..........39

Table 8. Surficial soil samples collected within the vicinity of the study area..........40

Table 9. Soil and groundwater pits sampled during May 2003..........42

Table 10. Samples collected and the sampling intervals at soil sampling pits..........45

Table 11. NLET detection limits (IDL) for 1 L and 20 L water and soil analyses..........52

Table 12. Results of particle size analysis, % organic matter and % organic carbon with depth at CHO, SHO and AO as determined from sampling during May 2003. 64

Table 13. Gravimetric and volumetric soil moisture contents, bulk densities, and porosity with depth at CHO, SHO and AO. 68

Table 14. Field saturated K_{fs} and log K_{fs} with depth at CHO, SHO, and AO..........70

Table 15. Measured depths to the water table and estimated ground surface elevations for the groundwater samples sites and the three soil sampling pits. 73

Table 16. Analytical results of DDT compounds in the shallow soil samples collected during July 2002. 77

Table 17. ΣDDT, ΣDDE, ΣDDD, Total DDT and %DDT, %DDE, %DDD from shallow (0-5 cm) soil samples adjacent to the 12 groundwater sampling sites. 79

Table 18. Analytical results of DDT compounds in soil with depth below ground surface at CHO, SHO and AO. 84

Table 19. ΣDDT, ΣDDE, ΣDDD, Total DDT and %DDT, %DDE, %DDD for soil samples obtained with depth at CHO, SHO and AO on May 12-14, 2003. 86

Table 20. Analytical results of DDT compounds in groundwater............................88

Table 21. Results of groundwater sampling for DDT, DDE and DDD throughout PPNP including replicate samples. 90

Table 22: Soil properties and flow parameter values used in LEACHMP simulations. 123

Table 23. Initial values assigned to solute transport parameters employed in LEACHMP calibrations. 131

Table 24. Reported vapour pressures and calculated vapour densities for DDT, DDE and DDD at 20 °C. 133

Table 25. Octanol-water partition coefficients (K_{ow}) and organic carbon partition coefficients (K_{oc}) for DDT, DDE and DDD...134

Table 26. Total DDT added as an initial condition to achieve calibration of simulations...145

Table 27. Final Calibrated fit between measured and simulated %DDT : %DDE : %DDD in the whole profile and DDE/DDT or DDD/DDT ratios with depth. 147

Table 28. Transformation and degradation half-lives employed for best-fit simulations after matching DDT, DDE and DDD concentrations in soil. 148

Table 29. Range of values tested for flow parameters tested during sensitivity analysis. 151

Table 30. Values tested for solute transport parameters during sensitivity analysis......157

Table 31. Transformation and degradation half-lives employed uniformly with depth at SHO. 163

Table 32. Values assigned to model parameters required by GW-WETLAND...........182

Table 33: GW-WETLAND simulations run to examine DDT transport scenarios.......194

Table 34: Total DDT loading approximations employed in GW-WETLAND simulations...195

CHAPTER 1: INTRODUCTION

1.1 Introduction

Approximately 70% of Point Pelee National Park (PPNP) is occupied by a marsh that provides habitat for both resident and migratory wildlife populations. As an area that is important to migratory bird populations, the wetland at PPNP is recognized and protected as a wetland of international importance under the RAMSAR convention (Mitsch and Gosselink, 2000). Each year, over 300,000 people visit the Park, with the majority of visitors coming to observe birds during the spring and fall migrations. In addition to birds, a large population of butterflies migrate through PPNP during the fall.

Many of the birds and wildlife within the Park rely on the rich habitat provided by the marsh for both feeding and breeding.

PPNP has not always been a natural area. Extensive development, including commercial establishments, agricultural activities, campgrounds, and numerous houses and seasonal dwellings continued to exist within PPNP until the late 1970's. Between 1948 and 1970, the insecticide DDT was used within PPNP to control both pests within the orchards and vegetable fields, and mosquitos within campgrounds, picnic areas, and residential areas. DDT, also known by its chemical name dichloro-diphenyl-trichloroethane is a hydrophobic and highly persistent organochlorine-based insecticide, that kills both target and non-target insects by attacking their nervous system. Because applications of DDT at PPNP ceased in 1970, it was thought that DDT would no longer be a problem at PPNP. However, when biologists from the University of Windsor attempted to identify the causes for the decline in the Park's population of amphibians, they noticed that spring peepers (Russell et al., 1995), and green frogs (Russell et al., 1997) exhibited unusually high concentrations of DDT. These findings are in agreement with other research conducted within southern Ontario, which showed general decline of amphibian and reptile populations resulting from DDT exposure (Gillan et al., 1998; Herbert et al., 1993). Subsequent studies tracked the source of this DDT to the soil within PPNP (Russell and Haffner, 1997), and showed that concentrations at several areas of the Park exceeded Ontario Ministry of Environment and Energy (OMOEE) guidelines of 1.6 μg/g for total DDT (OMOEE, 1997). Safety concerns relating to exposure to Park personnel and visitors resulted in the immediate closure of some public facilities and prompted the need for additional studies.

In 1998, Parks Canada requested the assistance of Environment Canada's National Water Research Institute (NWRI) to further quantify the extent of DDT contamination in the soil (both spatially and with depth) in two high-risk areas of the Park; the old Camp Henry and the Maintenance Compound, and in several shallow wells (sand points) used as a source of drinking water. This study (Crowe, 1999) confirmed that DDT was present at concentrations in shallow soil that often exceeded OMOEE guidelines for recreational/parkland land-use, but contamination was confined to the uppermost 20 centimetres of the soil profile. Additional sampling programs were undertaken by NWRI and PPNP to determine the spatial extent of the area of soil contamination, and these (see review in Crowe et al., 2002) confirmed that DDT contamination is widespread but limited to certain portions of the Park and that the soil contamination is confined to the upper several centimetres of the soil profile. Concerns about DDT in groundwater supply wells were addressed through analysis of groundwater samples taken at the tap; concentrations of DDT were several orders of magnitude below former Canadian Drinking Water Guidelines of 30 μg/L total DDT (CCREM, 1987). While the groundwater guidelines for Total DDT were removed in 2002 (CCREM, 2002), they serve as a reference point to which groundwater concentrations of Total DDT can be compared. It should be noted that the primary reasons that guidelines pertaining to Total DDT were removed relate to the lack of data on toxicity of DDT in groundwater to humans and the unlikely occurrence of DDT in groundwater because it was banned over 30 years ago and is no longer in use in Canada.

Recent studies by Crowe (1999), Crowe et al. (2002) and Marenco (2002) focused on the reasons for the persistence of DDT in soil at PPNP and specifically, characterizing DDT concentrations: (1) DDT concentrations by area and with depth, (2) past landuse practices to DDT concentrations, and (3) the impact of soil and hydrology on DDT concentrations and persistence. These studies determined that DDT, and its metabolites, DDE and DDD, which are also harmful to the environment, are spatially highly variable (over several orders of magnitude), but DDT is essentially confined to the A-horizon of the soil profile where organic matter content is highest. High concentrations are prevalent within the former agricultural areas, with very low levels in other land use areas. The DDT metabolite DDD is a prominent degradation product within the marsh. DDE is the main degradation product in the sandy soils that are never flooded by the marsh and the water table is well below ground surface. Also, half-lives in transitional soils are much shorter than half-lives in dry sand-dune soils.

The few analyses of DDT in groundwater below the former orchards (Crowe et al., 2002) showed that although DDT was present in groundwater samples, concentrations were very low. Both Crowe (1999) and Marenco (2002) suggested that DDT and its metabolites were attenuated on organic carbon within the soil profile and postulated this mechanism as a control on migration of DDT, DDE and DDD through the soil profile to the water table. However, no studies have been undertaken to characterize the mechanisms controlling DDT migration to the water table, present and historical fluxes at the water table (especially during the time DDT was widely applied), or if groundwater presents a possible pathway for DDT loading to the marsh, lake and drinking-water wells.

1.2 Objectives and Hypotheses

With extensive DDT contamination in former recreational and agricultural areas of the Park, contaminant leaching to groundwater and subsequent flow to the marsh could represent a potentially important pathway for delivering DDT-contaminated groundwater to the marsh, especially because some of these contaminated areas are often within a hundred metres of the marsh. Also, because groundwater is the Park's source of drinking water (through shallow sand points), groundwater flow to these wells could represent a pathway for delivering DDT to people. As a result of the potential for exposure of DDT to both humans and wildlife within PPNP, a thorough analysis of the behaviour of DDT within the subsurface and potential DDT loadings to groundwater merits further investigation.

The objectives of this thesis are:

1. To determine concentrations of DDT and its transformation products DDE and DDD in shallow groundwater at PPNP;
2. To determine the soil properties and hydrologic factors controlling leaching of DDT and its transformation products to the water table through both (a) field investigation, and (b) numerical modelling of DDT, DDE and DDD transport within the subsurface at PPNP.

The hypotheses used to test these objectives include:

1. DDT concentrations in groundwater correspond to the DDT concentrations in the overlying shallow soil; with concentrations in groundwater highest beneath soil with the highest concentrations of DDT.
2. Mechanisms controlling DDT persistence and mobility at surface are the same with depth and in groundwater; thus, relative proportions of the compounds DDT, DDE and DDD are the same in surficial soil, the soil profile, and groundwater.
3. DDT concentrations in groundwater are higher under areas where soil organic carbon concentrations are low, and concentrations in groundwater are lower beneath soils having high levels of organic carbon.
4. Depth to the water table from ground surface (i.e., length of pathway for leaching), is inversely related to concentrations of DDT in groundwater.
5. DDT concentrations in groundwater (i.e., below the water table) are lower due to dilution from annual recharge fluxes across the water table and dispersive and diffusive processes.

These objectives will be met through a combination of field, laboratory and numerical modelling studies. The field studies will be undertaken for two reasons. First soil and groundwater samples will be collected to assess the extent of DDT contamination within both the soil and groundwater. Secondly, soil samples will be collected for physical analysis in the laboratory to determine soil characteristics, and field tests will be conducted to determine the hydrologic properties of the field soils. Laboratory studies will quantify the physical properties of the soil and DDT distribution with depth, and this data will then assist in the conceptualization of the soil profile for numerical modelling purposes. Numerical modelling studies will focus on providing insight into the processes controlling pesticide fate and migration in the subsurface, and estimate pesticide fluxes across the water table. Numerical modelling studies will be undertaken to determine if DDT can migrate to the marsh by groundwater flow within the saturated zone, and if so, to establish the migration times to the marsh-aquifer interface.

1.3 Geographical Setting

Point Pelee National Park (PPNP) occupies the southern-most 12 km of Point Pelee, which extends southward approximately 15 km into western end of Lake Erie (Figure 1). It is located at 4638400 Northing and 366750 Easting (41°54' North Latitude and 82°22' West Longitude) and forms the southernmost point of mainland Canada. Point Pelee is surrounded by Lake Erie on the west, south and east and abuts farmland to the north. Approximately 70% or 1050 hectares of PPNP consists of a marsh that is separated from lake Erie by barrier bars on the west and east sides of the marsh. The western barrier bar increases in width from 70 m at the north end of the Park to over 800 m wide in the south. The width eastern barrier bar is fairly constant at approximate 25 m.

Point Pelee was established as the first National Park in Canada in May 1918. Numerous agricultural, recreational and commercial activities continued to exist, and in some cases expanded within PPNP (Battin and Nelson, 1978). Agriculture accounts for some of the most widespread impacts as a result of both commercial vegetable growing and fruit orchard operations (Figure 2). Some of the crops produced include beans, peppers, tomatoes, watermelons, strawberries, asparagus, tobacco, peaches and apples. By 1954, the apple, peach and asparagus demand had increased substantially and orchards were once again expanded by 30.4 hectares from 20.2 hectares between 1955 and 1963 (Battin and Nelson, 1978). During the late 1960's and throughout the 1970's, Parks Canada purchased much of the agricultural property within PPNP and the land was allowed to regenerate naturally. (Battin and Nelson, 1978). Restoration of the natural areas, including removal of non-native vegetation and animals, and reduction of the human impact though removal of building, roads, power lines, etc. continues to this day.

Between 1918 and 1954, numerous homes, seasonal cottages and campgrounds were built on the western barrier bar. During the 1970's Parks Canada purchased and removed most of the homes and cottages. Today only two of the former cottages remain within the Park, which are used to house research and park staff, (Harvey, personal communication, 2003). During the 1930's, some of the campgrounds were closed, and the land allowed to regenerate naturally. Camping within PPNP was effectively eliminated in 1972, with only two group campsites capable of accommodating 90 people remaining in operation. Only one of these campsites remains in use today, although it has since been moved to another area of the Park.

1.4 Climate

Point Pelee is classified as a humid continental climate. According to Canadian Climate Normals (Environment Canada, 2000), the mean annual temperature over the period from 1971 to 2000 within the Park was 9.2°C ±1.9°C, and the average annual precipitation was 908.3 mm of which 98.9 mm fell as snow. Because of the moderating effects of Lake Erie that surrounds Point Pelee, PPNP has one of the warmest mean January temperatures in all of Ontario. Accordingly, July mean temperatures are the highest in the province as well and it receives the fewest days of precipitation in the province with only 75 days of rain each year (Canadian Climate Normals, 2000, Environment Canada). Monthly average temperatures and total precipitation based on 30-year data sets from 1971-2000 are presented in Table 1.

Table 1. 30-year average monthly temperatures and precipitation values for PPNP (modified from Canadian Climate Normals, 2000, Environment Canada).

Monthly Average	Jan.	Feb.	Mar.	April	May	June	July	Aug.	Sept.	Oct.	Nov.	Dec.	30-Year Average
Temp. (°C)	-4.5	-3.6	1.3	7.2	13.7	19.3	22.3	21.5	17.6	11.1	5.5	-0.9	9.2
Precip. (mm)	57.6	53.6	78.2	79.9	79.3	84.5	73.9	89.3	94.2	61.2	83.7	72.9	908.3

In addition, evapotranspiration can be highly variable in space within PPNP due to both differences in depth to the water table as a result of elevation changes, and type of vegetation growing on the land surface. The majority of evapotranspiration occurs between mid-May and late-October (Crowe et al., 2004).

1.5 Geological Setting

The formation and evolution of the marsh and barrier bars comprising Point Pelee are related to local geology, the postglacial history of lake level fluctuations in the western basin of Lake Erie, and to long term isostatic rebound (Terasmae, 1970; Coakley, 1976; Trenhaile and Dumala, 1978; Coakley et al., 1998). Point Pelee developed at the location of the Pelee moraine that crosses Lake Erie to the south shore near Lorain, Ohio. High water levels and counter-rotating long shore currents caused the progressive shoreward migration of beach ridges and dune complexes on both sides of the Pelee-Lorain moraine, where they eventually met. The ancestral Point Pelee is believed to have extended much further south and east of its present position (Coakley, 1976). Its present configuration of a central marsh and coalesced barrier beaches to the east and west was initiated around 3.5 ka B.P. presumably soon after the Nipissing "flood" event around 4 ka B.P. Since then, Point Pelee has retreated primarily on the eastern side and southern-most point to where its present size is about two-thirds its original size. There is evidence of continuing accretion seen on the west-facing side as indicated by the sequence of preserved beach ridges. The current rise and fall of lake levels, coastal currents, coastal erosion and deposition continues to play a dominant role in the development of the southernmost portion of Point Pelee.

Recent studies by Coakley et al. (1998) identified four major sedimentary units; three within the barrier bar and one within the marsh. The lower-most unit is a clay-rich till which forms the moraine on which Point Pelee was formed. A fine-grained, grey glaciolacustrine sand rests on the clay-till but it is present only south of the Marsh Boardwalk site. The upper-most sediments comprising the barrier bar are a shoreface sand and gravel and an aeolian (dune) sand. The poorly sorted shoreface sand and gravel, composed of essentially the same material found along the present beach, varies in thickness from 7 m at the beach to 1 m adjacent to the marsh. An aeolian (dune) sand derived from the shoreface sand and gravel, varies in thickness from 0 m at the beach to

8 m within the largest dunes, and overlies the shoreface sand. The base of the marsh is composed of an organic marsh deposit (gyttja and peat), which sits on top of the clay-till.

The spatial distribution of these sediment units are shown in Figure 3. The surface of the till slopes southward from an elevation of ~172 m a.s.l. at the Park Gate transect to 164.5 m a.s.l. at the DeLaurier transect. South from here, the surface of the till is apparently flattened by erosion. The glaciolacustrine sand is absent from the eastern and northern portion of Point Pelee. Its top surface is essentially level at an elevation of 169.5 m a.s.l., and its absence corresponds to where the surface of the till exceeds an elevation of 169.7 m a.s.l. Its absence from the northern portion of Point Pelee and its level surface suggests that it is an erosional remnant of a once-extensive deposit. The aeolian and shoreface sands are present along the entire length of the western barrier bar, and rest on the glaciolacustrine sand, or directly on the till where the glaciolactustrine sand is absent. The elevation of the base of the aeolian sand rises towards the west to the present day high waterline. Although there was an overall rising trend in Lake Erie levels from 10 ka B.P., two major intervals in which the lake levels were at a stand-still are documented by the sediments at Point Pelee. First, the surface of the till below the south end of Point Pelee was eroded by waves to a planar surface at about 164 m a.s.l. Second, the upper portion of the glaciolacustrine sand was also eroded by wave action forming a planar surface at an elevation of approximately 169.5 m a.s.l. The initial deposition of the sand and gravel forming the barrier bar commenced at the same time as the formation of the marsh.

Recent aeolian processes have generated sand dunes up to 5 metres above ground surface, with relatively uniform soil properties. Studies within PPNP have shown that the dune sediments are typically 99% sand and 1% silt and clay, with a mean grain size of 470 μm. The sand contains 60% quartz, 25% limestone as well as smaller amounts of Ca-plagioclase, magnetite, epidote, amphibole and kyanite (Ptacek, 1998).

1.6 PPNP Soils

A soil survey of PPNP was undertaken in 1939 as part of a soil survey of Essex County and the soils within PPNP were classified as Eastport sands within the Regosolic Soil Order of the Canadian System of Soil Classification throughout both the eastern and western barrier bars (Richards et al., 1949). Soils bordering the marsh near the eastern extremity of the western barrier bar have been classified as Marsh soil under the Organic Soil Order. The Eastport sand profile exhibits little horizon differentiation, but is described as: one-half inch organic a horizon; a thin grey A horizon approximately 5 cm thick; a yellow B horizon less than 2 cm in thickness; and grey sand, which is the parent material. The presence of buried soil horizons was also suggested (Richards et al., 1949). Soils within the Camp Henry orchard have been classified as Melanic Brunisols according to Badley (2003), based on a 1.5 m by 3 m by 1 m deep soil pit excavation.

1.7 PPNP Groundwater

Groundwater levels within the barrier bars at Point Pelee National Park have been monitored by the NWRI for over 10 years, providing an assessment of the groundwater flow regime (Crowe et al., 2004; Crowe and Shikaze, 2004). The seasonal effects of precipitation and evapotranspiration exert controls on the groundwater flow regime. During the spring, the water table rises substantially due to infiltration of spring rains and snow melt (Crowe et al., 2004), and the water table declines throughout the remainder of the year due to evapotranspiration and drainage of groundwater towards the lake and marsh (Figure 4b). The lowest water table elevations occur between November and January. Also, rapid but short term rises of the water table are also seen in response to rain storm events during the spring, summer and fall, especially where the water table is very shallow.

Both long-term and seasonal fluctuations in the surface levels of Lake Erie and the Point Pelee marsh have a major impact on the groundwater flow regime within the barrier bars (Crowe et al., 2004). Water levels of both Lake Erie and the marsh rise in the spring to essentially the same elevation, decline throughout the remainder of the year (Figure 4a). The seasonal fluctuation of the lake is approximately 0.5 - 0.7 m, while the marsh only fluctuates approximately 0.1 - 0.2 m. This difference in surface elevations between the lake and the marsh imposes a hydraulic gradient on the groundwater flow regime within the barrier bar and influences the direction of groundwater flow. However, the magnitude of this imposed hydraulic gradient, and corresponding groundwater velocities, are a function of the width of the barrier bar; they are reduced as the width of the barrier bar increases (Crowe et al., 2004). Groundwater levels follow the long-term changes in marsh levels. The lowest marsh and water table elevations occurred during 1999, 2001, and 2002. The highest marsh and water table elevations occurred during

1996 and 1997. Thus, between 1994 and 2003 the water table fluctuated over a range of almost 1.0 m, the marsh ranged over 0.9 m and Lake Erie fluctuated over 1.6 m in elevation.

Where the barrier bar is relatively narrow (i.e., < ~350 m wide) the influence of the seasonally changing lake and marsh levels is the dominant factor affecting the groundwater flow regime. During the spring and early summer, when the lake and marsh levels are essentially the same, groundwater flows towards the marsh. However, from late summer to winter, when the lake level falls below that of the marsh, groundwater flows towards the lake. Thus, the changes in the relative elevations of the lake and marsh cause a seasonally oscillating direction of groundwater flow, with the hydraulic gradient, and hence groundwater velocity decreasing as the barrier bar width increases. As the barrier bar becomes wider, the infiltration rather than lake and marsh levels dominates the groundwater flow regime and groundwater flow velocity is relatively slow with essentially no flow reversal in wider areas of the western barrier bar. When the barrier bar is relatively wide (i.e., > ~350 m wide) the influence of the infiltration becomes significant relative to the seasonally changing lake and marsh levels in affecting the groundwater flow regime. The width of the barrier bar reduces the hydraulic gradient such that it has a minor impact on the direction of groundwater flow and groundwater velocity. Here the groundwater regime is characterized by a central groundwater divide with groundwater on either side of the divide flowing continuously towards the lake and the marsh throughout the year (Crowe et al., 2004). This assessment is supported by a stable oxygen isotope profile both with depth and over time and the determination that the largest infiltration of precipitation occurs during spring melt according to analyses of samples from nearby multi-level sampling wells (Huddart et al., 1999).

All study sites considered in this thesis are within areas of PPNP where the barrier bar is sufficiently wide such that the groundwater regime is dominated by infiltration and there is essentially no seasonal flow reversal in the direction of groundwater flow.

Sands and gravels within PPNP have calculated mean hydraulic conductivities of $6.7\text{x}10^{-2}$ cm/s for a study site close to the marsh on the western barrier bar (Ptacek, 1998). Another study reported conductivities of $2.52\text{x}10^{-2}$ cm/s for aeolian sand, $2.57\text{x}10^{-3}$ cm/s for shoreface sands, $4.17\text{x}10^{-3}$ cm/s for lacustrine sands and $1.9\text{x}10^{-4}$ cm/s for marsh sediments (Crowe et al., 2004). Saturated hydraulic conductivity of the sands have been measured using slug tests and ranged from 10^{-1} to 10^{-2} cm/s, declining slightly to the east corresponding to an increased clay content (Crowe and Ptacek, 1995).

1.8 DDT

When referring to the technical grade DDT insecticide that was sold commercially, the common name "DDT" will be used within this manuscript. The proper chemical name for the compound is dichloro-diphenyl-trichloroethane. Although the commercially available product consisted of up to 15 separate chemical constituents (Sayles et al., 1997), most commonly, technical grade DDT contained active ingredients in the following proportions: 77% *p,p'*-DDT, 14.9% *o,p'*-DDT, 0.3% *p,p'*-DDD, 0.1% *o,p'*-DDD, 0.1% *p,p'*-DDE, 4% *o,p'*-DDE, and up to 4% unidentified compounds (EHC 83, 1989). The terms ΣDDT, ΣDDE and ΣDDD will be used to refer to the sum of the *o,p'* and *p,p'* isomers of DDT, DDE and DDD, respectively. In addition, the terms "DDE-X" and "DDD-X" will be used to refer to the degradation products of DDE and DDD, respectively. A complete list and definition of terms used to refer to DDT and its transformation products is presented in Equations 1 through 7.

$$\Sigma\text{DDT} = \text{Sum of } o,p'\text{-DDT and } p,p'\text{-DDT} \tag{1}$$

$$\Sigma\text{DDE} = \text{Sum of } o,p'\text{-DDE and } p,p'\text{-DDE} \tag{2}$$

$$\Sigma\text{DDD} = \text{Sum of } o,p'\text{-DDD and } p,p'\text{-DDD} \tag{3}$$

$$\text{Total DDT} = \Sigma\text{DDT} + \Sigma\text{DDE} + \Sigma\text{DDD} \tag{4}$$

$$\%\text{DDT} = \frac{\Sigma\text{DDT}}{\text{Total DDT}} \times 100\% \tag{5}$$

$$\%\text{DDE} = \frac{\Sigma\text{DDE}}{\text{Total DDT}} \times 100\% \tag{6}$$

$$\%\text{DDD} = \frac{\Sigma\text{DDD}}{\text{Total DDT}} \times 100\% \tag{7}$$

During the early 1940's DDT was extensively used in agriculture as an insecticide and for pest control (e.g., lice, mosquitoes, spruce bud worm, etc.) because of its effectiveness, low cost, long-term persistence and thus, minimal need for repeated applications (Coulston, 1989; Wayland et al., 1991). Rachel Carson's 1962 book Silent Spring drew considerable attention to the persistent and bioaccumulative nature of DDT compounds, and to the deleterious effects DDT was having on humans and wildlife through exposure to contaminated food sources (Boul, 1994). The sales of DDT reached a maximum in 1969 in Ontario (Harris and Miles, 1975), when DDT use was severely restricted by the federal government in 1969. This eventually led to a ban in 1985, with the agreement that all outstanding stocks would be used or otherwise disposed of by December 31, 1990 (Environment Canada, 1997). Today, DDT is often found in soils in areas where it has been applied in the past (EPA, 1986; Aigner et al., 1998).

Within Canada, DDT is regulated under the Pest Control Products Act and as such, the use or sale of DDT in Canada represents a violation of the Act (PMRA, 1986). In addition, any export of DDT requires the appropriate authorities to be notified under the Canadian Environmental Protection Act (CEPA). Today, DDT is on the list of Tier 1 Substances and as such, is targeted for virtual elimination under the Canada-Ontario Agreement Respecting the Great Lakes Basin Ecosystem (1994) committed to restoring degraded areas; preventing and controlling pollution and conserving and protecting ecosystem health (Environment Canada, 1996).

DDT is still applied as an insecticide in developing nations to control mosquito populations and reduce deaths by malaria and Dengue fever. But it is targeted for elimination as part of many other treaties and agreements worldwide. In 1999, representatives from 110 countries met in Geneva and decided that use of DDT for agricultural purposes should be ceased immediately and its use for malaria control should be phased out in the near future. In addition, the World Wildlife Fund (WWF) proposed a target date for elimination of DDT use of 2007 to encourage funding for the development of alternatives to DDT (Hileman, 1999).

1.8.1 Properties of DDT

The behaviour of DDT and its metabolites in the subsurface is ultimately a result of its chemical and physical properties. Biological activity within the soil also affects the persistence of DDT and the formation of metabolites DDE and DDD. Some of the most important properties governing the behaviour of DDT include transformation/degradation rates, solubility, vapour pressures, octanol-water partion coefficient (K_{ow}) and organic carbon partition coefficient (K_{oc}). These are the primary factors affecting the mobility and persistence of DDT within a soil profile and thus influence leaching rates through the soil profile and pesticide fluxes across the water table.

1.8.2 Transformation of DDT

DDT is transformed to its primary metabolites, DDE and DDD along several degradation pathways that depend on soil redox and microbial conditions. The specific pathways have been observed to follow from DDT → DDE → DDD or from DDT → DDD directly as observed by Corona-Cruz and others (1999). Earlier research also claimed that both DDE and DDD could be formed concurrently (Guenzi and Beard, 1968). Following the transformation and/or degradation of DDT compounds, metabolites may be remobilized and either (1) be mineralized; (2) re-incorporated into soil organic matter or (3) released into solution leading to plant uptake or leaching to groundwater (Gevao et al., 2000). Generally, degradation proceeds most quickly in anaerobic environments, and much slower in aerobic environments.

In aerobic soils, DDE is the main dehydrochlorination product of DDT with little DDD forming (Spencer et al., 1996; Guenzi and Beard, 1968; Farmer et al., 1974; Boul et al., 1994). This reaction involves the loss of hydrogen chloride from DDT to form DDE through chemical reactions (Lichtenstein et al., 1971; Nash and Woolson, 1967; Parr et al., 1970) and/or via bacterially mediated processes (Guenzi and Beard, 1976).

DDD is the primary degradation product of DDT under anaerobic reducing conditions (Guenzi and Beard, 1968; Leahy and Brown, 1994; Parr et al., 1970), and the formation of DDE is not favoured (Farmer et al., 1974; Boul et al., 1994). This reaction involves the loss of a chlorine atom and reduces toxicity (Parr et al., 1970). It is important to note that the further degradation products of DDE and DDD are themselves rapidly degraded and less toxic.

The degradation half-life for DDT has been found to range from less than 10 years to greater than 40 years (Crowe et al., 1999), depending on soil conditions and climate. The range of half-lives reported in the literature are presented in Table 2. Nash and Woolson (1967) found a mean half-life of 10.5 years, with the longest half-life being 35 years in temperate agricultural soils in Maryland, USA. Another study by Dimond and Owen (1995) reported half-lives of 20-30 years for forest soils in Maine. Also Oliver et al. (1989) postulated both aerobic and anaerobic decay was occurring and estimated DDT half-lives of 14 to 21 years in Lake Ontario sediments.

Recent studies by Crowe (1999) have proposed that the degradation pathways and estimated half-lives of DDT at PPNP are influenced by soil conditions. Based on the relative proportions of DDT, DDE and DDD, Crowe (1999) proposed a half-life of less than 10 years in moist, organic rich soil adjacent to the marsh (maximum %DDT remaining in soils of <50%,) and a half-life of more than 40 years in dry, sandy soil in the sand dunes far from the marsh (maximum %DDT was >90%). After evaluation of an extensive number of DDT analyses conducted on soil within PPNP, Crowe et al. (2002) reported a linear 1:1 transformation of DDT to DDE in most areas of the park, with very little DDD produced outside areas covered by marshy sediment and marshy soils. This is in agreement with other studies of orchard soils reporting aerobic soil environments promoted DDT degradation to DDE rather than DDD (Kuhr et al., 1974; Lichtenstein et al., 1971). Marenco (2002) found that half-lives varied with depth in the soil profile and relative position to the marsh. DDT half-lives in soil at a depth of 0-5 cm were 30, 15 and 8 years at the sand-dunes soils, transitional soils and organic-rich transitional soils, respectively. At a depth of 10-15 cm, half-lives were shorter; about 15 years at both the

Table 2. Examples of reported half-lives for transformation of DDT, DDE and DDD.

$t_{1/2}$ - DDT (yrs)	$t_{1/2}$ - DDE (yrs)	$t_{1/2}$ – DDD (yrs)	Reference
20 - 30	-	-	Dimond and Owen (1995); forest soils
10.5 - 35	-	-	Nash and Woolson (1967); temperate agricultural soils
14 - 21	-	-	Oliver et al. (1989); Lake Ontario sediments
SHORT	SHORT	2.3	Guenzi and Beard (1976): anaerobic soils
LONG	LONG	< 0.08	Guenzi and Beard (1976): aerobic soils
< 10	-	LONG	Crowe (1999); PPNP organic soils
> 40	LONG	-	Crowe (1999); PPNP dry sandy soils
30	LONG	LONG	Marenco (2002); PPNP dune soils (0-5 cm)
15	LONG	LONG	Marenco (2002); PPNP transitional soils (0-5 cm)
8	LONG	LONG	Marenco (2002); PPNP organic transitional soils (0-5 cm)

SHORT and LONG refer to the rates of transformation/degradation relative to those measured in the study as they were not estimated or measured directly, but were referred to as "short" or "long" within the discussion section.

sand dune soils and transitional soils, and 6 years at the organic-rich transitional soils. Marenco (2002) confirmed that DDT degradation rates and pathways were related primarily to soil-moisture environments. In the transitional and organic-rich transitional soils below 175.3 m above sea level (a.s.l.), where the water table was close to ground surface and the soil is frequently flooded by the marsh, DDT degraded anaerobically to DDD preferentially. In the sand dune soils, at elevations above 175.3 m a.s.l, where seasonal flooding did not occur, DDT degraded to DDE preferentially through aerobic pathways.

1.8.3 Attenuation of DDT

Lichtenstein (1971) postulated that DDT would be retained in shallow soils much longer in areas rich in organic matter, while Bailey and White (1964) reported increased adsorption of DDT by organic matter with increasing contact time. Numerous studies have been undertaken in the laboratory targeted at determining the sorption properties of DDT, which ultimately controls the leaching of DDT under field conditions.

DDT has been reported in the literature as a compound representing the extreme case of long-term hysteretic sorption within the subsurface (Carter and Suffet, 1982; Champion and Olsen, 1971; Lichtenstein et al., 1971; Chiou et al., 1986; Guenzi and Beard; 1967). DDE binds more strongly to organic matter in soils than DDT or DDD (Ball and Roberts, 1991; Brusseau et al., 1991; Champion and Olsen, 1971). Thus, DDE is more resistant to leaching through the soil profile. Research continues at the field scale using aged DDT/sediment mixtures and using fresh DDT to generate sorption isotherms in the laboratory (Kan et al., 1998; Van den Hoop et al., 1999).

While some of the more recent research has focused on using extractability of DDT from soils as an indication of bioavailability to organisms (Kan et al., 1998; Reid et al., 2000), other focus has been given to implications for site remediation (Piwoni and Keeley, 1990; Cornelissen et al., 2000). Partition coefficients are a good indicator of the potential for leaching of pesticides to the water table. More specifically, the octanol-water (K_{ow}), organic matter (K_{om}) and organic carbon (K_{oc}) partition coefficients are used as an indicator for the leaching potential of DDT. Within the literature, the range of reported partition coefficients is quite large as illustrated in Table 3, because K_{oc} is dependent on both K_{ow} and percent organic carbon, which are highly variable themselves.

Pontolillo and Eganhouse (2001) undertook an extensive quality assurance and quality control (QA/QC) evaluation of reported solubility and K_{ow} values for DDT, DDE and DDD, with recommended values being marked with an asterisk in Table 3. They evaluated over 700 publications and stated that the best available K_{ow} values were those measured by de Bruijn et al. (1989) as the K_{ow} values for DDT, DDE and DDD were determined by the same laboratory and verified (Pontolillo and Eganhouse, 2001).

At PPNP, because no correlation between organic carbon content of soil and DDT concentrations in soil was observed, Crowe et al. (2002) suggested that given the very low levels of DDT, not all of the adsorption sites on the organic carbon are filled and thus, soil organic carbon content is not a predictor of DDT concentration in shallow soil. Although the K_{oc} values that received the highest QA/QC ranking according to Pontolillo

Table 3. Examples of log K_{ow}, log K_{om} and log K_{oc} values for DDT, DDE, and DDD.

	DDT	**DDE**	**DDD**	**Reference**
Log K_{ow} (-)	6.914*	6.956*	6.217*	De Bruijn (1989)*
“	5.33	-	-	Gustafson (1989)
“	6.307	-	-	Brooke et al. (1990)
“	6.36	-	-	Chiou (1982)
“	6.91	6.51, 6.00	6.02, 5.87	Howard and Meylan (1997)
“	5.98	-	-	Laskowski et al. (1982)
Log K_{om} (cm^3/g)	5.38	4.70	-	Sabljic (1984)
Log K_{oc} (cm^3/g)	5.35	-	5.18	Meylan et al., 1992 (estimated)
“	-	4.7, 5.19	5.19	Sabljic (1984)

* Received the highest QA/QC ranking after extensive evaluation by EPA: Pontolillo and Eganhouse (2001).

and Eganhouse (2001), the values may not be representative of PPNP soils. It is important to recognize that the values that received the highest ranking are also the highest values and represent the strongest sorption to soil.

1.8.4 Solubility of DDT

A wide range of solubility values for DDT, DDE and DDD have been reported in the literature, although values are usually only fractions of a milligram per litre at 25°C. Despite the fact that over 100 publications have looked at DDT dissolution and phase distribution, none received the highest ranking by Pontolillo and Eganhouse (2001). In addition, the solubility of DDD has rarely been investigated. Low solubility ultimately limits the amount of crystalline DDT that enters solution, which subsequently undergoes volatilization and sorption. Because only dissolved DDT is able to migrate vertically through the soil profile, when concentrations in shallow soils are high, leaching is restricted by solubility.

Guenzi and Beard (1967) were one of the first to study DDT leaching through porous media and found DDT remained in the upper regions of the soil column regardless of the volume of water applied for a variety of soil types including sandy loams, silty loams and clays. They concluded that the primary factor limiting DDT mobility was its extremely low solubility (Guenzi and Beard, 1967). The solubility of DDT, DDE and DDD are presented in Table 4 accompanied by their sources.

Table 4. Examples of solubility values reported in the literature for DDT, DDE and DDD.

	DDT	**DDE**	**DDD**	**Reference**
S @ 25°C (mg/L)	-	0.04	-	Chiou (1977)
"	0.005*	-	-	Chiou (1981)*
"	0.00012 - 6.21	0.0011 - 1.24	-	Pontolillo and Eganhouse (2001); synthesis of over 195 references
"	0.085	0.14	0.1	Howard and Meylan, 1997
"	0.0025	0.12	0.09	U.S. EPA, 1997; Howard and Meylan, 1997

* Received the best QA/QC ranking after extensive evaluation by EPA: Pontolillo and Eganhouse (2001).

1.8.5 Volatilization of DDT

Generally volatilization in temperate climates is quite low; however, in tropical climates DDT volatilization can contribute to significant losses from shallow soils (Boul, 1994). It has also been shown that the addition of water to a soil can dramatically increase the volatilization of DDT compounds (Spencer et al., 1996). Another important trend is that DDE has a higher vapour pressure than DDT or DDD and as a consequence, it is lost more readily through volatilization in well-aerated soils (Spencer, 1975). The vapour pressures, calculated vapour densities and Henry's Law constants are presented in Table 5 for DDT, DDE and DDD.

Table 5. Examples of reported values of vapour pressure (V_p), vapour density (V_d), and Henry's Law partition coefficient (K_H) for DDT, DDE and DDD.

	DDT	**DDE**	**DDD**	**Reference**
V_P (torr)	1.6×10^{-7} @25°C	6.0×10^{-6} @25°C	1.35×10^{-6} @25°C	Howard and Meylan, 1997
"	1.1×10^{-7} @25°C	6.2×10^{-6} @25°C	1.94×10^{-6} @25°C	Howard and Meylan, 1997
V_d (mg/L)	3.1×10^{-6} @25°C	1.0×10^{-4} @25°C	1.2×10^{-5} @25°C	Calculated from Howard and Meylan, 1997
K_H (atm·m^3/mol)	5.9×10^{-7}, 8.3×10^{-6}	1.8×10^{-5}, 2.1×10^{-5}	4.0×10^{-6}, 8.17×10^{-6}	Howard and Meylan, 1997

1.9 DDT in Soil

When DDT was first discovered, its long-term persistence was considered one of its most desirable attributes, reducing the number of applications required to ensure effective control of pests. This resistance to transformation and degradation is the primary reason why DDT contamination remains an issue today. The average DDT content for U.S. soils has been reported to be 0.168 g/m^2 for agricultural soils and 0.00045 g/m^2 for non-agricultural forest soils in Pennsylvania where DDT was known to have never been applied (Woodwell, 1971). It is important to recognize that measurements are rarely taken from agricultural areas where long-term use had not occurred (i.e., grain and fodder crops) and thus, the agricultural soil averages are likely biased to higher concentrations as a result of contamination concerns. Edwards (1970) reported an average value of 2 ppm in agricultural soils. Lichtenstein et al. (1971) studied persistence and vertical distribution of organochlorine pesticides both 10 and 15 years after a single application of DDT on a field plot in Wisconsin and found that cultivation practices led to enhanced disappearance of organochlorine pesticides with only 10.6% of the Total DDT remaining in loam soil 15 years after application. Kuhr et al. (1974) found that 12 years after the last application of DDT, over 70% of the Total DDT residues persisted as DDT in the upper layers of the soil profile in former orchard areas of New York State, and that DDE concentrations almost always exceeded DDT concentrations in shallow soil horizons. Nash and Woolson (1967) also studied DDT disappearance at the field scale and found 39% of the applied DDT remained 17 years after application on sandy loam soils in Maryland. Tarrant et al. (1972) reported that following aerial application of DDT by helicopter, essentially no percolation of DDT occurred after 36 months in forest soils receiving 20 inches of annual rainfall in Oregon, U.S.A. Soil organochlorine pesticide concentrations have also been measured in the soils of the U.S. corn belt from 1995-1996 and determined mean values of 9.6 ng/g Total DDT, with a maximum of 11846 ng/g (Aigner et al., 1998). Harner et al. (1999) determined that DDT concentrations were log-normally distributed in 36 Alabama farm soils and found that DDT concentrations were not related to organic carbon content of the soil. They also found mean DDT/DDE ratios ranging from 0.39 to 1.5 illustrating the role of degradation and differing application histories. Marenco (2002) and Crowe et al. (2002) also found that DDT concentrations were log-normally distributed at PPNP and there was no positive correlation between concentrations and organic carbon content.

Although DDT was used over broad areas in North America, both in the agricultural and residential environments, background DDT concentrations in Southern Ontario soils are generally below 10 parts per billion (Webber and Singh, 1995). Harris and Sans (1971) found that organochlorine pesticides including DDT residues were most persistent in orchard areas, followed by vegetable growing areas, tobacco fields and other field crops based on a study of 16 farms in south-western Ontario. Surveys of apple orchard soils in Southern Ontario have found concentrations approaching 43 ppm (Webber, 1994); with one study site being located between Windsor, Ontario and PPNP. During the early 1970's, Frank et al. (1976) reported a mean Total DDT concentration of 43.3 ppm for shallow soils from 0-15 cm below surface in 31 apple orchards located in Ontario and 5.83 ppm for soils from 15-30 cm below surface, and 9.22 ppm for peach orchards, all located in Ontario (Frank et al., 1976). Total DDT concentrations ranged from 1.33 to 334 ppm and the same authors also showed higher DDT concentrations in samples taken near tree trunks compared to samples equidistant from two trees.

1.10 DDT in Surface Water

During the 1970's, several studies focusing on DDT in surface waters and bottom sediments in southern Ontario were conducted and found that although DDT had not been applied in recent years, it was readily detected. Concentrations in southern Ontario streams between 1975 and 1977 revealed a range of concentrations for Total DDT from <0.4 ng/L to 347 ng/L, with a mean of 6.7 ng/L for 1976 and a mean of 7.7 ng/L for 1977, with International Joint Commission (IJC) objectives of 3 ng/L being exceeded 40.6% of the time (Frank et al., 1982). DDT was present in 93% of 949 stream waters analyzed between 1975 and 1977, with some of the highest concentrations in both of these studies being reported in Essex County which encompasses PPNP (Frank and Braun, 1981). They also determined that the majority of loss of DDT from watersheds occurred during the first 4 months of each year studied corresponding to spring melt and runoff events and found no decline in pesticide loads from year to year, indicating substantial storage of DDT in soil within the watersheds (Frank et al., 1981). This tailing effect is consistent with the findings of Harris and Miles (1975) who studied organic soils in central Ontario, Frank (1981) who studied DDT loading in the Grand and Saugeen river basins for 1975-1977, and Oliver et al. (1989) who investigated Lake Ontario sediments. Frank (1981) also noted an increased pesticide loading to surface waters in areas having a sandy soil texture. Local streams were also examined as part of the same study and found that residue concentrations peaked in the spring months when discharge volumes were highest and peaked at 45 ppt as a result of spring thaw, runoff, cultivation of the land and spraying of crops. It was also found that rainfall and runoff were not the primary controls on stream residue concentrations because residue concentrations declined during the summer despite heavier rainfall (Frank et al., 1974). Long Point Bay in Lake Erie has also been studied, having a mean of 12.5 ppt Total DDT in 1971 (Frank et al., 1974).

1.11 DDT in Groundwater

Studies of DDT in groundwater have focus on quantifying the contamination of drinking water supply wells for both private residences and municipalities in agricultural areas. DDT and its degradates were reported to range over three orders of magnitude in wells from just above detection limits (Kolpin et al., 1998) to an unusually high maximum value of 402 μg/L from point source contamination at an undisclosed location in the United States (Goodrich et al., 1991). Another point-source contamination problem in the Southeastern Coastal Plains, U.S.A. showed DDT and DDE concentrations of 1.5 and 0.5 ppb six months after construction and backfilling with contaminated soil, with concentrations in water declining within the year to between 0.1 and 0.3 μg/L over the remaining 4 years (Lewallen, 1971). During the 1990's, 4 of 97 wells sampled in North Carolina found concentrations of DDT and its degradates to be between 0.01 and 0.06 μg/L, although they were detected less frequently than in the 1960's (Wade et al., 1998). More recently, the United States Geological Survey (USGS) sampled 303 drinking water wells twice in 1991 across 12 states and revealed that the highest DDE concentrations in groundwater were found in areas where soil was sandy with a maximum observation of 0.05 μg/L (Kolpin et al., 1996). A comprehensive survey of groundwater conducted by the USGS encompassing 2485 sampling sites across the United States between 1992 and 1996, revealed a maximum DDE observation of 0.006 μg/L, being detected in 3.3% of the wells sampled (Kolpin et al., 2000). Hallberg (1989) reported average concentrations of DDD, DDE and DDT to be 3.0 μg/L, 5.0 μg/L and 20.0 μg/L in California during 1986.

Within Ontario, several studies have been undertaken at provincial, regional and local scales. Areas that experienced intensive cropping and orchard activity in Southern

Ontario have been studied in the past and it was found that Total DDT levels in shallow well water ranged from 0 to 2000 ng/L with a mean of 6.7 ng/L (Frank et al., 1982). Watersheds draining the tobacco belt bordering Lake Erie in southern Ontario were studied in the early 1970's and found that mean soil concentrations of Total DDT were 2.33 to 3.44 ppm and calculated a half-life of 3 to 4 years for DDT in the sandy loams that dominate these watersheds (Frank et al., 1974). As part of the same study, 14 shallow wells were sampled for organochlorine residues and found three containing Total DDT residues of 4, 40 and 50 ppt. DDT was also found in two of six spring-fed ponds sampled at 1 and 50 ppt, and four of nine surface-fed farm ponds sampled at 9, 35, 60 and 80 ppt. Mean Total DDT residues were calculated to be 6.7 ppt in shallow wells, 8.5 ppt in spring-fed ponds and 20 ppt in surface-fed ponds (Frank et al., 1974). They also concluded that volatile losses to air were insignificant during their study and that air transport was primarily due to spray drift and particulate transport by wind. Water samples were also collected from 11 wells located in an area of intensive vegetable production on an organic soil in Simcoe County, Ontario during 1981 and 1982. In addition, samples from 91 wells from farms on mineral soils across Ontario were analyzed from 1981 to 1984 for pesticide residues aimed at determining if normal field use of pesticides contaminated well waters. The study found that in all cases, no DDT residues were detected in well water samples (IDL <0.005 µg/L) (Frank et al., 1987a). An accompanying study by the same authors found that a DDT spill nearby a drilled well in Ontario resulted in residue concentrations of 0.5 and 2.1 µg/L 4 days after the spill occurred (Frank et al., 1987b). A study by Goss et al. (1998) showed almost 40% of the wells they tested in both summer and winter exceeded regulatory limits for pesticides in drinking water. Pesticides were detected in 7.4% of 1175 wells tested in the winter in Ontario, with 11.5% of the wells showing measurable pesticide concentrations in the summer of 1991, however no DDT residues were detected in any of the wells tested. They also reported increased contamination of wells located in permeable sands and gravels, with a rapid decrease in contamination in finer textured soils (Goss et al., 1998). The occurrence of contamination was also related directly to type, depth and age of the well. A continuation of this study utilized multi-level sampling wells and found very few pesticide detections during the 2 years following their installation in 1991, with no DDT residues being detected (Rudolph et al., 1998).

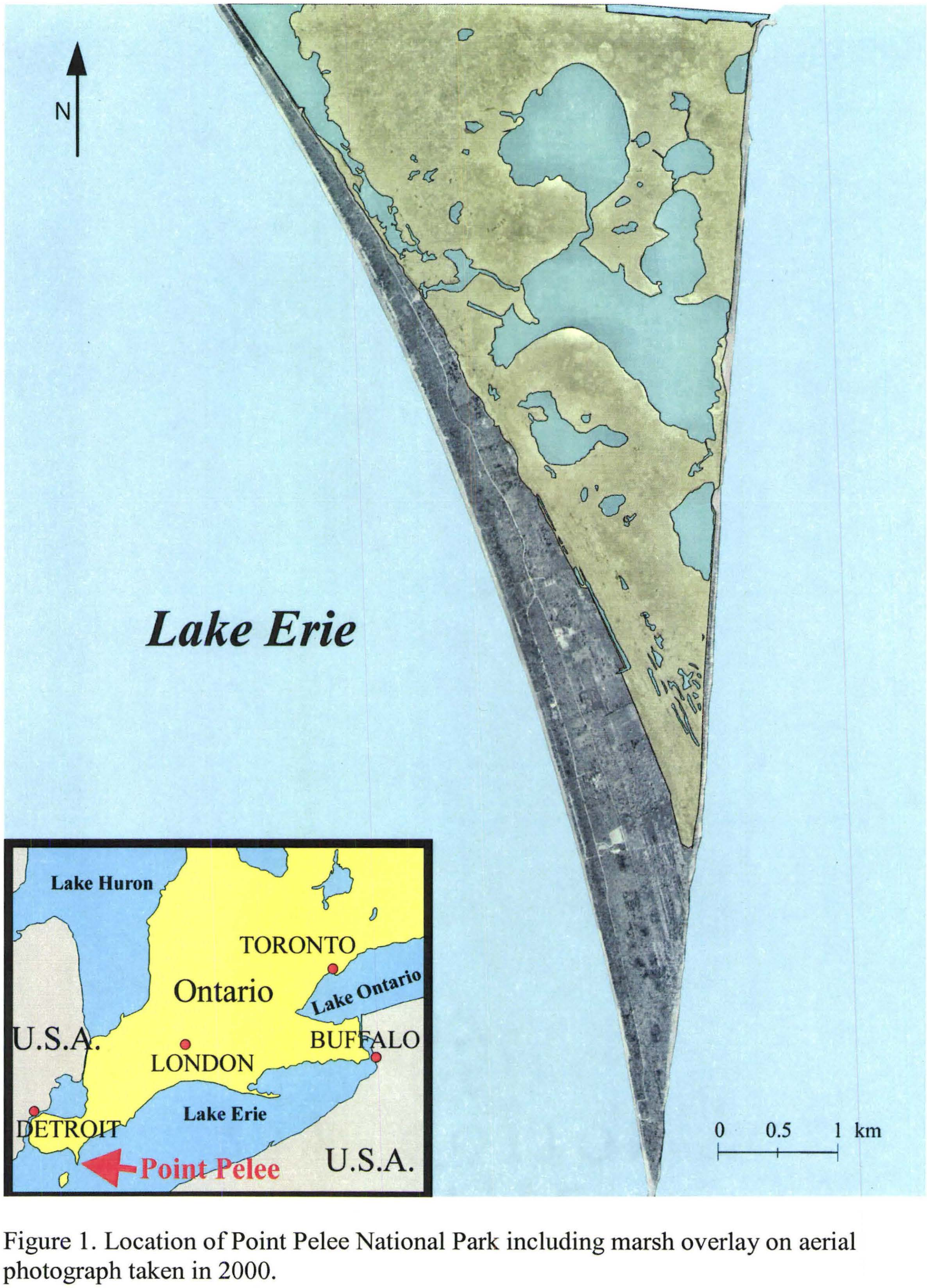

Figure 1. Location of Point Pelee National Park including marsh overlay on aerial photograph taken in 2000.

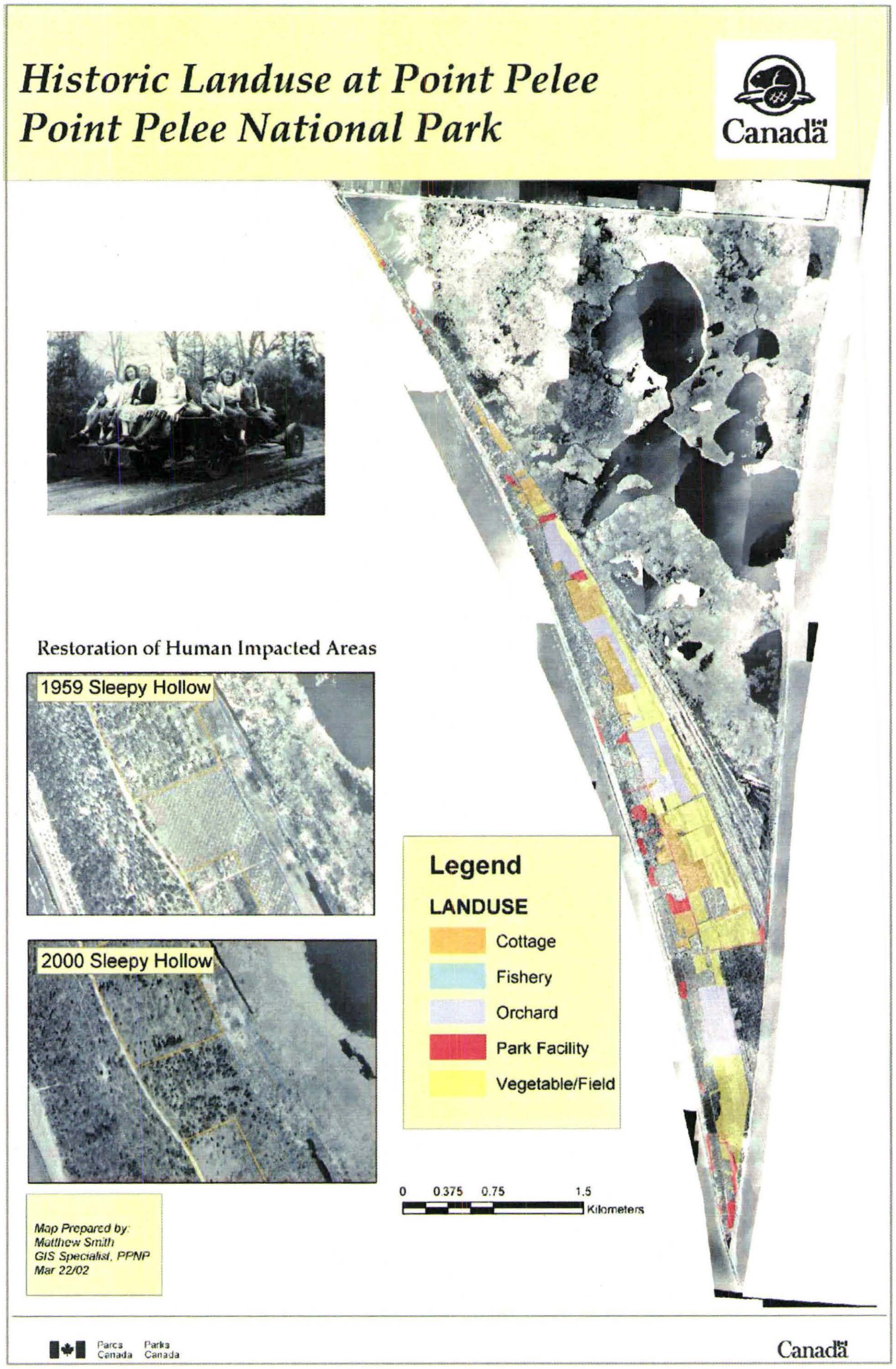

Figure 2. Historical landuse at PPNP highlighting former agricultural areas (prepared by Matthew Smith, Parks Canada, 2002).

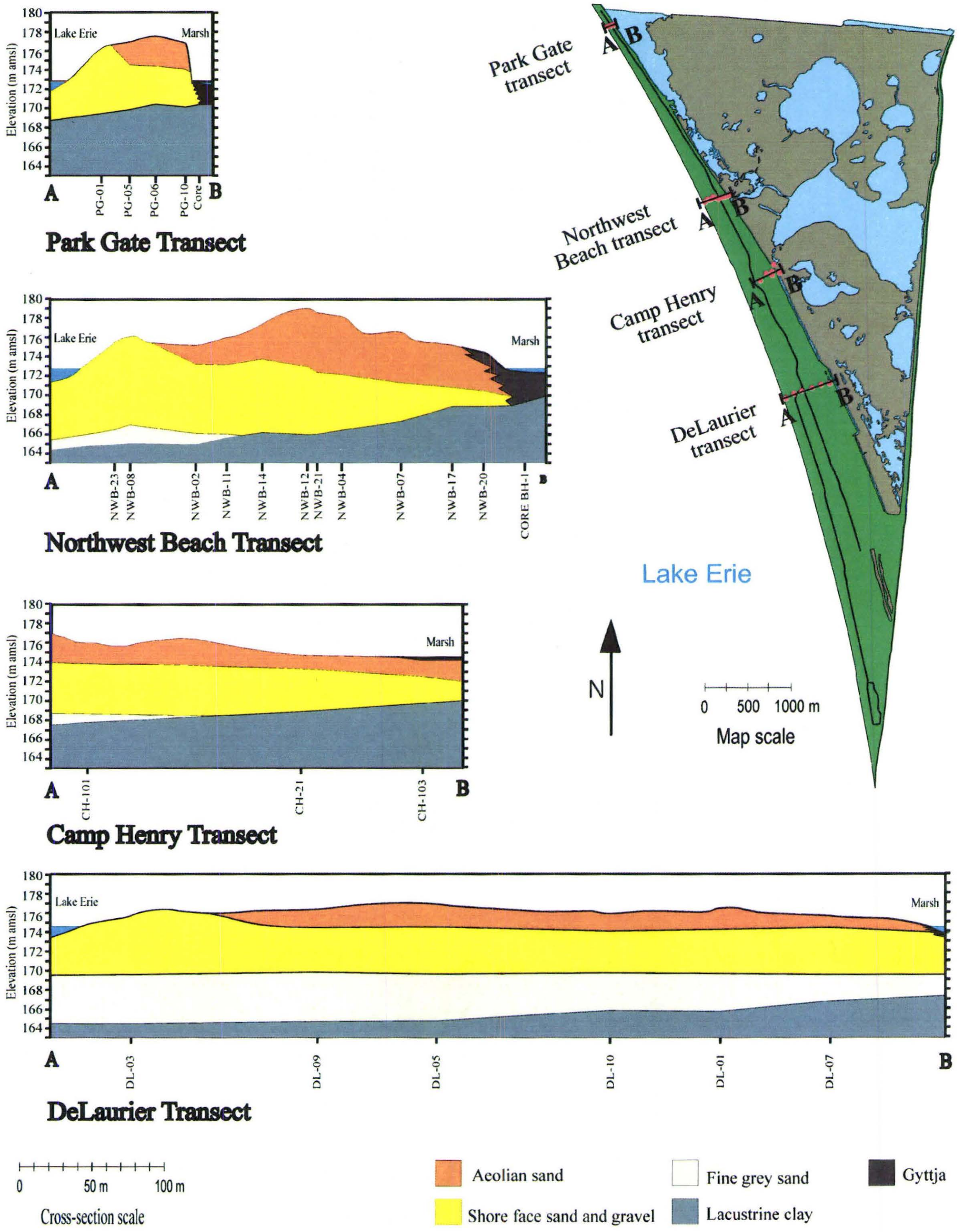

Figure 3. Geological cross-sections through the western barrier bar at PPNP (modified from Coakley et al., 1998).

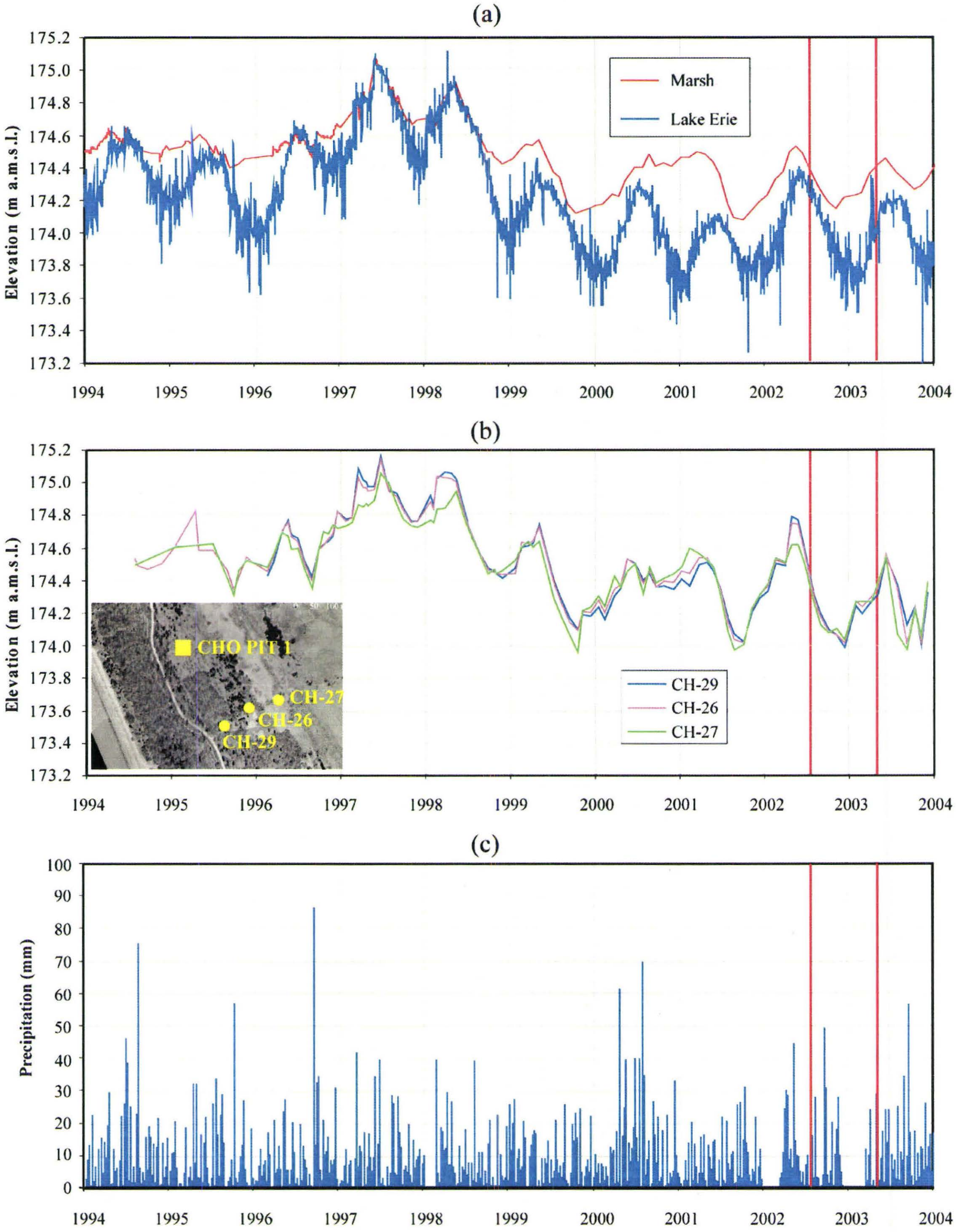

Figure 4. Seasonal fluctuations of (a) Point Pelee marsh and Lake Erie, (b) the water table at NWRI's Camp Henry transect and (c) daily total precipitations measured at the PPNP weather station from 1994 to 2004. July 2002 and May 2003 sampling dates are shown as red lines.

CHAPTER 2: FIELD AND LABORATORY METHODS

Field and laboratory work was conducted over a period of two field seasons. The first field program was undertaken to better understand the relationship between DDT in soil and DDT in the underlying groundwater at several sites throughout former orchard areas of PPNP, and to guide future detailed sampling programs. This study was conducted over a period of five weeks during June, July and August 2002. The second field program, conducted during May 2003, was undertaken to gather information on both soil DDT concentrations and soil/hydraulic properties with depth and groundwater samples at three selected sites within the park to support one-dimensional modelling of pesticide leaching from surface to the water table. The various types of samples collected and the analyses conducted in the field and laboratory are presented in Table 6.

Table 6: Parameters measured in the field and laboratory during 2002/2003.

Parameter Measured	**Field**	**Laboratory**
Depth to water table	X	
Field-saturated hydraulic conductivity	X	
Groundwater concentration of DDT, DDE and DDD		X
Soil concentration of DDT, DDE and DDD		X
Gravimetric soil moisture		X
Volumetric soil moisture		X
Bulk density of soil		X
% Organic matter		X
% Organic carbon		X
Particle size analysis (soil texture)		X
% Porosity		X

2.1 Field Methods

2.1.1 Site Selection

Locations of the sampling sites for the initial assessment of DDT contamination were selected within areas that were known to have different depths to the water table. The sites were also chosen based on areas known to have elevated concentrations of Total DDT within the shallow soil environment as reported in previous studies (Russell and Haffner, 1997; O'Connor Associates, 2001; Crowe et al., 2002). Selection of sites based on this methodology permitted the testing of the relationship between DDT (concentrations, relative proportions) in soil and groundwater and the depth to the water table. Soil and groundwater samples were taken from 12 sites during July and August 2002 (Figure 5). Ten sites were located within four former orchards; Camp Henry Orchard, DeLaurier Orchard, Sleepy Hollow Orchard, and Anders Orchard. Two additional sites were located outside of former orchard areas including one in a marshy soil environment and one in a natural vegetated area; both had not previously been occupied by agriculture or housing. Samples from an undisturbed natural sand-dune area provided background DDT concentrations in soil and groundwater. Only one sample from the natural sand-dune area was obtained because several analyses of soil within the natural areas existed (Crowe et al., 2002) and these analyses showed that concentrations of DDT were barely detectable. A single groundwater sample, collected at the water table, was obtained at each of the 12 sites. Replicate groundwater samples, spaced about 5 m from the initial groundwater sample were also taken at four sites to define the local variability of DDT concentrations in groundwater, giving a 16 groundwater samples (Table 7).

Previous studies (Marenco, 2002) showed that concentration of Total DDT and compounds DDT, DDE and DDD in soil at PPNP varies by several orders of magnitude within several metres of each other. Further, this degree of variation has been shown to be represented on the 10 cm scale within the former Camp Henry Orchard (Badley, 2003).

Table 7. Groundwater samples and replicates collected during July 2002.

Sample I.D.	UTM's – NAD 83 Easting	 Northing	Land Use Area
PPGW-01	373411	4646568	Former Orchard
PPGW-02	373696	4646029	Former Orchard
PPGW-03	374034	4645595	Former Orchard
PPGW-04	374347	4644858	Former Orchard
PPGW-05	374308	4644652	Former Orchard
PPGW-06	374076	4645083	Former Orchard
PPGW-07	373917	4645864	Former Orchard
PPGW-08	374441	4644708	Former Orchard
PPGW-09	373630	4646475	Natural Marsh Area
PPGW-10	374006	4645684	Former Orchard
PPGW-11	373519	4646608	Former Orchard
PPGW-12	373360	4646475	Natural Dune Area
PPGW-01-R	373412	4646577	Former Orchard
PPGW-02-R	373697	4646025	Former Orchard
PPGW-03-R	374029	4645596	Former Orchard
PPGW-04-R	374333	4644914	Former Orchard

Therefore, in order to obtain a representative soil concentration for comparison between concentrations in the soil and concentrations in groundwater, multiple soil analyses were required at each groundwater sampling site. Six of the groundwater sampling sites were located in close proximity to multiple previous soil samples collected within 100 metres of the sites and no further soil samples were collected. But at the remaining six of the groundwater sampling sites, only one previous soil analysis had been performed, and thus two replicate soil samples were collected here. The location of all soil samples (12 for this study, 56 from previous studies) used in this analysis, including those collected during the summer 2002 sampling program, are summarized in Table 8.

The following year (May 2003), a detailed study of physical and hydraulic properties of the soil with depth was undertaken to provide information to be used in

Table 8. Surficial soil samples collected within the vicinity of the study area.

Corresponding GW Sample	**Sample I.D.**	**UTM's – NAD 83**		**Land Use Area**	**Source of Data**
		Northing	**Easting**		
PPGW-01	S grid (S-1)	4646547	373429	Former Orchard	Marenco (2002)
	S grid (S-2)	4646550	373432	Former Orchard	Marenco (2002)
	S grid (S-3)	4646548	373433	Former Orchard	Marenco (2002)
	S grid (S-4)	4646544	373439	Former Orchard	Marenco (2002)
	S grid (S-5)	4646540	373434	Former Orchard	Marenco (2002)
	S grid (S-6)	4646538	373437	Former Orchard	Marenco (2002)
	S grid (S-7)	4646538	373443	Former Orchard	Marenco (2002)
	S grid (S-8)	4646535	373442	Former Orchard	Marenco (2002)
	S grid (S-9)	4646534	373431	Former Orchard	Marenco (2002)
	S grid (S-10)	4646533	373446	Former Orchard	Marenco (2002)
PPGW-02	PP-DDT-S05	4646034	373719	Former Orchard	Crowe et al. (2002)
	PP-DDT-S23	4646034	373703	Former Orchard	Current Study
	PP-DDT-S24	4646026	373702	Former Orchard	Current Study
PPGW-03	OC SS05	4645594	374042	Former Orchard	O'Connor + Assoc. (2001)
	SHPLT1Y02-1	4645589	374030	Former Orchard	Crowe (2002), pers. comm.
	SHPLT1Y02-2	4645584	374029	Former Orchard	Crowe (2002), pers. comm.
	SHPLT1Y02-3	4645589	374029	Former Orchard	Crowe (2002), pers. comm.
	SHPLT1Y02-4	4645588	374032	Former Orchard	Crowe (2002), pers. comm.
	SHPLT1Y02-5	4645586	374027	Former Orchard	Crowe (2002), pers. comm.
PPGW-04	OC-SS08	4644937	374348	Former Orchard	O'Connor + Assoc. (2001)
	AOPLT1Y02-1	4644913	374322	Former Orchard	Crowe (2002), pers. comm.
	AOPLT1Y02-2	4644911	374329	Former Orchard	Crowe (2002), pers. comm.
	AOPLT1Y02-3	4644908	374326	Former Orchard	Crowe (2002), pers. comm.
	AOPLT1Y02-4	4644913	374327	Former Orchard	Crowe (2002), pers. comm.
	AOPLT1Y02-5	4644915	374325	Former Orchard	Crowe (2002), pers. comm.
PPGW-05	OC-SS10	4644653	374302	Former Orchard	O'Connor + Assoc. (2001)
	PP-DDT-S25	4644652	374307	Former Orchard	Current Study
	PP-DDT-S26	4644668	374320	Former Orchard	Current Study
PPGW-06	PP-DDT-S02	4645068	374114	Former Orchard	Crowe et al. (2002)
	PP-DDT-S27	4645078	374076	Former Orchard	Current Study
	PP-DDT-S28	4645076	374077	Former Orchard	Current Study
PPGW-07	OC-SS04	4645820	373934	Former Orchard	O'Connor + Assoc. (2001)
	PP-DDT-S29	4645901	373829	Former Orchard	Current Study
	PP-DDT-S30	4645900	373833	Former Orchard	Current Study
PPGW-08	OC-SS09	4644710	374446	Former Orchard	O'Connor + Assoc. (2001)
	PP-DDT-S31	4644721	374459	Former Orchard	Current Study
	PP-DDT-S32	4644722	374458	Former Orchard	Current Study

Table 8. (cont.).

Corresponding GW Sample	Sample I.D.	UTM's – NAD 83 Northing	UTM's – NAD 83 Easting	Land Use Area	Collected This Study
PPGW-09	PP-DDT-S01	4646246	373600	Natural Marsh	Crowe et al. (2002)
	CHM-1	4646452	373628	Natural Marsh	Marenco (2002)
	CHM-2	4646454	373643	Natural Marsh	Marenco (2002)
	CHM-3	4646456	373636	Natural Marsh	Marenco (2002)
	CHM-4	4646459	373641	Natural Marsh	Marenco (2002)
	CHM-5	4646463	373629	Natural Marsh	Marenco (2002)
	CHM-6	4646464	373636	Natural Marsh	Marenco (2002)
	CHM-7	4646465	373645	Natural Marsh	Marenco (2002)
	CHM-8	4646467	373626	Natural Marsh	Marenco (2002)
	CHM-9	4646468	373642	Natural Marsh	Marenco (2002)
	CHM-10	4646470	373631	Natural Marsh	Marenco (2002)
PPGW-10	RR-14	4645451	374003	Former Orchard	Russell + Haffner (1997)
	PP-DDT-S33	4645676	374025	Former Orchard	Current Study
	PP-DDT-S34	4645682	374020	Former Orchard	Current Study
PPGW-11	M-1	4646614	373526	Former Orchard	Marenco (2002)
	M-2	4646613	373527	Former Orchard	Marenco (2002)
	M-3	4646613	373534	Former Orchard	Marenco (2002)
	M-4	4646612	373539	Former Orchard	Marenco (2002)
	M-5	4646609	373534	Former Orchard	Marenco (2002)
	M-6	4646610	373543	Former Orchard	Marenco (2002)
	M-7	4646603	373528	Former Orchard	Marenco (2002)
	M-8	4646604	373539	Former Orchard	Marenco (2002)
	M-9	4646604	373540	Former Orchard	Marenco (2002)
	M-10	4646596	373540	Former Orchard	Marenco (2002)
PPGW-12	PP-DDT-S07	4644928	374237	Natural Dune	Crowe et al. (2002)
	PP-DDT-S08	4645582	373808	Natural Dune	Crowe et al. (2002)
	PP-DDT-S09	4645789	373715	Natural Dune	Crowe et al. (2002)
	PP-DDT-S10	4646137	373514	Natural Dune	Crowe et al. (2002)
	PP-DDT-S11	4646506	373342	Natural Dune	Crowe et al. (2002)
	PP-DDT-S12	4644750	373975	Natural Dune	Crowe et al. (2002)
	PP-DDT-S13	4644478	374018	Natural Dune	Crowe et al. (2002)

modelling efforts aimed at elucidating the principal mechanisms controlling the migration of DDT from surface to groundwater within PPNP. Three study sites within former orchard areas of the park were selected based on, first, elevated concentrations of Total DDT within shallow soil and groundwater identified during the July 2002 field program, and second, varying depths to the water table. The three chosen study sites were within Camp Henry Orchard (CHO), Sleepy Hollow Orchard (SHO) and Anders Orchard (AO) (Figure 5). At each site a 0.75 m by ~1.5 m soil sampling pit was dug from surface to the water table. Samples at incremental depths were collected for laboratory analysis of soil and hydrologic properties. A groundwater sample was collected immediately below each pit and labelled CHO-PIT1-GW, SHO-PIT1-GW, and AO-PIT1-GW.

Table 9. Soil and groundwater pits sampled during May 2003.

Sample I.D.	Corresponding 2002 GW Sample	UTM's – NAD 83 Easting	UTM's – NAD 83 Northing	Land Use Area
CHO-PIT1-GW	PPGW-01	373386	4646581	Former Orchard
SHO-PIT1-GW	PPGW-03	374020	4645591	Former Orchard
AO-PIT1-GW	PPGW-05	374305	4644675	Former Orchard

All study sites were located using a handheld Garmin 12XL global positioning system (GPS). The positions were acquired in a NAD 83 datum and display the position in universal transverse mercator (UTM) mode. The position of the south western corner of each soil pit was then recorded, which constituted one end member of the pit face from which soil samples were extracted. All samples were extracted in vertical profiles near the south-west corner of each of the 3 soil pits, within a few centimeters of the recorded GPS co-ordinates.

The elevation of the ground surface at the 12 groundwater sampling sites and the three soil sampling pits were obtained from the 1987 topographic maps 1:3,000 Point Pelee National Park 1:3,000 Map Series. Elevations were interpolated from the contour lines, having a contour interval of 0.5 m, which are more accurate than GPS elevations.

2.1.2 Soil Sampling Techniques and Pit Excavation:

All soil collected during July 2002 for analysis of DDT was sampled using the following procedure. Latex gloves were worn at all times and changed frequently to ensure no cross-contamination of samples occurred. A stainless steel trowel, rinsed with a 50/50 mixture of residue analysis grade hexane/acetone, was used to first remove vegetation and organic debris from the ground surface, and then obtain the uppermost 2 - 3 cm of mineral soil. The trowel was rinsed with a 50/50 mixture of residue analysis grade hexane/acetone before each sample was collected to ensure all DDT from the previous sample was removed. The soil was placed in 75 mL VWR® pre-rinsed amber jars certified for organochlorine pesticide analysis. All jars were rinsed immediately before use with the same 50/50 solution of hexane and acetone and allowed to dry. The soil was deposited in the jar and covered with aluminum foil that had been rinsed with the hexane/acetone solution to ensure the sample did not make contact with the plastic lid. The samples were labeled and stored for a maximum of one week prior to submission to Environment Canada's National Laboratory for Environmental Testing (NLET) in Burlington, Ontario for organochlorine pesticide analysis.

During May of 2003, each pit was dug, samples taken and the pit refilled within a 12 hour period, as follows. The overlying grass was skimmed from the surface, set aside and the bulk of the soil was removed from rectangular areas of approximately 75 cm by 150 cm to a depth where soil became moist (i.e., the capillary fringe). Digging, to define the depth to the water table, was continued only at the end of the pit opposite to the intended sampling face. Soil samples were then obtained at opposite end of the pit to eliminate the possibility that the digging process would contaminate the groundwater or soil. Vertical samples were collected for the following analyses: (1) DDT concentrations; (2) organic carbon content; (3) organic matter content; (4) grain size analysis; (5) gravimetric and volumetric soil moisture; and (6) bulk density. Each of the DDT and bulk soil samples was extracted from a 2 - 3 cm depth interval and roughly 10 cm by 10 cm horizontal area. All samples for each analysis type were taken immediately below one another, forming a series of vertical profiles. The samples were separated laterally by a maximum of 15 cm and the sampling interval with depth was varied according to field observed conditions to target different soil horizons. A more frequent sampling interval was adopted in the organic rich zone near the surface, with less frequent sampling from the bottom of the organic rich layer to the water table. Additional samples were collected to characterize features of interest as they were observed in the soil profile. The samples collected for each type of analysis and the depths of sampling are presented in Table 10.

A total of twenty-seven 60 mL soil samples were collected from the three sampling pits for pesticide analysis; 14 from the CHO pit, 6 from the SHO pit, and 7 from the AO pit. Prior to sampling, a stainless steel trowel was rinsed with a 50/50 mixture of residue analysis grade hexane/acetone. The trowel was inserted horizontally into the soil profile to yield a sample from a discrete vertical interval of 2 - 3 cm, which was placed in a labelled pre-rinsed amber jar and capped with aluminum foil and the lid. Subsequent samples were collected immediately below one another and the samples were stored in a cool place for a maximum of one week prior to being frozen awaiting analysis at NLET.

Table 10. Samples collected and the sampling intervals at soil sampling pits.

Type of Analysis	Sample Size	Sampling Depths (cm)		
		CHO	SHO	AO
DDT	60 mL	10, 20, 30, 40, 50, 60, 80, 100, 120, 140, 60, 180, 200	0, 10, 20, 30, 40, 60	0, 10, 20, 30, 40, 60, 80
%O.C.	15 mL	10, 20, 28, 30, 40, 50, 60, 70, 80, 90, 100, 110, 120, 130, 140, 150, 160, 170, 180, 190, 200	0, 10, 20, 30, 40, 50, 60, 70, 80	0, 10, 20, 30, 40, 50, 60, 70, 80, 90, 100
%O.M.	100 - 150 g	10, 20, 30, 40, 50, 60, 80, 100, 120, 140, 160, 180, 190, 200	10, 20, 30, 40, 60, 80	10, 20, 30, 40, 60, 80, 90
B.D. / V.S.M. / G.S.M.	60 cm^3	10, 20, 30, 50, 80, 120, 160, 200	10, 20, 30, 40, 60	10, 20, 30, 40, 60, 80
Porosity	60 cm^3	10, 20, 30, 50, 80, 120, 160, 200	10, 20, 30, 40, 60	10, 20, 30, 40, 60, 80
Particle size analysis	100 - 150 g	10, 20, 30, 40, 50, 60, 80, 100, 120, 140, 160, 180, 190, 200	10, 20, 30, 40, 60, 80	10, 20, 30, 40, 60, 80, 90

An additional 41 samples were collected in labeled 15 mL vials from the three detailed sampling sites for organic carbon analysis; 21 samples from the CHO pit, 9 from the SHO pit and 11 from the AO pit. Each vial was pressed into the soil profile at the pre-determined depth, removed and the cap was replaced. Samples were stored in a cool place awaiting analysis at NLET.

Nineteen core samples of 60 cm^3 were collected from three study locations using stainless steel coring rings, which were approximately 3.3 cm height and 4.8 cm inside diameter with one end beveled to ease sample collection. These samples were to be used in the determination of gravimetric/volumetric soil moisture and bulk density. The samples were wrapped in Saran Wrap at the time of sample collection and inserted in labelled Ziploc bags awaiting analysis at the McMaster University laboratory.

Additional bulk sediment samples were collected from the excavated soil pits at 10 cm intervals near the ground surface and at 20 centimetre intervals deeper in each profile for use in organic matter analysis and grain size analysis. In total, 27 bulk samples were collected; 14 from the CHO pit, 6 from the SHO pit and 7 from the AO pit. Samples were returned to the McMaster University laboratory and analyzed.

2.1.3 Groundwater Sampling:

Once the site had been located, the vegetation overlying the groundwater sampling point was removed and set aside. Each of the groundwater samples collected during July 2002 used a temporary well technique, whereby a borehole was dug using a 10-inch manual post hole digger from the ground surface to a depth of approximately 20 - 50 cm above the water table. Digging was stopped based on observed soil moisture conditions and did not penetrate more than a few centimetres below the top of the capillary fringe. Boreholes were not dug to the water table in order to prevent potentially contaminated surficial soil from reaching the groundwater table and contaminating samples. All sampling equipment was rinsed with a 50:50 solution of residue analysis grade n-hexane and acetone to remove any traces of organic contaminants from the apparatus prior to sampling. Latex gloves were worn at all times and changed frequently to ensure no cross-contamination of samples occurred. A stainless steel drive point was driven to approximately 0.25 - 0.50 m below the water table, the sampling point protector was retracted 10 - 15 cm to expose the well screen and facilitate extraction of the groundwater sample through 1/4 – inch Teflon tubing using a Masterflex Model 07571-00 peristaltic pump. A 20 litre groundwater sample was collected instead of traditional one litre samples in order to lower the detection limit of the DDT analyses to the ng/L range from the μg/L range. This allowed for a much more accurate quantification of DDT concentrations in groundwater, as DDT is typically present in the sub-microgram range.

During the 2003 sampling, once the depth of the water table had been located, the peristaltic pump tubing and temporary stainless steel drive point assembly were cleaned with a 50/50 mixture of residue analysis grade hexane and acetone in order to remove any pre-existing organic compounds from the apparatus. A new piece of Teflon tubing and pump tubing was used for each sample. The drive point was subsequently driven to approximately 10 cm below the known level of the water table and retracted 5-7 cm to expose the screen through which samples were drawn. The Masterflex Model 07571-00 peristaltic pump was turned on at a flow rate of 5 mL/min to develop the well and sampling was begun after 1-2 minutes of pumping, or when the groundwater being pumped was observed to be free of particulate matter. The 4 L amber glass bottles were pre-rinsed in the laboratory according to the standard protocol outlined by NLET Container Washing Procedure Method #9 (NLET, 2002). Samples were collected in five VWR Trace-clean amber bottles certified for organochlorine pesticide residue analysis. The bottles were 4 litres in size and samples were collected immediately below the profile from which soil samples were to be extracted, yielding a total of 20 L of groundwater from each of the three sites. As each labeled bottle became full, aluminum foil rinsed with hexane/acetone was placed over the top of the bottle, the bottle was capped and Parafilm was used to seal the bottle. No air space remained at the top of each bottle. Each of the five bottles per sampling site was filled until 20 L of groundwater had been extracted when the drive point was removed such that soil sampling could be undertaken.

The bottles were labeled and stored for a maximum of four days at room temperature before submission to the National Laboratory for Environmental Testing, Environment Canada, Burlington, Ontario, for analysis.

2.1.4 Depth to Water Table Measurements:

The depth from surface to the water table was obtained each time a groundwater sample was extracted. The following method was used during the July 2002 sampling program. Once the groundwater sample had been extracted, the manually augered hole was deepened until ponded groundwater was observed. This ponded groundwater was allowed to equilibrate for a minimum of 15 minutes. The water table depth was measured by lowering a measuring tape down the hole until it reached the water table. This yielded a depth to the water table for each of the 16 groundwater samples.

During 2003 detailed pit sampling, the depth to groundwater was obtained by digging to the water table at the end of the pit opposite that from which soil and groundwater sampling would be conducted. Again, ponded water was permitted a minimum of 15 minutes to equilibrate before a measurement of the distance from surface to groundwater was made using a measuring tape. This procedure was repeated at each of the three soil pits, giving a total of three depths to the water table in 2003.

The elevations of the ground surface at each of the groundwater sampling sites and the three soil sampling pits were estimated from the topographic maps, with a 0.5 metre contour interval, of PPNP (Point Pelee National Park 1:3,000 Map Series, 1987). Using UTM coordinates measured in the field, the sites were plotted on the maps, and the ground surface elevations were interpolated from the contour lines

Additional water table well data was obtained from three well transects extending across the western barrier bar at PPNP; Park Gate transect, Northwest Beach transect and Camp Henry transect. These wells, which were installed in 1994 and have been monitored monthly since that time, were used to characterize groundwater flow within the barrier bars (Crowe et al., 2004). The long-term water levels from wells located along the Camp Henry transect provided information on seasonal and annual trends in water table fluctuations within PPNP for the current study.

2.1.5 Hydraulic Conductivity Measurements:

Measurements of in-situ field saturated hydraulic conductivity were made using a model 2800KI Guelph Permeameter manufactured by Soilmoisture Equipment Corp. It is a constant-head device that operates on the Mariotte siphon principle and provides a quick and simple method to calculate hydraulic conductivity in the unsaturated zone in the field. After each of the three pits had been excavated and the samples of groundwater and soil had been taken, hydraulic conductivity measurements were made at the end of the pit opposite the sampling face to eliminate the possibility that the soil profile had been disturbed. The measurements were taken approximately 50 centimetres from the edge of the pit to ensure a representative reading. After assembling the Guelph permeameter and the soil auger, a hole was augered to the desired depth below surface and sized properly with the sizing auger attachment. The well prep brush was then used to remove any smear layer present within the well and the permeameter was mounted on the tripod to provide support. Before filling the reservoir and making measurements, the reservoir valve was rotated to the 12 o'clock position that activated both the inner and outer reservoirs. The permeameter was then filled with water using the plastic water container and hose attachment provided and the fill plug was replaced in the filling hole. Subsequently, the permeameter was lowered into the prepared well hole and the water outlet tip was rested on the bottom of the hole, taking care not to disturb the sides of the open well. For deep measurements, the tripod was not necessary and thus, the permeameter was held in a vertical position using only the tripod bushing.

The air inlet tip was then slowly raised using the upper air tube to the 5 cm marking on the well head scale to achieve 5 cm of ponded head in the well. The water level in the reservoir was then recorded at 30 second or 15 second time intervals at the discretion of the operator to allow for a sufficient number of observed water level measurements for each trial. Repeated measurements were made until a constant rate of fall over three consecutive readings was achieved, or the water within the reservoirs was depleted. The upper air tube was then moved to the zero position to stop flow and the reservoir was then refilled as described above and the well was deepened for the following measurement. Field saturated hydraulic conductivity (K_{fs}) was calculated using the one ponded-height analysis technique (Elrick et al., 1989) using:

$$K_{fs} = \frac{Q}{\frac{2\pi H^2}{C} + \pi a^2} \tag{8}$$

where: $Q = R_1 \times A$ (9)

$$C = \left[\frac{H/a}{2.074 + 0.093H/a} \right]^{0.754} \tag{10}$$

and where Q is the volumetric flux of water (cm^3/s), H is the height of ponded water in the well (cm), C is the dimensionless well shape factor, a is the radius of the well (cm), R_l is the steady-state rate of fall of water (cm/s), and A is the area of soil through which infiltration of water takes place (cm^2). The two-ponded height method was not used as additional encapsulation of air within the soil adjacent to the well has been shown to substantially reduce the seconded ponded head measurements and can result in a negative K_{fs} (Elrick et al., 1989).

Several permeameter readings were taken with depth at each soil pit, producing a total of 14 measurements; seven at CHO pit, three at SHO pit, and four at AO pit. Readings were made beginning with the shallowest depth and after each measurement, the well was deepened to the required depth, where a new measurement was made. Because the Guelph Permeameter is only capable of extending 75 cm below the surface, prior to making readings below 60 cm the soil near the ground surface was excavated. During the excavation of the surficial soil, the soil auger was placed in the hole to prevent backfilling of the well. Care was taken to ensure that the soil was not disturbed and that excavation was kept to a minimum. Following the last reading, all excavated soil was placed back into the pit and the surficial vegetation replaced.

2.2 Laboratory Methods:

2.2.1 Groundwater Analysis for DDT, DDE and DDD:

Groundwater samples were stored in a cool location and submitted for analysis within 4 days of sample collection. After the groundwater samples were delivered to Environment Canada's National Laboratory for Environmental Testing (NLET), samples were analysed according to NLET Method Number 03-3251 (NLET, 2002). The method was modified to analyse 20 litre samples instead of the 1 litre samples normally used in order to lower instrument detection limits for each compound (Table 11). Extraction of organochlorines from the groundwater samples was performed using a Goulden Large Volume Extractor and 250 mL of dichloromethane at a feed rate of 500 mL/minute. Each sample maintained contact with the dichloromethane in the mixing chamber for about 4 minutes, on average. The extract was then dried, concentrated, cleaned up and fractionated on a 3% (w/w) deactivated silica gel column. It was then reconcentrated to a final volume of 1 mL prior to analysis. Dual column capillary gas liquid chromatography with dual electron capture detectors was used for quantification of DDT and Dieldrin.

Table 11. NLET detection limits (IDL) for 1 L and 20 L water and soil analyses.

	***o,p'*-DDT**	***p,p'*-DDT**	***o,p'*-DDE**	***p,p'*-DDE**	***o,p'*-DDD**	***p,p'*-DDD**
1-Litre IDL (ng/L)	0.75	1.30	-	1.28	-	2.24
20-Litre IDL (ng/L)	0.15	0.17	0.88	0.08	0.88	0.38
Soil IDL (ng/g)	4.85	2.07	0.29	2.25	0.58	0.76

2.2.2 Soil Analyses for DDT, DDE and DDD

Each of the DDT soil samples were analyzed at the National Laboratory for Environmental Testing (NLET) following NLET Method Number 03-3751 (NLET, 2003; Environment Canada, Burlington, Ontario) for analysis of organochlorine pesticides in sediment samples. The analysis was modified from standard protocol to include the *o,p'*- and *p,p'*- isomers of DDT, DDE and DDD. Each 20 gram wet sediment sample was ultrasonically extracted using a 1:1 mixture of pesticide grade acetone and hexane. The concentrated extract was partitioned with water and back-extracted with dichloromethane. The combined extract was then concentrated, cleaned up and fractionated on a 3% (w/w) deactivated silica gel column. The sample was then reconcentrated to a final volume of 10 mL prior to analysis. Dual column capillary gas liquid chromatography with electron capture detectors was used for analysis of organochlorines, typically yielding detection limits between 1 and 5 ng/g.

2.2.3 Gravimetric Soil Moisture

The gravimetric soil moisture is expressed as mass of water per unit mass of dry soil. Determination of gravimetric soil moisture, volumetric soil moisture and bulk density was carried out using soil cores obtained from an undisturbed vertical profile from the ground surface to the water table on one face of a dug soil pit using the most common procedure as outlined in Methods of Soil Analysis – Part 1 (Klute, 1986). In the laboratory, the samples were removed from the coring rings and placed in previously weighed and labelled aluminum dishes for drying. Wet sample weights were recorded and samples were oven dried for 24 hours at 105°C and placed in desiccators containing activated calcium chloride desiccant to cool. All sample weights were determined using the same Mettler Toledo PG5002-S Delta-Range® Balance and samples were dried in a Fisher Scientific Isotemp Drying Oven. The samples were then reweighed and the percent gravimetric soil moisture (θ_g) calculated as:

$$\theta_g = \left(\frac{M_{water}}{M_{dry}} \right) x100 \qquad (11)$$

where M_{water} is the mass of water in the wet sediment and M_{dry} is the mass of the oven dried sample (Klute, 1986).

2.2.4 Volumetric Soil Moisture

Using the same 19 soil samples as used to determine gravimetric soil moisture and knowing the volume of the coring rings, the volumetric soil moisture (θ_v) was determined using the following calculation (Klute, 1986):

$$\theta_v = \left(\frac{V_{water}}{V_{soil}} \right) x100 \qquad (12)$$

where V_{water} is the volume of water in the wet sample and V_{soil} is the volume of the core sample (Klute, 1986). The volumetric soil moisture represents the volume of water present in a given volume of soil. The wet soil samples were placed in clean, tared and labeled aluminum weighing dishes and dried for 24 hours at 105°C and reweighed after cooling in desiccators. Using cores of a known volume of 60 cm^3, the percent volumetric soil moisture was calculated for each sample.

2.2.5 Bulk Density

Bulk density is used as an indication of soil structure and is defined as the mass of dry soil per unit volume, which includes solid mineral matter, organic matter and pore space. Bulk density (ρ_B) was calculated for the same 19 soil core samples using the following equation (Klute, 1986):

$$\rho_B = \left(\frac{M_{dry}}{V_{soil}} \right) \tag{13}$$

where M_{dry} is the mass of oven dried soil and V_{soil} is the volume of the core sample. The mass of oven dried soil was obtained during gravimetric soil moisture determination and the known sample volume is 60 cm^3.

2.2.6 Organic Matter Content by Loss on Ignition

Organic matter loss on ignition was determined using the method described by Sparks (1996). Crucibles were initially placed in a Fisher Scientific Isotemp muffle furnace for two hours at 550°C to remove any organic matter residues and cooled in desiccators. Once labeled, the crucibles were weighed and filled with between 100 and 150 grams of sediment and placed in the drying oven at 105° C for 24 hours to remove any soil moisture. Samples were then removed from the oven, placed in desiccators to cool and reweighed. They were then placed in the muffle furnace at 550° C for 16 hours to burn any organic matter contained within the samples. After cooling in desiccators, the samples were once again weighed and the percent organic matter (*%OM*) determined by:

$$\%OM = \left(\frac{M_{105} - M_{550}}{M_{105}}\right) x100 \qquad (14)$$

where M_{105} is the mass of dried soil and M_{550} is the mass after burning off the organic matter in the furnace. Each soil sample was retained for later use in grain size analysis.

Organic carbon (*%OC*) content of the same soil samples was calculated using the equation developed by Olsen and Davis (1990):

$$\%OC = \frac{\%OM}{1.724} \qquad (15)$$

where *%OM* is the percent organic matter content as determined above.

2.2.7 Particle Size Analysis

Mechanical dry sieving was used to determine the grain size distribution for 27 samples at each of the three sites; 14 at the CHO pit, 6 at the SHO pit, and 7 at the AO pit. Loose sediment samples were collected at intervals of 10 cm near the surface and 20 cm at depth, with additional samples collected where features of interest were seen in the soil profile. Sub samples of between 100 and 150 grams of the loose soil samples were oven dried and organic matter was removed in the muffle furnace during the quantification of organic matter by loss on ignition. These same samples were processed by mechanical sieving using a nest of 10 six inch diameter stainless steel sieves of 2000, 1400, 1000, 710, 500, 355, 180, 90, 45 and 20 μm sizes, as well as a bottom pan.

Each sample was weighed prior to sieving, placed in the nest of sieves and shaken for 10 minutes on a Humboldt Testing Equipment H-4325 mechanical sieve shaker that had been secured to the laboratory bench. The fraction of sediment trapped within each sieve *(% Caught)* was carefully transferred to pre-weighed weighing paper and the mass recorded. By adding the masses of each size fraction, the total mass that passed through the sieve nest was calculated and the percent caught by each sieve was determined using the following equation (Klute, 1986):

$$\% Caught = \left(\frac{W_s}{W_t} \right) x100 \tag{16}$$

where W_S is the mass of soil caught in each sieve, and W_T is the total mass of soil that passed through the nest of sieves. The cumulative percent passing was calculated using:

$$\text{Cumulative} \% Pas \sin g = X - \% Caught \tag{17}$$

for each sieve, where X is the percent passing from the sieve above (100% initially). The cumulative percent passing was plotted against the grain diameter on a log scale to produce a grain size distribution curve. The % sand (2 mm to 50 μm), % silt (50 μm to 20 μm) and % clay (< 20 μm) were calculated from the data. The boundary between silt and clay was defined as 20 μm instead of 2 μm due to a finer sieve being unavailable.

2.2.8 Porosity

Through the measurement of bulk density of each of the core samples and the estimation of particle and organic matter density, the porosity (η) of each of the core samples was calculated as follows (Klute, 1986):

$$\eta = 1 - \left[\frac{\rho_B}{(f_{MM} \times \rho_{MM}) + (f_{OM} \times \rho_{OM})} \right] \times 100 \qquad (18)$$

where ρ_B represents the bulk density of the soil, f_{MM} represents the mass fraction of mineral matter and f_{OM} is the mass fraction of organic matter, ρ_{MM} represents the particle density of mineral matter and ρ_{OM} is the density of organic matter. The density of mineral matter was assumed to be 2.65 g/cm^3 and the density of organic matter was assumed to be 1.6 g/cm^3 (Brady and Weil, 2002).

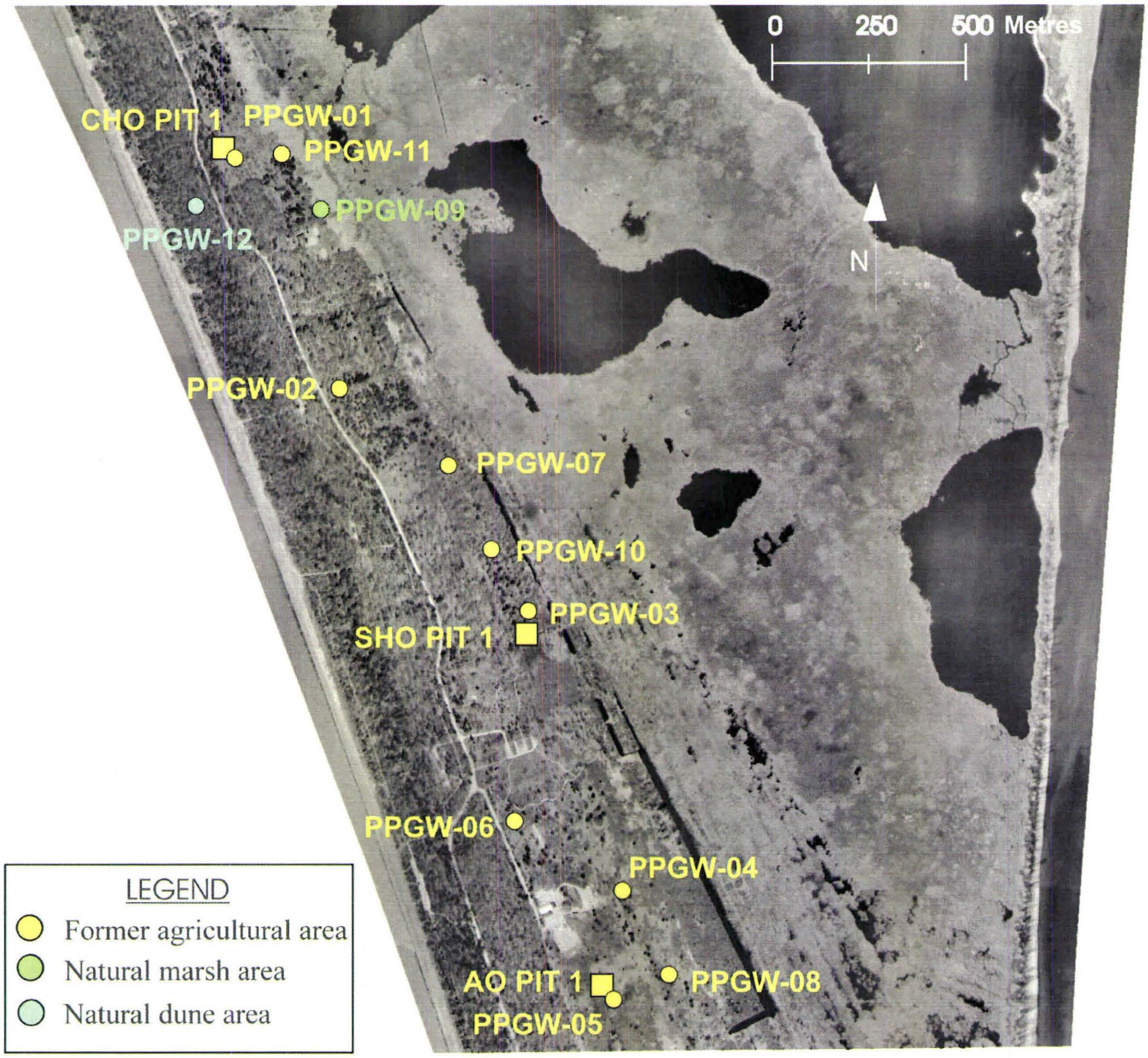

Figure 5. Location of groundwater sampling locations (circles) and detailed soil sampling pits (squares) sampled during this study.

CHAPTER 3: FIELD AND LABORATORY RESULTS AND DISCUSSION

Chapter 3 presents the results and the interpretation of the physical, hydrological, and chemical analyses that were undertaken in the laboratory and in the field as discussed in Chapter 2. The results of the analyses include concentrations of the DDT compounds in soil and groundwater, physical properties of the soil, and hydrogeological characteristics of the study sites. The interpretation of these analyses provides an overview of the spatial distribution of DDT in soil and groundwater, the relationship between concentrations of DDT in surficial soil and at the underlying water table, and the processes affecting the fate and migration of DDT within the subsurface.

3.1 Soil Classification

The type of soil depends on parent material, mineral content, organic matter content, grain-size distribution, extent of soil development, and land-management history. Photographs of the soil profiles at the CHO, SHO and AO sampling pits and their interpreted soil horizons are presented in Figure 6.

At CHO, a 7 cm thick dark brown Of-fibric soil layer consisting of slightly decomposed organic matter and numerous roots is present, underlain by a 30 - 35 cm thick very dark brown Ah horizon consisting of well-sorted medium-grained sand and abundant roots of varying thickness. Extending from 30-35 cm to 80-90 cm is a medium brown Bm horizon consisting of a well-sorted medium sand. Infrequent tap roots extend over 1 m into the profile. The C horizon, of unknown thickness, represented the bottom layer of the profile and consisted of light brown well-sorted medium to coarse grained aeolian sand. The water table was located at 2.00 metres below ground surface and the capillary fringe was observed to be approximately 20 cm thick.

At SHO, a 5 cm thick dark brown Of-fibric layer consisting of moderately decomposed organic matter and abundant fibrous plant roots is underlain by a 18 cm thick very dark brown Ah horizon consisting of medium grained well-sorted aeolian sand and numerous plant roots. Several snail shells were noted at ground surface, indicating somewhat wetter surface conditions. Extending from 20 cm to 75 cm is the mottled brown and grey weakly gleyed Bmgj horizon consisting of well-sorted medium to coarse grained sand and very few roots that extend up to a maximum of 5 cm into the top of the Bmgj horizon. The water table was located at 0.75 metres below ground surface and the capillary fringe was observed to be 15 cm thick.

At AO, a 5 cm thick Om-fibric layer consisting of slightly decomposed organic matter and numerous *Equisetum* roots represents the uppermost segment of the 15 cm thick Ah horizon of medium-dark brown, well-sorted sand. Beneath that, the red-brown and grey gleyed Bmgj horizon extended from 20 cm to the water table and consisted of infrequent thick *Equisetum* (herbaceous perennial plant) rhizomes penetrating to the bottom of the profile. At the water table, another horizon of unknown vertical extent was encountered consisting of well-rounded, moderately sorted pebbles up to 3 mm in length. The water table was located at 0.88 metres below ground surface and the capillary fringe was 13 cm thick.

The soil observed in the three test pits was classified according to the Canadian System of Soil Classification. At all three soil pit excavation sites, there exists an Ah horizon greater than 10 cm thick underlain by a Bm horizon that is more than 5 cm thick and finally, a C horizon of undetermined thickness at all three profiles (CHO, SHO, AO), meeting the requirements of the Brunisolic Soil Order. Because each of the soil profiles have an Ah horizon greater than 20 cm thick, the criteria for classification as a Melanic Brunisol are met in all three locations. Further, at both SHO and AO, an indistinct gleyed

Bmgj horizon was present below the Ah horizon, leading to their classification as Gleyed Melanic Brunisols. Thus, CHO was classified as a Melanic Brunisol and both SHO and AO were classified as Gleyed Melanic Brunisols.

The soil classifications described above are contradictory to the profile described by the 1938 Soil Survey of Essex County Report No. 11 (Richards et al., 1949), which classifies the soils throughout the study area as Eastport sands belonging to the Regosolic Soil Order. Based on the 1938 soil survey and observations within the Ah-horizon, Marenco (2002) referred to the soil as a humic Regosol (Regosolic Soil Order). Badley (2003) dug a 1.5 metre deep by 3 metre long trench and classified the soil in the vicinity of CHO as a Melanic Brunisol, which is in agreement with this study.

3.2 Soil Texture and Structure

3.2.1 Grain size

From visual inspection alone, the soils at the three field sites appeared similar in texture. Particle-size analyses were performed on samples obtained from soil pits dug from ground surface to the water table at CHO, SHO and AO. Samples were obtained at 10 cm intervals from ground surface to 40 cm depth, and at 20 cm intervals below that to the depth of the water table. The grain-size distributions for the CHO, SHO and AO sampling pits are tabulated in Table 12 and plotted in Figure 7. The percent sand varies between 96.40% and 99.31%. The grain size distribution for sand above 80 cm at SHO, above 90 cm at AO, and throughout the 200 cm profile at CHO, represents that of

Table 12. Results of particle size analysis, % organic matter and % organic carbon with depth at CHO, SHO and AO as determined from sampling during May 2003.

Sample Name	Horizon	Depth (cm)	% Sand	% Silt	% Clay	%OM (LOI)	%OC (from %OM)
CHO-PIT1-010	Of-Ah	10	96.404	2.914	0.682	3.130	1.80
CHO-PIT1-020	Ah	20	96.745	2.602	0.653	2.786	1.60
CHO-PIT1-030	Ah	30	97.993	1.480	0.527	0.926	0.53
CHO-PIT1-040	Bm	40	98.611	1.077	0.311	0.635	0.36
CHO-PIT1-050	Bm	50	99.004	0.803	0.193	0.551	0.32
CHO-PIT1-060	Bm	60	99.076	0.802	0.122	0.492	0.28
CHO-PIT1-080	Bm	80	99.172	0.706	0.122	0.509	0.29
CHO-PIT1-100	C	100	99.055	0.842	0.103	0.506	0.29
CHO-PIT1-120	C	120	99.306	0.629	0.065	0.442	0.25
CHO-PIT1-140	C	140	99.224	0.702	0.074	0.403	0.23
CHO-PIT1-160	C	160	99.293	0.633	0.074	0.473	0.27
CHO-PIT1-180	C	180	99.300	0.640	0.060	0.493	0.28
CHO-PIT1-190	C	190	99.196	0.708	0.096	0.485	0.28
CHO-PIT1-200	C	200	99.242	0.704	0.054	0.473	0.27
Mean			98.687	1.089	0.224	0.879	0.505
SHO-PIT1-010	Of-Ah	10	97.264	2.205	0.532	1.502	0.86
SHO-PIT1-020	Ah	20	97.910	1.583	0.507	1.127	0.65
SHO-PIT1-030	Bm	30	98.600	1.090	0.310	0.814	0.47
SHO-PIT1-040	Bm	40	98.564	1.152	0.284	0.771	0.44
SHO-PIT1-060	Bm	60	98.764	1.006	0.231	0.787	0.45
SHO-PIT1-080	Bm	80	98.051	1.491	0.459	0.868	0.50
Mean			98.192	1.421	0.387	0.978	0.562
AO-PIT1-010	Of-Ah	10	97.531	2.104	0.365	2.168	1.25
AO-PIT1-020	Ah-Bm	20	97.830	1.798	0.372	1.076	0.62
AO-PIT1-030	Bm	30	98.238	1.448	0.315	0.730	0.42
AO-PIT1-040	Bm	40	98.487	1.269	0.243	0.697	0.40
AO-PIT1-060	Bm	60	98.995	0.872	0.133	0.454	0.26
AO-PIT1-080	Bm	80	98.841	0.988	0.170	0.542	0.31
AO-PIT1-090	Bm	90	99.089	0.787	0.124	0.656	0.38
Mean			98.430	1.324	0.246	0.903	0.519

medium-fine grained sand. The grain size distributions compare favourably to the aeolian sand in Coakley et al. (1998) who observed medium grained, well sorted sediments (unimodal) with no pebbles or shells present and a median grain size of 1-2 ϕ (0.25 - 0.45 μm). The deepest samples at SHC (80 cm) and AO (90 cm) are coarser than the rest of the profile and contain many pebbles and are likely part of the shoreface sand gravel deposited during formation of the barrier bar as described by Coakley et al. (1998).

3.2.2 Bulk density

Soil cores were collected in the field at 10 cm intervals near the surface and at greater intervals (20-40 cm) deeper in the soil profiles to facilitate bulk density measurements and calculate porosity with depth at the three soil pits. Calculated bulk density values are presented in Table 13. The bulk density profiles with depth are presented in Figure 8. Bulk density values among the three soil sampling pits range from 1.18 g/cm^3 at ground surface to 1.60 g/cm^3 at 2 m depth. Each of the three profiles show a consistent pattern from surface to depth, with low values at the surface where organic matter content is highest and a transition to higher bulk densities with depth, where the soil is primarily mineral matter and under increasing sediment loads from above. Closer to the water table, bulk densities again increase. Mean bulk densities were 1.41 g/cm^3, 1.43 g/cm^3 and 1.42 g/cm^3 at CHM, SHO and AO, respectively. These values are consistent with average bulk densities of 0.97 g/cm^3 for the Ah horizon and 1.47 g/cm^3 for the Bm horizon, reported by Badley (2003).

Table 13. Gravimetric and volumetric soil moisture contents, bulk densities, and porosity with depth at CHO, SHO and AO.

Sample Name	**Horizon**	**Depth** (cm)	**% GSM**	**% VSM**	**Bulk Density (g/cm3)**	**Porosity (%)**
CHO-PIT1-010	Ah	10	10.960	12.900	1.18	55
CHO-PIT1-020	Ah	20	11.529	14.983	1.30	50
CHO-PIT1-030	Ah	30	8.369	11.517	1.38	48
CHO-PIT1-050	Bm	50	6.037	9.000	1.49	44
CHO-PIT1-080	Bm	80	5.713	8.550	1.50	43
CHO-PIT1-120	C	120	5.675	8.150	1.44	46
CHO-PIT1-160	C	160	5.937	8.667	1.46	45
CHO-PIT1-200	C	200	20.321	32.500	1.60	40
Mean					1.42	46
SHO-PIT1-010	Ah	10	6.711	8.833	1.32	50
SHO-PIT1-020	Bmgj	20	5.779	7.867	1.36	48
SHO-PIT1-030	Bmgj	30	6.203	8.850	1.43	46
SHO-PIT1-040	Bmgj	40	6.648	9.567	1.44	46
SHO-PIT1-060	Bmgj	60	21.936	33.267	1.52	43
Mean					1.41	46
AO-PIT1-010	Ah	10	7.689	9.450	1.23	53
AO-PIT1-020	Bmgj	20	5.902	8.317	1.41	47
AO-PIT1-030	Bmgj	30	5.293	7.733	1.46	45
AO-PIT1-040	Bmgj	40	5.220	7.817	1.50	43
AO-PIT1-060	Bmgj	60	16.849	24.150	1.43	46
AO-PIT1-080	Bmgj	80	22.357	34.183	1.53	42
Mean					1.43	46

3.2.3 Porosity

The porosity of a soil determines the maximum amount of water that can be held in a given volume of soil. Porosity was calculated from organic matter content and bulk density using assumed particle densities of 1.60 g/cm^3 for organic matter and 2.65 g/cm^3 for mineral matter (Brady and Weil, 2002). Calculated porosity values for CHO, SHO and AO soil pits are also presented in Table 13 and porosity profiles are plotted in Figure 8. Porosity ranged from 55% at ground surface at CHO to 42% at the water table at AO and showed an inverse relationship with bulk density. Badley (2003) found the average porosity of the Ah horizon to be 50%, and 42.3% for the Bm horizon. The average porosities at CHO, SHO and AO are 46%, 47% and 46%, respectively, which are consistent with Badley (2003).

3.3 Soil Organic Matter

Organic matter (OM) content acts to increase the amount of water stored by a given volume of soil and also increases the number of sites available for sorption of organic molecules including pesticides in the unsaturated zone. The %OM as determined by loss on ignition and calculated percent organic carbon (OC) are listed in Table 12. The mean %OM is highest at CHO (1.16%) and lowest at AO (0.94%), ranging from 0.45% (AO, 60 cm) to 3.13% (CHO, 10 cm) for the three study sites. Within the Ah horizons (0-20 cm), the mean %OM is highest at CHO (2.96%) and lowest at SHO (1.31%). Within the B and C horizons (30 cm to bottom of pit), mean %OM is lowest at CHO (0.56%) and highest at SHO (0.84%). Badley (2003) found %OM values to range from 2.4% to 14.5% near CHO, with an average of 7.05%. The %OM profiles for CHO, SHO and AO are listed in Table 12 and presented in Figure 8. There is a sharp boundary between the Ah and the B horizons exists at both CHO and AO, while a less defined boundary was observed at SHO. In each case, the %OM was uniformly low throughout the B and C horizons.

3.4 Soil Moisture

Moisture content of a given soil controls both the rate of flow of water and solutes vertically through the soil profile and it is a factor that in part determines the rate at which a given pesticide will be metabolized by soil microorganisms and/or degraded chemically (Marenco, 2002; Guenzi and Beard, 1976; Spencer et al., 1996).

Gravimetric and volumetric soil moisture contents were determined on the same samples for which bulk density and porosity were measured and calculated. The gravimetric water contents and volumetric water contents obtained with depth are presented for the CHO, SHO and AO soil pits for May 12-14, 2003, respectively, are listed in Table 13 and presented graphically in Figure 8. Gravimetric and volumetric soil moisture profiles are quite similar in shape at all 3 soil sampling pits, with volumetric soil moisture values between 5 and 10% through much of the profile and a well-defined capillary fringe at depth. This is consistent with the similar soil textures and bulk density values reported in Tables 12 and 13, respectively. Badley (2003) found volumetric soil moisture as determined using time-domain reflectometry (TDR) to range from 3.5% to 15.9% within shallow soils near CHO, which is consistent with the present study. In the shallow portion of the three profiles, soil moisture is slightly elevated, corresponding to the organic rich Ah horizon capable of storing more water than the B horizon.

The capillary fringe was observed to be 15-20 cm thick at all three locations, with large increases in water content observed in the soil samples obtained at the water table for each of the three sites. The thinner capillary fringe at SHO is attributed to the slightly coarser nature of the soils at SHO relative to the other sampling sites. At the water table, volumetric soil moisture contents were 32.5% at CHO, 33.27% at SHO and 34.18% at AO, with corresponding porosities of 40%, 43% and 42%, respectively. The 7.5%, 9.73% and 7.82% differences between porosity and volumetric water content at the water table can be attributed to entrapped air within the system as is often the case near the water table in natural systems (Ronen et al., 1989).

3.5 Field-saturated Hydraulic Conductivity

The rate of movement of water through the unsaturated zone is ultimately determined by the field saturated hydraulic conductivity (K_{fs}) and the degree of saturation of the porous media, with water moving under the influence of hydraulic gradients. K_{fs} values were measured at the three sampling pits (CHO, SHO and AO) using a Guelph Permeameter on May 12-14, 2003. The calculated field-saturated hydraulic conductivities are tabulated in Table 14 and presented in Figure 8. K_{fs} ranged over approximately one order of magnitude from 3.44×10^{-4} cm/s to 3.47×10^{-3} cm/s among all three sites, with the lowest values at surface where organic carbon, silt and clay contents are highest. This range of values is slightly lower than previous work that reported field-saturated hydraulic conductivities of ~5×10^{-3} cm/s for the Ah horizon and ~1×10^{-2} cm/s

Table 14. Field saturated K_{fs} and log K_{fs} with depth at CHO, SHO, and AO.

Sample Name	**Horizon**	**Depth (cm)**	**K_{fs} (cm/s)**	**log K_{fs} (cm/s)**
CHO-PIT1-020	Ah	20	3.44×10^{-4}	-3.46
CHO-PIT1-040	Bm	40	2.09×10^{-3}	-2.68
CHO-PIT1-060	Bm	60	2.13×10^{-3}	-2.67
CHO-PIT1-080	Bm	80	1.67×10^{-3}	-2.77
CHO-PIT1-100	C	100	1.41×10^{-3}	-2.85
CHO-PIT1-140	C	140	3.01×10^{-3}	-2.52
CHO-PIT1-180	C	180	3.44×10^{-3}	-2.46
Log Mean (40-180 cm)			2.20×10^{-3}	-2.66
SHO-PIT1-020	Bmgj	20	1.07×10^{-3}	-2.97
SHO-PIT1-040	Bmgj	40	3.47×10^{-3}	-2.46
SHO-PIT1-060	Bmgj	60	2.45×10^{-3}	-2.61
Log Mean (40-60 cm)			2.92×10^{-3}	-2.54
AO-PIT1-020	Bmgj	20	1.04×10^{-3}	-2.98
AO-PIT1-040	Bmgj	40	1.54×10^{-3}	-2.81
AO-PIT1-060	Bmgj	60	2.48×10^{-3}	-2.61
AO-PIT1-080	Bmgj	80	1.41×10^{-3}	-2.85
Log Mean (40-80 cm)			1.75×10^{-3}	-2.76

for the Bm horizon near CHO (Badley, 2003). Large reductions in K_{fs} were observed for the lowest sampling points at SHO and AO, but not at CHO. Through comparison with volumetric soil moisture profiles, it was determined that the measurements corresponding to SHO-60 and AO-80 were taken near the capillary fringe and thus, were not obtained in unsaturated soils as required by the Guelph Permeameter method. The decrease in K_{fs} at CHO from 60 to 100 cm is also explained by the increase in bulk density over the 50 to 120 cm interval, effectively reducing porosity and resulting in a lower K_{fs}. Because K_{fs} is log-normally distributed, log-transformed K_{fs} was used for statistical analyses. The in-situ K_{fs} for the Ah horizon at all three profiles were 3.44×10^{-4} cm/s at CHO,

1.07×10^{-3} cm/s at SHO and 1.04×10^{-3} cm/s at AO. The in-situ K_{fs} of soils beneath the Ah horizon were 2.20×10^{-3} cm/s at CHO, 2.92×10^{-3} cm/s at SHO and 1.75×10^{-3} cm/s at AO. While roots were observed in all 3 soil profiles, making preferential pathways possible, the hydraulic conductivity data does not show this is occurring. Although the 3 sampling pits were between 260 and 1900 m apart, the mean K_{fs} values are essentially the same; this is expected, given the common depositional environment of the barrier bar (Coakley et al., 1998; Crowe et al., 2004).

3.6 Ground Surface Elevation & Depths to Water Table

The proximity of the water table to ground surface has two important implications on levels of DDT in soil and groundwater. First, the closer the water table is to ground surface, the shorter the distance (thickness of unsaturated zone) that DDT must leach to the water table. Second, in soils that are periodically flooded by a high water table, DDT degrades along an anaerobic pathway to DDD. However, in soils where the water table is always well below ground surface, DDT degrades aerobically to DDE (Marenco, 2002).

The elevation of the ground surface at the 12 groundwater sampling sites, and the three soil sampling pits were obtained by interpolation from the 1:3000 Point Pelee Map Series; these maps have a contour interval of 0.5 m (Table 15). Surveyed ground surface elevations presented by Marenco (2002) are consistent with interpolated elevations within CHO and at PPGW-01, PPGW-13, PPGW-11 and PPGW-09. Other groundwater sampling locations were too far from surveyed elevations to make a direct comparison.

While more expensive global positioning systems could provide better elevation estimates in open areas (no tree cover), the system used for this study was restricted to 5 to 10 metre accuracy.

The depth to the water table (Table 15) was measured concurrently with the collection of every groundwater sample obtained for a DDT analysis in order to provide a measure for assessing whether or not the distance from surface to the water table was a factor influencing DDT migration to groundwater.

Surface topography does not have a major impact on the elevation of the water table because of the high hydraulic conductivity of the sands in the barrier bars and proximity of the surface water-groundwater interface at Point Pelee. Since 1994, the difference in elevation of the water table across the barrier bar at NWRI's Camp Henry transect on any given day was never more than 25 cm and typically less than 10 cm. Hence, the depth to water table is effectively proportional to the elevation of ground surface (Crowe et al., 2004). Among the 12 groundwater sites sampled during July 2002, the shallowest depth to the water table was 0.70 m at PPGW-09 (lowest ground surface elevation of 174.9 m a.m.s.l.) which was closest to the marsh, and the deepest water table was 2.70 m at PPGW-01 (highest ground surface elevation of 176.8 m a.m.s.l.) within the area dominated by dune topography.

The depth to the water table was also measured on May 12-14 2003 during the excavation of the three soil sampling pits CHO, SHO, and AO; these pits were located within a few metres of groundwater sampling sites PPGW-01, PPGW-03 and PPGW-05, respectively, and at the same elevation (Table 15). The depths to the water table during

Table 15. Measured depths to the water table and estimated ground surface elevations for the groundwater samples sites and the three soil sampling pits.

Sampling Location	Measurement Date	Elevation of Ground Surface (m amsl)	Depth to Water Table (m)	Elevation of Water Table (m amsl)
PPGW-01	July 8, 2002	176.8	2.70	174.10
PPGW-02	July 10, 2002	176.8	2.60	174.20
PPGW-03	July 15, 2002	175.6	1.33	174.27
PPGW-04	July 17, 2002	175.8	1.25	174.55
PPGW-05	July 23, 2002	175.7	1.17	174.53
PPGW-06	July 11, 2002	176.0	1.50	174.50
PPGW-07	July 24, 2002	176.2	1.25	174.95
PPGW-08	July 23, 2002	175.4	1.18	174.22
PPGW-09	July 18, 2002	174.9	0.70	174.20
PPGW-10	July 16, 2002	175.5	1.23	174.27
PPGW-11	July 23, 2002	175.6	1.15	174.45
PPGW-12	July 22, 2002	176.3	1.85	174.45
PPGW-01-R	July 9, 2002	176.8	2.77	174.03
PPGW-02-R	July 11, 2002	176.8	2.68	174.12
PPGW-03-R	July 16, 2002	175.6	1.36	174.24
PPGW-04-R	July 18, 2002	175.8	1.30	174.50
CHO-PIT1-GW1	May 12, 2003	176.9	2.00	174.90
SHO-PIT1-GW1	May 13, 2003	175.6	0.75	174.85
AO-PIT1-GW1	May 14, 2003	175.7	0.88	174.82

May 2003 were much shallower than those measured in July 2002 because infiltration of spring snowmelt raised the water table during May 2003 which had been lowered during the previous summer by evapotranspiration. The differences in water levels from July 2002 to May 2003 were 0.70 m at CHO, 0.58 m at SHO and 0.29 m at AO.

The depth to the water table was not measured at the NWRI wells on the same days as the depth to the water table was measured at the 12 groundwater sampling sites and the three soil sampling pits. Measurements along NWRI's Camp Henry transect were obtained on June 18, 2002 giving water table elevations of 174.504 to 174.589 and on August 1, 2002, giving water table elevations of 174.258 to 174.302 m a.m.s.l. Water table elevations obtained between July 8 and July 23, 2002 at the 12 groundwater sampling sites fall within the range of the NWRI groundwater elevations. Water table measurements along the NWRI Camp Henry transect were obtained on May 5, 2003, giving elevations between 174.312 and 174.388 m a.m.s.l. Although these water table elevations are much lower than those measured at CHO, SHO and AO on May 12-14, 2003, 44.6 mm of precipitation fell between the time of the water table measurements at the NWRI wells and water table measurements at CHO, SHO and AO (Figure 4).

Because the long-term elevation of the water table near the sampling sites follows the trends the marsh, high marsh levels induce a high water table, and low marsh levels cause a low water table (Crowe et al., 2004). Between 1994 and 2004, the range of marsh surface fluctuations was about 1 metre, from 174.1 to 175.1 m a.m.s.l. (Figure 4). Marenco (2002) stated areas of the Park whose elevation are below 175.1 m a.m.s.l. (e.g., PPGW-09) have likely been flooded during periods of elevated marsh levels in the past. Marenco (2002) also suggested that because the water table is typically higher that the elevation of the marsh, it is likely that during times of high marsh levels and with the capillary fringe, soil profiles could be saturated up to 174.3 m a.m.s.l. Consequently the elevation of the marsh, it is likely that during times of high marsh levels and with the capillary fringe, soil profiles could be saturated up to 174.3 m a.m.s.l. Consequently DDT within the soil at elevations above 174.3 m a.m.s.l. predominantly follow an aerobic transformation pathway (Marenco, 2002). Conversely, if the DDT in the soil is below an elevation of 174.3 m a.m.s.l., it is likely that DDT could have undergone anaerobic transformation at times in the past, with the frequency of anaerobic periods increasing as the elevation decreases (Marenco, 2002). Thus, it is likely that an anaerobic transformation occurs during periods of high marsh levels at PPGW-09, and aerobic transformation dominates at the remainder of the sampling locations.

3.7 Statistical Analyses of Physical and Hydrological Soil Properties

To compare physical and hydrological soil properties of the three soil sampling pits, ANOVA analyses were conducted employing Tukey-Kramer tests to determine if significant differences exist among population means at the 95% level. Soil properties, including gravimetric soil moisture, volumetric soil moisture, bulk density, porosity, organic matter content, and field-saturated hydraulic conductivity were statistically compared. No significant differences were found at the 95% level of confidence between the three pairs (CHO:SHO, CHO:AO, SHO:AO). Thus, the physical and hydrological properties of the soil at the three sites were not found to be significantly different from one another.

3.8 DDT in Soil and Groundwater at PPNP

The assessment of DDT in soil and groundwater at PPNP is presented in three parts; (i) a spatial assessment of DDT in shallow soil based on the sampling program conducted during July 2002 throughout the park (sites PPGW-01 to PPGW-12) and the assessment with depth conducted at the three soil sampling pits (CHO, SHO, AO) during May 2003, (ii) a spatial assessment of DDT in groundwater based on the groundwater sampling program (PPGW-01 to PPGW-12) and at the three soil sampling pits, and (iii) an assessment of the relationship between DDT in soil and DDT in groundwater.

The assessments in soil and groundwater were conducted using concentrations of ΣDDT, ΣDDE, ΣDDD and Total DDT. Further analyses were conducted using the relative proportions of ΣDDT, ΣDDE and ΣDDD. Relative proportions were calculated as defined in Chapter 1.

3.8.1 DDT in Soils - Spatial Distribution

Prior surveys of soil contamination within PPNP have determined that the primary areas of contamination lie within former orchard land-use areas, specifically within the former Camp Henry Orchard, DeLaurier Orchard, Sleepy Hollow Orchard and Anders Orchard (Crowe et al., 2002). All soil concentrations are reported to 3 significant digits by NLET and thus, all Total DDT concentrations are reported in the same manner. Concentrations of Total DDT in the 12 shallow soil samples collected during July 2002 ranged from 1,560 to 20,100 ng/g (Table 16). The highest average concentration was

Table 16. Analytical results of DDT compounds in the shallow soil samples collected during July 2002.

Soil Sample I.D.	***o,p'*-DDT** (ng/g)	***p,p'*-DDT** (ng/g)	***o,p'*-DDE** (ng/g)	***p,p'*-DDE** (ng/g)	***o,p'*-DDD** (ng/g)	***p,p'*-DDD** (ng/g)	**Total DDT** (ng/g)
PP-DDT-S23	104	390	9.6	1,020	10.0	21.4	1,560
PP-DDT-S24	580	1,200	185	8,240	149	94.6	10,400
PP-DDT-S25	75.3	557	7.87	2,000	9.26	38.2	2,690
PP-DDT-S26	59.8	610	9.85	2,150	11.7	31.8	2,870
PP-DDT-S27	1,230	3,580	139	11,000	203	175	16,300
PP-DDT-S28	556	3,120	58.5	7,520	76.1	140	11,500
PP-DDT-S29	162	396	36.0	2,830	30.4	36.0	3,490
PP-DDT-S30	220	475	79.0	2,730	35.8	51.9	3,590
PP-DDT-S31	1,360	5,570	120	12,300	164	259	19,800
PP-DDT-S32	1,160	3,620	125	9,280	106	190	14,500
PP-DDT-S33	1,470	4,130	108	10,300	135	188	16,300
PP-DDT-S34	1,710	9,190	64.6	8,830	110	237	20,100

found within the former Camp Henry Orchard. These concentrations values and large variability are consistent with the findings of Crowe et al. (2002) and Marenco (2002), who reported concentrations of Total DDT in shallow soil in the former orchard areas ranging from 319 to 87,500 ng/g, and from 5,690 to 316,000 ng/g, respectively.

Total DDT concentrations are highly spatially variable as a result of non-uniform application rates, different degradation rates, and post-agricultural disturbances to the soil. Thus, 56 additional soil analyses previously collected within a few metres of present sites were pooled with the 12 samples discussed above, giving a combined total of 68 soil analyses, were used in the analysis of DDT characteristics in the shallow soil above the 12 groundwater sampling locations. All 68 analyses, corresponding to each of the 12 groundwater sampling sites, are presented in Table 17.

The mean soil concentrations of Total DDT at the 12 groundwater sampling sites in the former agricultural areas range from 2,700 ng/g to 79,400 ng/g, with the highest concentration at the site corresponding to PPGW-01 within the former Camp Henry Orchard (Figure 9). The mean concentration of Total DDT within the natural dune area was orders of magnitude lower (19.6 ng/g near PPGW-12) than concentrations found in the former agricultural areas. These results are consistent with Crowe et al. (2002) who noted concentrations of Total DDT in natural dune areas ranged from 4.9 ng/g to 35.5 ng/g. Thus, the natural dune area (PPGW-12) has little DDT contamination at surface even though it was less than 100 m from the most contaminated site (PPGW-01). Possible explanations for the presence of DDT found in shallow soils within the natural dune area include spray drift during application of DDT, and/or translocation of contaminated sediments by aeolian transport processes. With the exception of the natural dune site, every mean shallow soil concentration was well above OMOEE guidelines of 1600 ng/g, 1600 ng/g, and 2200 ng/g for DDT, DDE, and DDD, respectively, for residential/parkland land use (OMOEE, 1997).

Although concentrations of Total DDT are highly variable throughout PPNP, the relative proportions of ΣDDT, ΣDDE, and ΣDDD (%DDT : %DDE : %DDD) within each soil sample, provides an indication of the consistency of degradation rates and pathways throughout PPNP. %DDT and %DDE in soil at each of the 12 groundwater sampling sites (Figure 10) range from 16.0% - 54.1% and 44.2% - 82%, respectively (Table 17).

Table 17. ΣDDT, ΣDDE, ΣDDD, Total DDT and %DDT, %DDE, %DDD from shallow (0-5 cm) soil samples adjacent to the 12 groundwater sampling sites.

Location	Sample Name	ΣDDT (ng/g)	ΣDDE (ng/g)	ΣDDD (ng/g)	Total DDT (ng/g)	%DDT	%DDE	%DDD
PPGW-01	S grid (S-1)	67,600	56,200	991	125,000	54.2	45.0	0.8
Former	S grid (S-2)	43,700	58,300	2,840	105,000	41.7	55.6	2.7
Orchard	S grid (S-3)	5,050	9,760	252	15,000	33.5	64.8	1.7
	S grid (S-4)	18,600	30,100	500	49,200	37.8	61.2	1.0
	S grid (S-5)	24,300	14,000	820	39,200	62.1	35.9	2.1
	S grid (S-6)	57,400	37,200	4,000	98,600	58.2	37.8	4.1
	S grid (S-7)	2,400	6,160	84.0	8,650	27.8	71.3	1.0
	S grid (S-8)	154,000	152,000	10,400	316,000	48.7	48.0	3.3
	S grid (S-9)	8,900	16,100	350	25,400	35.1	63.5	1.4
	S grid (S-10)	4,090	8,040	106	12,200	33.4	65.7	0.9
	Mean	38,600	38,800	2,030	79,400	43.2	54.9	1.9
PPGW-02	PP-DDT-S05	18,600	24,300	1,570	44,500	41.8	54.6	3.5
Former	PP-DDT-S23	494	1,030	31.4	1,560	31.8	66.2	2.0
Orchard	PP-DDT-S24	1,780	8,420	244.0	10,400	17.0	80.6	2.3
	Mean	6,960	11,200	616	18,800	30.2	67.2	2.6
PPGW-03	OC-SS05	22,100	33,300	428	55,900	39.6	59.6	0.8
Former	SHPLT1Y02-1	9,390	14,300	4,910	28,600	32.9	49.9	17.2
Orchard	SHPLT1Y02-2	15,500	18,700	1,500	35,700	43.4	52.4	4.2
	SHPLT1Y02-3	35,500	38,600	2,760	76,900	46.2	50.2	3.6
	SHPLT1Y02-4	15,900	20,100	1,740	37,700	42.2	53.2	4.6
	SHPLT1Y02-5	15,100	18,800	719	34,600	43.5	54.4	2.1
	Mean	18,900	24,000	2,010	44,900	41.3	53.3	5.4
PPGW-04	OC-SS08	5,280	13,000	199	18,500	28.6	70.3	1.1
Former	AOPLT1Y02-1	28,100	18,100	1,450	47,700	58.9	38.0	3.0
Orchard	AOPLT1Y02-2	6,680	11,800	1,520	20,000	33.4	59.0	7.6
	AOPLT1Y02-3	1,660	7,160	309	9,130	18.2	78.5	3.4
	AOPLT1Y02-4	4,460	5,100	4,180	13,700	32.5	37.2	30.4
	AOPLT1Y02-5	6,330	11,100	607	18,000	35.1	61.5	3.4
	Mean	8,750	11,000	1,380	21,200	34.5	57.4	8.1
PPGW-06	PP-DDT-S02	724	2,140	54.0	2,920	24.8	73.4	1.9
Former	PP-DDT-S27	4,810	11,100	378	16,300	29.5	68.2	2.3
Orchard	PP-DDT-S28	3,680	7,580	216	11,500	32.1	66.1	1.9
	Mean	3,070	6,950	216	10,200	28.8	69.2	2.0

Table 17 (cont'd).

Location	Sample Name	ΣDDT (ng/g)	ΣDDE (ng/g)	ΣDDD (ng/g)	Total DDT (ng/g)	%DDT	%DDE	%DDD
PPGW-07	OC-SS04	1,460	2,850	41	4,350	33.5	65.5	0.9
Former	PP-DDT-S29	558	2,870	66	3,490	16.0	82.1	1.9
Orchard	PP-DDT-S30	695	2,810	88	3,590	19.4	78.2	2.4
	Mean	904	2,840	65	3,810	23.0	75.3	1.8
PPGW-08	OC-SS09	16,600	33,200	260	50,000	33.2	66.3	0.5
Former	PP-DDT-S31	6,930	12,400	423	19,800	35.1	62.8	2.1
Orchard	PP-DDT-S32	4,780	9,400	296	14,500	33.0	65.0	2.0
	Mean	9,430	18,300	326	28,100	33.7	64.7	1.6
PPGW-09	PP-DDT-S01	69.0	999	87.0	1,160	6.0	86.5	7.5
Natural	CHM-1	29.0	1,710	19.0	1,760	1.7	97.3	1.1
Marsh	CHM-2	170	2,800	18.0	2,990	5.7	93.7	0.6
	CHM-3	64.0	2,110	20.0	2,200	2.9	96.2	0.9
	CHM-4	129	2,410	140	2,680	4.8	89.9	5.2
	CHM-5	713	8,410	80.0	9,210	7.7	91.4	0.9
	CHM-6	154	2,200	21.0	2,380	6.5	92.7	0.9
	CHM-7	273	4,000	16.0	4.290	6.4	93.3	0.4
	CHM-8	2,320	29,100	2,520	33,900	6.8	85.7	7.4
	CHM-9	120	1,200	41.0	1,360	8.8	88.2	3.0
	CHM-10	199	5,810	134	6,140	3.2	94.6	2.2
	Mean	385	5,520	281	6,190	5.5	91.8	2.7
PPGW-10	RR-14	5,660	9,700	212	15,600	36.4	62.3	1.4
Former	PP-DDT-S33	5,600	10,400	323	16,300	34.3	63.7	2.0
Orchard	PP-DDT-S34	10,900	8,900	347	20,100	54.1	44.2	1.7
	Mean	7,390	9,670	294	17,300	41.6	56.7	1.7
PPGW-11	M-1	1,440	4,150	96.0	5.690	25.3	73.0	1.7
Former	M-2	2,530	6,940	244	9,720	26.0	71.5	2.5
Orchard	M-3	3,960	7,230	118	11,300	35.0	63.9	1.0
	M-4	2,550	5,220	92.0	7,860	32.4	66.4	1.2
	M-5	4,580	10,000	28.0	14,600	31.4	68.5	0.2
	M-6	5,280	12,000	250	17,600	30.1	68.5	1.4
	M-7	5,900	8,630	277	14.800	39.9	58.3	1.9
	M-8	2,790	5,820	113	8,720	32.0	66.7	1.3
	M-9	3,900	11,000	117	15.000	25.9	73.3	0.8
	M-10	4,000	5,620	103	9,720	41.2	57.8	1.1
	Mean	3.690	7,670	144	11,500	31.9	66.8	1.3

Table 17 (cont'd).

Location	Sample Name	ΣDDT (ng/g)	ΣDDE (ng/g)	ΣDDD (ng/g)	Total DDT (ng/g)	%DDT	%DDE	%DDD
PPGW-12	PP-DDT-S07	7.92	11.8	0.96	20.7	38.3	57.1	4.6
Natural	PP-DDT-S08	6.16	11.5	<I.D.L	17.7	34.9	65.1	0.0
Dunes	PP-DDT-S09	4.04	9.62	<I.D.L	13.7	29.6	70.4	0.0
	PP-DDT-S10	3.74	6.32	<I.D.L	10.1	37.2	62.8	0.0
	PP-DDT-S11	10.9	19.1	1.12	31.1	35.0	61.4	3.6
	PP-DDT-S12	23.0	4.43	<I.D.L	27.4	83.9	16.2	0.0
	PP-DDT-S13	6.98	8.41	0.87	16.3	42.9	51.7	5.4
	Mean	8.96	10.2	0.42	19.6	43.1	55.0	1.9

The %DDT and %DDE in soil at each of the additional analyses range from 18.2 - 62.0% and 35.8 - 79.3%, respectively. %DDT and %DDE analyses are most frequently between 30 - 35% and 55 - 75%, respectively for both. %DDD in all 68 samples is substantially lower; < 5%. Thus, the analyses of the soil samples collected during July 2002 are consistent with the analyses of the soil samples previously collected in the vicinity of the 12 groundwater sampling sites. The %DDT, %DDE and %DDD in the natural dune area (i.e., PPGW-12) is consistent with those in the former agricultural areas (Table 17). However, although Total DDT concentrations are considerably lower in the marshy sediments (i.e., at PPGW-09) vs. the former agricultural areas, the %DDT, %DDE and %DDD organic-rich transitional soils are considerable different; 1.7 - 7.7%, 85.7 - 97.3%, and 0 - 7.5%, respectively. Thus, the distribution of %DDT : %DDE : %DDD throughout the former agricultural areas is quite consistent (Figure 10). This is consistent with the conclusion of Marenco (2002) that degradation rates were faster within the organic-rich transitional soils than within the higher-elevation soils of former agricultural areas.

A plot of %DDE vs. %DDT in the shallow soil in the vicinity of the 12 groundwater sampling sites (using all 68 surficial soil analyses) show that the majority of the analyses of soils in the former agricultural, natural dune, and marsh areas lie on a 1:1 line (Figure 11). The points on the %DDD vs. %DDT plot along the x-axis. This indicates that the primary degradation pathway in shallow soil at PPNP is essentially a 1:1 conversion of DDT to DDE along the aerobic pathway, with little production of DDD. However, Figure 11 shows two clusters of points along the 1:1 transformation line; the analyses of the agricultural soils are spread along the line from about 20% to 80% DDT, whereas the analyses of the organic-rich transitional soils are tightly grouped near 0% to 10% DDT. This indicates that the rate of transformation of DDT to DDE is faster in transitional soils (ground surface elevation <174.3 m a.m.s.l.) than the former agricultural areas (ground surface elevation >174.3 m a.m.s.l.). This is consistent with findings of Crowe et al. (2002) and Marenco (2002) who also found this relationship between %DDT, %DDE and %DDD.

3.8.2 DDT in Soils - Distribution with Depth

The analytical results of the DDT compounds with depth at CHO, SHO, and AO are presented in Table 18. Concentrations of ΣDDT, ΣDDE, ΣDDD and Total DDT are highest at surface and exhibit a rapidly decline with depth (Figure 12) of 3-4 orders of magnitude within the uppermost 40 cm of the three soil profiles. Concentrations at the surface of the soil profile at AO are not as large as at CHO and SHO. However, the initial concentrations of DDT at surface at AO were likely very similar to CHO and SHO in the past to produce essentially the same concentration profiles. Disturbances at the surface subsequent to application of DDT (e.g., during removal of the trees in the orchard) could have removed the uppermost layer of contaminated soil.

The total amount of DDT at each depth interval and the total mass of DDT in the soil profile are listed in Table 19. Total mass of DDT (M_{total}) within each soil profile was estimated by depth-weighted sum of the concentration at each profile assuming a unit soil profile surface area of 1 cm^2;

$$M_{total} = C_d \times z_d \times \rho_d \tag{14}$$

where C_d is the concentration of a given compound (ng/g) at a specific depth (d), z_d is the depth interval over which the concentration is assumed to represent (cm), and ρ_d is the bulk density of the soil within each depth interval (g/cm^3) as reported in Table 13. Essentially all of the mass of Total DDT (99.6% at CHO, 99.7% at SHO, 94.6% at AO) is contained within the uppermost 20 cm of the profile at each of the locations. This correlates with the distribution of organic matter with depth (Figure 8), where the highest concentrations of organic matter is within the upper 20 cm of the soil profile at all three sites. This trend is consistent with the ability of organic matter to bind DDT compounds, and thus limit leaching of DDT deeper within the soil profile and to the water table.

Table 18. Analytical results of DDT compounds in soil with depth below ground surface at CHO, SHO and AO.

Soil Sample I.D.	**Depth** (cm)	***o,p'*-DDT** (ng/g)	***p,p'*-DDT** (ng/g)	***o,p'*-DDE** (ng/g)	***p,p'*-DDE** (ng/g)	***o,p'*-DDD** (ng/g)	***p,p'*-DDD** (ng/g)	**Total DDT** (ng/g)
CHO-PIT1-000	0	2,820	15,500	121.3	12,900	793.53	1,430	33,600
CHO-PIT1-010	10	122	710	11.1	1,120	12.90	45.3	2,020
CHO-PIT1-020	20	<IDL	9.50	0.17	22.9	<IDL	<IDL	32.6
CHO-PIT1-030	30	<IDL	8.77	0.04	15.4	0.21	<IDL	24.4
CHO-PIT1-040	40	<IDL	8.11	<IDL	8.75	0.06	<IDL	16.9
CHO-PIT1-050	50	<IDL	<IDL	<IDL	5.56	0.06	<IDL	5.62
CHO-PIT1-060	60	<IDL	2.13	<IDL	2.99	0.06	<IDL	5.18
CHO-PIT1-080	80	<IDL	<IDL	0.03	<IDL	0.06	<IDL	0.09
CHO-PIT1-100	100	<IDL	<IDL	0.58	<IDL	0.06	<IDL	0.64
CHO-PIT1-120	120	<IDL	<IDL	<IDL	<IDL	0.10	<IDL	0.10
CHO-PIT1-140	140	<IDL	<IDL	<IDL	<IDL	0.06	<IDL	0.06
CHO-PIT1-160	160	<IDL	<IDL	<IDL	<IDL	<IDL	<IDL	<IDL
CHO-PIT1-180	180	<IDL	<IDL	<IDL	<IDL	<IDL	<IDL	<IDL
CHO-PIT1-200	200	<IDL	2.30	<IDL	<IDL	<IDL	<IDL	2.30
SHO-PIT1-000	0	2,930	13,400	194	30,300	331	391	47,500
SHO-PIT1-010	10	97.0	471	8.23	995	9.68	22.2	1,600
SHO-PIT1-020	20	9.29	64.2	0.97	229	0.99	3.18	308
SHO-PIT1-030	30	<IDL	8.54	0.03	30.1	0.11	<IDL	38.8
SHO-PIT1-040	40	<IDL	3.31	0.05	11.0	0.08	<IDL	14.4
SHO-PIT1-060	60	<IDL	<IDL	0.05	4.57	0.09	<IDL	4.71
AO-PIT1-000	0	67.1	641	6.25	2,020	6.30	26.8	2,770
AO-PIT1-010	10	126	846	17.0	2,310	23.69	56.6	3,380
AO-PIT1-020	20	13.5	85.3	3.68	749	3.21	9.19	864
AO-PIT1-030	30	<IDL	10.4	0.38	112	0.17	1.01	124
AO-PIT1-040	40	<IDL	6.90	0.15	53.4	0.16	<IDL	60.6
AO-PIT1-060	60	<IDL	19.8	0.05	6.09	0.82	1.06	27.8
AO-PIT1-080	80	<IDL	<IDL	0.03	3.15	<IDL	<IDL	3.18

* <IDL means compounds were below instrument detection limits.

When analyte concentrations are below or approach instrument detection limits, %DDT, %DDE and %DDD are highly variable because not all three of the compounds are detected. It is particularly important to note that the detection limits for each compound are different (Table 11) making comparisons based on relative proportions determined from concentration values near detection limits qualitative at best. For this reason, relative proportions of each compound are only calculated (Table 19) when concentrations are above detection limits (i.e., the uppermost 40 cm of the soil profiles). Generally, where more than one DDT compound is detected and concentrations are above detection limit (1) %DDE exceeds %DDT and %DDD, (2) %DDT generally decreases with depth, %DDE generally increases with depth, and %DDD remains essentially constant at <10%, and (3) the rate of %DDE increase and %DDT decrease with depth is very similar at all 3 sites (Figure 13). Also, %DDT with depth is consistently lower at AO than SHO, which is in turn consistently lower than CHO. Correspondingly, %DDE with depth at AO is consistently higher than SHO, which is in turn consistently higher than CHO. This indicates that transformation and/or degradation may be occurring somewhat slower at CHO vs. SHO vs. AO. Possibly this is because of the much deeper water table at CHO, or that DDT was more recently applied at CHO than it was at SHO and AO.

The similarity at all three sites with respect to (1) the decline of concentrations with depth below ground surface, (2) the %DDT : %DDE : %DDD with depth, and

Table 19. ΣDDT, ΣDDE, ΣDDD, Total DDT and %DDT, %DDE, %DDD for soil samples obtained with depth at CHO, SHO and AO on May 12-14, 2003.

Soil Sample I.D.	**Depth** (cm)	**ΣDDT** (ng/g)	**ΣDDE** (ng/g)	**ΣDDD** (ng/g)	**Total DDT** (ng/g)	**%DDT**	**%DDE**	**%DDD**
CHO-PIT1-000	0	18,300	13,000	2,220	33,600	55.0	39.0	7.0
CHO-PIT1-010	10	832	1,130	58.2	2,020	41.0	56.0	3.0
CHO-PIT1-020	20	9.50	23.1	<IDL	32.6	29.0	71.0	0.0
CHO-PIT1-030	30	8.77	15.4	0.21	24.4	36.0	63.0	1.0
CHO-PIT1-040	40	8.11	8.75	0.06	16.9	48.0	52.0	0.0
CHO-PIT1-050	50	<IDL	5.56	0.06	5.62	NC	NC	NC
CHO-PIT1-060	60	2.13	2.99	0.06	5.18	NC	NC	NC
CHO-PIT1-080	80	<IDL	0.03	0.06	0.09	NC	NC	NC
CHO-PIT1-100	100	<IDL	0.58	0.06	0.64	NC	NC	NC
CHO-PIT1-120	120	<IDL	<IDL	0.10	0.10	NC	NC	NC
CHO-PIT1-140	140	<IDL	<IDL	0.06	0.06	NC	NC	NC
CHO-PIT1-160	160	<IDL	<IDL	<IDL	<IDL	NC	NC	NC
CHO-PIT1-180	180	<IDL	<IDL	<IDL	<IDL	NC	NC	NC
CHO-PIT1-200	200	2.30	<IDL	<IDL	2.30	NC	NC	NC
Total Mass (ng)		118,000	90,800	13,800	222,000	53.0	40.8	6.2
SHO-PIT1-000	0	16,300	30,500	723	47,500	34.0	64.0	2.0
SHO-PIT1-010	10	568	1,000	31.9	1,600	35.0	63.0	2.0
SHO-PIT1-020	20	73.5	230	4.17	308	24.0	75.0	1.0
SHO-PIT1-030	30	8.54	30.1	0.11	38.8	22.0	78.0	0.0
SHO-PIT1-040	40	3.31	11.0	0.08	14.4	23.0	77.0	1.0
SHO-PIT1-060	60	<IDL	4.62	0.09	4.71	NC	NC	NC
Total Mass (ng)		116,000	218,000	5,240	339,000	34.2	64.2	1.5
AO-PIT1-000	0	708	2,030	33.1	2,770	26.0	73.0	1.0
AO-PIT1-010	10	972	2,330	80.3	3,380	29.0	69.0	2.0
AO-PIT1-020	20	98.8	753	12.4	864	11.0	87.0	1.0
AO-PIT1-030	30	10.4	112	1.18	124	8.0	91.0	1.0
AO-PIT1-040	40	6.90	53.6	0.16	60.6	11.0	88.0	0.0
AO-PIT1-060	60	19.8	6.14	1.88	27.8	71.0	22.0	7.0
AO-PIT1-080	80	<IDL	3.18	<IDL	3.18	NC	NC	NC
Total Mass (ng)		18,600	54,700	1,440	74,700	24.8	73.2	1.9

* NC means values were not calculated as compounds necessary for the calculation were below IDL.

* <IDL means both *o,p'*-DD_ and *p,p'*-DD_ isomers were not detected.

* Total mass is depth-weighted according to Equation 14.

(3) concentrations of Total DDT, ΣDDT, ΣDDE and ΣDDD, indicates that similar hydrological, biological and chemical processes are occurring at all three sites.

Because DDT compounds in near-surface soils are strongly adsorbed by organic matter in the Ah horizon, little leaching occurs, and thus results in essentially all of the mass of Total DDT being present in the upper ~20 cm of the soil profile. Both ΣDDE concentrations are much greater than ΣDDD concentrations, and relative proportion of DDE is much greater than DDD throughout the profile. This indicates that the dominant transformation pathway throughout the soil profile is aerobic transformation of DDT to DDE. There is very little DDD produced, suggesting that very little anaerobic degradation occurs anywhere in the soil profile. The DDT to DDE transformation rates increase slightly with depth. These findings are consistent with Marenco (2002).

3.8.3 DDT in Groundwater - Spatial Distribution

Because concentrations of the DDT isomers in groundwater are very low (Table 20), and approach instrument detection limits for 20 L samples, these compounds would likely not be detected if only 1 L samples were collected and analyzed. As discussed earlier, when concentrations are just above detection limits the reported values should be treated more qualitatively than quantitatively.

Concentrations of Total DDT in groundwater, collected from the 16 groundwater sampling sites, and 4 replicates (Table 20), are consistently low throughout PPNP (Figure 14), whether the sample was collected from a former agricultural area or a natural

Table 20. Analytical results of DDT compounds in groundwater.

GW Sample I.D.	**o,p'-DDT** (ng/L)	**p,p'-DDT** (ng/L)	**o,p'-DDE** (ng/L)	**p,p'-DDE** (ng/L)	**o,p'-DDD** (ng/L)	**p,p'-DDD** (ng/L)	**Total DDT** (ng/L)
PPGW-01	0.039	0.027	<IDL	0.069	<IDL	<IDL	0.135
PPGW-02	<IDL	<IDL	<IDL	0.063	<IDL	<IDL	0.063
PPGW-03	0.104	0.162	<IDL	0.281	<IDL	<IDL	0.548
PPGW-04	0.015	0.019	<IDL	0.064	0.002	<IDL	0.100
PPGW-05	<IDL	0.073	<IDL	0.270	<IDL	<IDL	0.342
PPGW-06	<IDL	0.025	<IDL	0.073	<IDL	<IDL	0.098
PPGW-07	<IDL	0.039	<IDL	0.107	<IDL	<IDL	0.146
PPGW-08	<IDL	0.046	<IDL	0.077	<IDL	<IDL	0.123
PPGW-09	<IDL	0.017	<IDL	0.080	<IDL	<IDL	0.097
PPGW-10	0.017	0.008	<IDL	0.068	<IDL	<IDL	0.092
PPGW-11	<IDL	0.026	<IDL	0.046	<IDL	<IDL	0.072
PPGW-12	<IDL	<IDL	<IDL	0.021	<IDL	<IDL	0.021
PPGW-01-R	<IDL	0.010	<IDL	0.043	<IDL	<IDL	0.054
PPGW-02-R	<IDL	<IDL	<IDL	0.033	<IDL	<IDL	0.033
PPGW-03-R	<IDL	0.019	<IDL	0.056	<IDL	<IDL	0.075
PPGW-04-R	<IDL	<IDL	<IDL	<IDL	<IDL	<IDL	0.000
CHO-PIT1-GW1	0.0510	0.375	0.000	0.252	<IDL	<IDL	0.68
SHO-PIT1-GW1	0.753	1.56	0.0360	1.83	<IDL	<IDL	4.18
AO-PIT1-GW1	0.037	0.383	0.000	3.36	<IDL	<IDL	3.65

* <IDL means compounds were below instrument detection limits.

setting. The highest concentration of Total DDT was 0.548 ng/L at PPGW-03, and the lowest was below detection limits (Table 11) for all DDT compounds at PPGW-15. Mean Total DDT concentrations in groundwater were calculated to be 0.153 ng/L. All groundwater concentrations were in excess of 2 orders of magnitude below the former Canadian Drinking Water Guideline of 30 μg/L Total DDT (CCREM, 1987).

Concentrations of Total DDT in groundwater collected at the three soil sampling pits were higher, ranging from 0.679 ng/L at CHO-PIT1-GW1 to 4.18 ng/L at

SHO-PIT1-GW1 (Table 20). At the three sites sampled in 2003, concentrations increased by a factor of 5.03 for CHO, 7.63 for SHO and 11.05 for AO as compared with samples obtained during 2002 which were within 5 metres of each location sampled during 2003 and the same sample procedure and analytical methods were used. This increase in DDT concentrations at the water table could be the results of a large spring infiltration event in 2003 flushing DDT from the soil surface to the water table.

The relative proportions of DDT and DDE at the 12 groundwater sampling sites ranges from 0 to 63% and from 51% to 100%, respectively (Table 21). %DDE was consistently greater than %DDT throughout PPNP (Figure 15). At two of the three soil sampling pits, %DDT exceeds %DDE. However, as discussed in Section 3.8.2, when concentrations are just above detection limits, relative proportions are more variable than they are when concentrations of all compounds are well above detection limits and thus, they should be considered only qualitatively. DDD was not detected in groundwater, with the exception of PPGW-04 with 2.0% DDD.

When compared to previous sampling of groundwater within PPNP, the samples collected during 2002 and 2003 are within the range of variability seen previously, although, with lower detection limits as a result of increased groundwater sample volumes, DDT compounds were detected in every case except PPGW-04-R, where all DDT compounds were below detection limits. While many of the initial groundwater and drinking water samples collected by NWRI, Parks Canada, and O'Connor and Associated Environmental between 1998 and 2001 exhibited concentrations of DDT compounds

Table 21. Results of groundwater sampling for DDT, DDE and DDD throughout PPNP including replicate samples.

GW Sample I.D.	ΣDDT (ng/L)	ΣDDE (ng/L)	ΣDDD (ng/L)	Total DDT (ng/L)	% DDT	% DDE	% DDD
PPGW-01	0.066	0.069	<IDL	0.135	49.0	51.0	0.0
PPGW-02	<IDL	0.063	<IDL	0.0623	NC	NC	NC
PPGW-03	0.267	0.281	<IDL	0.548	49.0	51.0	0.0
PPGW-04	0.034	0.064	0.002	0.100	34.0	64.0	2.0
PPGW-05	0.073	0.270	<IDL	0.342	21.0	79.0	0.0
PPGW-06	0.025	0.073	<IDL	0.098	26.0	74.0	0.0
PPGW-07	0.039	0.107	<IDL	0.146	27.0	73.0	0.0
PPGW-08	0.046	0.077	<IDL	0.123	37.0	63.0	0.0
PPGW-09	0.017	0.080	<IDL	0.097	17.0	83.0	0.0
PPGW-10	0.024	0.068	<IDL	0.092	27.0	73.0	0.0
PPGW-11	0.026	0.046	<IDL	0.072	36.0	64.0	0.0
PPGW-12	<IDL	0.021	<IDL	0.021	NC	NC	NC
Mean	0.051	0.102	0.000	0.153	34.0	66.0	0.0
PPGW-01-R	<IDL	0.033	<IDL	0.033	NC	NC	NC
PPGW-02-R	0.010	0.043	<IDL	0.054	19.0	81.0	0.0
PPGW-03-R	0.019	0.056	<IDL	0.075	25.0	75.0	0.0
PPGW-04-R	<IDL	<IDL	<IDL	<IDL	NC	NC	NC
CHO-PIT1-GW1	0.427	0.252	<IDL	0.679	63.0	37.0	0.0
SHO-PIT1-GW1	2.317	1.863	<IDL	4.181	55.0	45.0	0.0
AO-PIT1-GW1	0.420	3.364	<IDL	3.784	11.0	89.0	0.0

* NC means values were not calculated as compounds necessary for the calculation were below IDL.
* <IDL means both *o,p*'-DD_ and *p,p*'-DD_ isomers were not detected.

below detection limits for 1 L samples, this study detected DDT and DDE compounds in groundwater in nearly all of the samples by employing 20 L samples, thus reducing detection limits by a factor of 20. The concentrations of Total DDT in prior groundwater analyses directly from water table samples showed concentrations ranging from 1.40 to 7.56 ng/L at Camp Henry (Crowe et al., 2002), and 3.00 to 23.0 ng/L near the former maintenance compound (O'Connor and Associated Environmental, 1998). While other analyses of water have been undertaken within PPNP, they are derived from either groundwater supply wells, which exhibit much lower Total DDT concentrations or monitoring wells for which sampling depths are not clearly presented. Analyses of samples collected during 2002 and 2003 compare favourably with previous work within PPNP specifically. The relative proportions of DDT, DDE and DDD from previous analyses generally report greater proportions of DDE than DDT in groundwater and drinking water, and have also found large fluctuations in relative proportions of each compound as a result of concentrations near instrument detection limits. The relative proportions of DDT, DDE and DDD in groundwater are consistent with those seen in PPNP soils and reflect a linear 1:1 transformation of DDT to primarily DDE (Figure 16).

While the concentrations of DDT reported for 2002 and 2003 analyses within PPNP are lower than concentrations reported elsewhere in southern Ontario, Canada and the United States, they are indicative of concentrations you would likely find at the water table in areas where agriculture was historically intensive and widespread within sandy soils with relatively thin surficial organic matter. Maximum concentrations observed at the water table at PPNP in 2003 are within a factor of 10 of maximum concentrations observed by Kolpin et al. (2000) after sampling at 2,485 sites across the Unites States between 1992 and 1996. Within Ontario, during the late 1970's and early 1980's, the maximum observed concentration in shallow well water was 2000 ng/L, with a mean concentration of 6.7 ng/L within historically intensively cropped areas (Frank et al., 1982). These concentrations are much higher than any concentrations observed as part of this study. This could be partly due to the long period of time since the last application of DDT within PPNP (at least 30 years), and subsequent degradation and flushing.

3.8.4 Relationship Between DDT in Groundwater and Depth to Water Table

Figure 17 shows that no clear relationship between Total DDT concentrations in groundwater and the depth to the water table among the analyses from the 12 groundwater sampling sites obtained during July 2002. However, the samples collected in early May 2003, show higher concentrations at the water table. While there are limited data (only 3 data points), it is suspected that this could be the result of a spring flushing event that flushes DDT to a shallower water table. The higher concentrations do not appear in the 2002 samples because of considerably less infiltration, a deeper water table, and advective and dispersive processes in the groundwater flow system have reduced Total DDT concentrations from the spring flushing.

To further assess the relationship between soil and groundwater concentrations and the depth to the water table, the ratio of Total DDT in groundwater to Total DDT in soil was plotted against the depth to the water table (Figure 17b). This removes the variability in surficial soil concentrations among groundwater sampling sites by assessing the proportion of DDT at surface leached to the water table and the depth to the water table. Again, there is no clear relationship between the proportion of Total DDT leached to the water table and the depth to the water table, suggesting that surficial soil concentration have no clear effect on concentrations at the water table.

During the month prior to sampling in May 2003, a total of 98.4 mm of precipitation fell within PPNP, with 53.8 mm falling during the week prior to sampling. The amount of precipitation that fell during July 2002 was only 45.6 mm, substantially less than during May 2003. July 2002 was also much hotter (T_{ave} = 23.6°C) than for the month prior to sampling in May 2003 (T_{ave} = 8.4°C). Consequently, a larger proportion of the precipitation would have evaporated prior to infiltrating to the water table in July 2002, than in May 2003. Also, groundwater flow at the water table between a spring infiltration event and the mid-summer could have transported and dispersed the DDT that is transported to the water table during a spring infiltration event. There is also no relationship between Total DDT in groundwater and ground surface elevation (Figure 17c) among the sample collected both in 2002 and 2003. This is consistent with the relationship between surface elevation and depth to the water table.

There is no apparent relationship between the fractions of DDT, DDE and DDD and the depth to the water table (Figure 18). This shows that there are no fractionation processes occurring, whereby DDT, DDE or DDD are being preferentially leached or degraded with depth. If this were occurring, an enrichment of the compound that was preferentially leached would be expected at the water table. While the sorption coefficients for DDT, DDE and DDD are somewhat different, with DDD being a full order of magnitude lower than DDT and DDE, there is little DDD produced and thus, the difference is not manifested at the water table. The sorption coefficients for DDT and

DDE only differ by a factor of 1.1 and thus, are not expected to show significant differences in leaching behaviour.

3.8.5 Relationship Between DDT in Soil and DDT in Groundwater

A plot of Total DDT in soil against Total DDT in groundwater (Figure 19a) shows orders of magnitude difference between soil and groundwater concentrations. However, no strong positive correlation between soil and groundwater concentrations exists. When plotted on log-log axes, concentrations cluster between 1 and –2 on the x-axis and between 3 and 5 on the y-axis, although DDD concentrations plot at –4 on the x-axis, corresponding to detection limits. The range in concentrations in soil extends over 4 orders of magnitude, while concentrations in groundwater cover 2 orders of magnitude.

When the concentrations of individual DDT compounds in soil are plotted against the same compounds in groundwater (Figure 19b), again there is no strong positive correlation, and concentrations in soil cannot predict concentrations in groundwater. This illustrates that no preferential leaching of any DDT compounds through the soil profile is occurring and that concentrations in groundwater are not determined by concentrations in the overlying soil alone. Thus, concentrations of DDT in surficial soils cannot be used alone as a reliable predictor of concentrations of DDT in groundwater.

Relative proportions of DDE vs. DDT in both soil and groundwater (Figure 20) generally plot along the same region of the 1:1 transformation line, illustrating that no preferential degradation or adsorption of DDT, DDE or DDD occurs during leaching from shallow soil to the water table. DDD was only detected on one occasion at the water table, while relative proportions in soil ranged from 1.16% to 6.50%, thus the points corresponding to DDD lie near the origin (0,0). Because relative proportions of DDT, DDE and DDD in groundwater plot in the same locations of the %DDE and %DDD vs. %DDT in soil graphs, it can be inferred that the processes controlling DDT transformation and degradation in surficial soils also dictate the relative proportions of DDT, DDE and DDD in groundwater. Again, potential degradation pathways will be given further consideration in subsequent sections.

The relative proportions of DDT, DDE and DDD in groundwater were plotted against the Total DDT concentrations in groundwater to assess whether the degradation of DDT compounds in groundwater was related to the Total DDT concentration in groundwater (Figure 21). There is no clear relationship between concentrations of Total DDT in groundwater and the relative proportions of DDT compounds. Thus, degradation of DDT compounds seems to occur at a similar rate, irrespective of concentrations in groundwater. It could be that the degradation is primarily occurring in shallow soils and groundwater concentrations and relative proportions of each compound in groundwater are the result of processes occurring in soil, prior to reaching the water table.

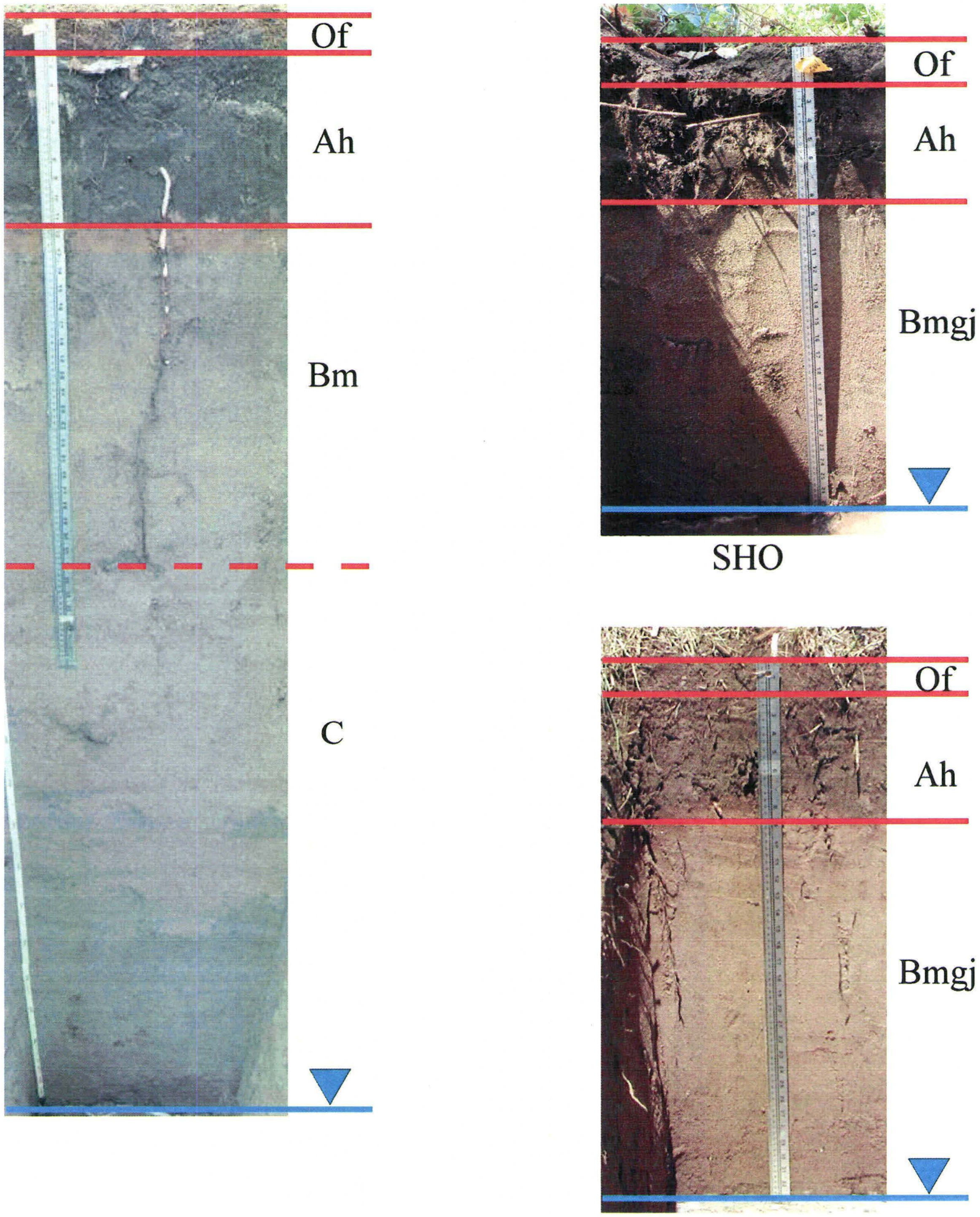

SHO

CHO

AO

Figure 6. Soil profiles at CHO, SHO and AO.

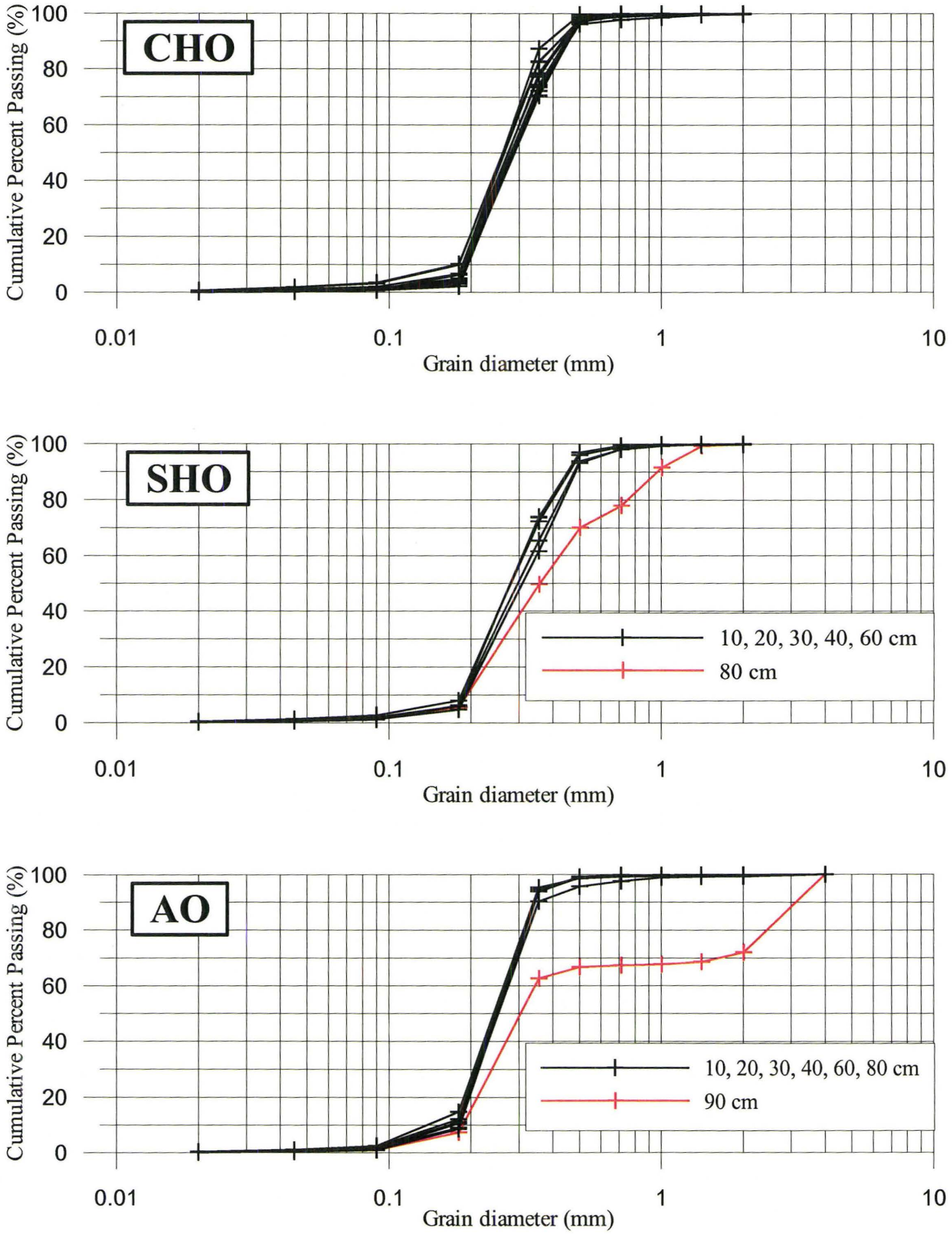

Figure 7. Grain-size distributions with depth at CHO, SHO and AO.

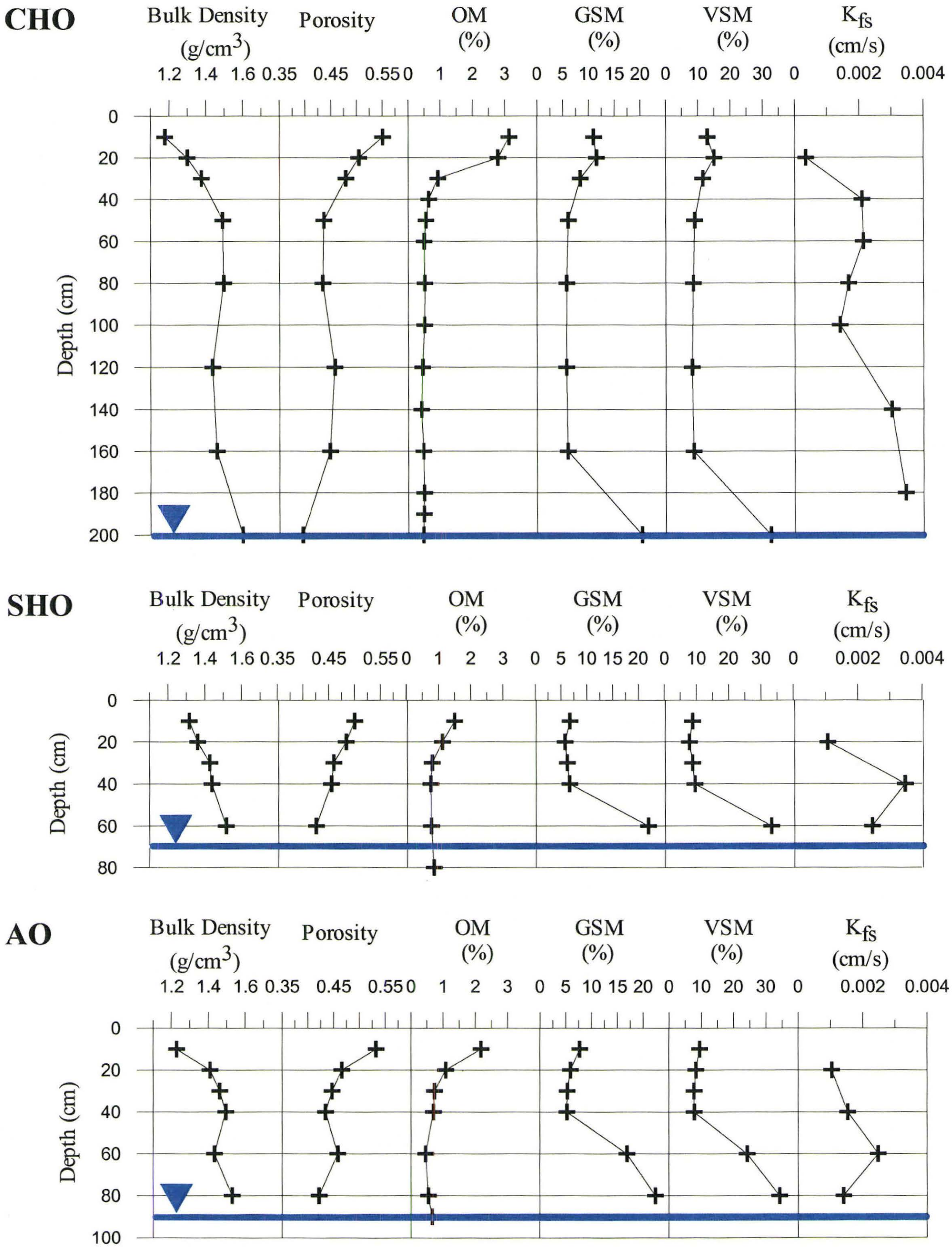

Figure 8. Soil and hydraulic properties measured with depth at CHO, SHO and AO.

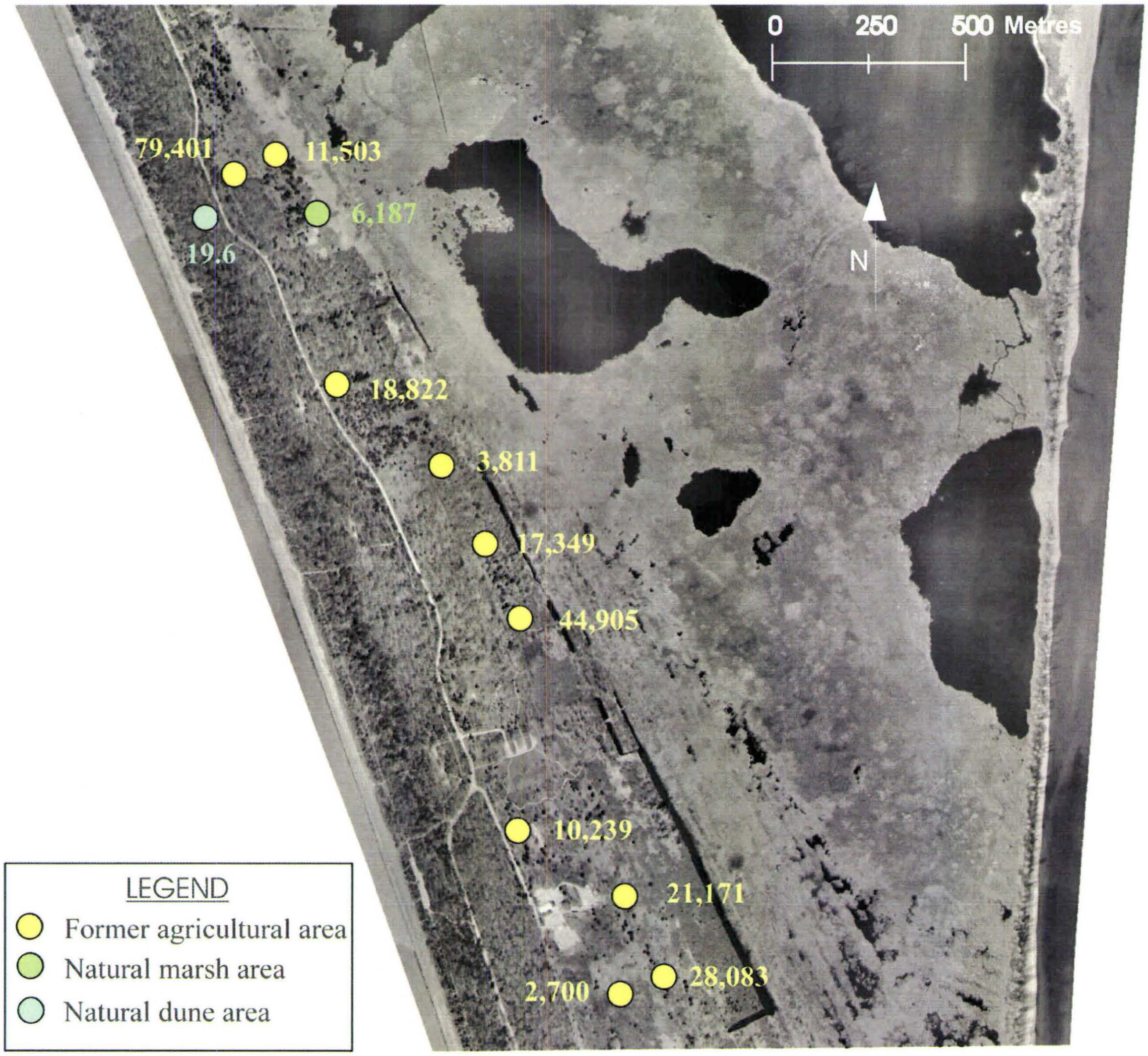

Figure 9. Mean Total DDT concentrations (ng/g) in shallow soil (0-5 cm) at the 12 groundwater sampling sites.

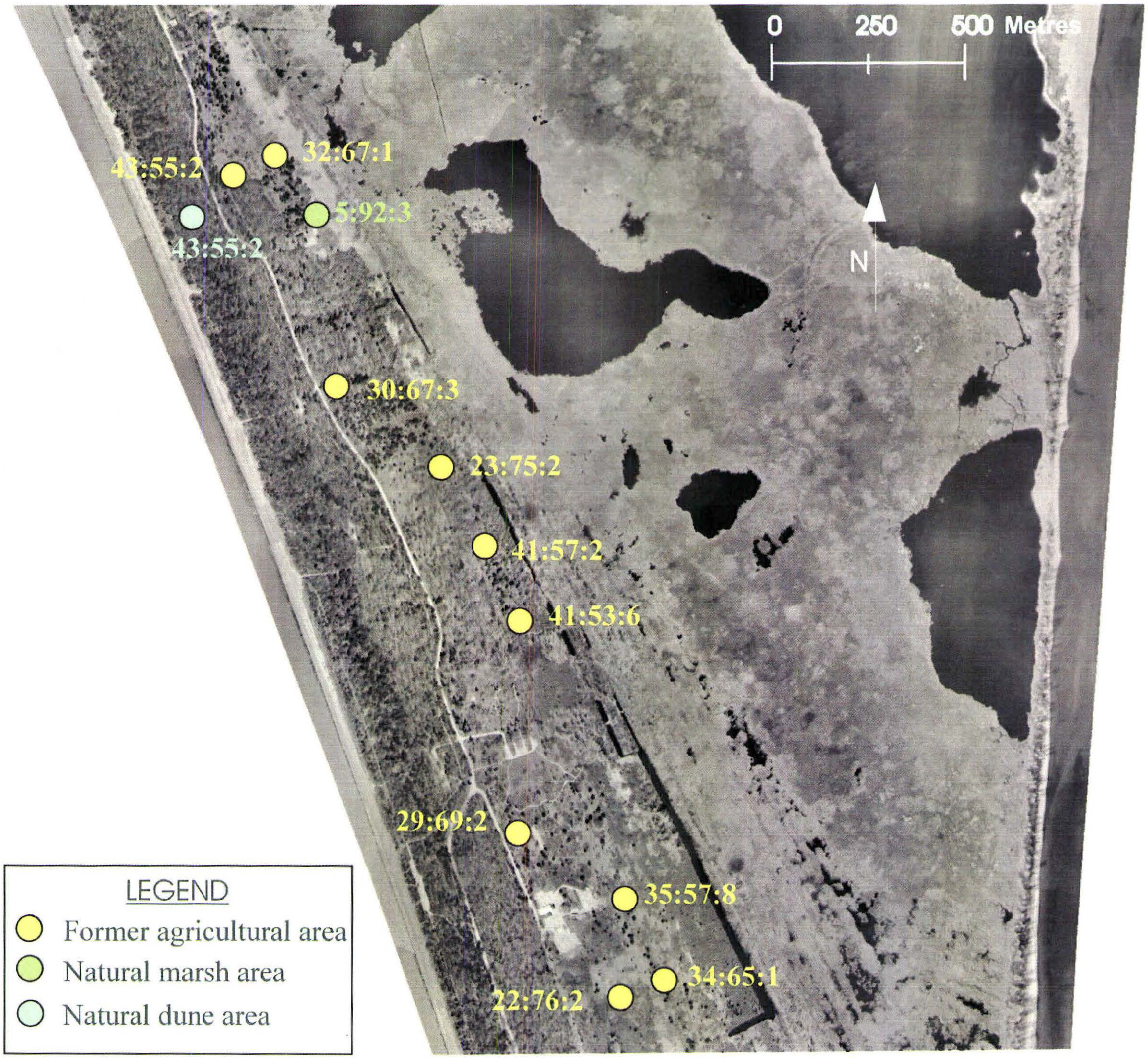

Figure 10. %DDT : %DDE : %DDD in shallow soil (0-5 cm) collected at the 12 groundwater sampling sites.

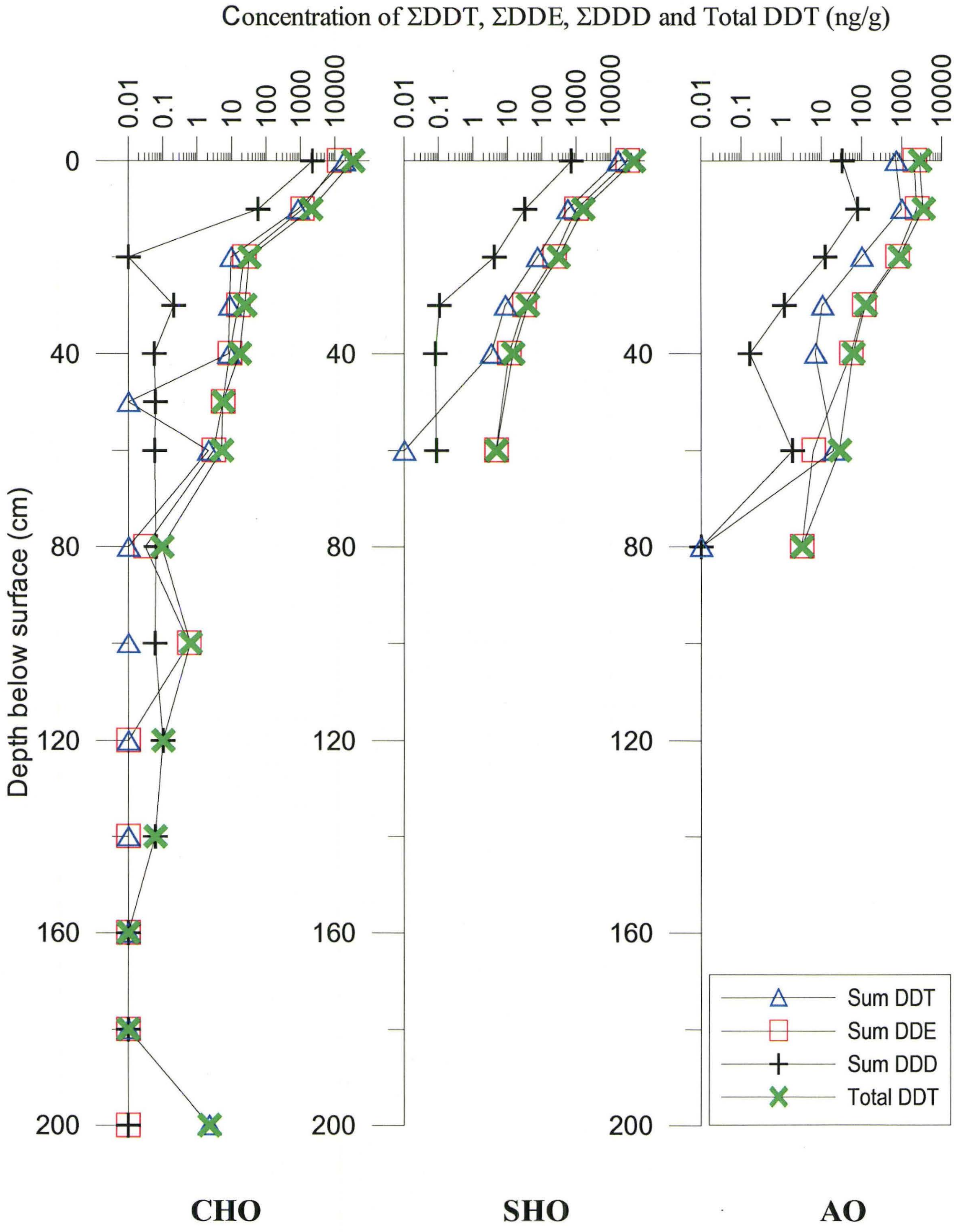

Figure 12. Distribution of ΣDDT, ΣDDE, ΣDDD and Total DDT concentrations with depth at CHO, SHO and AO soil sampling pits.

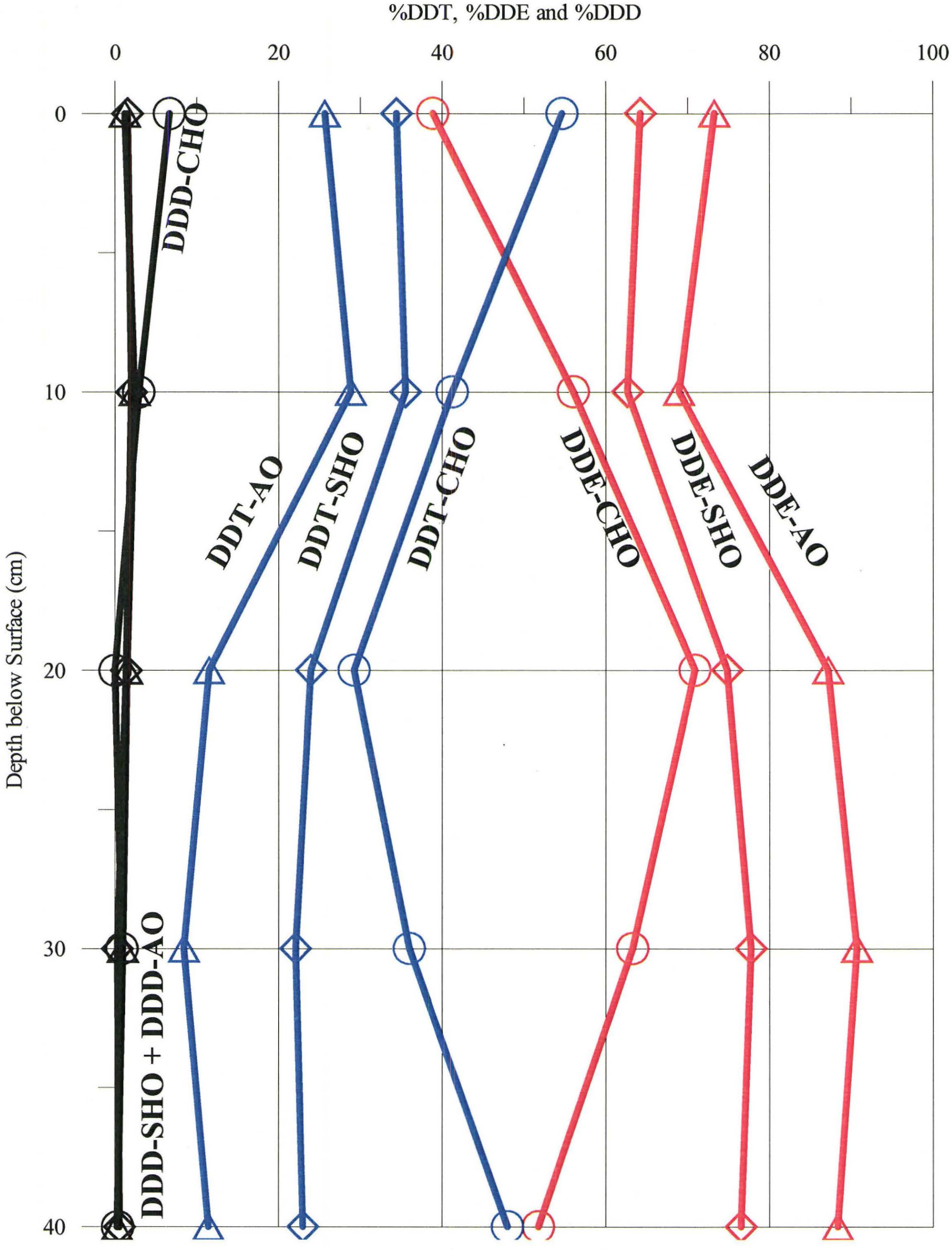

Figure 13. %DDT, %DDE and %DDD from 0-40 cm at CHO, SHO and AO.

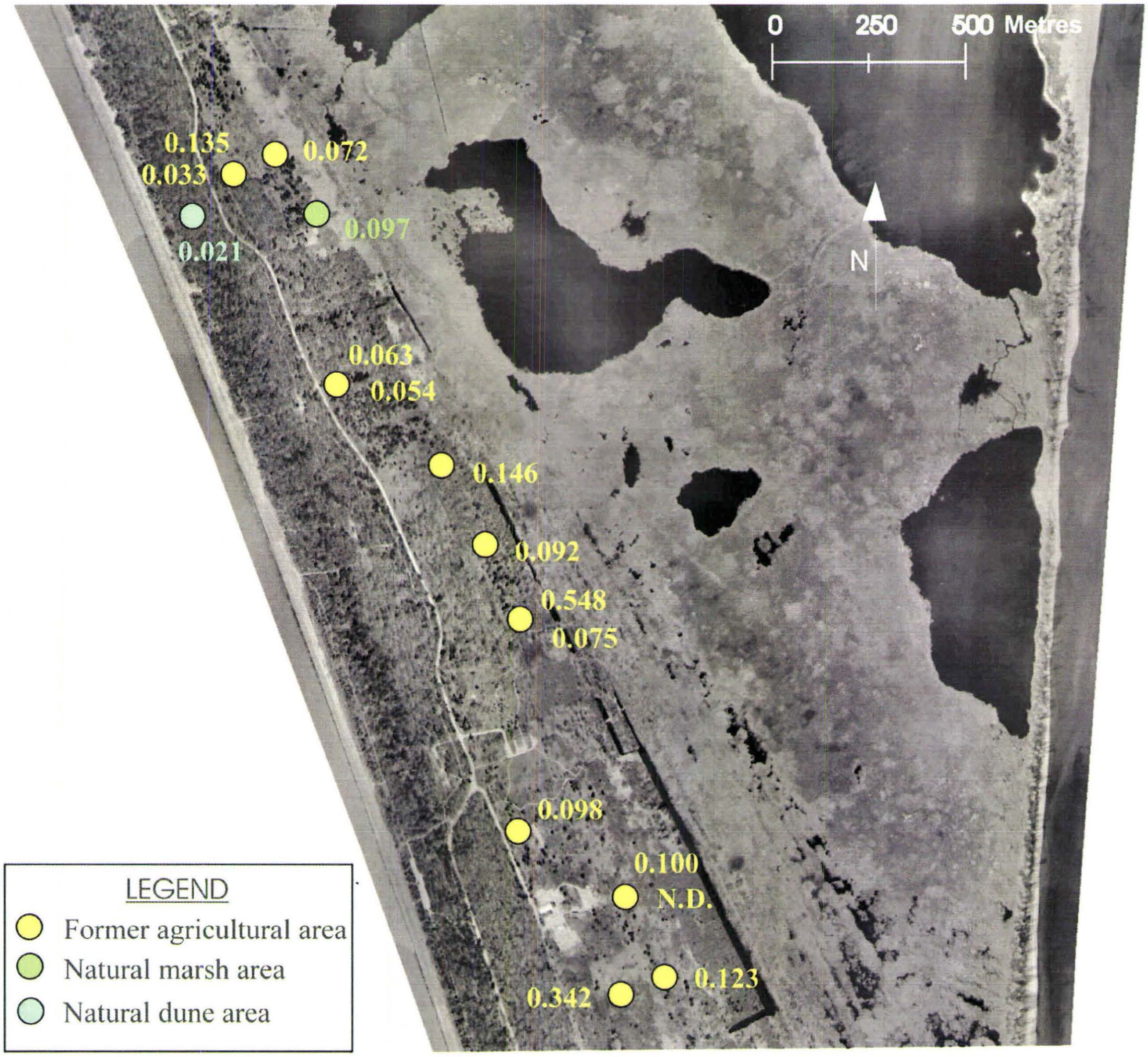

Figure 14. Total DDT concentrations in groundwater (ng/L) at the July 2002 groundwater sampling locations.

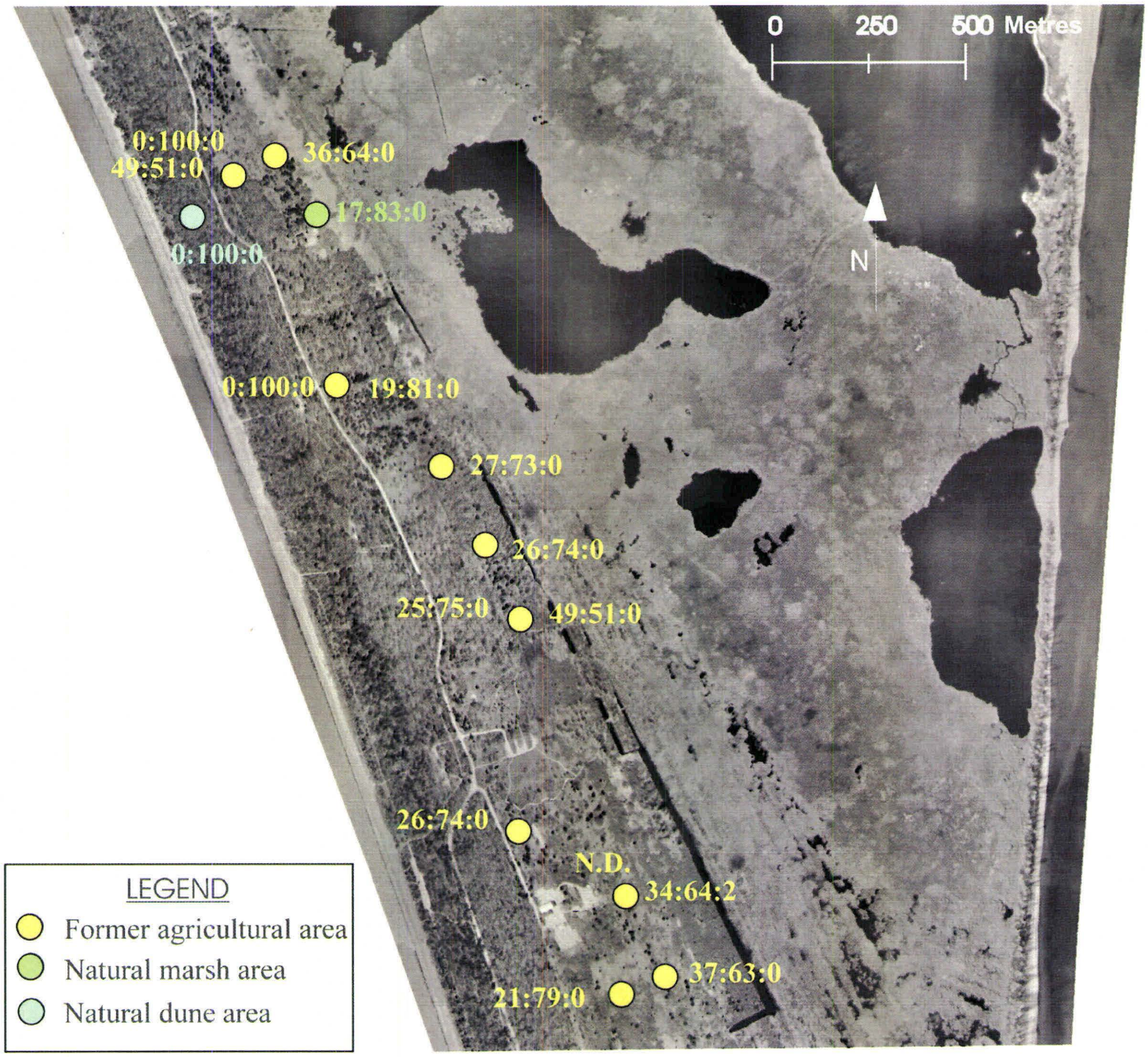

Figure 15. %DDT : %DDE : %DDD in groundwater at the July 2002 groundwater sampling locations.

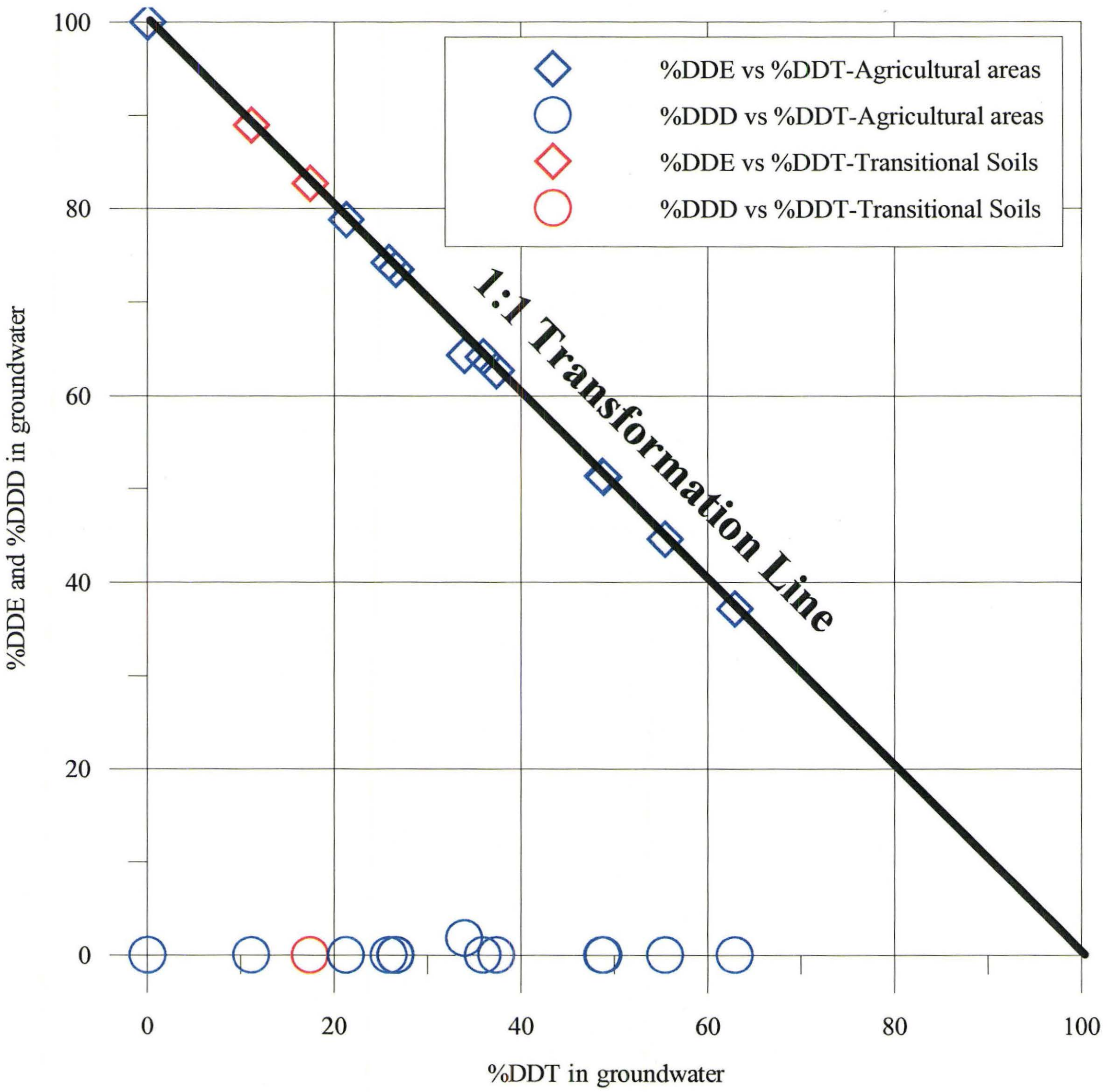

Figure 16. %DDE vs. %DDT and %DDD vs. %DDT in groundwater at the July 2002 groundwater sampling locations. Included is the 1:1 transformation line between DDT and DDE or DDD.

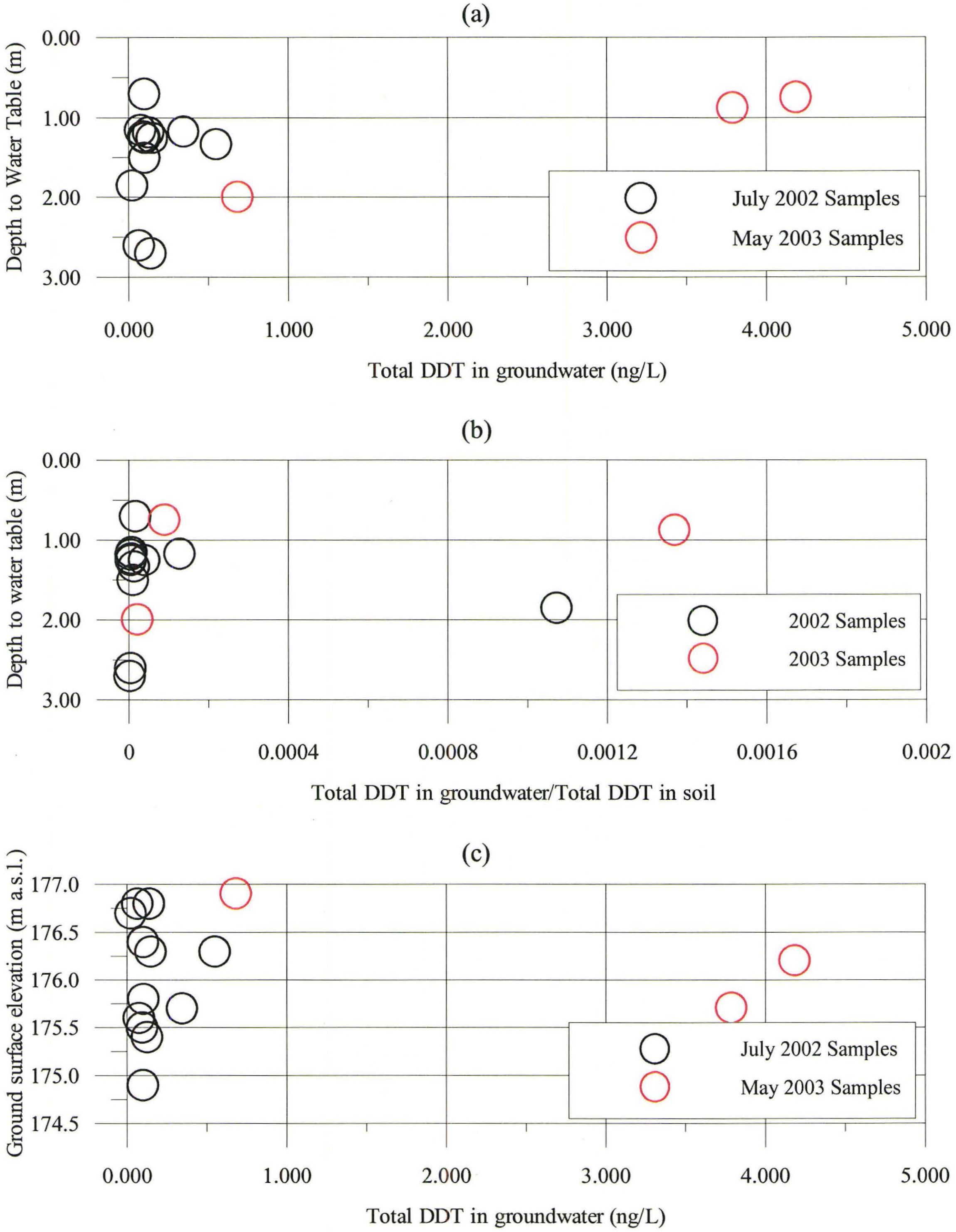

Figure 17. Relationship between (a) depth to water table and Total DDT in groundwater, (b) depth to water table and the ratio of DDT in groundwater to DDT in soil and (c) ground surface elevation and Total DDT in groundwater.

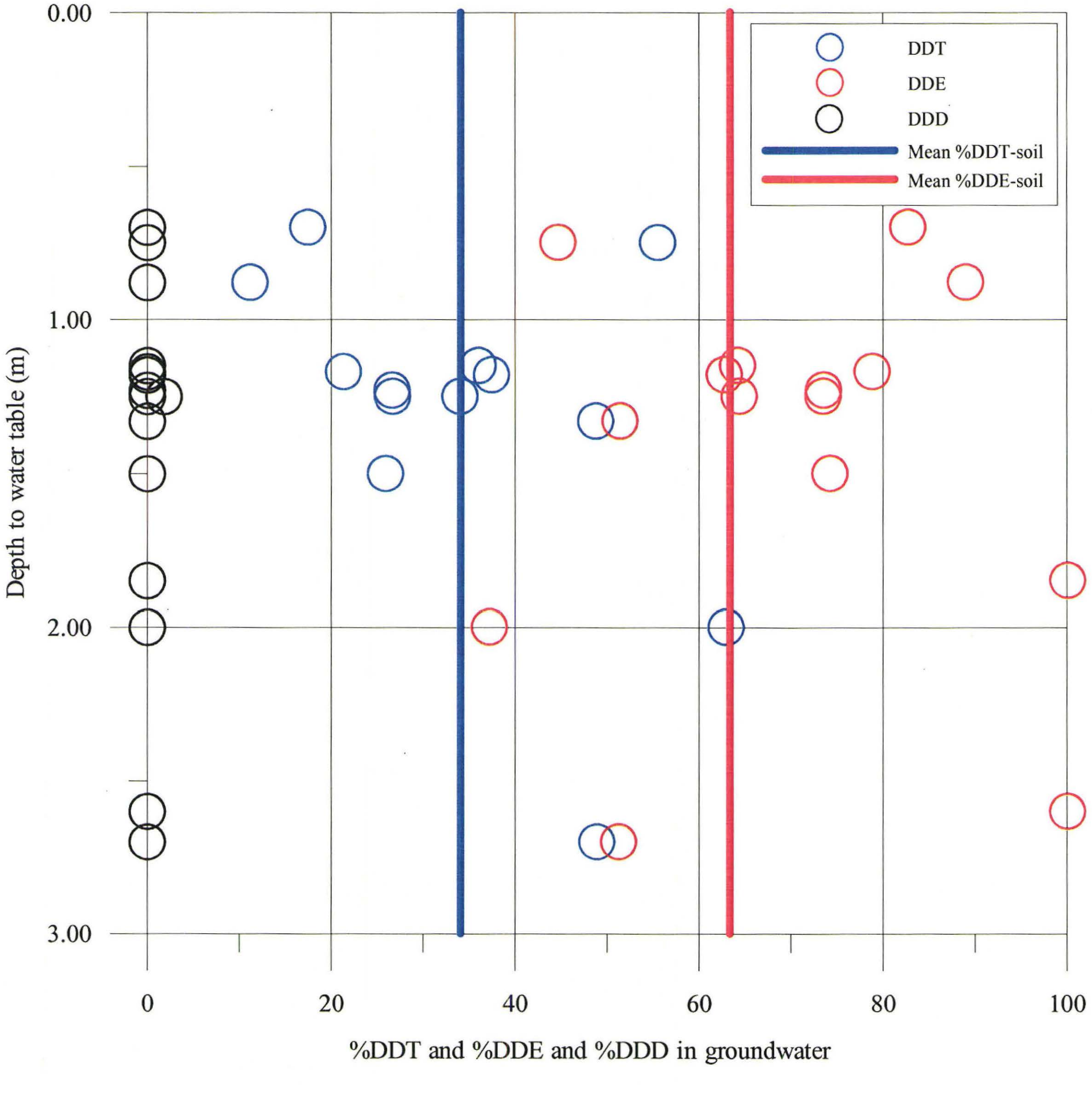

Figure 18. Relationship between depth to water table and %DDT, %DDE and %DDD in the July 2002 and May 2003 groundwater samples. Included are the mean %DDT and %DDE from all 68 shallow soil samples.

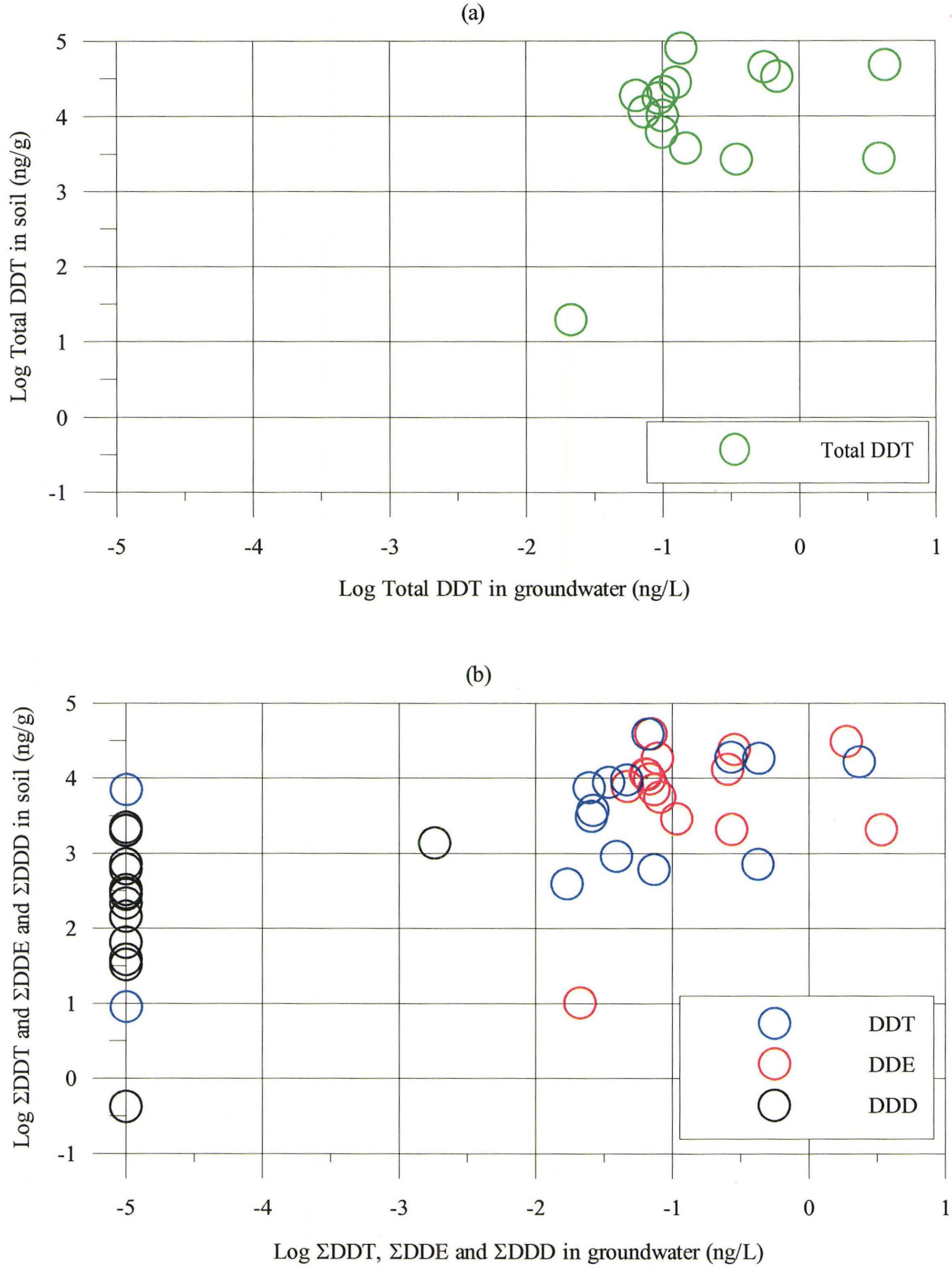

Figure 19. Relationship between (a) Log Total DDT in soil vs. log Total DDT in groundwater and (b) Log ΣDDT, ΣDDE and ΣDDD in soil vs. Log ΣDDT, ΣDDE and ΣDDD in groundwater. Values plotted at –5 represent analyses <IDL.

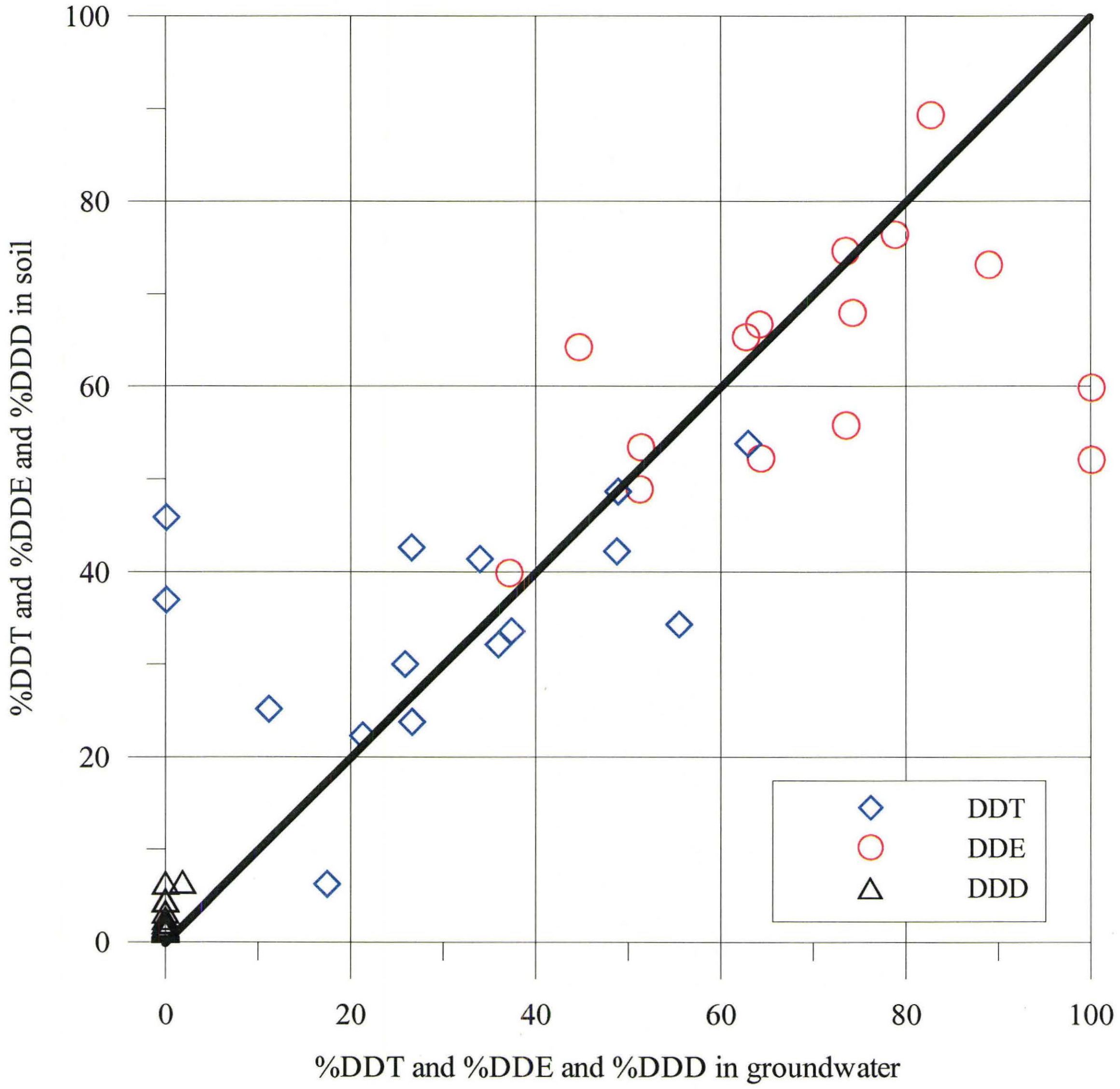

Figure 20. %DDT, %DDE and %DDD in soil vs. %DDT, %DDE and %DDD in groundwater. Included is the 1:1 relationship line between relative proportions in soil and groundwater.

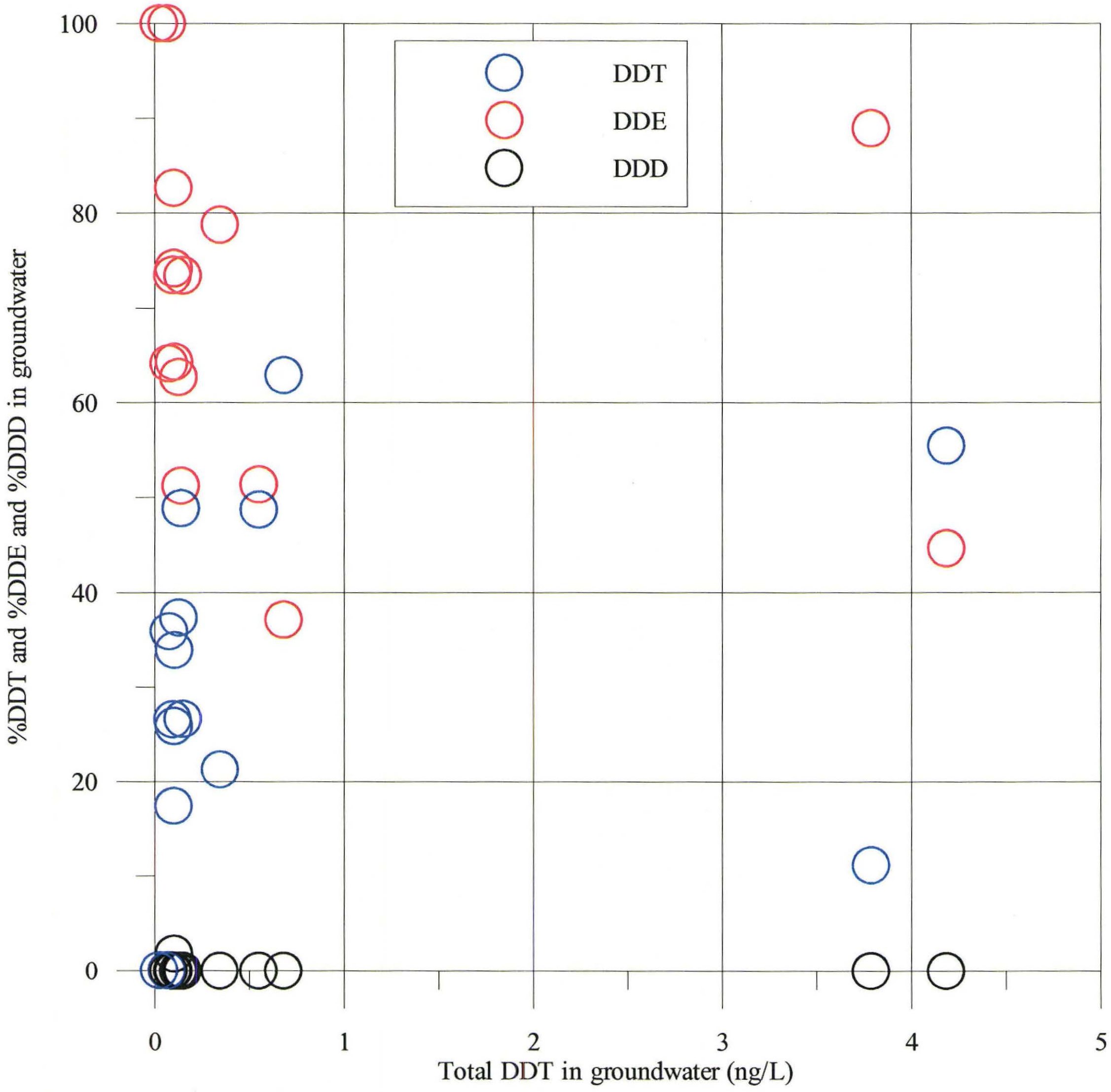

Figure 21. %DDT, %DDE, and %DDD in groundwater vs. Total DDT in groundwater for samples collected in May 2002 and July 2003.

CHAPTER 4: NUMERICAL MODELLING OF DDT TRANSPORT AND FATE AT PPNP

Many different physical, chemical and biological processes affect the migration, retention, and persistence of a pesticide in the subsurface. Field and laboratory studies are invaluable in understanding individual processes and the eventual impact of these processes or the complex interactions among processes and their effect on the fate of pesticide in the subsurface. But in some cases field and laboratory studies have limitations. For example, assessing the fate of pesticides over long periods of time and into the future; pesticide problems are often encountered for which the history of contamination and application are unknown; and field and laboratory studies can not assess the fate of pesticides in the subsurface under every possible soil, geological, hydrological, meteorological, and contaminant loading condition in a timely and practical manner. Numerical models offer an effective means of addressing many of these problems. When properly calibrated using site-specific data, models can provide insight into processes controlling pesticide fate and migration, and provide a basis upon which management decisions can be made.

Numerical modelling involves the representation of the physical, biological and chemical processes affecting the migration, retention and persistence of a contaminant in the subsurface with mathematical expressions. There are several types of numerical models that differ in the complexity of their description of processes occurring in the physical system or biological and chemical processes acting on the contaminant. Contaminant transport models have historically been developed for unsaturated and saturated conditions independently, primarily due to: (1) the different mathematical expressions for the flow of water within each region, (2) their numerical methods, and (3) the type of field information required for each is generally different.

Many numerical models have been developed specifically for simulating the leaching and fate of pesticides within a soil profile or unsaturated zone (Mutch et al, 1992). Most of these models simulate: (1) 1-D advective and 1-D or 2-D dispersive transport due to infiltration; (2) pesticide degradation by microorganisms; (3) pesticide sorption to mineral and organic matter; (4) volatilization; and (5) plant uptake (Wagenet and Rao, 1990). They are able to quantify the amount of pesticide in the aqueous, sorbed and vapour phases, calculate leaching rates, and present concentration with depth and over time. The most complex type of numerical model is a research model, which attempts to describe in detail all of the physical processes within the system and allow for a number of boundary and initial conditions to be employed (Mutch et al., 1993). They typically provide detailed quantitative output. However, this often comes at the expense of substantially long execution times, the requirement of very detailed input data that are often difficult and/or time consuming to measure, and long learning curves to properly use them. The pesticide model known as LEACHMP (Wagenet and Hutson; 1987) will be used to investigate the processes controlling DDT persistence in former orchard areas of PPNP and will be discussed in more detail in subsequent sections.

Unlike numerical models for simulating pesticide transport in the unsaturated zone, no saturated transport models have been developed specifically for pesticides. However, numerous numerical models are available that can simulate the transport and fate of a multitude of contaminants, which could include pesticides. Also unlike unsaturated zone pesticide transport models, saturated zone models simulate 2-D or 3-D advective and dispersive transport.

The processes affecting the transport and persistence of pesticides in the unsaturated zone are mostly the same in the saturated zone (i.e., advection, dispersion, diffusion, degradation, adsorption, etc.), and the mathematical relationships governing groundwater flow and solute transport in saturated zone is well known. Numerical modelling within the saturated zone is very well developed. Some of the principal differences between numerical groundwater models include the representation of boundary conditions (e.g., how the model simulates the water table, fluxes across the groundwater-surface water interface and transient changes in surface water body levels), the numerical methods used to solve groundwater flow equations (e.g., finite element, finite difference, integrated finite differences, boundary integral equation, analytic elements) and the contaminant fate and transport processes described within the model (e.g., adsorption, degradation, multiple solutes).

The GW-WETLAND model (Shikaze and Crowe, 1999; 2000; 2001; Crowe et al., 2004) will be used here because the mathematical framework on which the model is based is proven, and it can account for the complex boundary conditions that control the groundwater flow regime at PPNP (e.g., fluctuating water table, groundwater-surface water interaction, changing areal extent of the groundwater-surface-water interface) and incorporates reactive contaminant transport as well.

4.1 Model Description: LEACHMP

The LEACHM (Leaching Estimation And Chemistry Model) is a numerical model developed by Wagenet and Hutson (1987) to simulate the transport of agricultural chemicals through the vadose zone. The model has been released as several modules including LEACHMC, which simulates inorganic species, LEACHMB, which simulates subsurface microbial population dynamics, LEACHMN, which simulates nitrogen cycling, and LEACHMP (Leaching Estimation And Chemistry Model for Pesticides), which is used to simulate pesticide fate and transport in the subsurface. Because only LEACHMP will be used in this study, only this model will be discussed further.

LEACHMP incorporates detailed representations of the processes governing the leaching of up to 40 pesticides and daughter products through a heterogeneous vadose zone. Subsurface processes considered by the model include sorption, dissolution, volatilization, temperature dependent degradation, advective and dispersive transport, and heat flow (Wagenet, 1986; Wagenet and Hutson, 1987; Hutson, 2003). LEACHMP also accounts for factors affecting pesticide introduction to the subsurface such as plant processes and uptake, application methods and rates and timing, meteorological conditions, surface runoff, and agricultural land management practices. LEACHMP generates concentration and soil moisture profiles, time series plots, phase-partitioning information, and water and pesticide fluxes and storage for a soil profile. LEACHMP has been widely used and verified to model field-scale problems relating to both water movement and solute leaching through the vadose zone within the regulatory, agricultural, management and scientific communities (Jones, 1986; Priddle et al., 1988; Pennell et al., 1990; Boesten and van der Linden, 1991; Hutson and Wagenet, 1992, Mutch et al., 1992; Costa et al., 1994; de Jong et al., 1994; Brown et al., 1996; Caux et al., 1996; Guo et al., 1997; Roy et al., 2001; Paramasivam et al., 2002). Many of the processes accounted for by LEACHMP are employed in other models, such as PESTAN (Enfield et al., 1982; Ravi and Johnson, 1992), PRZM (Carsel et al., 1985), DRASTIC (Aller et al., 1987), SESOIL (Bonazountas and Wagner, 1984), VULPEST (Villeneuve et al., 1987, 1990), MACRO (Jarvis, 1995), but rarely to the same level of detailed mathematical description as in LEACHMP. When compared with models used by European regulatory agencies such as PESTLA, LEACHMP provided the most quantitative representation of field observations (Vink et al., 1997). LEACHMP has evolved over the past 15 years (Wagenet and Hutson, 1987, 1989; Hutson and Wagenet, 1992; Hutson et al., 1997; Hutson, 2003). The most current version of LEACHM (Version 4.0) was used for all numerical modelling conducted as part of this thesis.

4.1.1 Flow Representation

LEACHMP solves Richard's equation for the 1-dimensional (vertical) transient flow of water through a heterogeneous soil profile:

$$\frac{\partial \theta}{\partial t} = \frac{\partial}{\partial z}\left[K(\theta)\frac{\partial h}{\partial z}\right] - U(z,t) \tag{19}$$

where θ is the volumetric water content (-), t is time (days), z is depth (mm), $K(\theta)$ is the unsaturated hydraulic conductivity (mm/d), h is hydraulic head (mm) and U is a sink term representing water lost per unit time by transpiration (d^{-1}). Water fluxes in the soil profile are driven by transient or steady-state boundary conditions at the soil surface (rainfall, irrigation, potential evapotranspiration) and at the lower boundary (fixed matric potential, unit gradient drainage, fixed or variable water table, zero flux). The distribution of water within the soil profile is determined through a finite-difference solution to Equation 19.

The hydraulic head distribution and water content relationship at each depth within the soil profile is defined for each element using the Campbell (1974) model:

$$h = a(\theta / \theta_s)^{-b} \tag{20}$$

where h is the pressure potential (kPa), a is taken as the air entry value (kPa) and b represents the slope of the soil moisture characteristic curve (kPa), θ is the volumetric water content (-) and θ_s is the volumetric water content at saturation (-). Hutson and Cass (1987) added a wet end modification for pressure potentials between 0 and h_c where h_c represents the point of intersection of the exponential equation described by Campbell (1974), and the parabolic wet-end modification described by Hutson and Cass (1987):

$$h = \frac{a(1-\theta/\theta_s)^{1/2}(\theta_c/\theta_s)^{b}}{(1-\theta_c/\theta_s)^{1/2}} \tag{21}$$

$$h_c = a[2b/(1+2b)]^{-b} \tag{22}$$

$$\theta_c = 2b\theta_s/(1+2b) \tag{23}$$

where h is the pressure potential (kPa), a is the air entry value (kPa), b is the slope of the soil moisture characteristic curve, θ is the volumetric water content (cm^3/ cm^3), θ_s is the volumetric water content at saturation (cm^3/ cm^3), θ_c is the water content (cm^3/ cm^3) at the point of intersection of the two curves, and h_c is the pressure potential (kPa) at the same point of intersection. A separate equation employing the same constants relates the unsaturated hydraulic conductivity ($K(\theta)$) and retentivity to the matric potential using the function proposed by Campbell (1974):

$$K(\theta) = K_s(\theta/\theta_s)^{2b+2+p} \tag{24}$$

where $K(\theta)$ is the unsaturated hydraulic conductivity (mm/day) at a water content θ, K_s is the saturated hydraulic conductivity at saturation θ_s (mm/day), and p is a pore interaction parameter (-) used to scale the hydraulic conductivity function.

The version of LEACHMP used for this study incorporates two-region flow that accounts for both macropore flow and flow through the porous media matrix, however, this was not employed because the model domain consists of medium grained sand (porous medium), and generally lacks structure. LEACHMP also includes a surface runoff routine, but it was not used because the ground surface is essentially flat and the soils are highly permeable in the vicinity of CHO and SHO (Marenco, 2002), and no surface runoff was observed at PPNP.

4.1.2 Solute Transport

Solute transport and reactions are calculated using a finite-difference solution to the advective-dispersion equation (Hutson, 2003):

$$\frac{\partial C_L}{\partial t}(\rho_B K_D + \theta + \varepsilon K_H) = \frac{\partial}{\partial z}\left[\theta D_D(\theta,q)\frac{\partial C_L}{\partial z} - qC_L\right] \pm \Phi \qquad (25)$$

where C_L is the solution concentration (mg/dm^3), ρ_B is the soil bulk density (kg/dm^3), K_D is the partition coefficient (dm^3/kg), θ is the volumetric water content (cm^3/cm^3), ε is the gas-filled soil porosity (cm^3/cm^3), K_H is the Henry's Law constant (-), $D_D(\theta,q)$ is the apparent diffusion coefficient (mm^2/day), q is the macroscopic water flux across a compartmental boundary (mm/day), and Φ is a source/sink term (mm/day). The water flux term (q) and the soil moisture content (θ) are calculated from the Richards equation and the Campbell equation, respectively, defined above.

Hydrodynamic dispersion is simulated through user to input diffusion and dispersion coefficients for both dissolved and vapour phases (Guo et al., 1997). Numerous flexible upper and lower boundary conditions make this model very flexible, although the short time steps precipitate longer computing times. Gas phase transport by diffusion is also simulated within the volatilization and transport modules.

4.1.3 Sorption

Adsorption is represented in LEACHMP using linear, Freundlich or Langmuir sorption isotherms that instantaneously achieve phase equilibrium and partition pesticides accordingly. Chemical equilibrium changes as a function of temperature within LEACHMP. The model also has the ability to attribute different sorption properties to each compound present, permitting the application of this model to multiple solutes that are not equally sorbed to organic carbon, as in the case of DDT compounds.

4.1.4 Degradation and Transformation

LEACHMP creates pesticide daughter products through both transformation and degradation reactions. Hutson (2003) defines a transformation reaction as a loss of a given species following first-order kinetics, with the product able to be defined as a source of another chemical species, which in turn, can undergo further reactions. Transformation rates can also be adjusted according to water content and temperature. Hutson (2003) defines a degradation reaction as loss of a given species following first-order kinetics, but, the mass of degradation products cannot be tracked. In addition, degradation reactions are insensitive to changes in soil moisture and temperature.

The degradation and transformation of pesticides in LEACHMP is simulated as a sink term in the advective-dispersion equation, using the exponential decay function:

$$C_t = C_0 e^{-kt} \tag{26}$$

where C_t is the concentration at a given time t (mg/kg), C_0 is the initial concentration (mg/kg) at time t_0, and k is the degradation or transformation rate (day^{-1}). The degradation pathways are specified by rate constants for each chemical and can be linked in series, where a degradation product of one reaction becomes the source for the ensuing reaction. Degradation of several different pesticides can also be simulated in parallel, where degradation of one species is independent of the presence of other species, although the separate parallel degradation pathways cannot be linked together. Additionally, transformation and degradation may be applied to both solution and sorbed phases. Some additional capabilities offered by recent versions allow for the simulation of biological degradation following Monod kinetics and degradation in multiple phases.

An important capability for shallow soil environments is the ability to adjust degradation rates according to both temperature and moisture conditions within the soil profile, using a heat balance approach. Accounting for temperature and saturation effects on degradation is often overlooked by simpler models, resulting in degradation, which is often faster under moist conditions, occurring at equivalent rates at residual water content. This has potentially large consequences for environments where the surficial soil remains dry for much of the year and would result in an overestimation of the degradation of pesticides if this mechanism was not employed.

4.2 Simulation of DDT Transport to the Water Table at PPNP

LEACHMP was used to simulate leaching, distribution, and degradation of DDT, DDE and DDD through both a Melanic Brunisol and Gleyed Melanic Brunisol soils at PPNP. Simulations focused on the soil profile at CHO because soil properties at CHO, SHO and AO were very similar, and the water table was deepest at CHO. Because CHO was the focus of previous work, (Badley, 2003; Marenco, 2002), additional field data was available to support the numerical modelling. Simulations were also undertaken at SHO because it represents a site having a different organic carbon distribution with depth and a water table closer to ground surface. The focus of the simulations was to evaluate the relative importance of different soil and hydrologic factors and land management practices on DDT leaching and persistence at PPNP.

Because both the exact DDT application history and amount of DDT applied within PPNP are unknown, two end members representing the earliest (1950) and latest (1970) dates of probable DDT application were utilized as starting dates for the simulations. Application rates were based on the Best Management Practices recommended by the Ontario Ministry of Agriculture and Food for recommended DDT application rates for use in apple orchards from 1949 to 1972 (OMAF, 1975). According to PPNP staff, 1970 corresponds to last DDT application within the park (Dan Rieve, pers. comm., 2003). These dates of application yield an extreme range of possible outcomes for DDT transport and persistence at PPNP. Thus, if the true application history were known, the outcome would fall within this range of possibilities. The application rate used for the initial calibration stage was 100 mg/kg applied as 95.3% DDT, 4.3 %DDE and 0.4% DDD within the uppermost 5 cm of the Ah horizon.

The physical properties of the soil profile and values assigned to model flow parameters are presented (Table 22).

Table 22: Soil properties and flow parameter values used in LEACHMP simulations.

Parameter	Units	Final Values Used	Measured Value / B.A.V.	Source
Soil Profile				
% Sand	%	96 - 99	96 - 99	Measured
% Silt	%	0.63 - 2.9	0.63 - 2.9	Measured
% Clay	%	0.05 - 0.68	0.05 - 0.68	Measured
% Organic carbon	%	0.23 - 1.80	0.23 - 1.80	Measured
Initial soil temperature	°C	9.2	9.2	30 yr. mean air temperature
Bulk Density	kg/dm^3	1.2 - 1.60	1.2 - 1.60	Measured
Particle Density	kg/dm^3	2.65	2.65	Brady and Weil (2002)
Density of Organic Matter	kg/dm^3	1.6	1.6	Brady and Weil (2002)
Depth to water table	mm	2000	2000	Measured
Water Flow				
Air entry value - Ah horizon	kPa	-0.32	-0.26	Marenco (2002), F.P.
Air entry value – B+C horizon	kPa	-0.56	-0.46	Marenco (2002), F.P.
Campbell's b - Ah horizon	-	1.48 - 1.80	2.73	Marenco (2002), F.P.
Campbell's b – B+C horizon	-	1.20 - 1.30	1.91	Marenco (2002), F.P.
Ksat - Ah horizon	mm/day	1728	297 (K_{fs})	Measured, F.P.
Ksat - B+C horizon	mm/day	3456	1884 (K_{fs})	Measured, F.P.
P-Pore interaction parameter	-	-0.3		F.P.
Daily total precipitation	mm/day	PPNP data		Measured
Weekly estimated PET	mm	Thornthwaite method		Thornthwaite method

F.P. – Used as a fitting parameter with initial values based on field measurements and/or best available literature values.
B.A.V. – Best available literature value.

4.2.1 Values Assigned to the Model Parameters:

Values assigned to the chemical and physical parameters were obtained from data measured under the same field conditions being simulated at PPNP and supplemented by values obtained from a substantial literature review. In the case of fitting parameters, initial input values were based on previously measured data or best available literature values where possible and modified thereafter to match field data.

4.2.2 Space and Time Discretization Parameters:

The four distinct soil horizons observed (Of, Ah, Bm and C) formed the basis for the model conceptualization. Only two layers, (1) the organic rich Ah horizon from 0 to 30 cm below surface and (2) the Bm and C horizons from 35 cm to the bottom of the profile at 200 cm, were considered to be significantly different from one another, based on organic carbon content (Table 12), porosity (Table 13) and field saturated hydraulic conductivity (Table 14) differences with depth. At CHO, the soil profile was divided into 40 compartments of 5 cm each to represent the 2 metre profile from ground surface to the water table, and the profile thickness remained constant during a simulation. Additional simulations conducted at SHO employed 12 soil compartments of 5 cm thickness each to represent a fixed distance of 60 cm from ground surface to the water table.

The simulation time steps were kept short to prevent numerical error (Mutch et al., 1993). The initial time step was 0.1 day and the maximum allowable time step was set at 0.1 day according to recommendations made by Hutson (2002).

4.2.3 Soil Hydraulic Properties

The soil profile flow domain is comprised of aeolian sands having Ah, Bm and C horizons with heterogeneous soil and hydraulic properties. The Of horizon was considered part of the Ah horizon within the model because no field measurements of soil properties were taken within the Of horizon, which was only 7 cm thick. At CHO, the mean of the log-transformed K_{fs} value for the entire CHO soil profile, 1.68 x 10^{-3} cm/s (Table 14) was used as a starting value throughout the profile, and was subsequently changed as a fitting parameter with best model fits achieved when hydraulic conductivity was 2.00 x 10^{-3} cm/s within the Ah horizon and 4.00 x 10^{-3} cm/s within the Bm and C horizons. This is consistent with current and former studies. Field measurements of K_{fs} at the CHO soil profile show K_{fs} for the Ah horizon to be 3.44 x 10^{-4} cm/s and 2.18 x 10^{-3} cm/s for the Bm and C horizons (Table 14). Marenco (2002) reported a mean for log-transformed field saturated hydraulic conductivity of 8.31 x 10^{-3} and 1.05 x 10^{2} cm/s in shallow and deep soils, respectively, near CHO. Badley (2003) reported a log-transformed mean K_{fs} values between 1.3 x 10^{-2} and 7.1 x 10^{-3} cm/s, also near CHO, and noted hydraulic conductivity was higher within the Bm horizon than the Ah horizon. Crowe et al. (2004) have reported K_s values ranging from 0.91 x 10^{-2} to 4.6 x 10^{-2} cm/s for aeolian sands at PPNP as determined using ex-situ falling head tests.

Soil moisture retention parameters (Campbell's a, b, and p parameters) required by LEACHMP were converted from Marenco's (2002) calculation of soil retention parameters fit by the van Genuchten-Mualem retention curve model. Marenco (2002) obtained the pressure head – water content data from laboratory measurements using the pressure plate apparatus with soil cores from within 50 metres of the soil profile under study. Campbell's (1974) retentivity function was used to fit known volumetric soil moisture and pressure head measurements for each horizon. The Of layer was included as part of the Ah layer for the purposes of generating soil moisture characteristic curve parameters because the Of layer is very thin (5 cm) and the contrast in hydraulic parameters between the Of horizon and the remainder of the Ah horizon would generate artificial capillary barrier effects. Figure 22 illustrates the modelled soil moisture characteristic curves for each horizon at CHO, and a comparison to Marenco's (2002) data. The difference in water retention parameters can be partly attributed to the fact that Marenco determined moisture retention data based on the main drainage curve, and not the main wetting curve. Thus, hysteresis could contribute to the difference. It should be noted that the water content drops very rapidly with small changes in pressure head for all 3 depths plotted.

The initial volumetric water content throughout the soil profile for the calibration of LEACHMP was arbitrarily set to 10% VWC. Because the calibration of the model was for an 8 year period of time and actual water content in the soil profile rapidly changes on a daily basis, the initial VWC assigned will have no impact on simulated VWC beyond a few simulation days.

Hydraulic conductivity and Campbell's parameters were subsequently used as fitting parameters during the calibration of the flow solution (Table 22) and thus, were slightly modified from the lab-measured values and will be discussed below in the flow calibration section. The unsaturated hydraulic conductivity function employed in LEACHMP simulations is presented in Figure 23.

For simulations conducted at SHO, the same values assigned to Ah and Bm horizons at CHO were assigned to the Ah and Bmgj horizons at SHO. However, the Ah horizon is somewhat thinner at SHO (20 cm thick instead of 30 cm thick) and the C horizon is absent at SHO (Figure 6).

4.2.4 Boundary Conditions for Water Flow

The upper flow boundary condition was specified as a variable flux boundary condition representing infiltration. The lower boundary condition was set as a permanent water table, according to Hutson (2003), whereby the pressure potential of the lowest node is fixed. The water table fluctuates by almost 1 m between spring and the rest of the year (Crowe et al., 2004). However, the depth to the water table was set at 2.00 m because it was measured depth at CHO on May 12th, 2003, and this date is used to calibrate the modeled moisture content against measured moisture contents. Also, the high water table during the spring is due to a rapid infiltration of snow melt, and it subsequently rapidly declines (Crowe et al., 2004). In addition, allowing a fluctuating water table within LEACHMP is not recommended when simulating solute transport as the magnitude and direction of water flux densities in the saturated zone may fluctuate considerably (Hutson, 2003). This flow boundary condition was used in all simulations.

4.2.5 Meteorological Data

Meteorological data (daily total precipitation, daily mean temperature, minimum and maximum temperatures) collected from nearby Leamington (~5 km from PPNP) from 1950 to 1974 and from an Environment Canada weather station within PPNP for the period from 1974 to 2003 was used to construct the flux across the upper boundary condition (Figure 24a). Data was rarely missing from a given station; however, when absent it was substituted with data from nearby Kingsville (~15 km from PPNP). Daily precipitation, times and surface flux densities were input along with mean weekly temperatures and weekly amplitude of temperature fluctuations. Surface flux densities were calculated as 4 times the magnitude of the precipitation event (Mutch et al., 1993), which corresponds to a 6 hour long precipitation event. The time at which individual precipitation events began were often not recorded, especially prior to automation and thus, all precipitation was applied at 6 a.m. Rainfall data was preprocessed to account for storage of water as snow on the ground surface when weekly mean temperatures were below 0°C seen as gaps during the winter (Figure 24b). All stored water was applied as precipitation after one week of daily mean temperatures above 0°C each year. For years with substantial storage of water as snow on the ground surface, the spring infiltration event was extended over 2 days to minimize mass errors. Otherwise, all of the snow melt would not infiltrate prior to the next precipitation event.

Before entering meteorological data into LEACHMP, recorded daily temperatures were converted into monthly mean temperatures to estimate the monthly potential evapotranspiration using the Thornthwaite (1948) method for a grass-covered field:

$$E_T = 1.62\left(\frac{10\,T_{ai}}{I}\right)^a \tag{27}$$

$$I = \sum_{i=1}^{12}\left(\frac{T_{ai}}{5}\right)^{1.5} \tag{28}$$

$$a = 0.492 + 0.01791I - 0.0000771I^2 + 0.000000675I^3 \tag{29}$$

where E_T is the potential evapotranspiration (cm/month), T_{ai} is the mean monthly air temperature in °C for month i, I is the annual heat index, and a is constant. This method assumes 12 hours of sunshine each day for 30 days each month. The latitude correction factor was applied to arrive at values to be used in field simulations.

The monthly potential evapotranspiration values were then converted to weekly values and input into the model by dividing monthly potential evapotranspiration by the number of days in the month. During the winter months, where recorded monthly temperatures were below 0°C, evapotranspiration was set to 0 based on the assumption that no plant growth would take place (Figure 24).

4.2.6 Soil Physical Properties

Measured and best-estimates of physical and chemical parameters for each soil profile were applied to each element within a given horizon. Physical properties of each element were based on field data for the CHO soil profile. After statistical comparison of soil properties between CHO, SHO and AO, it was determined that for the additional simulations conducted at SHO, soil properties need not be changed because there were no statistical differences between sites relative to any soil properties measured in the field and/or laboratory. Although small variations in bulk density (<0.10 g/cm^3) were observed in field data, bulk density for the Bm and C horizons within the model was assigned the mean of lab measured values (1.48 g/cm^3) to prevent capillary barrier effects (Table 13). A bulk density value of 1.60 g/cm^3 measured at the water table at 2.00 m was also used and a gradual transition from 1.48 g/cm^3 to 1.60 g/cm^3 was implemented over the bottom 20 cm of the profile to avoid capillary barrier effects deep in the profile.

4.2.7 Initial Soil Concentrations of DDT, DDE and DDD

The simulated profile was initially free of DDT, DDE and DDD, with the exception of the uppermost soil segment (0-5 cm), within which technical grade DDT (95.3% DDT: 4.3% DDE: 0.3% DDD) was applied at the beginning of each simulation (either 1950 or 1970). Although no additional DDT, DDE or DDD was applied during the remainder of the calibration simulations, DDT was introduced into the upper most cell during several of the scenario simulations.

4.2.8 Boundary Conditions for Solute Transport

The upper boundary condition for DDT, DDE and DDD was a no flux boundary, whereby no additional pesticide was added during a simulation. The lower boundary condition at the water table was a variable flux boundary that allowed DDT to pass directly across the water table.

4.2.9 Molecular Diffusion Coefficients

Diffusion coefficients for both air and water were obtained from the CRC Handbook Physical Properties of Organic Chemicals (Howard and Meylan, 1997) for each of DDT, DDE and DDD. The diffusion coefficients for DDT, DDE and DDD in air and water are presented (Table 23). Because LEACHMP requires only one diffusion

Table 23. Initial values assigned to solute transport parameters employed in LEACHMP.

Solute Transport Parameters	Units	Initial Value	Justification or Source
Chemical Parameters			
Molecular diffusion coefficient (water)	mm^2/day	44.84	Howard and Meylan (1997)
Molecular diffusion coefficient (air)	mm^2/day	1.296×10^5	Howard and Meylan (1997)
Barometric enhancement	mm^2/day	0	DDT compounds have low volatility
Dispersivity	mm	100	Domenico and Schwartz (1998)
Aqueous solubility - DDT	mg/dm^3	2.50×10^{-2}	Howard and Meylan (1997)
Aqueous solubility - DDE	mg/dm^3	1.20×10^{-1}	Howard and Meylan (1997)
Aqueous solubility - DDD	mg/dm^3	9.00×10^{-2}	Howard and Meylan (1997)
Vapour density - DDT	mg/dm^3	3.10×10^{-6}	Howard and Meylan (1997)
Vapour density - DDE	mg/dm^3	1.03×10^{-4}	Howard and Meylan (1997)
Vapour density - DDD	mg/dm^3	1.17×10^{-5}	Howard and Meylan (1997)
K_{oc} - DDT	L/kg	3.1×10^5	De Bruijn et al. (1989) and Karickhoff (1981), F.P.
K_{oc} - DDE	L/kg	3.4×10^5	De Bruijn et al. (1989) and Karickhoff (1981), F.P.
K_{oc} - DDD	L/kg	6.4×10^4	De Bruijn et al. (1989) and Karickhoff (1981), F.P.
Transformation Parameters			
Transformation Rate – DDT	day^{-1}	Various	Marenco (2002), F.P.
Transformation Rate – DDE	day^{-1}	Various	Marenco (2002), F.P.
Transformation Rate – DDD	day^{-1}	Various	Marenco (2002), F.P.
Degradation Rate – DDT	day^{-1}	Various	Marenco (2002), F.P.
Degradation Rate – DDE	day^{-1}	Various	Marenco (2002), F.P.
Degradation Rate – DDD	day^{-1}	Various	Marenco (2002), F.P.
Max. water content: Air filled porosity	cm^3/cm^3	0.08	Calculated from field data
Rate constant adjustment per 10 °C	-	3	Recommended by Hutson (2003)
Optimum temperature	°C	35	Recommended by Hutson (2003)
Maximum temperature	°C	50	Recommended by Hutson (2003)
Min. water content: Matric potential	kPa	-300	Recommended by Hutson (2003)
Min. matric pot. for transformation	kPa	-1500	Recommended by Hutson (2003)
Relative transformation rate at sat'n	-	1.0	Recommended by Hutson (2003)
Land Management Parameters			
Initial profile concentrations	mg/kg	0	Not previously applied
Pesticide applications	mg/m^2	1950, 1970	PPNP records (earliest, most recent)
Depth of incorporation	mm	0	DDT was applied at surface
Cultivation	mm	0	No evidence of tillage in soil profile
Initial application rate	mg/kg	100	Fitting estimate

F.P. – Used as a fitting parameter with initial values based on field measurements and/or best available literature values.
B.A.V. – Best available literature value.

coefficient in air and one for water, arithmetic means of the diffusion coefficients for DDT, DDE and DDD in air and water were used. No barometric enhancement was employed throughout the simulations because aged DDT, DDE and DDD are not volatile.

4.2.10 Solubility

Solubility values for DDT, DDE and DDD were taken from the CRC Handbook Physical Properties of Organic Chemicals (Howard and Meylan, 1997) and are presented in Table 23. These values were selected over those reported to have the best QA/QC ranking by Pontolillo and Eganhouse (2001) because only a value for DDT and none for DDE and DDD were reported. Howard and Meylan (1997) provided solubility values for all 3 compounds.

4.2.11 Vapour Density

The arithmetic means of the vapour pressures of o,p'- and p,p'- isomers for each of DDT, DDE and DDD at 20°C as taken from the CRC Handbook of Physical Properties of Organic Chemicals (Howard and Meylan, 1997) were subsequently converted to vapour density (*V_d*) values for input into LEACHMP as follows:

$$V_d = \frac{P \times M}{R \times T} \tag{30}$$

where *P* is the vapour pressure (mm Hg), *M* is the molecular weight of the compound (g/mol), *R* is the universal gas constant ($\mathrm{L \cdot atm \cdot mol^{-1} \cdot K^{-1}}$) and *T* is temperature (°K).

Table 24. Reported vapour pressures and calculated vapour densities for DDT, DDE and DDD at 20 °C.

Compound	Vapour Pressure @ 20°C (atm)	Vapour Density @ 20°C (mg/dm^3)
DDT	2.1×10^{-10}	3.1×10^{-6}
DDE	7.9×10^{-9}	1.03×10^{-4}
DDD	8.8×10^{-10}	1.17×10^{-5}

4.2.12 Sorption-K$_{oc}$

Because K_{oc} values for DDT, DDE and DDD, and the experimental conditions under which they were determined are rarely reported, K_{oc}'s for DDT, DDE and DDD were calculated using the relationship between K_{ow} and K_{oc} by Karickhoff (1981):

$$\log K_{OC} = 0.989 \times \log K_{OW} - 0.346 \qquad (31)$$

This relationship was derived for a number of hydrophobic organic pollutants of high molecular mass with aqueous solubility values < 10^{-3} mol/L (such as DDT) and for geologic materials with < 3 % organic carbon content, making it the best to use at PPNP. At CHO, the organic carbon content lies between 0 and 1.80 %, which is consistent with the conditions for which the sorption properties were determined. Values of K_{ow} reported by de Bruijn et al. (1989) were selected because they received the highest QA/QC ranking by Pontolillo and Eganhouse (2001). The values used within LEACHMP for K_{ow} and calculated for K_{oc} are presented in Table 25.

4.2.13 Isotherm Type

No sorption studies have been conducted at PPNP, and laboratory studies reported in the literature are often conducted using "fresh" technical grade DDT (Kan et al., 1998;

Table 25. Octanol-water partition coefficients (K_{ow}) and organic carbon partition coefficients (K_{oc}) for DDT, DDE and DDD.

Compound	Log K_{ow} [a] (L/kg)	Log K_{oc} [b] (L/kg)	K_{oc} (L/kg)
DDT	6.914	6.492	3.1×10^6
DDE	6.956	6.533	3.4×10^6
DDD	6.217	5.803	6.4×10^5

a. Taken from de Bruijn et al. (1989).
b. Calculated using equation proposed by Karickhoff (1981).

Van den Hoop et al., 1999). It has also been reported that as hydrophobic compounds age, their sorption properties often change (Luthy et al., 1997; Pignatello and Xing, 1996). Because the concentrations of dissolved DDT compounds are extremely low, and the corresponding lack of a direct correlation between DDT concentrations in both soil and water and %OC in soil, a linear sorption isotherm was implemented for DDT, DDE and DDD. The lack of correlation between %OC and concentrations of DDT in soil indicates that all sorption sites on the organic carbon have not been filled. While it is expected that the sorption behaviour of DDT will be different at higher concentrations as is often reported in the literature (Huang and Weber, 1998), there is no field data from PPNP to justify the selection of a non-linear model.

4.2.14 Crop Parameters

Because DDT has a low volatility, low solubility, and high K_{oc}, uptake and transpiration of DDT compounds by plants is not likely to be a significant pathway for DDT removal from shallow soils. Thus, crop growth and pesticide uptake by plants is not simulated. Transpiration of water by plants is accounted for by estimating potential evapotranspiration using the Thornthwaite method with grassland-specific plant parameters. Land-management practices including cultivation and additional chemical applications were not implemented during the calibration procedure, although scenario testing employing different land management practices was conducted.

4.2.15 Transformation Pathways and Rate Constants

Transformation and degradation rate constants were adjusted during the calibration process; however, initial values were based on the results Marenco (2002). These are rough estimates because Marenco (2002) matched relative proportions of DDT:DDE:DDD to an exponential decay model that assumed DDT was applied in 1970 and degraded according to first-order decay with no seasonal rate variation due to temperature and moisture contents. The LEACHMP simulations account for seasonal rate variation due to temperature and moisture contents

The capability of LEACHMP to consider the effects of temperature and moisture content variations was employed as the transformation and degradation rates were adjusted during model calibration. Three of the most likely transformation/degradation pathways for DDT at PPNP were investigated as follows:

$$\textit{Pathway \#1} \quad \begin{tikzcd} DDT \arrow[r] \arrow[d] & DDE \\ DDD & \end{tikzcd} \tag{32}$$

$$\textit{Pathway \#2} \quad \begin{tikzcd} DDT \arrow[r] \arrow[d] & DDE \arrow[r] & DDE - X \\ DDD & & \end{tikzcd} \tag{33}$$

$$Pathway\,\#3 \quad \begin{tikzcd} DDT \arrow[r] \arrow[d] & DDD \arrow[r] & DDD - X \\ DDE \end{tikzcd} \tag{34}$$

These three pathways were employed during the solute transport calibration and provide the basis for the simulations discussed throughout this chapter.

4.2.16 Output and Summary File Parameters

LEACHMP was set to print output parameters for the calibration of the solute transport module in mg/m^2 for all summary (*.SUM) files, and in µg/kg, µg/L, ng/L for sorbed, aqueous and vapour phases in the output (*.OUT) files. The units in which data are displayed are always printed above the values for each output and summary file. For the summary files, depths of interest were specified as 200, 500 and 1500 mm below surface, corresponding to depths within the Ah, Bm and C horizons. These depths provide the basis for all time-series plots generated from calibration/simulation outputs.

4.3 LEACHMP Model Calibration

Calibration of a numerical model is undertaken to demonstrate that the model is capable of reproducing field-measured data. This is accomplished by assigning a set of parameters and boundary conditions that reproduce simulated heads, water contents, and fluxes that match field-measured data within a pre-established range of error (Anderson and Woessner, 1992). Calibration of LEACHMP was undertaken by first calibrating to soil moisture content in the soil profile and secondly calibrating the pesticide distribution within the profile. All simulation names coincide with LEACHMP file names.

4.3.1 Flow Calibration: January 1, 1995 to September 30, 2003

The flow solution at CHO was first calibrated against field measured volumetric soil moisture profiles for the short period from January 1, 1995 to September 30, 2003 because (1) there is only one measurement of volumetric soil moisture content with depth at CHO on May 12, 2003, (2) given the high hydraulic conductivity and porosity, the volumetric water content is likely to change and equilibrate rapidly, and (3) computing time during the flow calibration process was thus minimized. Thus, results of the simulation were calibrated against the measured volumetric soil moisture profile of May 12, 2003. The soil moisture characteristic curve parameters measured by Marenco (2002) were used as an initial starting point but were subsequently adjusted by reducing the value of Campbell's b parameter incrementally until moisture content profiles had the same shape as field data, yet remained reasonable for the soil under consideration. Air entry values were kept as the values determined by Marenco (2002). The field-saturated hydraulic conductivity values as determined at CHO on May 12, 2003 were input as saturated hydraulic conductivity values, with increased hydraulic conductivity below the Ah horizon. During the calibration process, the hydraulic conductivity functions were scaled by altering Campbell's pore interaction parameter from 1.0 (the default value) to -0.3, which provided a much better fit to field data and retained the shape of field measured profiles. It was also observed that the moisture profile changed as expected in response to the transient atmospheric upper boundary condition.

A comparison between simulated and measured volumetric soil moisture (Figure 25a) content for the CHO profile was quantified using root mean squared error (*RMSE*):

$$RMSE = \left[\frac{1}{n} \sum_{i=1}^{n} (P_i - M_i)^2 \right]^{1/2} \tag{35}$$

where i is the measurement depth, n is the number of depths sampled, M_i is the measured average for the i^{th} depth, and P_i is the predicted value at the i^{th} depth. The RMS error for the 1995 - 2003 calibration period was 0.0164 ($n = 8$), or 1.64% volumetric soil moisture content. This is a relatively good fit to measured data, where volumetric soil moisture at CHO showed a range of 24.35% (8.15% - 32.50%) on May 12, 2003 (Table 13).

4.3.2 Flow Calibration: January 1, 1950 to September 30, 2003

The calibration period was extended backwards in time to include the earliest probable date that DDT would have been applied within PPNP; January 1, 1950, and extended to September 30, 2003. Again, results of the simulations were calibrated against the one measured volumetric soil moisture profile of May 12, 2003. Values of the model parameters obtained in the best-fit simulation of the January 1, 1995 to September 30, 2003 calibration were used as initial starting values and no changes to the soil and hydraulic parameters were necessary in order to calibrate the flow solution. Only meteorological data from January 1, 1950 to December 31, 1994 was added. The calculated RMS error values with respect to volumetric moisture contents within the soil profile were calculated to be 0.016439 (n=8) for the long-term simulation, consistent with that observed for the short-term flow calibration. The measured and simulated volumetric soil moisture profiles at CHO for May 12, 2003 are presented in Figure 25a. The rapid change in water contents within the soil profile (especially the shallow regions) was verified following initial calibration by observing that the %VWC changed daily and responded to precipitation events and dry spells within a 1-2 day time frame. A plot of %VWC versus depth for a number of consecutive days is presented in Figure 26. A comparison of modelled and measured volumetric water contents illustrates that the model adequately represents flow processes occurring in the natural system (Figure 27). A plot of a large precipitation event on July 17, 1989 illustrates the migration of water through the soil profile under gravity drainage over a 3-4 day period (Figure 28), and thus, infiltrating waters will reach the water table within a 3-4 day time frame. CHO flow parameters were also implemented at SHO (Figure 25b) and although the measured and modelled volumetric soil moisture profiles do not compare as well as at CHO, it is acceptable. The main differences between CHO and SHO include the organic carbon content and hydraulic conductivity profiles as well as vegetation, which is grass at CHO and trees at SHO. In reality, the differences will affect soil moisture, but the model shows that they do not significantly affect the volumetric soil moisture content. Flow parameters for the calibrated best-fit were utilized for the remainder of the simulations and no flow parameters were changed during solute transport calibration simulations. Sensitivity analyses for flow parameters were carried out and are discussed later.

4.3.3 Solute Transport Calibration

Calibration of solute transport was undertaken for each degradation pathway and timeline in four steps to match: (1) relative proportions of DDT, DDE and DDD within the entire CHO soil profile as on May 12, 2003; (2) DDT/DDE and DDT/DDD ratios within shallow and deep soils at CHO as on May 12, 2003; (3) concentrations and distribution of DDT, DDE and DDD present in the CHO soil profile as shown as on May 12, 2003; and, (4) concentrations of Total DDT in groundwater at CHO as on May 12, 2003. All solute transport simulations employed the previously calibrated flow solution with no further alteration of flow parameters.

In each simulation, the entire amount of DDT, DDE and DDD applied was set as an initial condition for pesticide concentrations in the uppermost soil layer (0-5 cm), with a DDT:DDE:DDD ratio corresponding to that of technical grade DDT as it would have been commercially available during 1950-1970. The initial mass of DDT within the upper portion of the soil profile was based on the total measured mass of DDT within the soil profile on May 12, 2003. While this is probably an underestimate of the mass that would have been present in 1950 or 1970 because of degradation during this time, the total mass was subsequently adjusted during calibration. Transformation and degradation rates were initially input based on the findings of Marenco (2002) and were subsequently adjusted to calibrate the relative proportions of each compound in the subsurface. Each stage of the calibration of solute transport at PPNP was undertaken using both the 1950-2003 and 1970-2003 timelines for each of the 3 degradation pathways discussed above. The calibration steps will be discussed in detail below. In all solute transport calibration simulations, the previously calibrated flow parameters were not altered.

Six simulations were conducted to investigate different half-life configurations for the three degradation pathways (Equations 32-34) and the two simulation periods (i.e., 1950-2003; 1970-2003). To explore the possibility of non-uniqueness, an attempt was made to fit field data employing different half-lives. Only 2 additional simulations based on Pathways #2 and #3 were able to fit field data. Thus, a total of 8 calibrated fits resulted and form the basis for further discussion of solute transport. It is recognized that calibrated half-lives of the second and third degradation pathways may not be unique; a second calibration was undertaken with different half-lives.

LEACHMP creates pesticide daughter products through both transformation and degradation reactions. As noted above, Hutson (2003) defines a transformation reaction as a loss of a given species with the product able to be defined as a source of another chemical species, which in turn, can undergo further reactions, and a degradation reaction as a loss of a given species but the mass of degradation products cannot be tracked. In addition, LEACHMP does not have the capability to transform one parent compound to multiple daughter products (i.e., DDT to both DDE and DDD); it can undertake only one transformation reaction per chemical species present. However, LEACHMP does have the capability of undertaking simultaneous degradation of the parent compound as well as other transformation products. There are two principal drawbacks of using the degradation module vs. the transformation module. First, the exact mass of the degradation product is not tracked and must be determined indirectly by subtracting the total mass in the soil profile of the other species present from the initial total mass introduced to the soil profile; transformation products are tracked. Second, degradation reactions occur at a constant rate with respect to both depth in the soil profile and with time and are not subject to temperature and moisture condition variations; transformation rates vary throughout the soil profile and with time as a function of temperature and moisture variations in the soil profile. Thus, the user-defined transformation rate occurs only during the most favourable soil conditions, and in effect it represents a maximum attainable transformation rate. Because soil conditions vary over time during a simulation, the same half-life will produce two disappearance curves over time, with conversion through transformation occurring at an overall slower rate than through a degradation reaction. A comparison for the calibrated flow solution that employs Pathway #1 (PPI3039D) is presented in Figure 29.

4.3.3.1 Calibration of Profile Total %DDT, %DDE and %DDD at CHO

The %DDT, %DDE and %DDD based on the sum of the mass of DDT, DDE and DDD within the entire CHO soil profile as of May 12, 2003 were calibrated by adjusting the half-lives for each transformation pathway described by Equations (32-34). This process resulted in 8 fits to %DDT, %DDE and %DDD for the entire profile employing different half-life combinations for the 3 transformation pathways. At this calibration stage, transformation and degradation rates do not vary with depth. The %DDT, %DDE and %DDD for the entire profile matched field data quite well for each of these fits, however, the resulting outputs did not adequately represent the relative proportion of each DDT compound at each specific depth. The %DDT, %DDE and %DDD measured in the soil profile were observed to be very different for shallow (0-10 cm) and deep (10-200 cm) soils at CHO. For this reason, it is necessary to implement depth-dependent transformation and degradation rates.

4.3.3.2 Calibration of DDT/DDE and DDT/DDD for Shallow and Deep Soils at CHO

Differences in the relative proportions of DDT, DDE and DDD based on the measured data from CHO vary with depth (Table 19) imply different degradation rates with depth and thus, depth-dependant half-lives must be determined. However, the ratio of DDT/DDE and DDT/DDD was used in this stage of calibration rather than %DDT : %DDE : %DDD because LEACHMP was not capable of tracking the mass of the degradation products of DDT (DDE and DDD) separately. DDT/DDE and DDT/DDD ratios within shallow (0-10 cm) and deep (10-200 cm) soils at CHO on May 12, 2003 were matched by adjusting half-lives in shallow and deep soils independently for each transformation pathway and timeline simulated. This suite of calibration simulations was based upon the previous 8 simulations. For Pathway #1 and #2, this meant that the mass of DDD in each depth segment was unknown, as was the mass of DDE for Pathway #3. Only the relationship between DDT and DDE for Pathways #1 and #2, or DDT and DDD for Pathway #3 could be known with depth. Thus, the DDT/DDE ratio could be matched for Pathways #1 and #2, and the DDT/DDD ratio could be matched for Pathway #3.

By adjusting half-lives in the shallow and deep soils, each of the 8 calibration simulations was able to match measured ratios and surface concentrations relatively well.

But DDT compounds were retained too strongly at surface; no DDT present at depth. Thus concentration profiles did not match (Figure 30) and K_{oc} was adjusted.

The K_{oc} values used up to this point were calculated from the K_{ow} values from de Bruijn et al. (1989) (Table 25), which also happened to be the highest values encountered during literature review. Concentration profiles of the calibrated model simulations showed that DDT compounds were being retained too strongly at ground surface and thus, K_{oc} was reduced by one order of magnitude to match concentrations with depth and half-lives were readjusted. Final K_{oc} values were 3.1×10^5 L/kg for DDT, 3.4×10^5 L/kg for DDE and 6.4×10^4 L/kg for DDD, which is well within the reported range of organic carbon partition coefficients for DDT compounds (Table 3).

Because half-lives vary with depth, each successive change in K_{oc} requires half-lives to be readjusted to generate the correct relative proportions of each DDT compound with depth, owing to the new vertical mass distribution within the profile. The resulting 8 simulation outputs matched both relative proportions of each DDT compound and the shape of the concentration profiles with depth, but the magnitudes of DDT, DDE and/or DDD concentrations were far too low at surface (Figure 31). Therefore initial concentrations in soil were adjusted.

4.3.3.3 Calibration to Total DDT in the Soil Profile on May 12, 2003

The next calibration stage focused on adjusting the initial concentrations of Total DDT applied in 1950 and 1970 to match simulated concentrations on May 12, 2003 to those measured with depth at CHO as of May 12, 2003. The 8 simulations were rerun.

The calibrated initial concentrations of Total DDT necessary to match the measured concentration profile at CHO as on May 12, 2003 are presented in Table 26. In order to match the relative proportions of DDT, DDE and DDD, half-lives were adjusted. The initial soil concentrations of Total DDT, if applied only during 1970, are almost twice the initial concentrations if the DDT had been applied only in 1950 because the half-lives used for 1950 – 2003 simulations were about one half of those used for 1970 - 2003 simulations. These 8 calibrated initial DDT loading rates were extrapolated to the application rates using equation (14) and bulk density values (1.18 g/cm^3) measured at CHO, with a thickness of the zone of application of 5 cm to yield conservative first approximations of past areal application rates necessary to reproduce current concentration profiles. The calculated loading rates reflect the amount of DDT in soil and not the amount of DDT applied through aerial spraying.

Table 26. Total DDT added as an initial condition to achieve calibration of simulations.

Simulation	**Initial concentration (mg/kg)**	**Initial concentration (ng/g)**	**Necessary loading rate (kg/ha)**
PPI3039D	43.0	43,000	25.2
PPI3118B	40.0	40,000	23.4
PPI4023B	44.8	44,754	26.2
PPI4034D	70.0	70,000	41.0
PPI4119C	41.0	41,000	24.0
PPI4125D	68.0	68,000	39.8
PPI5042G	45.0	45,000	26.3
PPI5127	42.0	42,000	24.6

4.3.3.4 Comparison to Total DDT in groundwater on May 12, 2003 at CHO

Breakthrough curves of DDT concentrations at the water table for each of the simulations listed in Tables 27 and 28, show that no DDT crossed the water table for any transformation/degradation pathways or time frames simulated. Total DDT concentration measured in groundwater at CHO on May 12, 2003 was 0.679 ng/L. It is suspected that DDT is so strongly adsorbed to the OM in the A horizon during the simulations that DDT is not leaching to the water table. In order to determine the factors that most strongly influence DDT leaching and retention within LEACHMP, sensitivity analyses were conducted on parameters that control the leaching and retention of DDT at PPNP.

4.3.3.5 Assessment of Calibration Simulations

The outputs from all calibration steps matched relative proportions of DDT, DDE and DDD for the soil profile as a whole, relative proportions with depth, shape of the concentration profiles and the magnitude of concentrations quite well (Figure 32). These simulations were considered calibrated to field data (Table 27) and provided the basis for further calibration of groundwater concentrations, sensitivity analysis and scenario testing. The final half-lives are listed in Table 28 and will be discussed below.

During the calibration process, the transformation/degradation pathways were calibrated with no limits placed on the magnitude of the contrast between transformation/degradation rates at soil surface and those employed at depth at CHO. While many of the half-lives that resulted from the calibration process were within the range of values reported in the literature (Table 2), some of the transformation pathways and half-life combinations were unrealistic and these can be dismissed.

The two calibrations employing Pathway #1 (Eq. 32), employing the production of both DDE and DDD but no further degradation of DDE or DDD, matched relative

Table 27. Final Calibrated fit between measured and simulated %DDT : %DDE : %DDD in the whole profile and DDE/DDT or DDD/DDT ratios with depth.

Simulation	Trans.	Start of	Proportions for Entire Profile			Ratios with Depth		
	Pathway	Simulation	%DDT	%DDE	%DDD	Depth (cm)	DDT/DDE	DDT/DDD
Measured			54	40	6	0-10	1.41	8.24
						10-200	0.73	14.68
PPI3039D	1	1950	54	40	6	0-10	1.41	-
						10-200	0.73	-
PPI3118B	1	1970	55	39	6	0-10	1.40	-
						10-200	0.73	-
PPI4023B	2	1950	54	39	7	0-10	1.42	-
						10-200	0.73	-
PPI4034D	2	1950	54	40	6	0-10	1.40	-
						10-200	0.78	-
PPI4119C	2	1970	55	39	6	0-10	1.40	-
						10-200	0.74	-
PPI4125D	2	1970	54	41	5	0-10	1.33	-
						10-200	0.71	-
PPI5042G	3	1950	55	38	7	0-10	-	8.17
						10-200	-	8.85
PPI5127	3	1970	53	41	6	0-10	-	8.92
						10-200	-	5.51

proportions of DDT, DDE and DDD for the entire profile and DDT/DDE ratios with depth quite well for both 1950 and 1970 applications and utilized realistic half-lives consistent with those reported by Marenco (2002) at a nearby field site, although field data suggests that DDD and DDE may be degrading further. Because we know further degradation of DDE occurs under similar field conditions, Pathway #1 is likely not the primary route for DDT transformation within former agricultural areas at PPNP.

The four calibrations using Pathway #2 (Eq. 33), employing the production of DDT and DDE, with further degradation of DDE only, produced half-life estimates that

Table 28. Transformation and degradation half-lives employed for best-fit simulations after matching DDT, DDE and DDD concentrations in soil.

Simulation	Trans. Pathway	Start of Simulation	Depth (cm)	Transformation Half life (years)		Degradation Half life (years)
				DDT→ DDE		**DDT→ DDD**
PPI3039D	1	1950	0-10	32	Not simulated	450
			10-200	10	Not simulated	450
PPI3118B	1	1970	0-10	20	Not simulated	300
			10-200	6	Not simulated	300
				DDT→ DDE	**DDE→ DDE-X**	**DDT→ DDD**
PPI4023B	2	1950	0-10	30	100	450
			10-200	9	100	450
PPI4034D	2	1950	0-10	16	9	650
			10-200	7	9	650
PPI4119C	2	1970	0-10	19	90	300
			10-200	6	90	300
PPI4125D	2	1970	0-10	9	5	500
			10-200	4	5	500
				DDT→ DDD	**DDD→ DDD-X**	**DDT→ DDE**
PPI5042G	3	1950	0-10	150	2000	80
			10-200	150	1	80
PPI5127	3	1970	0-10	113	450	45
			10-200	113	1	45

were also in line with Marenco (2002), and also fit field-measured data well. But this step afforded two potential half-life combinations for each application date that differed in the relative rates of production and further degradation of DDE for a total of 4 calibrated simulations. Two simulations achieved a good fit to field data when DDE degradation was faster than DDE production from DDT. The rates were not realistic because DDE is known to persist in PPNP soils. In addition, the predicted disappearance rate for DDT and DDE was much shorter than has been determined from field data collected between

1998 and 2003. Thus, the simulations entitled PPI4034D and PPI4125D were not considered possible because the half-lives were inconsistent with field data. While the simulation from 1970 to present entitled PPI4119C also fit data fairly well, the fit was not quite as good as achieved when loading of DDT occurred in 1950. In addition, it was known that DDT had been applied prior to 1970. Therefore, Pathway #2 is the best pathway, and of all of the simulations, PPI4023B best fit field data.

The two calibrations based on Pathway #3 (Eq. 34), employing the production of both DDE and DDD, and further degradation of DDD only, necessitated a marked contrast between transformation rates needed at soil surface (0-10 cm) and at depth (10-200 cm) for the further degradation of DDD and did not match measured DDT/DDD ratios deep in the profile. Because the soil properties were relatively uniform from 0-30 cm depth at CHO, it did not seem reasonable that a contrast of this magnitude over a distance of centimeters would be observed in a natural system with similar soil properties. In addition, because Pathway #3 focused primarily on DDD and its further transformation products make up very little of the mass in the subsurface, and treated DDE as a degradation product rather than a transformation product, the mass distribution of DDE with depth was unknown for all simulations employing Pathway #3. PPNP dune soils are also known to be aerobic and DDD production is more prevalent in anaerobic environments. Thus, Pathway #3 was also not considered to be a primary transformation pathway occurring at CHO.

Overall, the calibrated simulation from 1950 to 2003 entitled PPI4023B is deemed to best describe the leaching behaviour at CHO and provided the basis for further scenario testing because it matched (1) relative proportions of DDT, DDE and DDD in the profile as a whole, (2) DDT/DDE ratios with depth, and (3) the transformation rates of DDT to DDE in shallow and deep soils at CHO are consistent with those found in the literature (Table 2) and those calculated by Marenco (2002). Based on the calibration values for simulation PPI4023B, at CHO, the half-life for the transformation from DDT to DDE was approximately 30 years at surface and 9 years at depth. The half-lives for DDE to DDE-X and DDT to DDD were estimated to be 100 years and 450 years, respectively, and both are uniform with depth. Although these half-lives are very high these values indicate that the further degradation of DDE to DDE-X and degradation of DDT to DDD proceeds relatively slowly, and are probably not important primary reactions at PPNP. The calibration values for simulation PPI4023B will provide the basis for further scenario testing.

4.4 Sensitivity Analysis

The purpose of sensitivity analyses is to quantify the uncertainty in the calibrated model caused by uncertainty in the estimates of parameters and boundary conditions, and represents an essential part of applying models to natural systems (Anderson and Woessner, 1992). The outcome of the sensitivity analysis can be used to identify parameters that are most influential in controlling the flow of water and the fate and migration of DDT. By identifying the importance of each parameter, sensitivity analyses can provide an indication of the parameters that need to be well characterized, and conversely point to those that do not need to be well characterized in the field. The flow sensitivity analysis and solute transport sensitivity analysis will be discussed separately.

4.4.1 Sensitivity Analyses for Flow Calibration

Sensitivity analyses were conducted to evaluate the relative importance of flow parameters that were adjusted during the calibration process. The model parameters evaluated as part of the flow sensitivity analyses are presented in Table 29. Several simulations for each parameter between lower and upper limits were conducted, but only the upper and lower limits are discussed in the following analyses. Parameters relevant to the flow of water in the subsurface were adjusted one at a time and model outputs for each simulation on May 12, 2003 were compared to measured volumetric water contents with depth as well as the calibrated best-fit simulation output. All simulations were undertaken from January 1, 1950 to September 30, 2003 and utilized the calibrated best-fit simulation PPI4023B.

Table 29. Range of values tested for flow parameters tested during sensitivity analysis.

Parameter Name	Lower Value	Upper Value
Daily total precipitation (P)	P x 0.80	P x 1.20
Weekly potential evapotranspiration (PET)	PET x 0.80	PET x 1.20
Air entry value (AEV)	AEV x 0.80	AEV x 1.20
Campbell's b coefficient (b)	b x 0.5	b x 2.0
Pore interaction parameter (p)	p = -0.6	p = 0.0
Saturated hydraulic conductivity (K_{sat})	K_{sat} x 0.10	K_{sat} x 10

Sensitivity to Precipitation Values

The 30-year mean annual precipitation at PPNP is 908.3 mm (Table 1); however, over the 10-year period from 1994 to 2004, the minimum total annual precipitation was 558.6 mm (1998) or 61.5% of the 30-year mean, and the maximum was 924.6 mm (2000) or 101.7% of the 30-year mean. This actual total annual precipitation varied over 40% of the 30-year mean annual precipitation. In order to assess the effect of variability in precipitation at PPNP, and the impact of not having precipitation measured at the field site during the past 54 years, on the outcome of the flow calibration, daily total precipitation values were increased by 20% and reduced by 20%.

The model outputs (Figure 33a) illustrate that the model is relatively insensitive to precipitation when it is varied by ±20%. Increased precipitation values are reflected by increased volumetric soil moisture contents with depth, which are more pronounced from 500 to 1500 mm below ground surface as a result of the timing of the precipitation events on May 11th and 12th, 2003. The pulse of water resulting from recent precipitation events results in an increase of approximately 1-2% volumetric soil moisture contents. Conversely, reduced precipitation results in 1-2% decreased volumetric soil moisture contents with depth, again, with the effects being more pronounced from 500 to 1500 mm below ground surface. While the quality of the calibration is slightly reduced by ±20% changes in daily precipitation values, the impact on volumetric soil moisture content are small. Hence the lack of precipitation measured at the site is not crucial to the calibration.

Sensitivity to Potential Evapotranspiration Estimates

The 30-year mean annual potential evapotranspiration was 664.0 mm based on estimates using the Thornthwaite method, with minimum and maximum values of 574.8 mm (1996) or 86.5% of the 30-year mean, and 739.3 mm (1999) or 111.3% of the 30-year mean, respectively, between 1994 and 2003. Increasing and decreasing weekly potential evapotranspiration estimates by 20% tested the sensitivity of the model to variability potential evapotranspiration at PPNP.

The calibrated model was insensitive to variations in potential evapotranspiration on the calibration date (Figure 33b). Only the uppermost 150 mm of the soil profile show any deviation from the calibrated best-fit simulation output, with a maximum deviation of less than 1% volumetric soil moisture content. This could be in part because the calibration date was in early May, when evapotranspiration estimates were relatively low. Because the soils at CHO are very permeable, much of the precipitation that falls rapidly infiltrates to deeper soils, reducing actual evapotranspiration.

Sensitivity to Air Entry Values

The air entry value of a soil determines the pressure at which water will drain from a soil pore filled and be replaced by air. The capillary fringe at CHO was observed in the field to be approximately 20 cm thick and was clearly visible based on changes in soil colour and consistency. In order to assess the effect of changing air entry values on the calibrated best-fit simulation, air entry values were increased and decreased by 20%.

Because the soil profile shows the highest water content at and just above the water table at CHO, the effects of changing air entry values is most pronounced near the capillary fringe (Figure 33c); there is essentially no change in the volumetric soil moisture content above the capillary fringe. Higher air entry pressures increased the thickness of the capillary fringe by tens of millimetres, while reduced air entry values decreased the thickness of the capillary fringe by tens of millimetres. Thus, the calibrated best-fit simulation was relatively insensitive to air entry values.

Sensitivity to Campbell's b Coefficient

The volumetric soil moisture content depends on pressure head in the unsaturated zone according to the shape of the soil moisture characteristic curve. LEACHMP employs Campbell's model and the Hutson-Cass wet-end modification to define this relationship. The slope of the soil moisture characteristic curve is defined as Campbell's b coefficient (BCAM). Because soil moisture content also determines in part, unsaturated hydraulic conductivity, Campbell's b coefficient is important to understand relative to flow of water and ultimately, solutes in the unsaturated zone. Best-fit b values were multiplied by 50% and 200% uniformly with depth in order to assess the effect of varying soil moisture characteristic curves on model outputs.

When the soil moisture characteristic curve was steepened (by reducing b) or broadened (by increasing b), the volumetric soil moisture content profile essentially retained its shape (Figure 33d). However, the moisture content was reduced by approximately 4-6%, and increased by approximately 2-4% with depth, respectively.

Thus, when the slope of the soil moisture characteristic curve is changed, the volumetric water content profile scales to reflect increased or reduced storage of water in the unsaturated zone. Even though the modelled soil moisture profiles change, increased and decreased b values do not cause a substantial deviation from measured field data and calibrated value.

Sensitivity to Pore Interaction Parameter

The pore interaction parameter, p, scales the unsaturated hydraulic conductivity function according to user input. It represents the connectivity of pores in the flow domain and is often used as a fitting parameter. Values for p for the best-fit simulation were –0.3. In order to evaluate model sensitivity, values were adjusted to 0.0 and –0.6.

When the pore interaction parameter was increased or decreased, the volumetric soil moisture content above 1500 mm increased and decreased, but by only approximately 1%; there is essentially no change below a depth of 1500 mm (Figure 33e). However, the shape of the soil moisture content profile remains essentially the same. Thus, the model appears to be relatively insensitive to the value of p.

Sensitivity to Saturated Hydraulic Conductivity (K_{sat})

Saturated hydraulic conductivity values employed in LEACHMP simulations were 1728 mm/day (2×10^{-3} cm/s) in the Ah horizon and 3456 mm/day (4×10^{-3} cm/s) in the Bm and C horizons. Values for the Ah horizon varied slightly from field-saturated hydraulic conductivity values measured at 20 cm in the field. The difference between model and measured hydraulic conductivity values was less than one order of magnitude, which is within the typical range of values seen in PPNP soils (Crowe et al., 2004). In addition, field saturated hydraulic conductivity values are often lower than laboratory derived saturated hydraulic conductivity values as a result of entrapped air (Ronen et al., 1989). In order to assess the effect of variability of hydraulic conductivity values, best-fit simulation values were both increased and decreased by a factor of 10.

The model is sensitive to the value specified for hydraulic conductivity (Figure 33f). When hydraulic conductivity values are increased, volumetric soil moisture contents are reduced by approximately 5-6% of the initial value at surface, with the difference declining with depth. When hydraulic conductivity is decreased by an order of magnitude, volumetric soil moisture contents increase by approximately 10% at surface due to the much slower migration of a recent large precipitation event on May 10th -11th.

4.4.2 Sensitivity Analyses for Solute Transport Calibration

LEACHMP simulated DDT and DDE or DDD concentrations within the soil profile at CHO quite well, matching both the shape of the concentration profile and concentrations. Sensitivity analyses were conducted to evaluate the importance of flow and solute transport parameters adjusted during the calibration process and their effect on the leaching of DDT compounds at CHO. Several model parameters were evaluated as part of the flow sensitivity analyses (Table 30). All simulations were undertaken from January 1, 1950 to September 30, 2003 and utilized the calibrated best-fit solute transport simulation that employs transformation Pathway #2 (PPI4023B).

Table 30. Values tested for solute transport parameters during sensitivity analysis.

Parameter Name	Lower Value	Upper Value
Daily total precipitation (P)	P x 0.80	P x 1.20
Potential evapotranspiration (PET)	PET x 0.80	PET x 1.20
Saturated hydraulic conductivity (K_{sat})	K_{sat} x 0.10	K_{sat} x 10
Organic carbon partition coefficient (K_{oc})	K_{oc} x 0.10	K_{oc} x 10
Half life ($t_{1/2}$)	$t_{1/2}$ – 5 years	$t_{1/2}$ + 5 years
Organic carbon content (%OC)	%OC x 0.5	%OC x 2.0

Sensitivity to Precipitation Values

Because infiltration of water through the unsaturated zone determines in part, the potential for leaching of pesticides to the water table, a sensitivity analysis on the daily total precipitation was undertaken to determine its impact on DDT concentrations throughout the soil profile. Precipitation values were again varied by ±20% to address the spatial variability of precipitation and examine the effect of these adjustments on long-term leaching of DDT compounds at CHO. Figure 34a shows that the largest effect on the concentration profile is observed near the ground surface, with DDT compounds being retained higher in the soil profile when lower precipitation amounts are used. The opposite holds true when precipitation values are increased. The trend is consistent for both DDT and DDE. While the changes in precipitation values are reflected by changes in the modelled concentration profiles, the magnitude of these changes is relatively small, changing shallow soil concentrations by approximately ±5%. The magnitude of the effect of precipitation value adjustments is dampened as the distance from the upper boundary increases. Overall, the model is relatively insensitive to precipitation values.

Sensitivity to Evapotranspiration Estimates

Temperatures recorded at PPNP and nearby weather stations were used to estimate potential evapotranspiration values for the entire duration of the simulations from January 1, 1950 to September 30, 2003. Because there is some uncertainty related to these estimates, evapotranspiration values were varied by ±20% to provide some insight into the dependency of model predictions on evapotranspiration values. Figure 34b shows that the leaching behaviour, and hence the concentrations and distribution of DDT within the soil profile, is insensitive to evapotranspiration within the range of values tested. While it is expected that the quality of the flow calibration would be negatively affected, the vertical distribution of DDT compounds within the soil profile do not change with the increased or decreased evapotranspiration values.

Sensitivity to Saturated Hydraulic Conductivity Values (K_{sat})

The sensitivity of the model's predicted concentrations and distribution of DDT to variability in saturated hydraulic conductivity was investigated using the same range of values previous run; saturated hydraulic conductivities were adjusted uniformly with depth and were both increased and decreased by a factor of 10. Figure 34c shows increased retention at surface is predicted when hydraulic conductivity is reduced; however, the changes in concentration are very small. The effects of changing hydraulic conductivity values become even less pronounced at depth. Overall, solute leaching is relatively insensitive to hydraulic conductivity values employed for simulations at CHO.

Sensitivity to the Organic Carbon Partition Coefficient (K_{oc})

DDT has an extremely high organic carbon partition coefficient, and although authors report K_{oc} values for DDT, very few report values for its transformation products DDE and DDD. In addition, reported values are often based on empirically derived equations relating K_{ow} to K_{oc}. These empirical relationships are only consistent within a narrow range of physical conditions (%OC, temperature, soil type), but these conditions are rarely reported. Under field conditions with soil types and organic carbon contents different from those for which the empirical relationships were derived, the range of expected K_{oc} values is much greater. Also, a search of literature values exhibited a range of approximately two orders of magnitude for K_{ow}. In order to examine the effect of varying sorption coefficients on the shape of the concentration profile, K_{oc} values were adjusted by an order of magnitude.

Figure 34d shows that vertical migration of DDT compounds is sensitive to the value of K_{oc}; the fundamental shape of the concentration profile changes dramatically when K_{oc} is adjusted by only one order of magnitude. When K_{oc} is reduced by an order of magnitude, the DDT compounds are redistributed throughout the profile because the lower K_{oc} causes less retention in the upper portion of the soil profile. Concentrations of DDT and DDE at surface due to the lower K_{oc} are ~8,000 ng/g less and now DDT compounds penetrate to a depth of 375 mm vs. ~170 mm. When K_{oc} is increased by an order of magnitude, more of the DDT compounds are retained in the organic matter at surface, and less is leached downward. Concentrations of DDT and DDE at surface due to the higher K_{oc} are ~5,000 and ~4,000 ng/g, respectively, and the maximum depth to which DDT compounds migrate within the soil profile is only approximately 125 mm.

The dramatic change in concentration profiles when the K_{oc} is changed illustrates the importance of sorption in controlling the migration of DDT compounds from ground surface to the water table, and in fact it is the most important parameter. Kinetic and/or depth-dependent sorption models were not tested within this study, however further laboratory and modelling investigations of sorption behaviour could significantly benefit the understanding of DDT fate and migration at PPNP.

Sensitivity to Transformation and Degradation Rates

Transformation and degradation rates were used as fitting parameters to calibrate the model to relative proportions of DDT compounds with depth at CHO. Because soil moisture regimes are variable within PPNP (Marenco, 2002), and transformation rates vary with temperature and moisture content, a sensitivity analysis for transformation and degradation rates was conducted. A change in half-lives of 5 years was selected for testing of the sensitivity of LEACHMP to transformation and degradation rates. All three transformation/degradation rates were adjusted uniformly each time that reaction rates were changed.

As expected, model outputs (Figure 34e) show that the model is somewhat sensitive to changes in half-lives. While the shape of the concentration profile remains relatively consistent, the concentration profile shifts as concentrations with depth increase or decrease when rates are increased or decreased, respectively. However, the increase and decrease in concentrations due to the half-lives change is only 12% and 9% for DDT and DDE, respectively. The changes in concentrations at ground surface could have been matched by adjusting initial loadings, but matching relative proportions with depth would not be possible as the relative proportions were initially matched by changing transformation/degradation rates.

Sensitivity to Organic Carbon Content with Depth

Organic carbon content and the organic carbon partition coefficient determine the role of sorption of DDT compounds in the subsurface. Because the organic carbon content of soils can vary spatially and with depth, a sensitivity analysis on organic carbon contents with depth was conducted to assess the impact on DDT leaching. Analyses for organic carbon content from 83 soil samples collected at depth greater than 10 cm and throughout PPNP (Crowe et al., 2002; Marenco, 2002; this study) indicate that %OC ranges from ~0.5% - 7.0%, with the majority of values <2.0%. Organic carbon contents are already quite low at CHO, so values were only reduced to half of the field-measured values, as a further reduction would have generated rapid flushing of DDT to the water table providing little insight. Organic carbon contents were also increased by a factor of 2 to examine leaching behaviour in soils richer in organic carbon.

Because DDT is readily adsorbed onto organic carbon within the soil profile, increasing or decreasing the organic carbon content will corresponding decrease and increase the leaching of DDT compounds. Thus, the shape of the concentration profile and concentrations with depth change as the organic carbon content changes. When the organic carbon content is reduced (Figure 34f), the surficial soil concentration is reduced by 19% and DDT compounds migrate deeper into the soil profile. When the organic carbon content is increased, the surficial soil concentration is increased by 13% and DDT compounds are retained shallower in the soil profile. Overall, the model is sensitive to changes in organic carbon content with depth, meaning that organic carbon contents are important to quantify when simulating the fate and transport of DDT compounds.

4.5 Simulation of Solute Transport at SHO

All simulations up to this point were based on soil and hydraulic properties and DDT concentrations measured for the CHO soil profile. In order to assess the leaching of DDT compounds through a soil profile at a different location within PPNP, a shallower depth to the water table (75 cm), and soil having a lower organic carbon content and distribution with depth, simulations were undertaken with the SHO soil profile. Because there are no statistically significant differences at the 95% confidence level between CHO and SHO with respect to soil or hydraulic properties, simulations at SHO were based on the flow calibration parameters used at CHO and values were changed. While this did not match water contents with depth as well as at CHO, it provides a water balance estimate of flow behaviour at SHO sufficient for scenario testing purposes (Figure 25b).

The organic carbon distribution with depth was adjusted to reflect field measurements at SHO (Table 12). The organic carbon contents at surface at SHO were less than half of those seen at CHO and the distribution of organic carbon was more uniform with depth than at CHO (Figure 8).

Solute transport was calibrated by adjusting half-lives to match relative proportions of DDT, DDE and DDD as measured at SHO (Table 19) for Pathway #2 using a 1950 starting date. Because relative proportions of DDT were consistently less than DDE with depth, uniform half-lives were calibrated with depth (Table 31) to a loading rate of 100 mg/kg of Total DDT applied in the upper 5 cm of the soil profile.

Table 31. Transformation and degradation half-lives employed uniformly with depth at SHO.

Simulation	Half-life (years)		
	DDT->DDE	**DDE->DDE-X**	**DDT->DDD**
SHO4002 *	14	100	1200

* Based on PPI4023A parameters, with altered DDT loading rates, OC distribution and depth to W.T.

After transformation and degradation rates at SHO were calibrated, solute concentration profiles with depth and solute breakthrough curves at the water table were assessed to determine if DDT, DDE and/or DDD were leaching to groundwater.

Simulation outputs show that DDT and DDE reaches the water table beginning in 1998, with Total DDT concentrations reaching approximately 2.25 x 10^{-16} mg/L on May 13, 2003 (Figure 36). The measured concentration of Total DDT in groundwater at SHO on May 13, 2003 was 4.181 x 10^{-6} mg/L (Table 21). There are two possible reasons why DDT reaches the water table at SHO (however at very low concentrations) but not at CHO. First, the organic carbon content of the Ah horizon at SHO is ~50% lower than that in the CHO soil profile and the thickness of the Ah horizon is small than that at CHO. Previous sensitivity analyses (Figure 35) show that a 50% reduction in organic carbon content in the Ah horizon will cause significant desorption and leaching of DDT to the Bmgj horizon. However, the organic carbon of the Bmgj horizon at SHO is about 50% greater than that of CHO (Table 12), thus increasing adsorption in the Bmgj horizon. But the organic carbon content here is still sufficiently low to permit leaching of some DDT to the water table. Secondly, because the depth to the water table at SHO is only 70 cm, the distance for DDT to travel from ground surface to the water is only about one third of that at CHO. Simulations undertaken at CHO (with a higher organic carbon content in its Ah horizon than that at SHO) still showed DDT moved over 70 cm downward through the soil profile (Figure 32c). Thus, SHO could represent a soil profile in which sorption may be limited by lower organic carbon content in the Ah horizon, and short travel distances to the water table enable DDT to enter the groundwater. This suggests that leaching to the water table at PPNP is more likely to occur where the organic carbon content is lower and the water table is shallower and implies that leaching of DDT to groundwater will vary seasonally in response to water table fluctuations.

4.6 Scenario Testing

Because of the inability to match concentrations seen in groundwater today at CHO (Figure 35) and SHO (Figure 36), further scenario testing was undertaken to determine what is limiting the leaching of DDT to the water table. The scenarios chosen for testing included: (1) removal of organic carbon content from the B and C horizons, (2) direct application of DDT below the organic rich Ah horizon, (3) homogenizing of DDT within the Ah horizon by ploughing, (4) assessing the adsorption behaviour of DDT, and (5) assessing the historical application rates of DDT. As with the solute transport sensitivity analysis, all simulations were undertaken using simulation PPI4023B.

Note that all of the following breakthrough curves exhibited numerous low amplitude, short duration spikes superimposed on the long-term slow increase in DDT and DDE concentrations due to pesticide leaching occurring during the infiltration events.

4.6.1 Removal of Organic Carbon Content from the Bm and C Horizons

The soil profile at CHO was shown to contain up to 1.80% organic carbon within the Ah horizon (0-30 cm), and less than 0.36% organic carbon within the B and C horizons (30-200 cm). Even this very small amount of organic carbon is sufficient to adsorb the DDT compounds as they migrate through the B and C horizons. In order to investigate the possibility that the organic carbon in the B and C horizons is the limiting factor controlling DDT leaching to the water table, organic carbon of the B and C horizon (30 cm below ground surface to the water table) was set to 0.

Simulation results for CHO show that with no organic carbon in the B and C horizons, DDT that migrates through the Ah horizon will reach the water table (Figure 37). Concentrations at both CHO and SHO gradually increase over time beginning approximately 20 years after the beginning of the simulations as more DDT correspondingly leaches through the Ah horizon. At CHO, DDT and DDE concentrations at the water table are ~1 x 10^{-7} mg/L and ~7 x 10^{-8} mg/L, respectively, on May 12, 2003 (Figure 37).

Simulated concentrations of DDT and DDE on May 12, 2003 at SHO, with no organic carbon in the B and C horizons (depths of 20 cm to the water table) are approximately 5 x 10^{-6} mg/L and 7 x 10^{-6} mg/L, respectively (Figure 38). These concentrations are within an order of magnitude of concentrations seen at the water table today (Table 21). As the mass of contaminant migrates deeper into the soil profile, and if current meteorological conditions persist, it is likely that concentrations at the water table will continue to increase until the majority of the mass of DDT has leached through the Ah horizon. While field data and the previous simulations show that DDT is strongly adsorbed, preventing leaching though the Ah horizon, the results of the present simulation shows that either the relatively low organic carbon content of the Ah horizon (~1.3%) permits some leaching of DDT, or DDT is essentially not adsorbed within the B and C horizon (e.g., preferential pathways), or a different adsorption mechanism is occurring from that being simulated (non-equilibrium adsorption).

4.6.2 Application of DDT below the Ah horizon

At PPNP, it is possible that DDT was placed below the Ah horizon (e.g., deep ploughing, very thin or absent Ah horizon, removal of roots or stumps, etc.). To assess the leaching behaviour that would result from DDT being directly introduced into the Bm horizon within former agricultural areas of PPNP, DDT was applied at a depth of 30 cm on four occasions at 5 year intervals; no DDT was placed in the Ah horizon. The amount of DDT, DDE and DDD applied was equivalent to that applied to shallow soil during the calibration process. Only the depth at which DDT was applied was changed (i.e., surficial soil vs. 30 cm below ground surface).

In the first simulation, the soil profile contains the field-measured organic carbon contents (1.80% organic carbon within the Ah horizon (0-30 cm), and less than 0.36% organic carbon within the Bm and C horizons (30-200 cm)). LEACHMP again predicts no leaching of DDT compounds across the water table. Hence, even if large amounts of DDT were applied below the organic-rich Ah horizon at PPNP, there is still sufficient organic carbon in the Bm and C horizons to adsorb all this DDT.

In the second simulation, all the organic carbon below the Ah horizon is removed, as discussed previously. As expected, the resulting breakthrough curve (Figure 39) shows that within one year, DDT and DDE concentrations at the water table rapidly increase to levels approaching the solubility limit of DDT. High DDT concentrations persist for approximately one year after DDT is introduced into the soil and then began to decline rapidly as the DDT is rapidly flushed from the Bm and C horizons as water infiltrates through the soil profile to the water table. Because DDE make up a much smaller fraction of the total mass applied (4.3%) and because there is little time for the transformation of DDT to DDE before being flushed, the peak concentration of DDE is much lower, despite having a greater aqueous solubility than DDT. A tailing effect is also apparent for DDT and DDE caused by the upward movement of DDT and DDE into the Ah horizon during periods of evapotranspiration, subsequent adsorption to organic matter in the Ah horizon, and later release during infiltration events. The same trend is repeated for each of the four applications at depth. Following the final application, the effects of transformation of DDT to DDE can be seen, with concentrations of DDT crossing the water table declining exponentially over time, with proportional increases in DDE concentrations.

4.6.3 Ploughing of the Ah horizon

DDT could also have been placed within the Ah horizon, but at the interface between the Ah and the Bm horizon as a result of disturbances to the Ah horizon, such as ploughing in the vegetable fields or during the restoration of former orchard areas within PPNP when tree stumps were removed and pushed into piles for burning. As a result of these activities, it is possible that contaminated soil was overturned and left in direct contact with deeper soils containing minimal organic carbon. As such, simulations were run where the top 30 cm of the soil profile was ploughed in 1955 or five years after the beginning of the simulation. Within LEACHMP, ploughing will homogenize DDT concentrations within the user-defined depth interval. As a result of ploughing, DDT is spread throughout the top 30 cm, including being adjacent to the Bm horizon. Simulations were conducted with field-measured organic carbon contents throughout the soil profile, but again, no leaching of DDT compounds to groundwater occurred throughout the duration of the simulation. Further simulations with organic carbon contents reduced to 0 below the Ah horizon were conducted to investigate the leaching behaviour under these conditions.

When organic carbon was present in the Bm and C horizons, no DDT was leached to the water table during the entire 54 year simulation. However, when the organic carbon content of the soil is set to 0, simulation outputs (Figure 40) show that DDT compounds leach to groundwater within one year of ploughing because the large contaminant mass is in direct contact with deep soils having no organic carbon (below 30 cm), and subsequent rapid leaching through the Bm and C horizons to the water table due to no absorption. Total DDT concentrations in groundwater decline slowly due to continued leaching of the DDT from the portion of the Ah horizon immediately adjacent to the Bm horizon. This is in contrast to leaching behaviour observed in an undisturbed soil profile, where no leaching of DDT compounds to groundwater occurs. Overall, leaching after a ploughing event is very similar to that after a direct application of DDT at depth. Both types of loading results in a short-lived pulse of contaminants leaching to the water table, but ploughing (i.e., DDT remains in the Ah horizon) results in long-term inputs into the Bm and C horizons, and subsequently to the water table.

4.6.4 Assessment of Adsorption Behaviour of DDT at PPNP

The calibrated solute transport simulations for CHO were able to match DDT and DDE or DDD concentration profiles in soil well, but they were unable to match concentrations of DDT compounds measured in groundwater. This implies that the selected K_{oc} values were fairly accurate. The LEACHMP calibration simulations predicted that no leaching of DDT compounds to groundwater occurred at CHO. However, measurable concentrations of DDT, DDE and/or DDD were reported in a groundwater sample collected beneath the CHO on May 12, 2003 (0.68 ng/L Total DDT), as well as all other groundwater samples analysed. Only when organic carbon was removed from the Bm and C horizons, did leaching of DDT compounds to the water table occur. Similarly, simulations at SHO showed when organic carbon was present in the Bmgj horizon, concentrations of dissolved DDT at the water table were orders of magnitude lower than that measured. Only when the organic carbon content of the Bmgj horizon at SHO was reduced to zero, was there a large increase in groundwater concentrations predicted by the solute breakthrough curve, which was the only means by which the field-measured groundwater concentrations could be matched.

Although under field conditions the B and C horizons at PPNP do have an organic carbon content, the assignment of no organic carbon to these two horizons can be justified when considering an alternative leaching model. LEACHMP assumes adsorption occurs under equilibrium conditions; this ignores the time-variant sorption behaviour of pesticides in solution. If sufficient adsorption sites (organic carbon) are available, DDT will be instantaneously removed from, or transferred to, solution according to a linear equilibrium isotherm. Because concentrations of DDT in solution at PPNP are extremely small relative to the amount of sorption sites, this implies that all DDT that dissolves and is transported to the Bm and C horizons will be instantaneously partitioned according to the equilibrium isotherm.

However, if adsorption occurred under non-equilibrium conditions, the amount of DDT adsorbed from solution would depend on not only on concentrations in solution, K_{oc} of DDT compounds, and amount of adsorption sites but also the time in which the DDT was in contact with the adsorption sites. Several studies of DDT compounds have shown that sorption is not always an instantaneous process (Bailey and White, 1964; Brusseau et al., 1991). In the laboratory, samples may take weeks to months to achieve equilibrium partitioning between phases (de Bruijn et al., 1989). At PPNP, water infiltrates from ground surface to the water table in a matter of a few days to weeks (Figure 28), thus offering insufficient time for equilibration. Thus if a kinetic or the depth-dependent sorption mechanism was employed in LEACHM, and given that water (and associated dissolved DDT) moves through the soil profiles in a matter of days, under these conditions some of the DDT would not adsorb and thus reach the water table.

The body of sorption literature reports a wide range of K_{ow}'s for DDT, DDE and DDD, and after numerical modelling it is clear that additional study is necessary to quantify the sorption of DDT and DDE at PPNP in the laboratory and/or field.

At PPNP, the leaching of DDT to the water table likely began earlier in areas of the park where organic carbon contents are lower and the water table is shallower. Over time, leaching of DDT to the water table will be more common and frequent within former agricultural areas of the park that have shallow depths to the water table and lower organic carbon contents within the Ah horizon as seen at SHO.

4.6.5 Assessment of the Historical Application Rates of DDT at PPNP

The Ontario Ministry of Agriculture and Food (OMAF, 1975) recommendations for DDT use within apple orchards, from 1949-1972, were up to five applications each year at a rate of 3.4 - 5.0 kg/ha per application, or 17 to 25 kg/ha per year. Thus, the amount of DDT that may have been applied to a field or orchard at PPNP between 1950 and 1970 is between 3.4 kg/ha (1 application) and 500 kg/ha (5 kg/ha applied 5 times per year for 20 years). Several studies have reported volatilization losses of DDT; volatilization is the main loss of pesticide. Willis et al. (1980) reported a 44% loss over 120 days, while another study reported a 58% loss over a period of 11 days (Willis et al., 1980). This is supported by Lichtenstein et al. (1961) who reported 50-60% loss of DDT in 6-12 months, and measurable volatilization continuing thereafter. Similar organochlorine compounds have been shown to experience 90% volatilization loss from orchard grasses after 30 days (Taylor et al., 1977). Some of the DDT applied would also be lost through drift, plant and animal uptake, etc. Therefore, the actual amount of DDT in the shallow soil before degradation and leaching commences and considerably less than the application rate. While the fraction of DDT that enters the subsurface at PPNP is unknown, it is assumed here that $^{1}/_{10}$ of the applied DDT entered the shallow soil, thus the total amount of DDT to enter the soil at PPNP over 20 years should be between 0.34 kg/ha and 50.0 kg/ha, or a maximum annual soil accumulation rate of 2.5 kg/ha.

Extrapolating the depth-weighted profile mass of Total DDT from Table 19, calculated per cm^2 of the soil profile, at CHO (0.223 mg), SHO (0.339 mg) and AO (0.075 mg), to a hectare scale gives Total DDT at CHO, SHO, and AO of 22.3 kg/ha, 33.9 kg/ha, and 7.5 kg/ha, respectively. Based on the best-fit calibration simulation (PPI4023B), only 5.9% of the Total DDT was lost due to degradation and leaching over the 54 year period. Thus, even considering a loss of DDT after it entered the subsurface, the present amounts of DDT in the soil at PPNP are within the range of probable amounts to have entered the soil.

Although there were no records of DDT application to agricultural areas at PPNP, the 8 calibration simulations for CHO provide application rates (i.e., DDT to have entered the soil) at CHO of 23.4 to 26.4 kg/ha if applied only during 1950, and 39.8 to 41.0 kg/ha if applied only during 1970 (Table 26). Greater quantities of DDT were applied within the 1970 – 2003 suite of simulations because half-lives were much shorter relative to the 1950 – 2003 suite of simulations. Thus, as indicated by these LEACHMP simulations for CHO, it would appear that DDT could not have been applied only during 1970; 40 kg/ha to have entered the soil during only 1 year is unrealistically higher than even if all DDT applied at Ontario Ministry of Agriculture and Food's (OMAF) maximum recommended rate of 25 kg/ha entered the soil. Similarly, the simulated application of DDT only during 1950 is still above the range of DDT levels in shallow soil that could occur if the OMAF recommended application rate for one year was followed.

Thus, DDT would have to have been applied several times over a number of years. The Total DDT that historically entered soil at CHO is between 23.0 kg/ha and 41.0 kg/ha. Based on maximum loading rates (2.5 kg/ha/yr to enter soil), at least 10 years would be required for CHO, 14 years at SHO and 3 years at AO to attain field-measured values prior to further loss in the subsurface. Because application of DDT in 1970 requires unrealistic application rates, and applications over a period of 14 years are required at SHO, DDT was likely applied early in the time frame being simulated (i.e., 1950-1960).

When modelled application rates were compared with an application rate calculated from the depth-weighted profile Total DDT for CHO (Table 18), it showed that between 1.0 kg/ha and 18.8 kg/ha had either degraded or been removed from the system through volatilization and/or leaching to groundwater. The simulation selected to be the best fit to field data (PPI4023B) required that technical grade DDT be applied at a rate of 26.2 kg/ha.

Because the depth-weighted profile Total DDT mass was fairly low relative to the best management practices, a simulation employing the absolute minimum application of DDT was not conducted. Thus, the maximum amount of DDT that was applied is approximately 20 times higher than what currently exits within the soil profile at CHO as measured on May 12, 2003. It is unlikely that DDT was applied at such high rates; so loading was increased by a factor of 10, with organic carbon again removed from deep soils (30-200 cm). Breakthrough curves (Figure 41) predicted DDT and DDE concentrations on May 12, 2003 were approximately 7 ng/L and 5 ng/L, respectively. At early times the abundance of DDT over DDE, and slightly lower sorption coefficient of DDT, results in an earlier appearance of DDT at the water table. At late times, the higher solubility of DDE relative to DDT and conversion of DDT to DDE, generates higher concentrations of DDE at the water table. In the future, DDE concentrations in groundwater will dominate as DDT continues to be transformed to DDE in soil.

4.7 Discussion of LEACHMP Modelling Results

One-dimensional modelling with LEACHMP showed that the primary transformation/degradation pathway in the soils of the former agricultural areas at CHO is via the aerobic transformation of DDT to DDE, with half-lives of ~30 years at ground surface and ~9 years at depth. Very little transformation of DDT to DDD or DDE to further degradation products occurs (estimated half-lives of 450 and 100 years, respectively). Simulations at SHO (shallower depth to water table, different organic carbon content, lower elevation) illustrated that degradation was occurring at a uniform half-life with depth of ~14 years. No leaching was predicted at CHO with the present levels of organic carbon found in the soil profile throughout the time period that was simulated. Only when organic carbon was removed from the Bm and C horizons, did leaching begin after approximately 40 years, producing concentrations of Total DDT at the water table within one-order of magnitude of field-measured groundwater concentrations. The factor limiting the leaching of DDT to groundwater is the binding of DDT to the organic carbon in the Ah horizon. Once DDT enters the Bm and C horizons, it is flushed to the water table within a few days with infiltration. This suggests that the sorption mechanism at PPNP is probably either kinetic, or depth-dependent. At SHO, where the water table is shallower and Ah horizon organic carbon contents are lower, leaching was predicted but at levels 10 orders of magnitude less than measured. Again, when organic carbon was removed from deep soils, concentrations at the water table compared very favourably to measured data in May 2003. This implies that if the depth to the water table is sufficiently shallow, some DDT will reach the water table even if some organic carbon is present.

4.8 GW-WETLAND Simulations

4.8.0 Model Description: GW-WETLAND

The GW-WETLAND model was developed to simulate both groundwater flow, groundwater-surface interaction, contaminant transport within the saturated zone, and solute fluxes across the groundwater-surface water interface, in a 2-D heterogeneous cross section in response to transient hydrological and meteorological conditions (Shikaze and Crowe, 1999). The model has been used to simulate groundwater flow and contaminant transport within the barrier bar between the marsh and a lake at PPNP (Crowe et al., 2004), infiltration of contaminated water from a river during flooding (Shikaze and Crowe, 1998), groundwater flow in the vicinity of drainage ditches and responses to ditch blockages (Crowe et al., 2000), impact of dewatering at a quarry on an adjacent wetland (Crowe et al., 2002), and the groundwater flow regimes adjacent to coastal wetlands (Crowe and Shikaze, 2004). A brief description of the GW-WETLAND model is provided below and the reader is directed to the users' guides for detailed descriptions of the model (Shikaze and Crowe, 1999, 2000, 2001).

Within the context of this thesis, GW-WETLAND was used to model the transport and persistence of DDT within the saturated zone of a section of the western barrier bar at CHO from Lake Erie to the Point Pelee marsh. The model simulated the 54-year period of time from the first applications of DDT in 1950 through the last applications of DDT in 1970 to the present time (2003). The specific objective of the GW-WETLAND modeling was to evaluate the transport of DDT within the saturated zone in response to both actual meteorological conditions measured between 1950 and

2004 and various DDT loading scenarios across the water table based on LEACHMP simulation outputs.

4.8.1 Flow Representation

GW-WETLAND simulates the 2-D transient flow of groundwater in the saturated zone within a heterogeneous cross-section. The hydraulic head distribution within the heterogeneous flow domain is solved using the transient groundwater flow equation:

$$\frac{\partial}{\partial x}\left(K_x \frac{\partial h}{\partial x}\right) + \frac{\partial}{\partial z}\left(K_z \frac{\partial h}{\partial z}\right) = S_s \frac{\partial h}{\partial t} \tag{44}$$

where K_i is the saturated hydraulic conductivity [LT^{-1}], h is the hydraulic head [L], S_s is the specific storage coefficient [L^{-1}], x and z are directions [L] and t is time [T]. The solution to this equation is solved using a standard Galerkin finite-element method employing linear triangular elements (Pinder and Gray, 1977). Left, right and bottom boundary conditions for the cross-section are no-flow boundaries represented by:

$$\left.\frac{\partial}{\partial x}\right|_{x=0} = 0 \qquad \left.\frac{\partial}{\partial x}\right|_{x=s} = 0 \qquad \left.\frac{\partial}{\partial z}\right|_{z=0} = 0 \tag{45}$$

where $x = 0$ is the left boundary of the cross section, $x = s$ is the right boundary of the cross-section, and $z = 0$ is the base of the cross-section. The upper boundary of the saturated domain is either a Dirichlet (specified head) or a Neumann (specified flux) boundary condition. Infiltration and evapotranspiration may vary both spatially and with time, and are simulated using the following Neumann type boundary condition equation:

$$K_x \frac{\partial h}{\partial x} + K_z \frac{\partial h}{\partial z} = \left[I - S_y \frac{\partial h}{\partial t} \right] \tag{46}$$

where I is the rate of infiltration [LT^{-1}] across the water table and S_y is the specific yield within the unsaturated zone immediately above the water table.

GW-WETLAND simulates a fluctuating water table that rises and falls in response to the calculated pressure head distribution within the saturated flow domain and boundary conditions. In order to accurately simulate the position of the water table and to maintain the integrity of hydrostratigraphic units, the geometry of the uppermost portion of the finite element grid moves in response to a rise or fall of the water table. When the fluctuation of the elevation of the water table is small when compared to vertical grid spacing, elements along the water table are stretched or compressed. However, if the change in elevation of the water table is large, new elements are added (rising water table) or removed (falling water table) along the water table. Thus an accurate solution is obtained when elevation of a node along the water table is equal to the value of hydraulic head at that node:

$$\delta(x,z,t) = h(x,z,t) \tag{47}$$

where δ [L] is the elevation of the water table at a given point and h [L] is the hydraulic head at the same point in space and time. The GW-WETLAND model simulates the formation or removal of seepage faces as the water table rises to intersect ground surface, or falls below ground surface, respectively.

The hydraulic head distribution within the flow domain and the geometry of the flow domain are both unknown at each time step. Therefore, the solution can be obtained only through an iterative technique. At each iteration, the calculated head for each node along the water table is compared to the elevation of the corresponding node. The position of the nodes along the water table are adjusted as necessary until the residual for all nodes along the water table is less than specified convergence criteria:

$$residual = \sum \left| \delta(x,z,t) - h(x,z,t) \right| \tag{48}$$

The GW-WETLAND model is capable of simulating single or multiple surface water bodies within the 2-D cross section whose lateral extent and surface elevation change (i.e., a rising marsh moving lateral over the shoreline) in response to meteorological, hydrological, and hydrogeological conditions. These are simulated as a transient specified head boundary along the top of the saturated zone where the surface water body intersects ground surface. The hydraulic head along the groundwater-surface water interface is equal to the elevation of the surface water body:

$$H(x,z,t) = L(t) \tag{49}$$

where L is the surface elevation of the wetland [L]. The nodes along the surface of the saturated flow domain are switched from free nodes to specified head nodes as the lateral extent of surface water body expands across the shoreline. Nodes are switched from specified head nodes to free nodes when the surface water body retreats. The model can be executed using long-term water level records for the surface water bodies to fix the elevation of the surface water body at each time step or secondly, by allowing the groundwater flow discharge or recharge to determine the level of the surface water body during each time step. For all simulations undertaken here, long-term water levels were available and thus, the first option was utilized.

4.8.2 Solute Transport

The transport of contaminants within the saturated zone is simulated using a numerical solution to the 2-D advective-dispersion equation:

$$\frac{\partial c}{\partial t} = -\frac{\partial}{\partial x} v_x c - \frac{\partial}{\partial z} v_z c + \frac{\partial}{\partial x}\left(D_{xx} \frac{\partial c}{\partial x} + D_{xz} \frac{\partial c}{\partial z} \right) + \frac{\partial}{\partial z}\left(D_{zx} \frac{\partial c}{\partial x} + D_{zz} \frac{\partial c}{\partial z} \right) \tag{50}$$

where c is the contaminant concentration [ML^{-3}], υ is the average linear porewater velocity in the x,z directions [LT^{-1}] and D is the hydrodynamic dispersion tensor [LT^{-1}].

Two methods for solution of the advective-dispersion equation are employed in GW-WETLAND. The first method is a standard Galerkin finite element scheme (Pinder and Gray, 1977), which directly solves the 2-D advective-dispersion equation throughout the cross-section. The second method is a deterministic-probabilistic particle-tracking solute transport model (Ahlstrom et al., 1977; Schwartz, 1978; Prickett et al., 1981), in which particles representing the mass of contaminant are added at a specific source location(s) within the saturated flow domain and move by advection according to the velocities calculated within each element in the direction of groundwater flow. Dispersion is handled by generating a random number to account for velocity variations within the porous medium. Utilizing this method, both the location of particles within the flow domain and concentrations within each element are provided.

In addition, the particle-tracking method is able to provide visualization of the flow pathways of contaminants by looking at particle locations at each time step. This method has the advantage of being more numerically stable in systems that are advectively dominated when compared to the direct Galerkin-finite element solution to the advective-dispersion equation that is unstable when Peclet numbers greater than 2 prevail in the system and contaminants travel distances greater than the dimensions of an element in a given time step. Because the sands at PPNP are relatively homogeneous and have very high hydraulic conductivity (~2.52 x 10^{-2} cm/s), and thus contaminant transport is likely advectively dominated, the particle tracking method will be utilized for investigation of DDT transport at PPNP. A variety of output files are also generated to provide a variety of information including hydraulic conductivity distribution, hydraulic head distribution, flow velocities, mass balance information, fluid fluxes, particle locations and solute concentration at user-specified times. The output files have also been constructed to allow for simple visual presentation within GridBuilder© software.

4.8.3 Values Assigned to the GW-WETLAND Model Parameters:

The model for the simulations is based on the previously published model presented in Crowe et al. (2004) for the Camp Henry Transect. All parameters remained the same as presented, with minor adjustments made to recharge and evapotranspiration. The length of the simulations was extended to 1950 to 2003. Model input parameters were based on field measurements and best available literature values (Table 32).

4.8.4 Space and Time Discretization Parameters:

The flow domain is 500 m wide and extends perpendicular across the western barrier bar near CHO between Lake Erie and the marsh. The cross section extends 25 m past each shore (Figure 4) to ensure that the groundwater flow and DDT transport here is

Table 32. Values assigned to model parameters required by GW-WETLAND.

Parameter	Units	Values Used	Source
Aeolian and Shoreface Sands			
Effective porosity	-	0.3	Measured
K_{sat} (aeolian sand, shoreface sand)	m day^{-1}	8.64	Measured
Specific storage	m^{-1}	0.0005	Domenico and Schwartz (1998)
Specific yield	-	0.20	Domenico and Schwartz (1998)
Glaciolacustrine Sand			
Effective porosity	-	0.3	Measured
K_{sat} (lacustrine sand)	m day^{-1}	0.864	Measured
Specific storage	m^{-1}	0.0005	Domenico and Schwartz (1998)
Marsh Sediments			
Effective porosity	-	0.3	Measured
K_{sat} (marsh sediments)	m day^{-1}	8.64 x 10^{-3}	Measured
Specific storage	m^{-1}	0.0005	Domenico and Schwartz (1998)
Glacial Clay			
K_{sat} (clay)	m day^{-1}	0	No flow boundary
Grid dimensions	# rows, # columns	126, 501	Field measurements
Cell height	m	0.1	
Cell width	m	5.0	
Initial time step size	day	0.5	
Maximum time step size	day	1.0	
Time step scaling factor	-	1.05	
Convergence criteria	m	0.001	
Monthly precipitation (P)	m	PPNP and Leamington weather station data	Measured
Recharge (January - April)	m	0.50 x P	Fitting parameter
Recharge (April - December)	m	0.25 x P (0 - 150 m) 0.00 x P (150 - 250 m) 0.25 x P (250 – 500 m)	Fitting parameter
Evapotranspiration (Oct. - April)	m day^{-1}	0	Fitting parameter
Evapotranspiration (May – Sept.)	m day^{-1}	0 (0 – 250 m) 0.0010 (251 – 350 m) 0.0015 (351 – 501 m)	Fitting parameter
Monthly Lake Erie levels	m above model datum	1950 – 2004	Daily measurements
Monthly PPNP Marsh levels	m above model datum	1950 - 1978 1978 - 2004	Extrapolated from L.Erie level PPNP / NWRI records
Initial water table elevation	m above model datum	9.4	Approximated

Table 32 (cont'd).

Parameter	Units	Values Used	Source
Dispersivity (longitudinal, transverse)	m	1.0, 0.1	Domenico and Schwartz (1998)
Contaminant source zone location (point source)	m (x,z)	225 - 230, 8.4 – 8.5 325 - 330, 8.4 – 8.5 425 – 430, 8.4 – 8.5	Western boundary, centre, and eastern boundary of former agricultural landuse area
Contaminant source zone location (non-point source)	m (x,z)	225 - 430, 8.4 – 8.5	Entire span of former agricultural landuse area
Initial mass per contaminant particle	mg	Varies	Dependent upon loading curve
Number of particle source zones	-	Varies	Dependent upon loading curve
Number of particles added per time step	-	Varies	Dependent upon loading curve
Start date, Stop date	day number	Varies	Dependent upon loading curve
Degradation half-life	day^{-1}	3650	Marenco (2002), approximated from LEACHMP simulations

controlled by lake or marsh fluctuations and is not constrained by boundary conditions. Due to the ability of the model to not only simulate the rise and fall of the lake and marsh levels, but to simulate the corresponding lateral movement of the lake and marsh across the shore, the actual width of the barrier bar changes with time.

The finite element grid consists of 126 rows that are 0.1 m in height, and 501 columns that are 1.0 m in width. The total number of elements changes in response to the fluctuating water table, but generally exceeded 66,000 linear triangular elements, or 33,000 cells consisting of 2 elements each. There were a total of 481 free water table nodes that were located in the uppermost row of the saturated flow domain. This row of nodes was permitted to change in response to fluctuating water table conditions that change the geometry of the flow domain over time.

Simulations of groundwater flow at CHO begin on January 1, 1950 and extend to December 31, 2003 for a total of 19723 days of simulation time and 19730 time steps. Initial time steps were set at 0.5 days, and incrementally increased by a factor of 1.05 to a maximum time step of 1 day for the duration of the simulation. Model tolerance for convergence of the solution to the water table elevations was set at 0.001 m, with the maximum number of iterations set at 100 within each time step. Simulations generally took between 18 and 72 hours to execute on a computer with a Pentium IV-2.8 GHz processor, with execution times lengthening with increasing numbers of particles.

4.8.5 Physical and Hydraulic Properties

The definition and hydraulic properties of hydrostratigraphic units along the modelled cross-section was based on information derived from NWRI boreholes in the vicinity of Camp Henry (Figure 3) and are described in Crowe et al. (2004). Five sedimentary units were identified along the Camp Henry transect including aeolian sand, shoreface sand and gravel, lacustrine sand, clay-rich till, and gyttja. However, because the hydraulic conductivity of the aeolian sand and shoreface sand and gravel is essentially the same (2.52×10^{-2} cm/s for aeolian sand; 2.57×10^{-2} cm/s for shoreface sand and gravel, respectively), these two units were treated as a single hydrostratigraphic unit with an assigned hydraulic conductivity of 8.64 m/day. Because the aeolian sand is variably saturated, it was assigned both a specific yield of 0.20 and a specific storage of 0.0005 m^{-1}. The lacustrine sand, glacial clay till and gyttja were modeled as separate hydrostratigraphic units. Average hydraulic conductivity values are 4.17×10^{-3} cm/s for lacustrine sands 1.9×10^{-4} cm/s for marsh sediments based on a total of 24 tests (Crowe et al., 2004). The glaciolacustrine sand was assigned a hydraulic conductivity of 0.864 m/day and effective porosity of 0.3 and a specific storage of 0.0005 m^{-1}. Marsh sediments were assigned a hydraulic conductivity of 3.64 x 10^{-2} m/day, an effective porosity of 0.3 and a specific storage coefficient of 0.0005 m^{-1}. The glacial clay till unit has a very low hydraulic conductivity and the top of this unit was treated as an impermeable (no flow) boundary.

4.8.6 Boundary Conditions for Water Flow and Solute Transport

The upper boundary of the saturated flow domain is a free surface that is permitted to fluctuate throughout the simulation in response to changes in lake and marsh levels, and precipitation, and evapotranspiration. Infiltration and evapotranspiration fluxes across the upper boundary change spatially and over time in response to meteorological conditions described in Section 4.2.5, as well as vegetation types and thickness of the unsaturated zone across the barrier bar. In the model, evapotranspiration and infiltration were used as fitting parameters to match measured hydraulic head distributions across flow domain. Evapotranspiration is assumed to occur from the beginning of May to the end of October each year corresponding to the period of active plant growth and hence, transpiration. It is assumed that no evapotranspiration occurs from late October to late April each year.

Lake Erie and the marsh were represented as separate surface water bodies along part of the west and east portions of the flow domain (Figure 42). These boundaries were treated as variable constant head boundaries, with values of head set equal to daily lake and marsh levels. Daily water levels in Lake Erie have been recorded throughout the duration of the simulation at the Canadian Hydrographic Survey's Kingsville station

(Station # 6134190). However, marsh levels were only recorded at regular intervals from 1978 to 2004 by Parks Canada, so they were extrapolated from 1950 to 1978 based on the relationship between marsh and lake levels for the time when they had both been recorded. Because marsh levels were recorded sometimes on a daily basis and other times on a monthly basis, and because marsh levels change very little from week to week, average monthly marsh levels were assigned to each day during the month. To eliminate any short term impact on lake levels due to storms (Figure 4), that have essentially no impact on groundwater levels, the daily lake levels used in the simulations were obtained by first calculating a monthly average Lake Erie water levels and then calculating the daily value by linear interpolation between monthly values.

The side boundaries of the flow domain are no flow boundaries, situated at a sufficient distance away from the shore of Lake Erie and the marsh such that they do not generate unrealistic flow conditions within the saturated zone. The placement of the side boundaries is further supported by the fact that groundwater discharge into a large surface water body decreases exponentially from shore (McBride and Pfannkuch, 1975).

The bottom boundary, which represents the top of the clay-till, is a no flow boundary that slopes upward in elevation from west to east (Figure 3).

Contaminant transport was simulated using the particle tracking method, and varying numbers of particles were added via user-defined source zone locations over user-specified time intervals to represent the loading of Total DDT from the unsaturated zone. Initial particle masses and loading rates and times were based on outputs from LEACHMP modelling, and parameter values varied between simulations. Two areal loading scenarios were adopted in order to investigate point-source and non-point source loading. Point-source loading was used to discern approximate flow pathways and observe the effect of dispersion on groundwater concentrations over time. Non-point source loading was used to evaluate the outcome of field-scale application and leaching of DDT on groundwater concentrations beneath former orchard areas at PPNP.

Particles were added to the saturated zone at an elevation below the lowest recorded water level at Camp Henry monitoring wells in order to ensure that no contaminants were artificially removed from the flow domain as elements became unsaturated. This loading scenario approximates the loading of DDT compounds at the water table via leaching from the unsaturated zone. Thus, all source zones were 0.1 m thick and 5 m wide and were situated at an elevation of 8.4 to 8.5 metres above model datum (165.0 m a.s.l.). Solute breakthrough curves obtained from LEACHMP simulations were divided into separate loading periods to approximate the actual shape of the breakthrough curve using continuous, constant loading rates within each source zone. While loading rates specified for each source zone were variable, particles were added at the water table during each time step at a fixed rate within each loading period, necessitating a compromise between number of particles, number of source zones and particle mass in order to maintain reasonable simulation times on the order of days, rather than weeks. Contaminants were not added to the flow domain until well after time step sizes reached daily increments and the flow system had stabilized.

The bottom and side boundaries for solute transport were no-flow boundaries and did not permit contaminant transport by advective, dispersive or diffusive processes across the boundary. Contaminants were permitted to discharge to Lake Erie and the marsh, where the solute flux across the groundwater-surface water interface over time could be known. Contaminant masses and concentrations were no longer recorded following discharge to the surface water bodies.

4.8.7 Initial Conditions for Water Flow and Solute Transport

The initial conditions for the flow domain were a flat water table at an elevation of 8.85 m above model datum, corresponding to an elevation of 173.85 metres above sea level. The initial water levels for Lake Erie and the marsh were 8.85 m and 9.26 m, (elevations of 173.85 m a.s.l. and 174.26 m a.s.l.) respectively, based on recorded lake levels and estimated marsh levels from the day the simulations commenced.

The flow domain was initially free of DDT.

4.8.8 Solute Transport Parameters

Longitudinal and transverse dispersivity values of 100 cm and 10 cm, respectively, were taken from previous modelling of a septic plume at the Camp Henry Transect (Crowe et al., 2004). The dispersivity values are consistent with reported standard values (Domenico and Schwartz, 1998).

A half-life of 3650 days (10 years) was implemented based on the best-fit half lives in deep soils achieved through LEACHMP modelling. This is also consistent with half-lives in deep soils reported in previous studies within PPNP (Marenco, 2002; Crowe et al., 2002), as well as the best fit LEACHMP calibration (PPI4023B).

Because there are no field measurements of organic carbon content within the saturated zone, and LEACHMP simulations illustrate that adsorption cannot be occurring within the saturated zone, the flow domain was assumed to be free of organic carbon and DDT compounds were non-sorbing within the flow domain. Thus, retardation (adsorption) of DDT was not employed in the GW-WETLAND simulations.

4.8.9 GW-WETLAND Output Parameters

Hydraulic head distribution, elevation of the water table, and the location and mass of particles were output at various times to allow for the visualization of the transient behaviour of flow and contaminant transport at Camp Henry using GridBuilder© software (McLaren, 1992) and spreadsheet software packages. GW-WETLAND output files were quite large owing to the long time period being simulation and thus, only 15 output times between 1950 and 1970 on days 1, 176, 2000, 4000, 5000, 6000, 7000, 7310, 8000, 10000, 12000, 14000, 16000, 18000 and 19477 were specified. This provided outputs that were approximately equally spaced throughout the duration of simulations, with additional outputs on the calibration date (May 12, 2003) and days after the largest pulse loading events had occurred. The elevation of the water table was printed at every time step, allowing for the comparison of water table elevations with measured data over on specific dates to evaluate the quality of the flow calibration. Output was post-processed and contoured within GridBuilder© in order to illustrate concentrations within groundwater. After plotting several different contour intervals and ranges of values, a compromise was reached affording the best resolution of concentrations. While the entire range of concentrations is not reflected in many simulations, they appear as blank areas and can be inferred to represent concentrations above the greatest value on the contour scale colour bar.

4.9 GW-WETLAND Flow Calibration

Only groundwater flow in the saturated zone was calibrated because DDT concentrations in groundwater have only recently been measured at the water table (1998, 2002, 2003) and most of the sampling locations were not located within the 2-dimensional flow domain being simulated. The simulations were undertaken from 1950 to 2003 but were only calibrated against 10 years of measured water table elevations (1994 - 2003) recorded by NWRI staff.

Because the exact magnitudes of infiltration and evapotranspiration were not known across the entire transect, they were used as fitting parameters to match the measured spatial and temporal distribution of the elevation of the water table at CHO. The transect was divided into 3 regions based on similarities in vegetation and depth to the water table, to which infiltration and evapotranspiration values were assigned. Evapotranspiration rates employed for the simulations at the Camp Henry transect were 0 m/day from 1 to 250 m east across the transect, 1.00×10^{-3} m/day from 251 to 350 m and 1.50×10^{-3} m/day from 351 to 501 m for May to September, and 0 m/day across the entire transect from October to April each year.

The model was able to simulate the elevation of the water table (Figure 43). When modelled elevations of the water table were compared to measured elevations of the water table along the Camp Henry transect, a relatively good correlation was observed, with all points clustering near the 1:1 line and RMS errors of 0.151 m, 0.124 m and 0.116 m for wells CH-29, CH-25 and CH-27, respectively (Figure 44). These errors were calculated based on a total of 292 water table elevation measurements, and the pooled RMS error for all 3 wells was 0.1308 m. This indicates that GW-WETLAND is able to accurately represent groundwater flow regime within the barrier bars at PPNP near CHO.

4.10 Solute Transport Simulations

The calibrated GW-WETLAND model of the flow domain across the barrier bar at CHO was used to evaluate the transport of DDT within the saturated zone in response to both meteorological conditions measured between 1950 and 2004 and various DDT loading scenarios across the water table based on LEACHMP simulation outputs. Only one cross section, that at Camp Henry Orchard, is simulated because former agricultural areas within PPNP from the Camp Henry Orchard southward to the former Ander's Orchard have a similar geology and groundwater flow regime. The model simulates the various DDT loading scenarios during the 54-year period of time from the first applications of DDT in 1950 through the last applications of DDT in 1970 to 2003.

Two types of DDT loadings to the saturated domain as a flux across the water table were simulated, (1) point source (scale of a few m^2) representing a spill or current location of very high concentrations in the shallow soil, and (2) non-point source (scale of 100's m^2) representing widespread DDT loading across a large portion of the barrier bar as would occur from an agricultural application of DDT to a field or orchard. The point-source loading is used to examine the direction of transport, either towards the lake or the marsh, depending on where across the barrier dissolved DDT entered the flow domain. The point-source loading is also used to examine the spreading of dissolved DDT due to dispersion and diffusion as it is transported with groundwater flow through the barrier bar. Non-point source loading is used to examine typical concentrations that would be seen in groundwater both historically as well as today under typical agricultural land-use areas (e.g.. vegetable field, orchard). Specifically, at CHO, the spatial distribution of the non-point source loading area matches the known extent of former agricultural areas within that region of the park (Figure 2).

4.10.1 DDT Source Zones within the Flow Domain

Three source zones were used for the non-point source loadings. Each source zone was 5 m or 5 cells wide by 0.1 m or 1 cell thick, and located at the water table. These source zones were located within the former Camp Henry orchard, at the most westerly edge of the former orchard at 225 - 230 m, the centre of the former orchard at 325 - 330 m, and the eastern edge of the former orchard at 425 - 430 m, or at distances of approximately 220 m, 120 m, and 20 m from the edge of the marsh (Figure 42).

Non-point source loading was simulated with one source zone 205 m wide by 0.1 m thick (205 x 1 cell) representing the entire width of the former Camp Henry orchard. It was located at 225 – 430 m or located between 225 m and 20 m from the marsh, and again placed along the water table (Figure 42). Another simulation employed a persistent addition of DDT for 54 years at 1 ng per time step from 325 - 326 m.

GW-WETLAND removes all contaminant mass from along the water table if the water table falls sufficiently to drain the element. To ensure that all DDT added to the saturated zone was conserved, source zones were placed at the lowest water table elevation recorded at Camp Henry monitoring wells (8.4 m - 8.5 m above datum).

4.10.2 DDT Loading Rates to the Flow Domain

A total of 11 scenarios were run with GW-WETLAND, based on: (1) point source or non-point source loading, (2) year the DDT loading occurred, and (3) the length of time in which loading occurred (Table 33). The loading of DDT to the water table in the GW-WETLAND simulations is based on the three different breakthrough curves from LEACHMP outputs: (1) single pulse input of DDT, (2) multiple pulses of DDT, (3) long-term continuously increasing loading rate of DDT, and (4) long-term constant loading rate of DDT (Table 33). Because LEACHMP simulated loading of DDT compounds in both 1950 and 1970, two suites of GW-WETLAND simulations were run for each LEACHMP loading scenario. In all cases, simulations began in 1950, although loadings started in either 1950 or 1970.

The particle tracking routine was utilized within GW-WETLAND for the PPNP simulations. The mass of each particle added to the flow domain remained the same throughout the duration of each simulation, but was changed from one simulation to another in order to keep the total number of particles between 5,000 and 20,000 and keep

Table 33: GW-WETLAND simulations run to examine DDT transport scenarios.

Simulation	Type of source zone(s)	LEACHMP loading	Loading schedule
CH 1a	point source	Figure 39	single 85 day pulse of DDT during 1950
CH 1b	point source	Figure 39	single 256 day pulse of DDT during 1970
CH 2a	non-point source	Figure 39	single 85 day pulse of DDT during 1950
CH 2b	non-point source	Figure 39	single 256 day pulse of DDT during 1970
CH 3a	point source	Figure 37	long slow increase in DDT loading to w.t. from 1950 to 2003
CH 3b	point source	Figure 37	long slow increase in DDT loading to w.t. from 1970 to 2003
CH 4a	non-point source	Figure 37	long slow increase in DDT loading to w.t. from 1950 to 2003
CH 4b	non-point source	Figure 37	long slow increase in DDT loading to w.t. from 1970 to 2003
CH 5a	point source	-	very low continuous leaching over 54 years (1950 - 2003)
CH 6a	point source	Figure 37	2 year pulse of DDT during 1955/56, 1960/61, 1965/66, 1970/71
CH 6b	non-point source	Figure 37	2 year pulse of DDT during 1955/56, 1960/61, 1965/66, 1970/71

simulation times reasonable. Particle loading times and number of particles loaded at each time step were determined based on the LEACHMP outputs for each leaching scenario, with LEACHMP solute breakthrough curves being approximated as a step function because the number of particles added to the flow domain must remain constant over time. Variable loading rates were accomplished by implementing multiple source zones at the same grid location at several different times (Table 34). In all situations the mass leached as predicted by LEACHMP simulations closely matched that input into GW-WETLAND simulations.

4.11 Discussion of GW-WETLAND Modelling Results

The outputs from all point source loading of DDT simulations generally show 3 distinct plumes. For the purposes of clarity, the westernmost plume will be referred to

Table 34: Total DDT loading approximations employed in GW-WETLAND simulations.

Simulation	Particle mass (mg)	Start time (day)	End time (day)	Particles added per time step	Number and Type of source zone(s)	Total mass added per zone per loading period (mg)	Total number of particles	
							Per zone	**Total**
CH 1a	1	90	100	317	3 P.S. zones	3170		
Figure 45	1	101	135	9	3 P.S. zones	306		
	1	136	175	3	3 P.S. zones	117		
						3593	**3593**	**10779**
CH 1b	1	7396	7406	240	3 P.S. zones	2400		
Figure 46	1	7407	7441	15	3 P.S. zones	510		
	1	7442	7652	3	3 P.S. zones	630		
						3540	**3540**	**10620**
CH 2a	20	90	100	690	1 N.P.S.	138000		
Figure 47	20	101	135	19	1 N.P.S.	12920		
	20	136	175	2	1 N.P.S.	1560		
						152480	**7624**	**7624**
CH 2b	20	7396	7406	525	1 N.P.S.	105000		
Figure 48	20	7407	7441	29	1 N.P.S.	19720		
	20	7442	7652	6	1 N.P.S.	25200		
						149920	**7496**	**7496**
CH 3a	0.001	6570	6571	150	3 P.S. zones	0.15		
Figure 49	0.001	7665	7666	150	3 P.S. zones	0.15		
	0.001	8760	8761	150	3 P.S. zones	0.15		
	0.001	9855	9856	150	3 P.S. zones	0.15		
	0.001	10950	10951	150	3 P.S. zones	0.15		
	0.001	12045	12046	150	3 P.S. zones	0.15		
	0.001	13140	13141	150	3 P.S. zones	0.15		
	0.001	14235	14236	1	3 P.S. zones	0.001		
	0.001	15330	15331	1	3 P.S. zones	0.001		
	0.001	15332	19710	1	3 P.S. zones	4.378		
						5.43	**5430**	**16290**

Table 34 (cont'd).

Simulation	**Particle mass** (mg)	**Start time** (day)	**End time** (day)	**Particles added per time step**	**Number and Type of source zone(s)**	**Total mass added per zone per loading period** (mg)	**Total number of particles**	
							Per zone	**Total**
CH 3b	0.0001	15774	15775	500	3 P.S. zones	0.05		
Figure 50	0.0001	16650	16651	500	3 P.S. zones	0.05		
	0.0001	17307	17308	500	3 P.S. zones	0.05		
	0.0001	17928	17929	500	3 P.S. zones	0.05		
	0.0001	13402	18403	500	3 P.S. zones	0.05		
	0.0001	18731	18732	500	3 P.S. zones	0.05		
	0.0001	19132	19133	500	3 P.S. zones	0.05		
	0.0001	19607	19608	500	3 P.S. zones	0.05		
						0.40	**4000**	**12000**
CH 4a	0.02	6570	6571	308	1 N.P.S.	6.16		
Figure 51	0.02	7665	7666	308	1 N.P.S.	6.16		
	0.02	8760	8761	308	1 N.P.S.	6.16		
	0.02	9855	9856	308	1 N.P.S.	6.16		
	0.02	10950	10951	308	1 N.P.S.	6.16		
	0.02	12045	12046	308	1 N.P.S.	6.16		
	0.02	13140	13141	308	1 N.P.S.	6.16		
	0.02	14235	14236	308	1 N.P.S.	6.16		
	0.02	15330	15331	308	1 N.P.S.	6.16		
	0.02	15332	19710	2	1 N.P.S.	175.12		
						230.56	**11528**	**11528**
CH 4b	0.001	15774	15775	2050	1 N.P.S.	2.05		
Figure 52	0.001	16650	16651	2050	1 N.P.S.	2.05		
	0.001	17307	17308	2050	1 N.P.S.	2.05		
	0.001	17928	17929	2050	1 N.P.S.	2.05		
	0.001	18402	18403	2050	1 N.P.S.	2.05		
	0.001	18731	18732	2050	1 N.P.S.	2.05		
	0.001	19132	19133	2050	1 N.P.S.	2.05		
	0.001	19607	19608	2050	1 N.P.S.	2.05		
						16.4	**16400**	**16400**

Table 34 (cont'd).

Simulation	**Particle mass** (mg)	**Start time** (day)	**End time** (day)	**Particles added per time step**	**Number and Type of source zone(s)**	**Total mass added per zone per loading period** (mg)	**Total number of particles**	
							Per zone	**Total**
CH 5a	0.000001	30	19722	1	325 - 326 m	0.019692		
Figure 53						**0.019692**	**19692**	**19692**
CH 6a	100	2008	2738	1	3 P.S. zones	73000		
Figure 54	100	3833	4563	1	3 P.S. zones	73000		
	100	5658	6388	1	3 P.S. zones	73000		
	100	7483	8213	1	3 P.S. zones	73000		
						73000	**730**	**2190**
CH 6b	1000	2008	2738	4	1 N.P.S.	2920000		
Figure 55	1000	3833	4563	4	1 N.P.S.	2920000		
	1000	5658	6388	4	1 N.P.S.	2920000		
	1000	7483	8213	4	1 N.P.S.	2920000		
						2920000	**2920**	**2920**

N.P.S. – Non-point source loading from 225-430 metres across the transect
P.S. – Point-source loading from 225-230, 325-330 and 425-430 metres across the transect.

as Plume #1, Plume #2 is the central plume and the easternmost plume is Plume #3. It should be noted that the cross sections showing the distribution of DDT in the saturated zone are drawn with a vertical exaggeration of 6.8 times.

Because GW-WETLAND does not simulate solubility reactions (i.e., dissolution and precipitation), some of the scenarios predicted DDT concentrations in groundwater above what would be expected natural system given that the solubility of DDT in water is 0.005 mg/L (Table 5). While such high concentrations are not likely accurate because DDT compounds would precipitate at these concentrations, these simulations do provide insight into where elevated concentrations of DDT would likely be found in the aquifer.

2-D groundwater flow conditions from 1950 to 2004

General statements can be made about the groundwater flow conditions at Camp Henry because the same calibrated groundwater flow solution was used for each simulation. Groundwater flow is infiltration dominated at Camp Henry between 1950 and 2003. Simulations predict groundwater flow divide exists within the central portion of the barrier bar and it fluctuates between 225 m and 325 m in response to annual changes in the relative elevations of Lake Erie and the marsh. Thus, groundwater flow in this 225 – 325 m portion of the barrier bar experiences a short-term reversal in flow direction. These observations are consistent with those of Crowe et al. (2004).

Distinct plumes develop as a result of the imposed DDT loading conditions and the system is advectively dominated, except in the small portions of the barrier bar where a reversal occurs and here dispersion dominates. An average linear pore water velocity can be calculated based on the position of the centre of the contaminant plumes over time. Based on the locations of the three plumes during 1950 and 1961 (Figure 45), groundwater velocities were calculated to be 3 - 5 m/yr for the eastern portion of the barrier bar, and 8 - 10 m/yr for the western the barrier bar. The higher groundwater velocities in the western portion of the barrier bar are a result of steeper hydraulic gradients due to a greater range of lake level fluctuations versus those in the marsh.

Short-term point source loading of DDT in 1950 and 1970

Scenarios CH 1a and CH 1b simulate short-term (85 days) point source loading of DDT at the water table as high-concentration pulse shortly after application of DDT in

1950 and 1970, respectively. The simulation results of both simulations produce three main observations (1) the plumes move either towards, and discharge into, the lake or marsh due to advective transport, (2) the plumes become more dispersed with time occupying a large vertical portion of the saturated domain, and (3) concentrations of DDT rapidly decline over time (Figures 45 and 46).

In both scenarios, Plume #1 migrates toward Lake Erie, while Plumes #2 and #3 migrate toward the marsh. When DDT loading occurred during 1950, Plume #3 and nearly all of Plume #2 have discharged to the marsh by 2003. But as expected due to the short time for contaminant migration, only all of Plume #3 and some of Plume #2 have discharged to the marsh by 2003. In both scenarios, substantial DDT from Plume #1 remains within the lacustrine sands below the western portions of the barrier bar by 2003. The lower hydraulic conductivity of the lacustrine sands means that it may take some time for the lacustrine sands to be free of DDT through discharge to Lake Erie. In both cases, a substantial portion of the aeolian sand is free of DDT contamination.

Within 10 years after loading of DDT at the water table in both scenarios, contaminants have spread throughout much of the vertical extent of the saturated zone. This is due to the dispersive nature of contaminant transport through the permeable sand, the length of time over which loading occurred (85 days and 256 days), recharge (especially the spring melt) pushing the contaminants downward within the saturated zone, and evapotranspiration pulling the contaminated groundwater upwards.

Concentrations of DDT in the source zones immediately below the water table are very high because contaminant loading into the source zone is faster than groundwater flow velocity to remove the contaminated water, and the loading is faster than degradation rates. Over time, concentrations of DDT in the contaminant plumes rapidly decline because of both a loss of mass due to degradation and spreading of mass due to dispersion. After 54 years of transport and degradation (Figure 45), maximum concentrations of DDT remaining in the aeolian sand (Plume #2) are less than 1 mg/L. But after only 30 years of transport and degradation (Figure 46), DDT concentrations in the aeolian sand are still quite high (>10 mg/L). Within the lacustrine sands, the predicted DDT concentrations for 2003 show a different pattern. Not only is there considerable DDT remaining in the lacustrine sand, but the difference in maximum concentrations between the 1950 and 1970 loading are much less than those in the aeolian sands to due greater dispersion. Maximum concentrations are approximately 1 mg/L and 5.0 mg/L, when DDT was introduced in 1970 and 1950, respectively.

Short-term non-point source loading of DDT in 1950 and 1970

Scenarios CH 2a and CH 2b simulate short-term, non-point source loading of DDT to the saturated zone below former agricultural areas near CHO. Both simulations show (1) DDT spreads through the saturated domain from the lake to the marsh, and discharges into the lake and marsh in less than 20 years due to advective transport, (2) the size of the plumes expanded due to dispersion, (3) the contaminant plumes moved downward to the base of the saturated zone, and (4) concentrations of DDT rapidly decline over time (Figures 47 and 48).

Again, flow of contaminants is towards both the marsh and Lake Erie, but most movement of contaminant mass was toward the marsh due to the position of the flow divide. The loading resulted in a large continuous plume that extended from Lake Erie to the marsh in less than 20 years. However, because recharge (especially spring melt) pushes the contaminant plume downward to the base of the saturated domain, the entire saturated domain is not contaminated. The plumes move upward with groundwater flow to discharge into the marsh, and also rise to the water table adjacent to the marsh due to evapotranspiration. Contamination still extends from the lake to the marsh by 2003 in both cases. Based on the 1950 loading scenario, it would appear that DDT will remain in the lacustrine sand far longer than in the aeolian sand.

Over time, concentrations rapidly decline due to dispersion, degradation, and mixing with infiltration. There does not appear to be a significant difference in concentrations between the portions of the plume within the aeolian sand and the lacustrine sand. Maximum concentrations in 2003 are 15 mg/L for a loading in 1950, and 80 mg/L for a 1970 loading.

Point source, slow increase in DDT loading from 1950 to2003 and 1970 to 2003

LEACHMP simulations indicate that because DDT is strongly bound within the Ah horizon, and is slowly moving downward to the B and C horizons, concentrations of DDT leaving the Ah horizon, and hence crossing the water table, will continuously and slowly increase with time (Figure 37). Scenarios CH 3a and CH 3b are designed to assess the distribution of DDT compounds in groundwater that would result from continuously increasing surficial loadings from 1950 to present from point sources. Due to restrictions in contaminant input in GW-WETLAND, the 54-year continuously increasingly loading at the water table is represented as a series of increasing pulses. For the 1950 loading, the pulses occur for 1 day every 1095 days, from 1968 to 1992 and continuously from 1992 to 2003. For the 1970 loading, the pulses occur for 1 day at 329 to 867 day intervals between 1993 and 2003. As a result of this loading schedule (pulse inputs), the contaminant plume often appears as a series of plumes.

As with the previous simulations, Figures 49 and 50 illustrate that the contaminant plumes (1) move towards, and discharge into, the marsh and lake over time, (2) move downward to the base of the flow regime due to recharge (especially spring melt), and (3) spread due to dispersion. Concentrations of DDT decrease as the plume migrates from the source zone. However, concentrations in the contaminant plumes adjacent to the source zones increase over time as flux loading at the water table increases, and by 2003 concentrations reach levels of 0.60 mg/L and 0.10 mg/L for the 1950 and 1970 loading scenarios, respectively. Mass loading also increases at a rate faster than the contaminants can be removed by degradation and advective transport. As the loading rates continue to increase, an increasing portion of the saturated zone will become contaminated by higher concentrations of DDT.

Non-point source, slow increase in DDT loading from 1950 to2003 and 1970 to 2003

Scenarios CH 4a and CH 4b are designed to assess the distribution of DDT compounds in groundwater that would result from continuously increasing loading of

DDT at the water table from 1950 to present (long-term slow leaching of DDT from the Ah horizon) from non-point sources. Again, due to restrictions in contaminant input in GW-WETLANDS, the 54-year continuously increasingly loading at the water table is represented as a series of increasing pulses, and the predicted contaminant plumes often appear as a series of plumes.

As with previous simulations, Figures 51 and 52 illustrate that the contaminant plumes (1) move towards, and discharge into, the marsh and lake over time, (2) move downward to the base of flow regime due to recharge, and (3) spread due to dispersion. A widespread plume of contaminated groundwater was observed under the entire area formerly used for agricultural. Due to the both the continuous loading of DDT and the increasing loading rate, concentrations increase over time at the source zone and in an increasingly larger area adjacent to the source zone. Because LEACHMP predicts that this loading scenario will continue at PPNP well into the future, a great portion of the saturated zone between Lake Erie and the marsh will be contaminated by increasing levels of DDT.

Point source, very low continuous leaching of DDT from 1950 to 2003

Scenario CH 5a was undertaken to assess the impact of continuous loading of small amounts of DDT at one location over a long period of time (1950-2003). In this scenario 1 ng (10^{-6} mg) of DDT was added at every time step (daily) for 54 years via a 1 m by 0.1 m source zone located in the centre of the former agricultural areas at the Camp Henry transect (325 m – 326 m).

A continuous contaminant plume develops that moves in the direction of groundwater flow towards, and discharges into, the marsh (Figure 53). The plume spreads due to dispersion and is pushed deeper into the aquifer by recharge. After a few decades, the entire portion of the aquifer between the source zone and the marsh is contaminated because of the continuous loading of DDT. However, groundwater to the west of this source zone is never contaminated by DDT. Concentrations within the contaminant plume continue to increase, especially adjacent to the source zone, because of continuous loading of DDT. Even though only 10^{-6} mg of DDT is loaded each day, concentrations reach a maximum of 1.2 x 10^{-3} mg/L near the source zone after 54 years. It can be expected that increased concentrations of DDT in groundwater will be seen in the future, although the portion of the aquifer contaminated will remain essentially the same, given that the leaching conditions simulated by LEACHMP will continue at PPNP well into the future. While this contaminant plume moves exclusively toward the marsh for this scenario, a similar migration scenario towards Lake Erie would occur if the source zone had been located to the west of the groundwater flow divide.

A corresponding non-point source continuous long-term loading was not tested due to limitations on the number of particles that could be added to the flow domain. However, based on the previous non-point source scenarios, it is expected that the continuous loading will rapidly cause contamination of essentially the entire aquifer.

Point source, multiple 2-year pulse loading in 1955/56, 1960/61, 1965/66, 1970/71

Scenario CH 6a represents multiple point-source additions of DDT to the saturated zone, corresponding to applications DDT at five-year intervals, and its subsequent pulse leaching to the water table. The loading history for this scenario consists of DDT loading to the water table for two years, followed by three years of no loading at the three loading zones; this sequence is repeated four times during 1955-1956, 1960-1961, 1965-1966, and 1970-1971.

Figure 54 shows the contaminants (1) move towards, and discharge into, the marsh and lake over time, (2) move downward to the base of flow regime due to recharge, and (3) spread due to dispersion. The individual plumes are separated during the first 20 years of the simulation because of the three–year pause between DDT loadings. Although concentrations at the source zone are equally high every five years, maximum concentrations of DDT within each successively earlier plume decrease over time. By 1980, the plumes from source zone #3 have discharged into the marsh, and the individual plumes from source zones #1 and #2 have started to amalgamate into single contaminant plumes. By about 1990, the plumes have either moved to the marsh or into the lacustrine sand, leaving most shallow groundwater uncontaminated. In 2003, the plume near the marsh appears to discharge slowly to the marsh as the plume is pushed towards the marsh during the winter and pulled away from the marsh during the summer due to evaporative fluxes near the marsh boundary. As in previous simulations, high concentrations of DDT persisted within the lacustrine sand on the western side of the barrier bar and DDT continued to discharge to Lake Erie in 2003.

Non-point source, multiple 2-year pulse loading in 1955/56, 1960/61, 1965/66, 1970/71

Scenario CH 6b represents multiple non-point source pulse loading of DDT to the saturated zone corresponding to applications of DDT at five-year intervals. This scenario is the non-point source equivalent of scenario CH 6a; with the same 2-year loading of DDT at the water table, followed by a 3-year gap, and this sequence repeated four times.

As expected, the contaminants (1) move towards, and discharge into, the marsh and lake over time, (2) move downward to the base of flow regime due to recharge (especially spring melt), and (3) spread due to dispersion (Figure 55). Groundwater contamination is very extensive and widespread, with very high concentrations persisting deep in the aquifer even during 2003. In fact the extent of groundwater contamination and concentrations are much greater than any previous non-point simulation. Based on this scenario, loading of DDT to the saturated zone in 1955, 1960, 1965 and 1970 will cause contamination to persist deep in the aquifer even though concentrations at the water table are essentially zero. The only location where concentrations were above zero at the water table resulted from enhanced evapotranspiration near the marsh boundary (Figure 55). Widespread loading of high concentrations DDT at multiple times indicated that if this type of loading had historically occurred, deep groundwater near the marsh and within the lacustrine sands near Lake Erie would remain contaminated today.

4.11 <u>1-D and 2-D Modelling Summary</u>

One-dimensional vadose zone modelling with LEACHMP showed that the primary transformation/degradation pathway in the soils of the former agricultural areas at CHO is via the aerobic transformation of DDT to DDE, with half-lives of ~30 years at ground surface and ~9 years at depth. Very little transformation of DDT to DDD or DDE to further degradation products occurs (estimated half-lives of 450 and 100 years, respectively). Simulations at SHO (shallower depth to water table, different organic carbon content, lower elevation) illustrated that degradation was occurring at a uniform half-life of ~14 years with depth. Simulations predicted no leaching at CHO with the present levels of organic carbon found in the soil profile throughout the time period that was simulated. When organic carbon was removed from the Bm and C horizons, leaching began after approximately 40 years, and concentrations of Total DDT crossing the water table were within one-order of magnitude of measured concentrations. The limiting factor in this case is that DDT is bound to the organic carbon in the Ah horizon, because once DDT enters the Bm and C horizons, it is flushed to the water table within a few days with infiltration. This suggests that the sorption mechanism at PPNP is probably either kinetic, or depth-dependent. At SHO, where the water table is shallower and Ah horizon organic carbon contents are lower, leaching was predicted but at levels 10 orders of magnitude less than measured. Again, when organic carbon was removed from deep soils, concentrations at the water table compared very favourably to measured data in May 2003. This implies that if the depth to the water table is sufficiently shallow, some DDT will reach the water table even if some organic carbon is present.

Two-dimensional GW-WETLAND modelling showed that whenever DDT enters the groundwater domain, no matter what the loading scenario, all contaminant plumes show (1) advective transport towards the lake or marsh, depending upon the location source zone with respect to the groundwater divide, (2) contaminants will always discharge into the lake or marsh, (3) dispersion spreads contamination as it moves via groundwater flow, (4) groundwater recharge across water table pushes the contamination to base of the aquifer and, (5) DDT can be "trapped" in lower K units, resulting in longer retention time in the saturated zone. As long as continuous loading of DDT to the water table occurs at a field scale even at a very small rate (1 ng/L per day), essentially the entire groundwater flow domain from the lake to the marsh will always be contaminated. However, if the loading of DDT were to stop, concentrations in the contaminant plume would decrease and contaminated groundwater would eventually be flushed from the aquifer, but this would still take several decades. Discharge to the marsh and Lake Erie will account for most of the mass removal assuming current degradation rates are accurate. Groundwater recharge across water table will push contaminated groundwater to the base of the aquifer, and thus although very high concentrations exist at the base of the aquifer, no contamination is seen near the water table well away from the source zone. Thus even if a large pulse of DDT reached the water table, little evidence of that contamination would be seen today based on samples collected at the water table. If, as suspected from the LEACHMP simulations, loading of DDT compounds to the saturated zone began recently, an increasing portion of the aquifer will be contaminated and DDT concentrations will continue to increase for decades to come, should present climatic and hydrological conditions continue into the future.

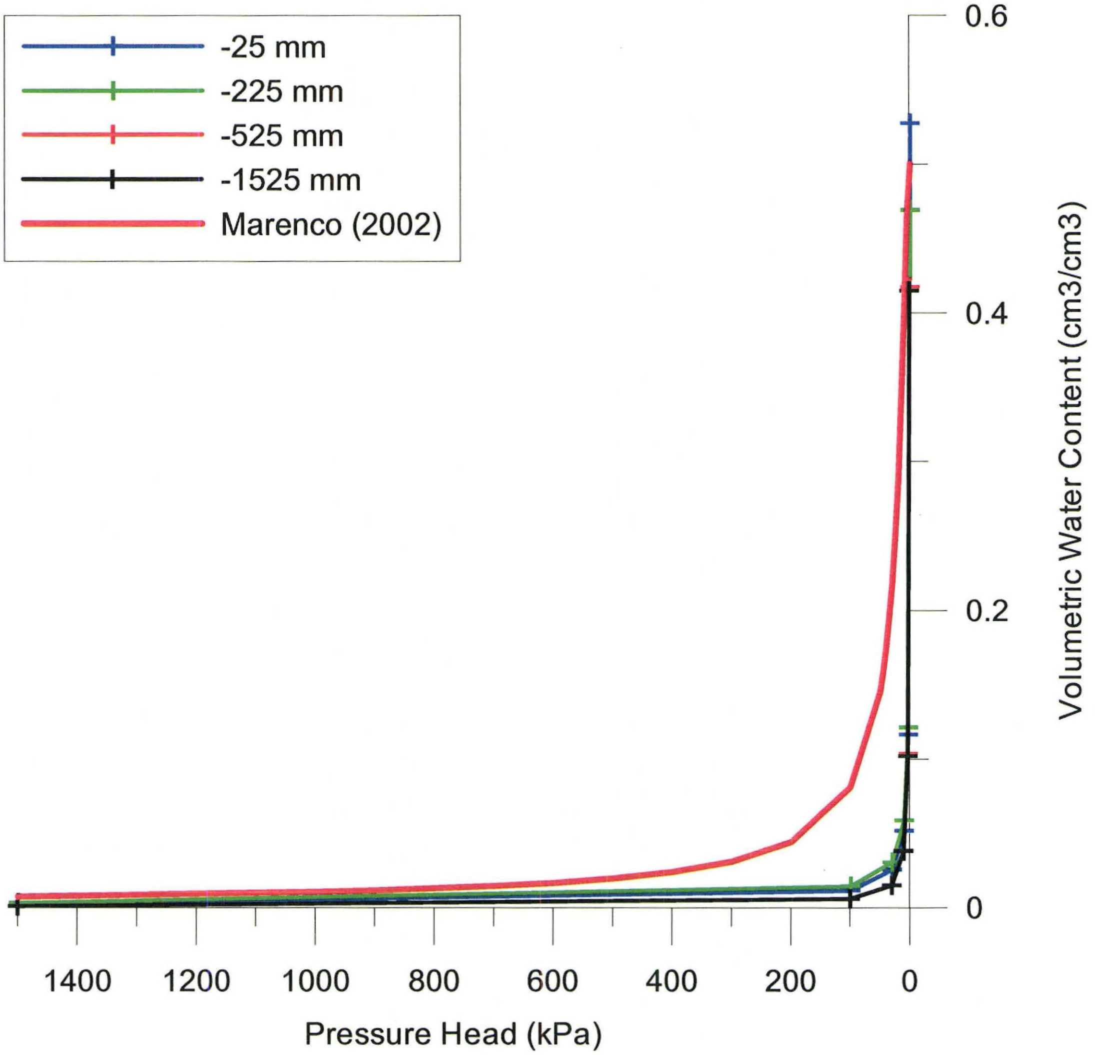

Figure 22. Soil moisture characteristic curves employed at 200 mm, 500 mm and 1500 mm for all LEACHMP simulations. Also presented is the best-fit soil moisture characteristic curve as measured by Marenco (2002) under drainage conditions.

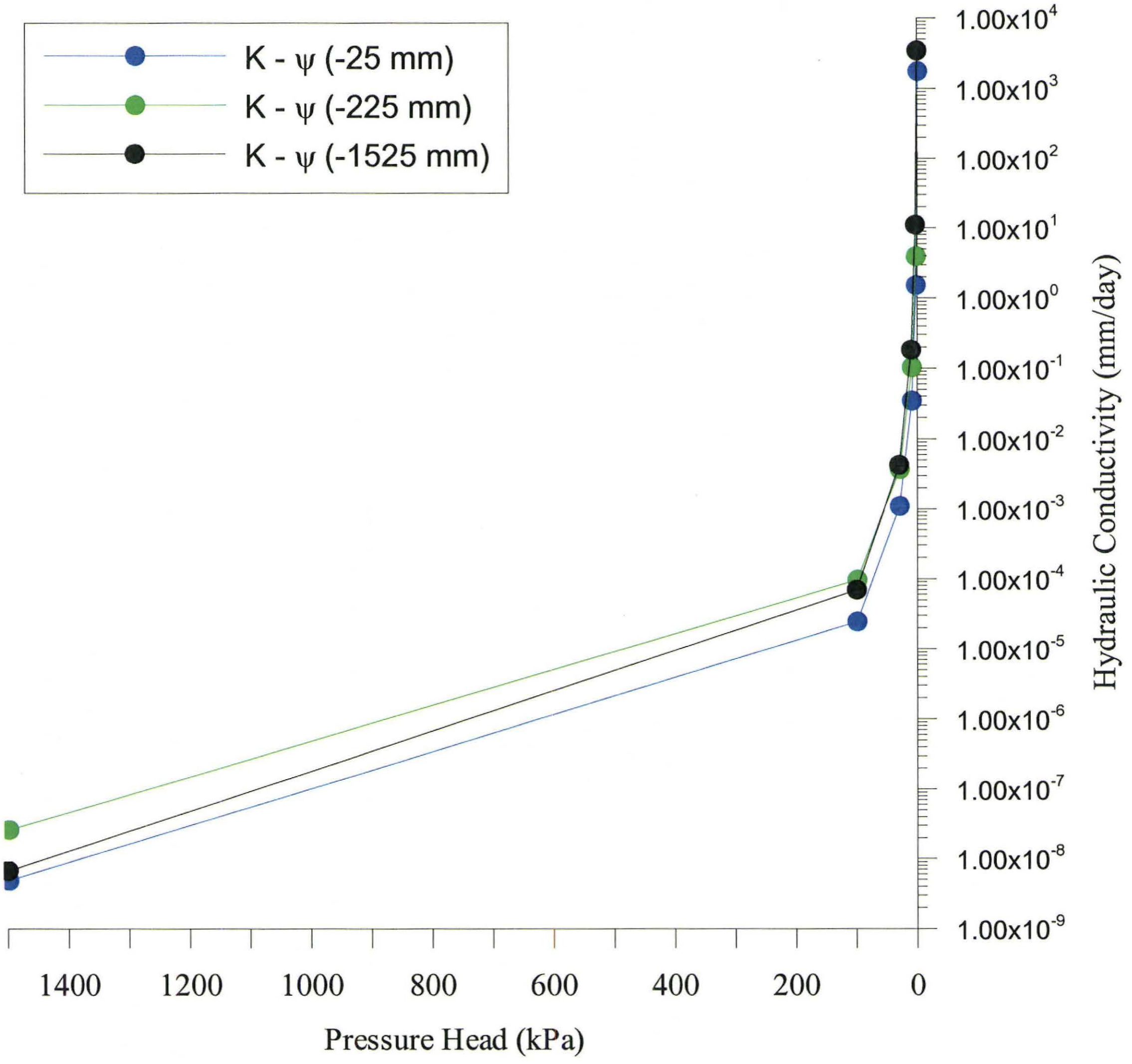

Figure 23. Modelled unsaturated hydraulic conductivity function employed in LEACHMP simulations.

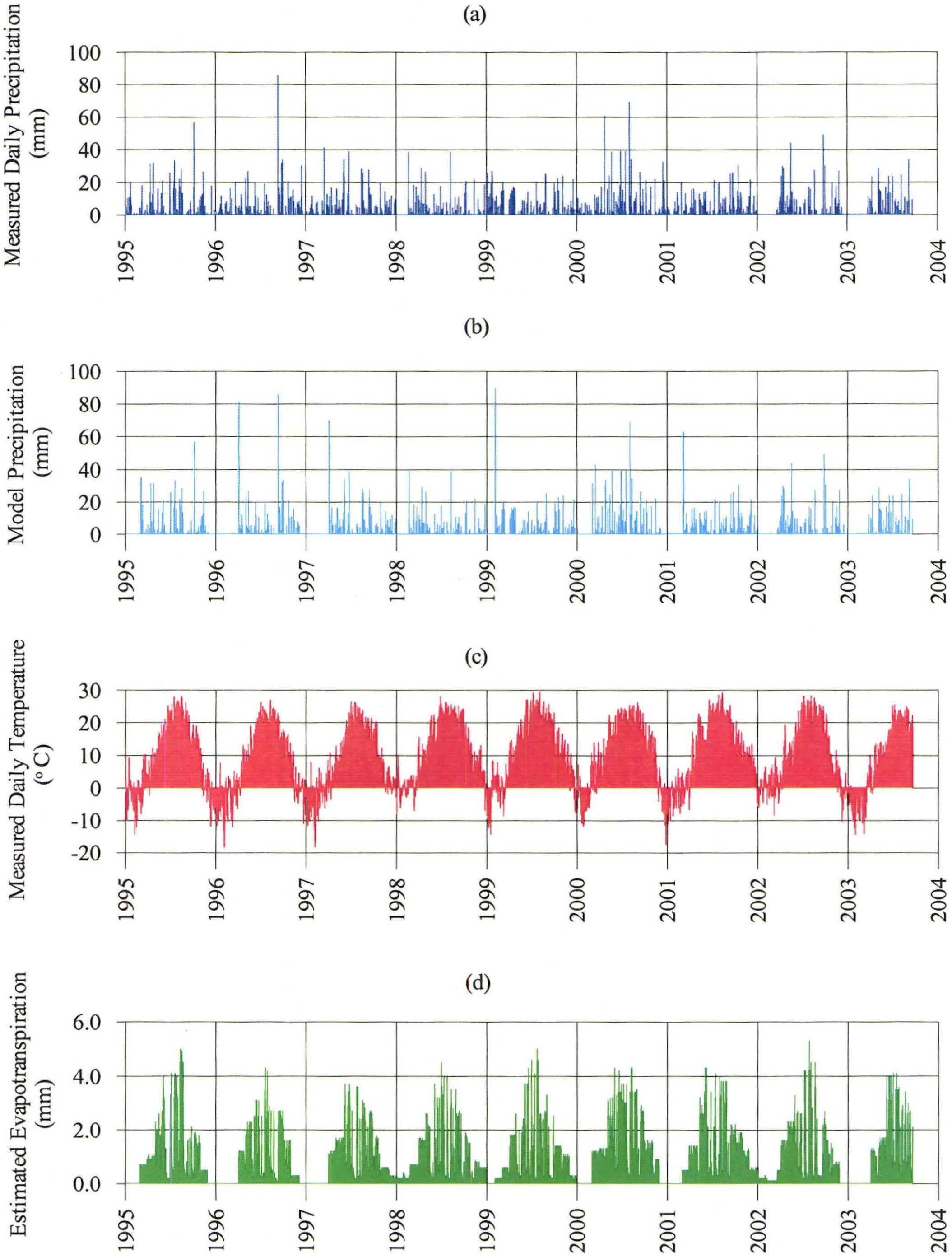

Figure 24. Measured total daily precipitation, model input precipitation, measured daily temperature and Thornthwaite estimated daily potential evapotranspiration for the calibration period from January 1, 1995 to September 30, 2003.

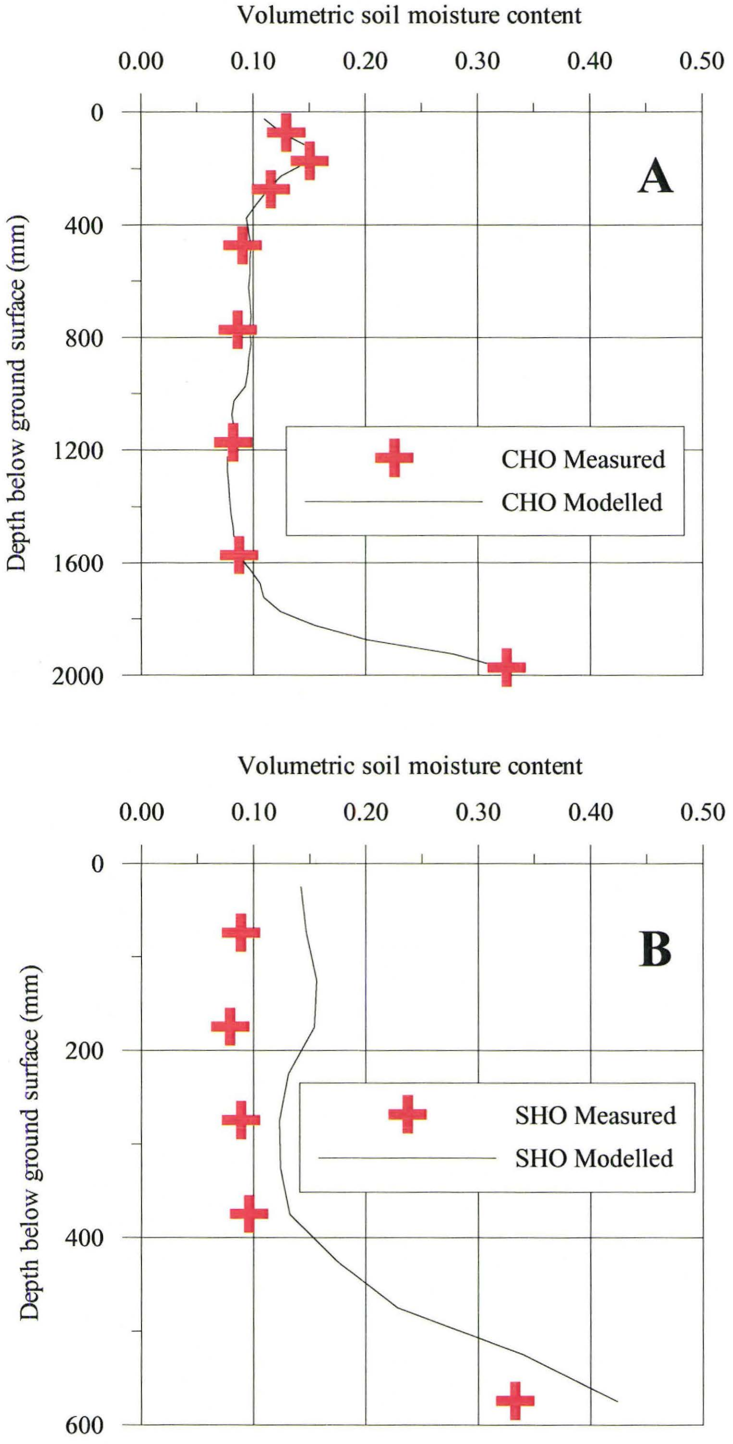

Figure 25. Measured and modelled volumetric soil moisture profile from ground surface to the water table at (a) CHO and (b) SHO on May 12, 2003 as employed in LEACHMP.

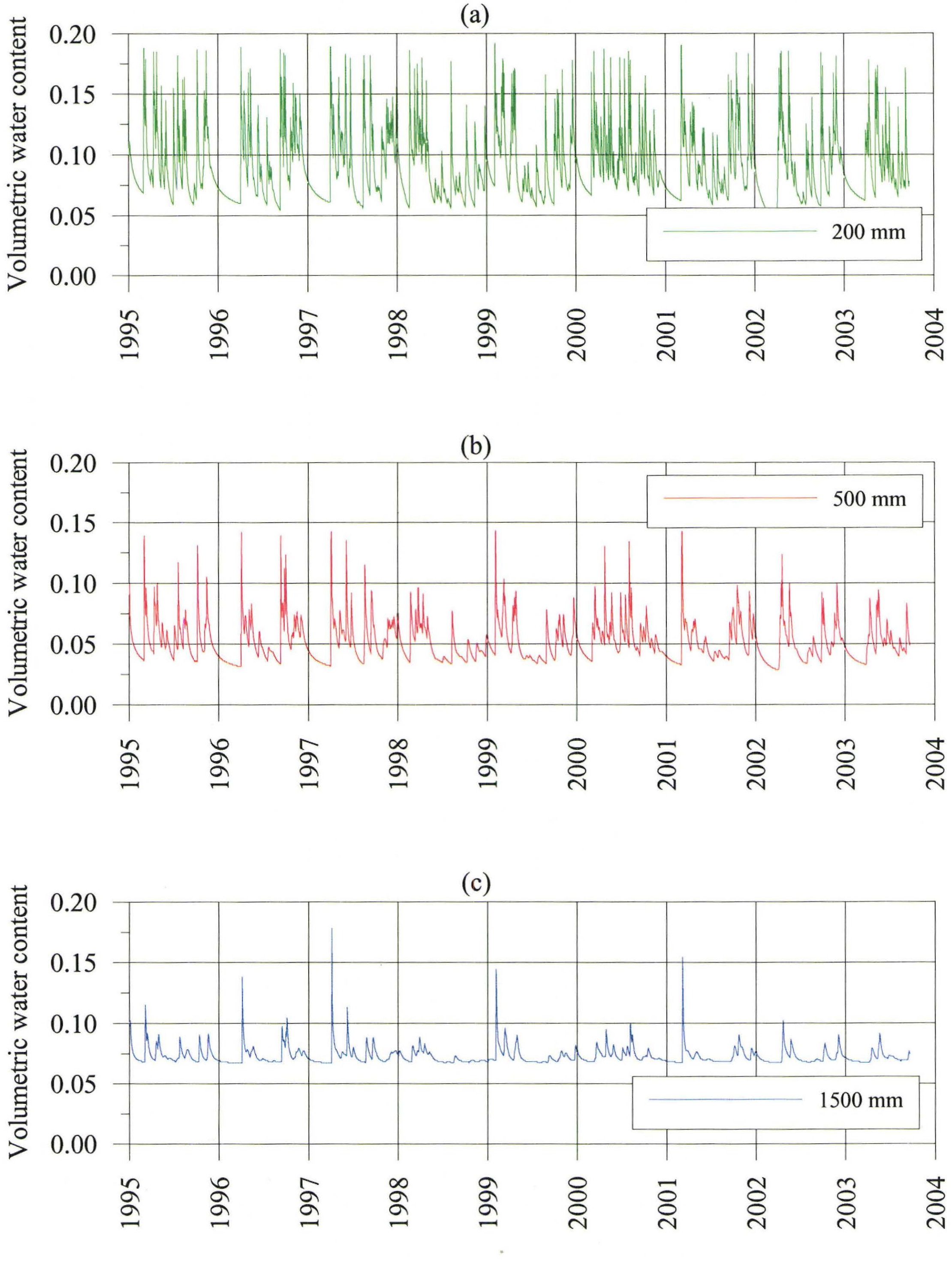

Figure 26. Modelled volumetric soil moisture content over time from January 1, 1995 to September 30, 2003 at (a) 200, (b) 500 and (c) 1500 mm below ground surface

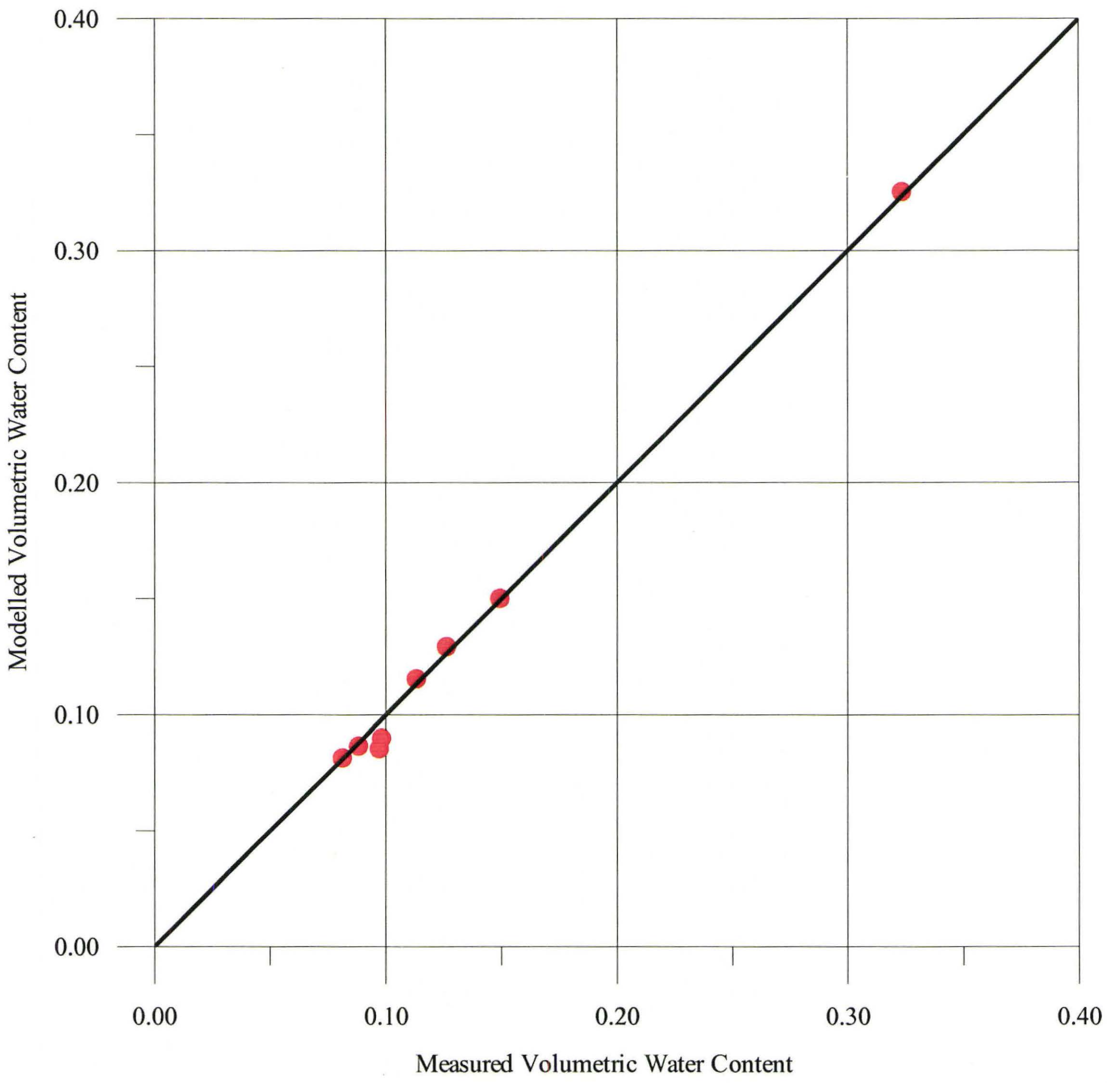

Figure 27. Calibrated fit between modelled and measured volumetric soil moisture contents with depth at CHO on May 12, 2003.

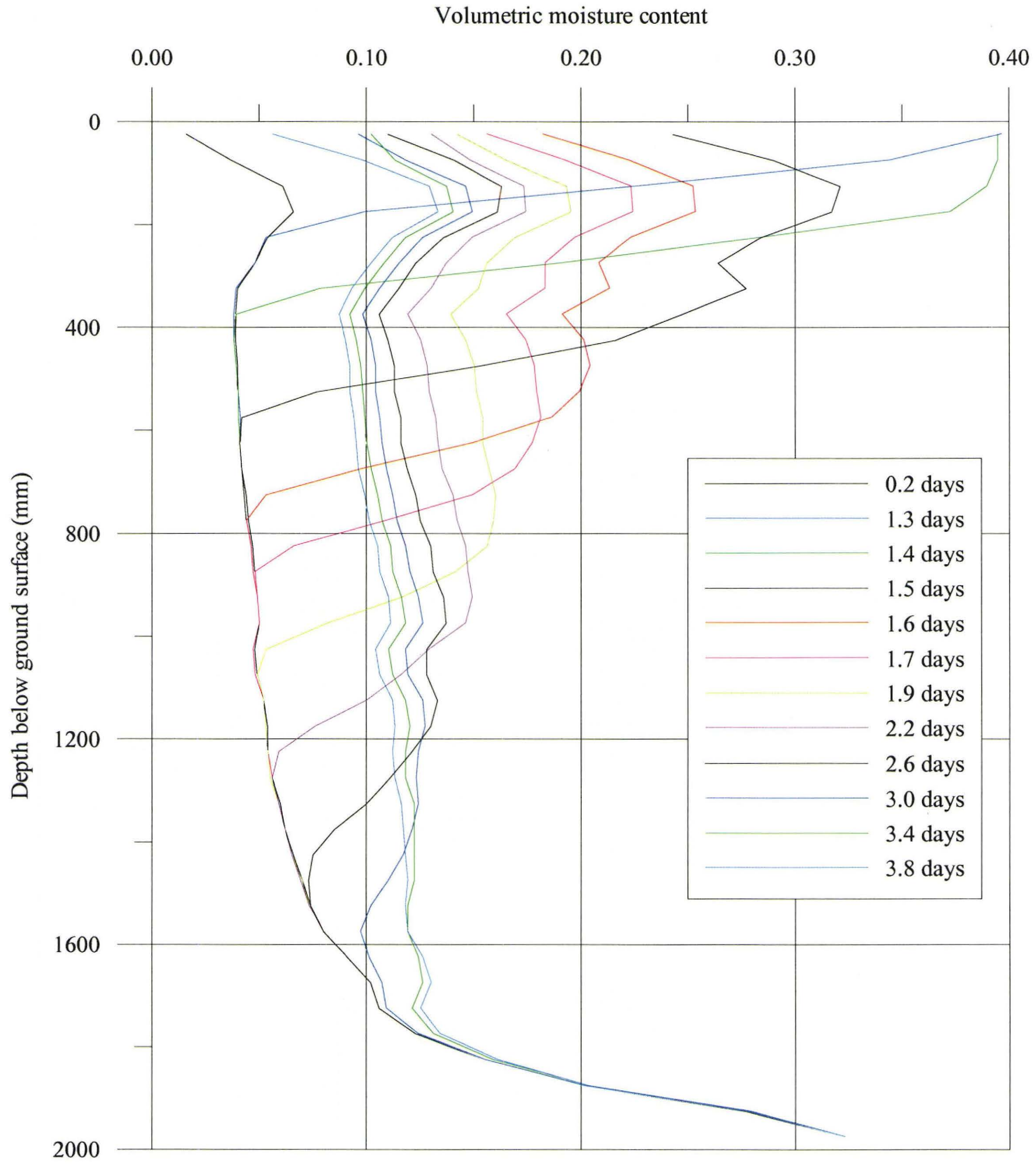

Figure 28. Volumetric soil moisture profile at various times after a large infiltration event on July 17, 1989 showing the migration of water through the soil profile.

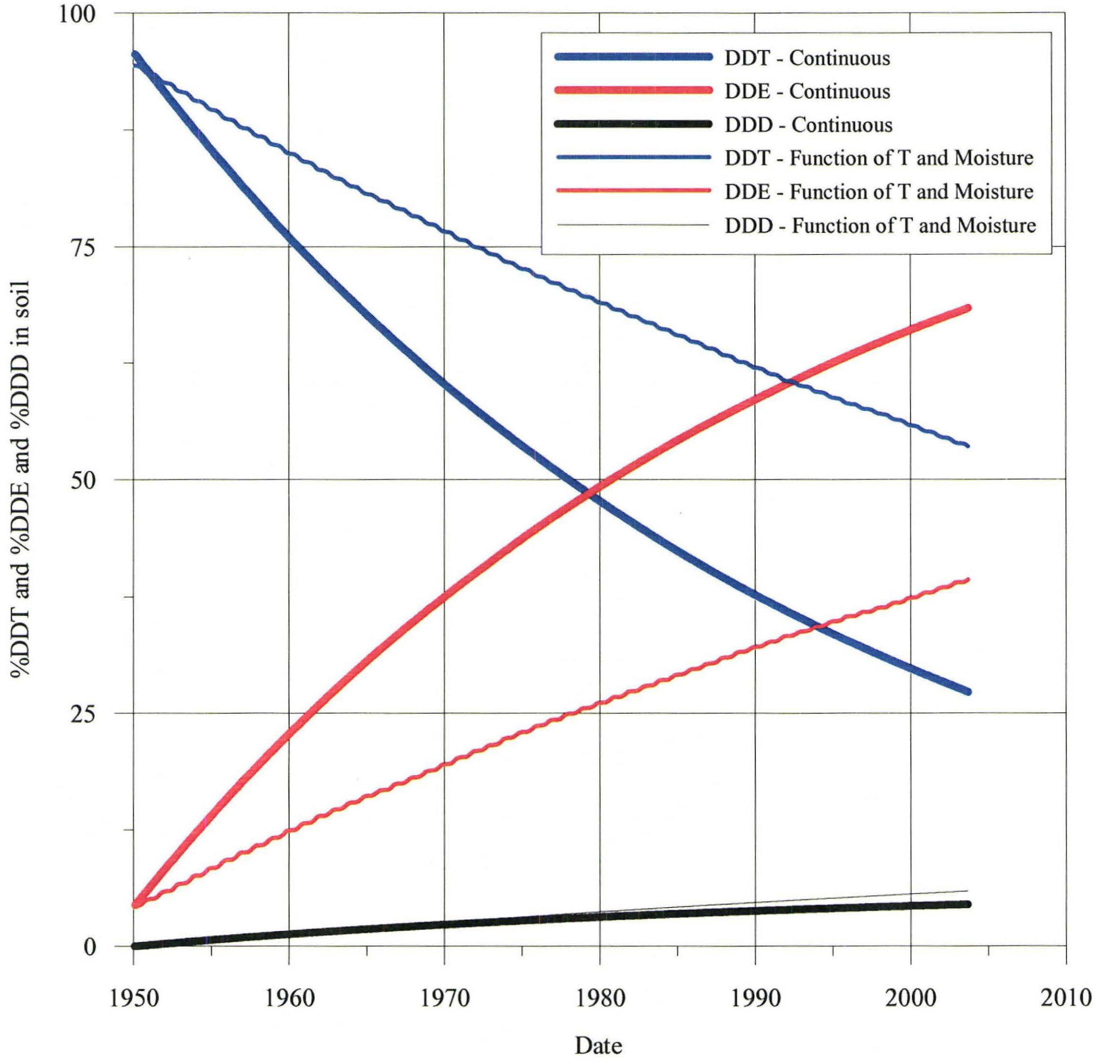

Figure 29. Comparison of DDT transformation and DDE formation when transformation rates are either sensitive or insensitive to moisture content and temperature variations over time.

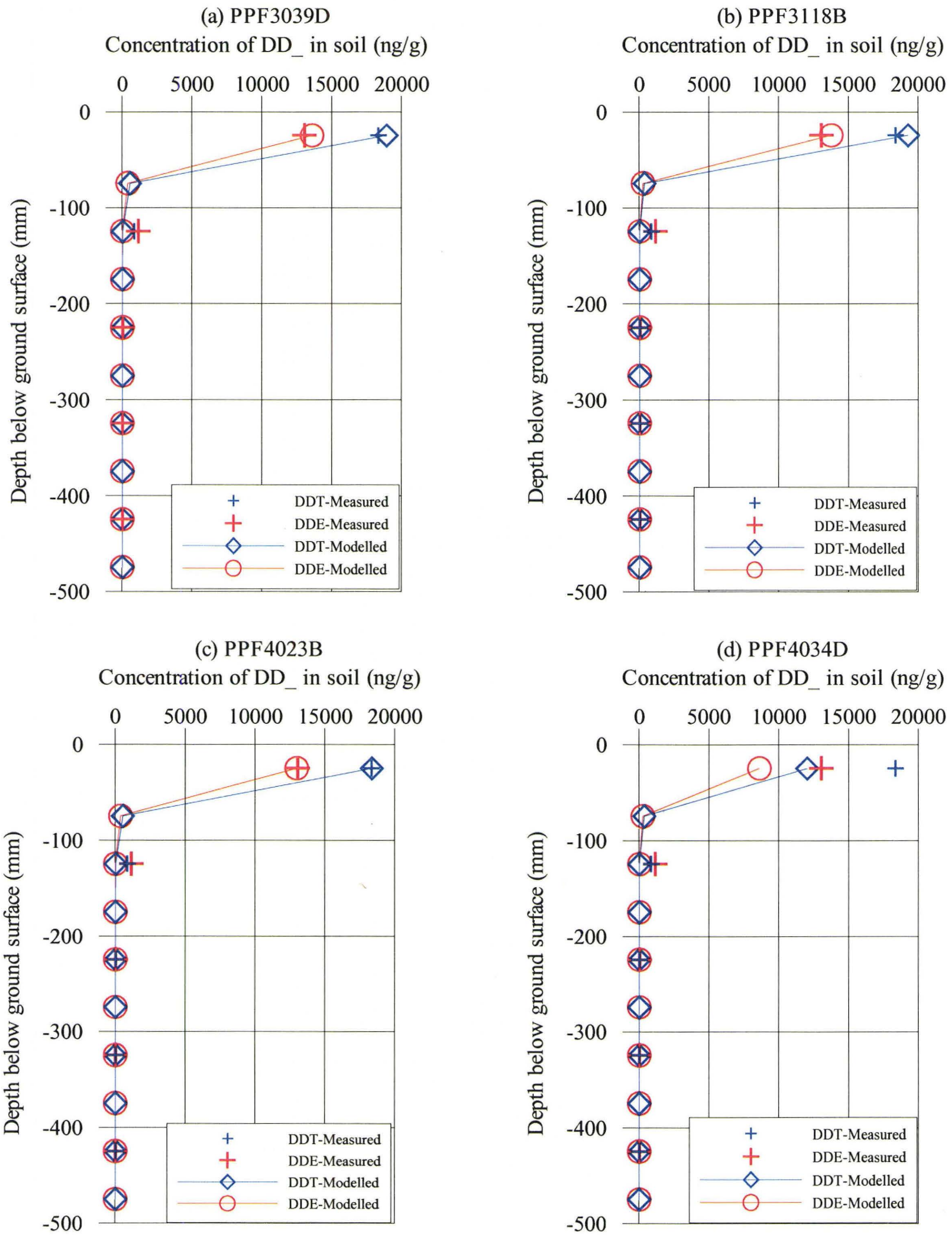

Figure 30. Measured and modelled concentration profiles for simulations where relative proportions of DDT and DDE or DDD were matched for the entire profile and with depth on May 12, 2003.

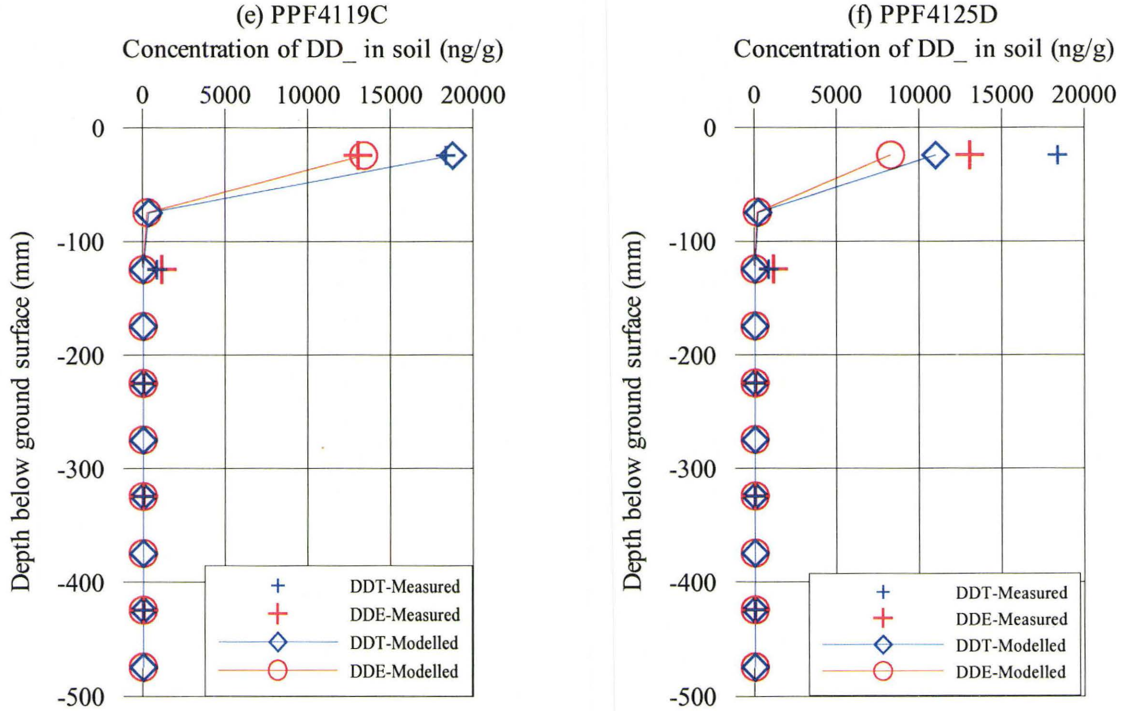
(e) PPF4119C

(f) PPF4125D

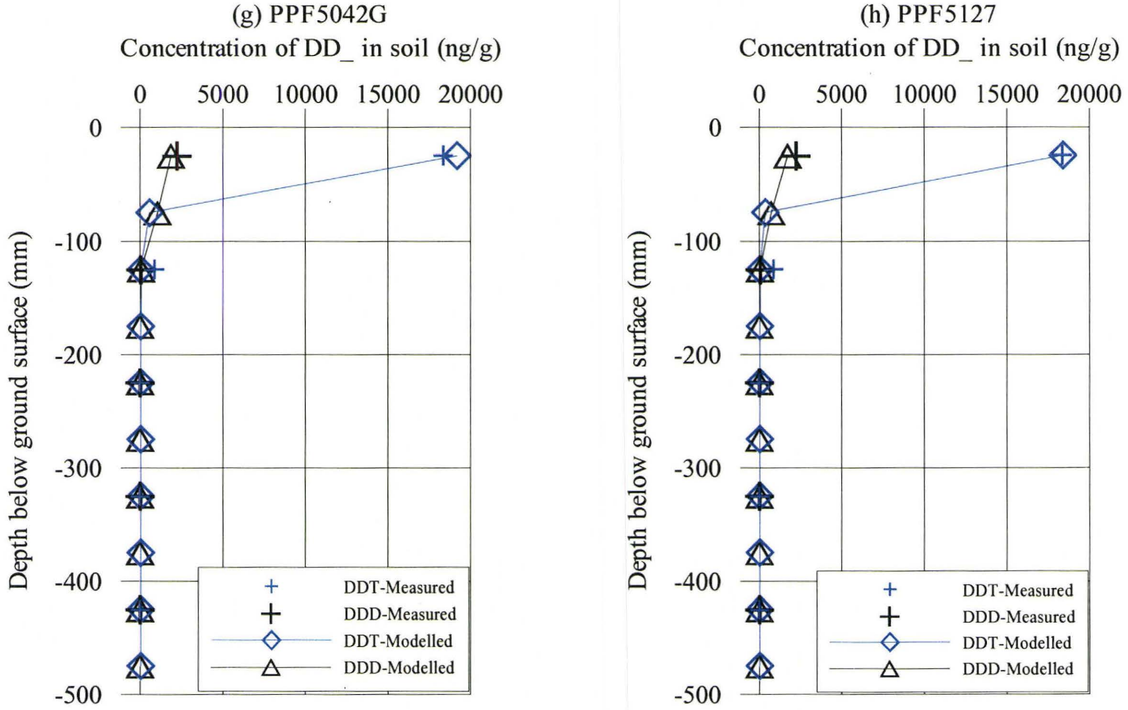
(g) PPF5042G

(h) PPF5127

Figure 30 (cont'd). Measured and modelled concentration profiles for simulations where relative proportions of DDT and DDE or DDD were matched for the entire profile and with depth on May 12, 2003.

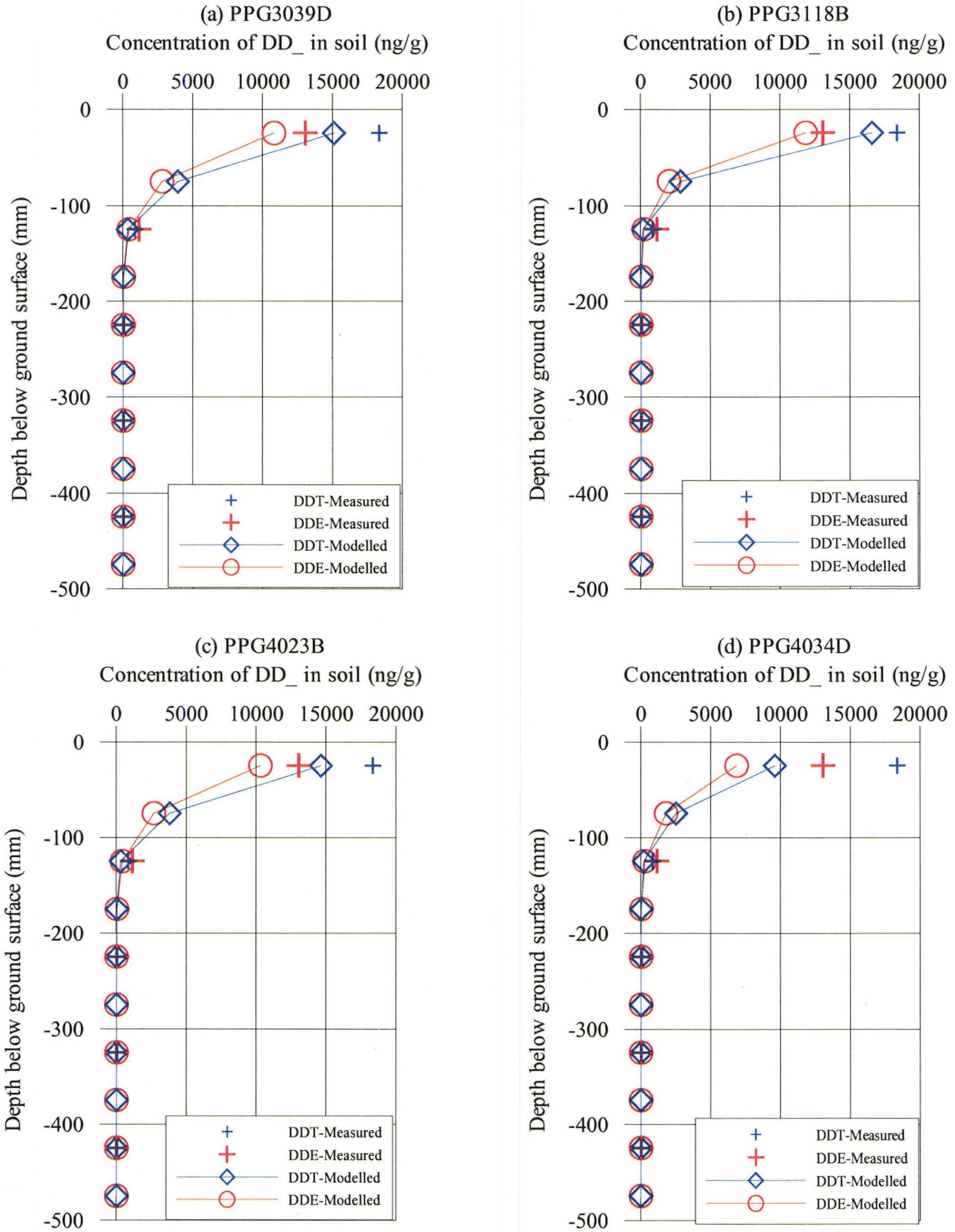

Figure 31. Measured and modelled concentration profiles for simulations where relative proportions of DDT and DDE or DDD were matched for the entire profile and with depth on May 12, 2003 after K_{oc} adjustments.

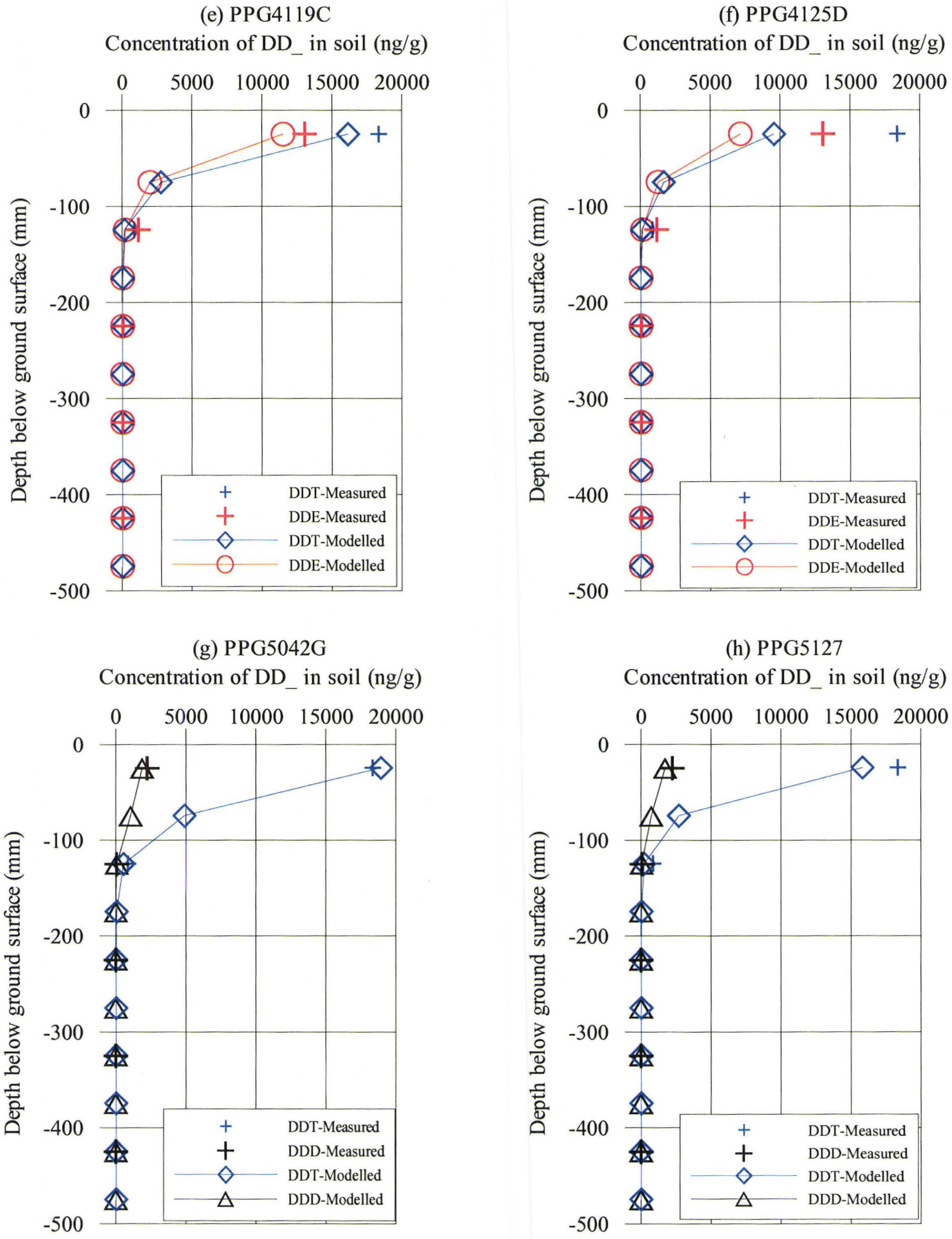

Figure 31 (cont'd). Measured and modelled concentration profiles for simulations where relative proportions of DDT and DDE or DDD were matched for the entire profile and with depth on May 12, 2003 after K_{oc} adjustments.

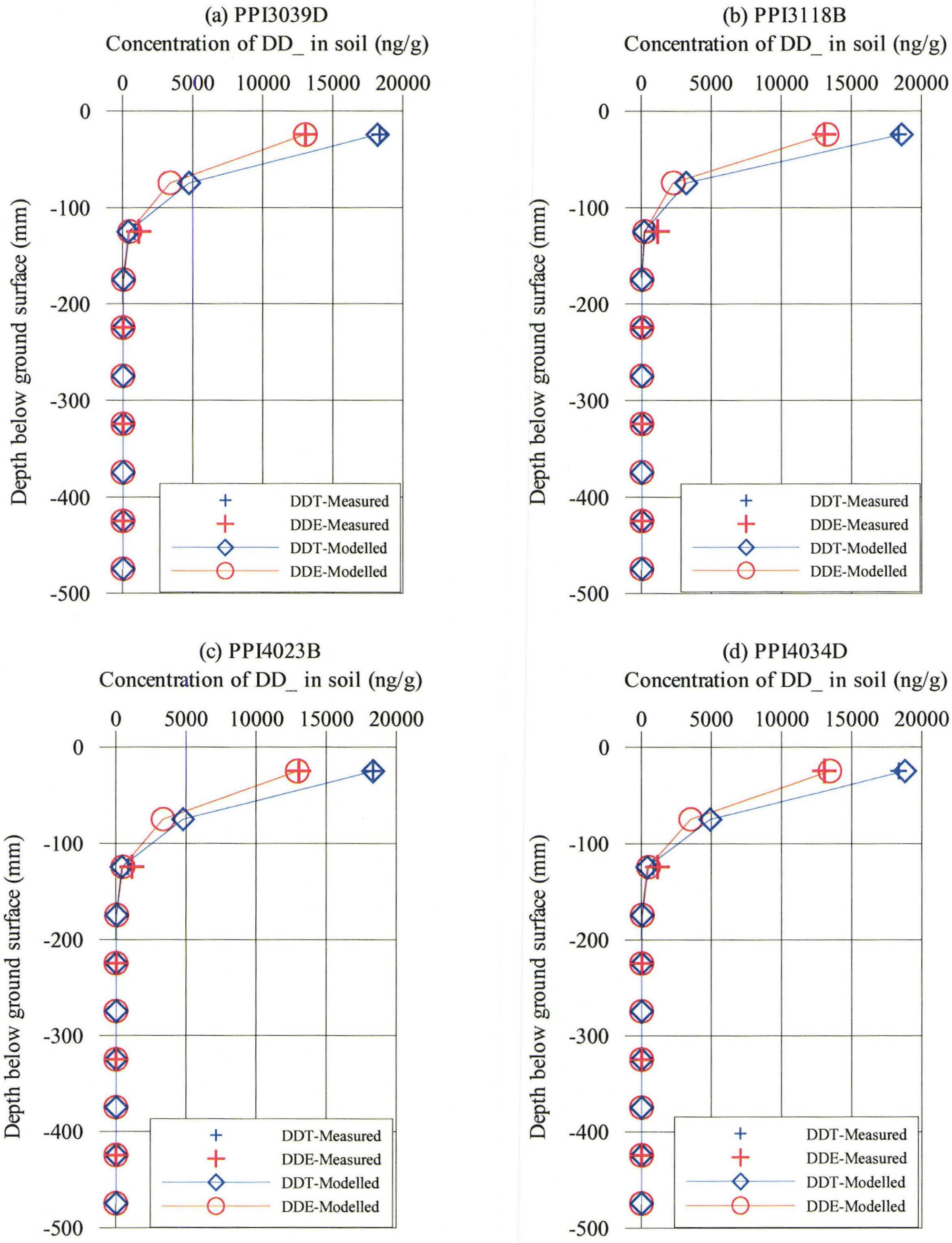

Figure 32. Measured and modelled concentration profiles for simulations where relative proportions of DDT and DDE or DDD were matched for the entire profile and with depth on May 12, 2003 after K_{oc} adjustments and concentrations with depth were matched.

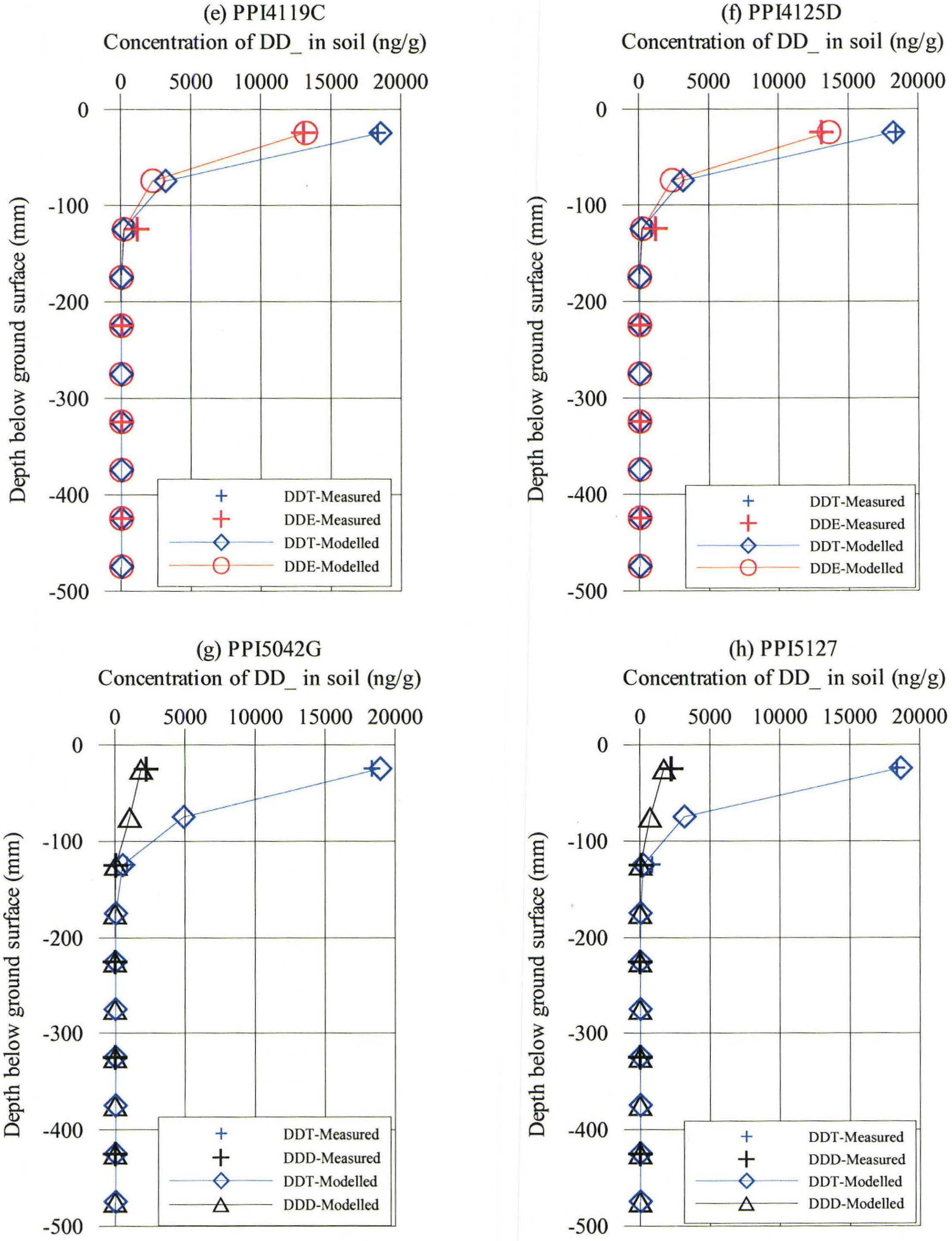

Figure 32 (cont'd). Measured and modelled concentration profiles for simulations where relative proportions of DDT and DDE or DDD were matched for the entire profile and with depth on May 12, 2003 after K_{oc} adjustments and concentrations with depth were matched.

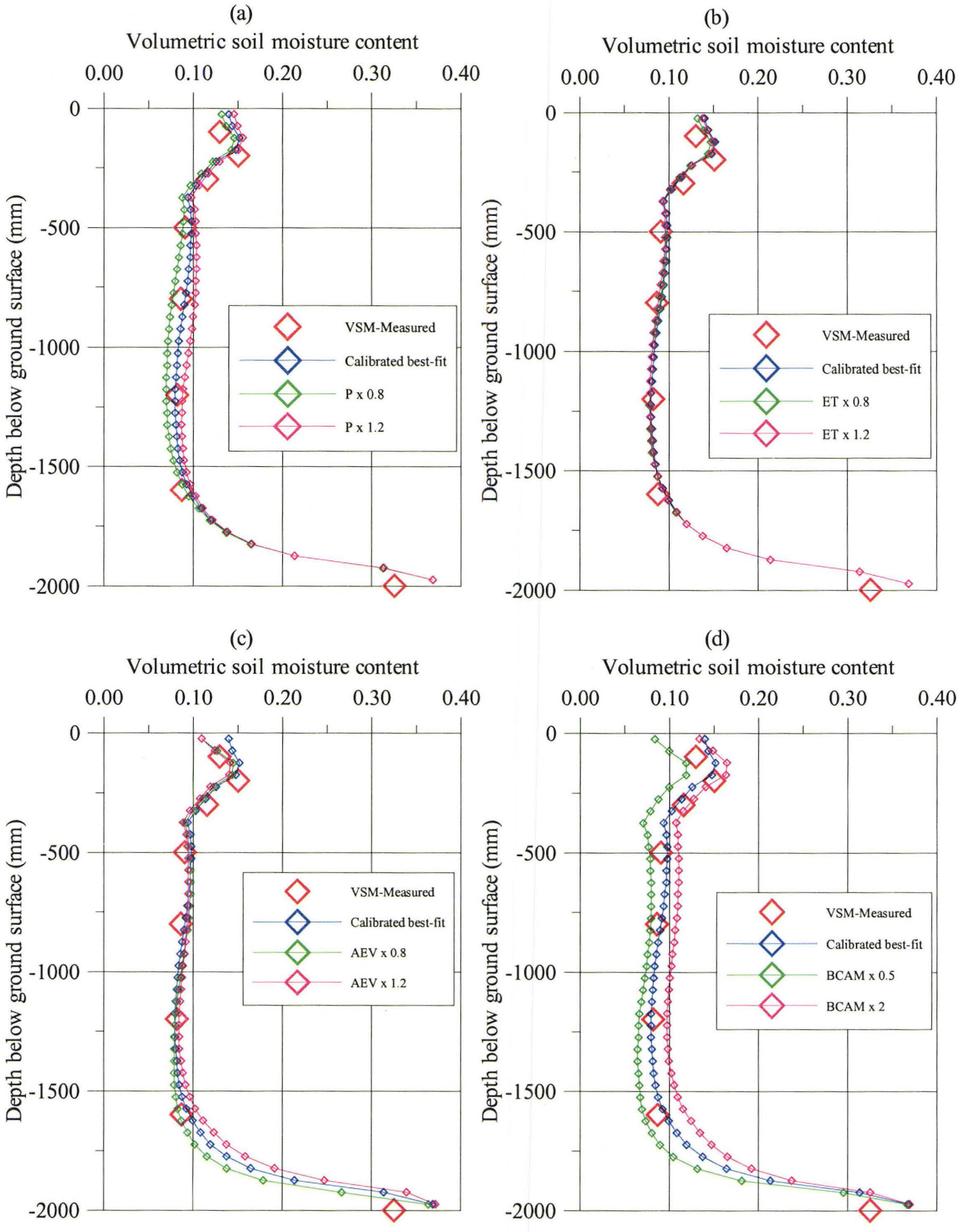

Figure 33. Sensitivity of flow calibration to values of (a) precipitation, (b) potential evapotranspiration, (c) air entry, and (d) Campbell's b parameter, (e) pore interaction parameter and (f) K_{sat}.

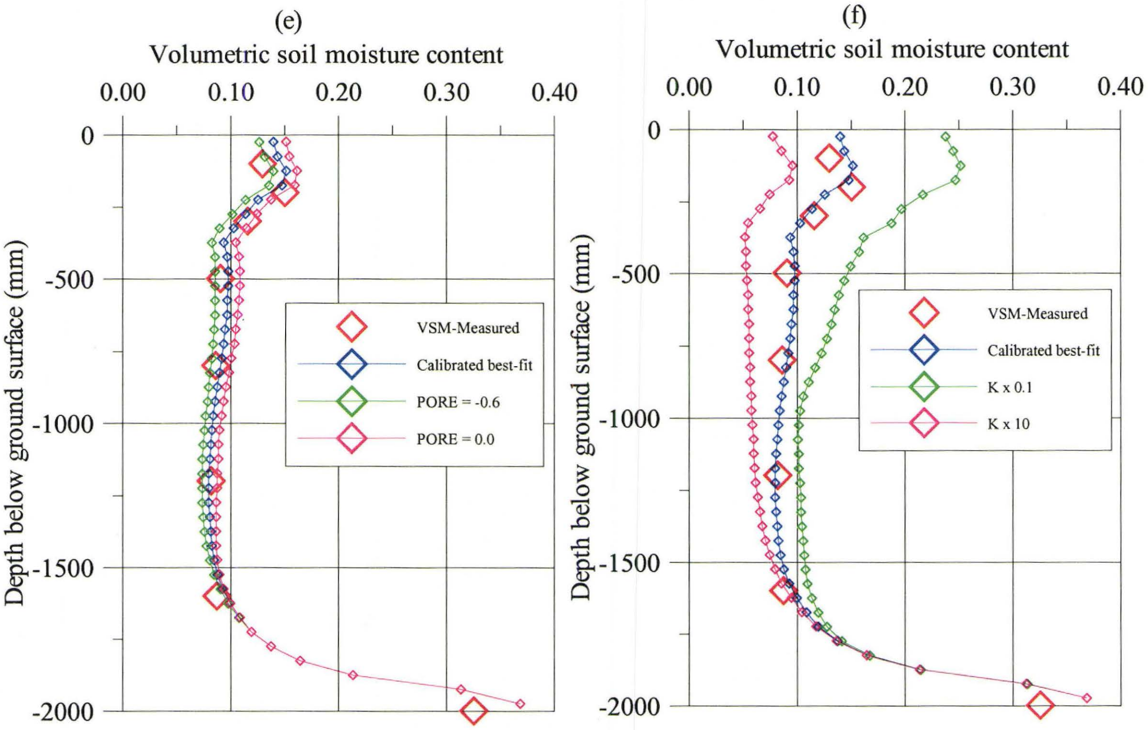

Figure 33 (cont'd). Sensitivity of flow calibration to values of (a) precipitation, (b) potential evapotranspiration, (c) air entry, and (d) Campbell's b parameter, (e) pore interaction parameter and (f) K_{sat}.

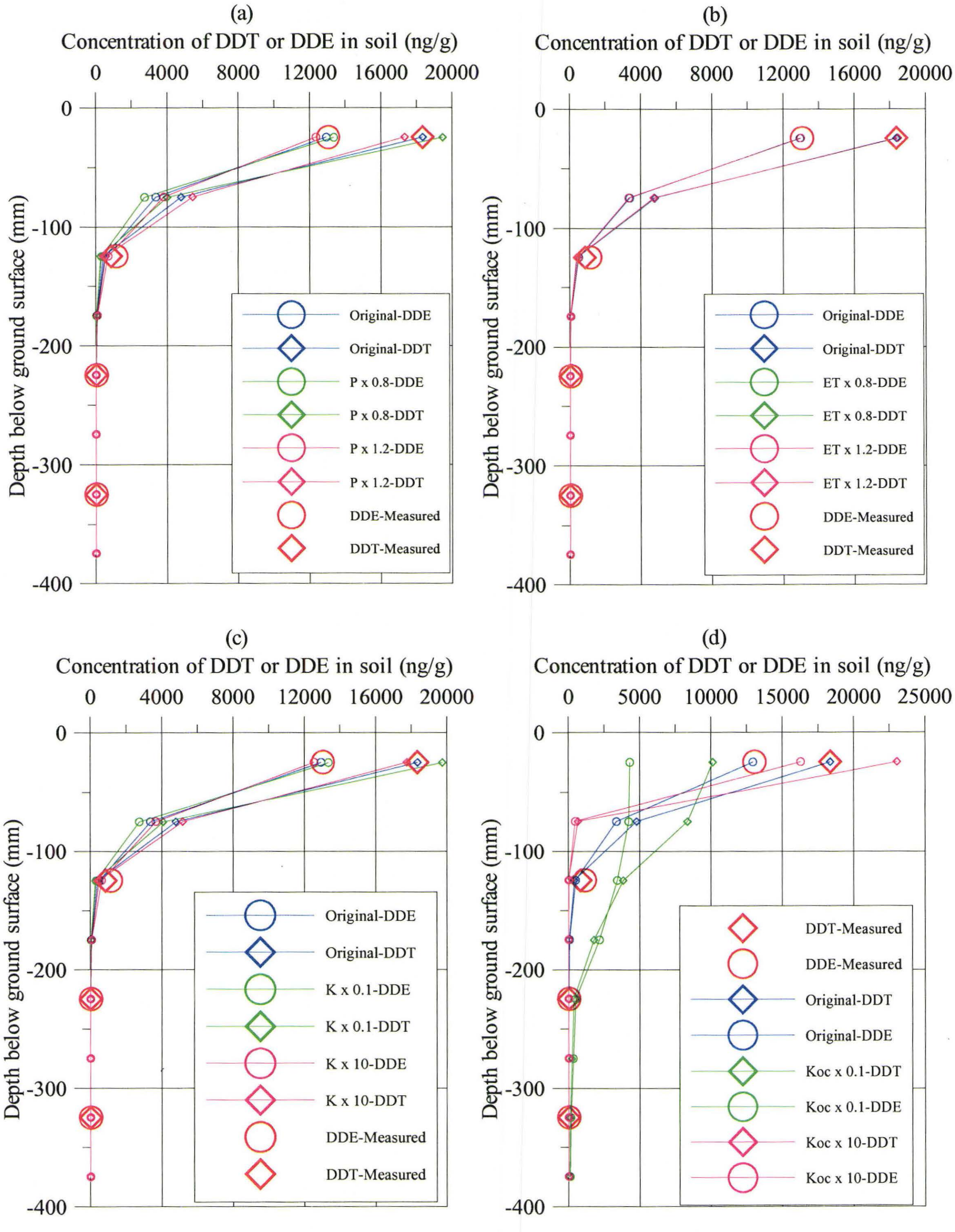

Figure 34. Sensitivity of solute transport calibration to values of (a) precipitation, (b) potential evapotranspiration, (c) K_{sat}, (d) K_{oc}, (e) half-live and (f) organic carbon content.

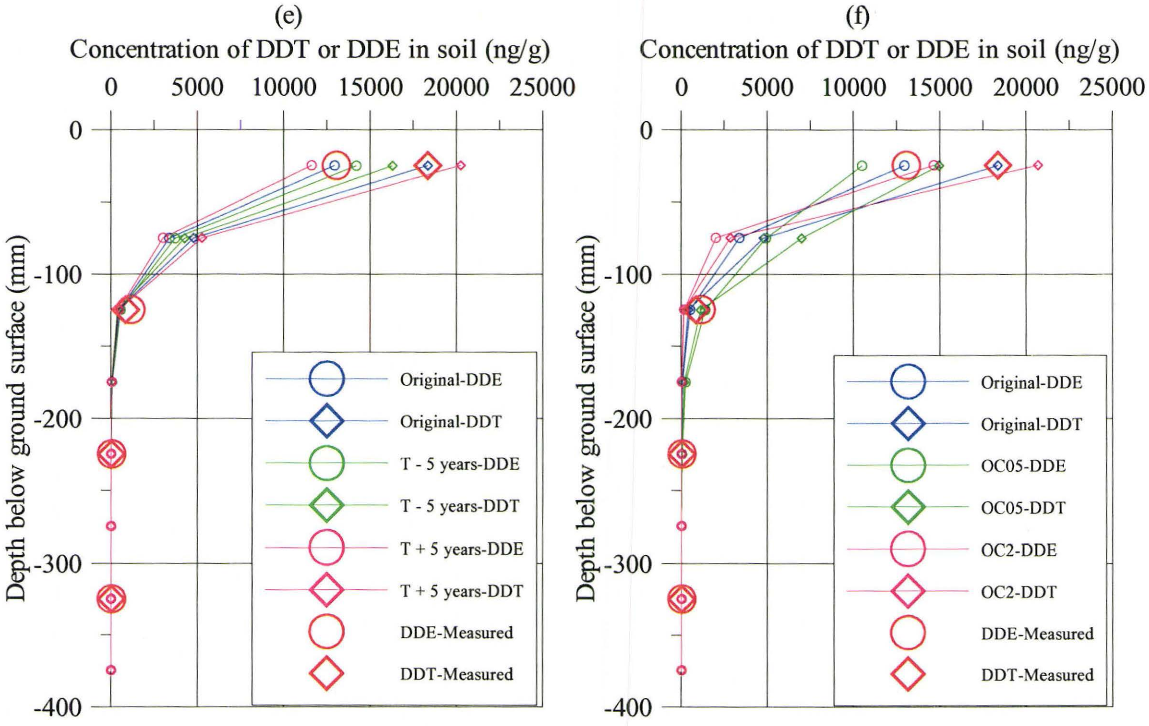

Figure 34 (cont'd). Sensitivity of solute transport calibration to values of (a) precipitation, (b) potential evapotranspiration, (c) K_{sat}, (d) K_{oc}, (e) half-live and (f) organic carbon content.

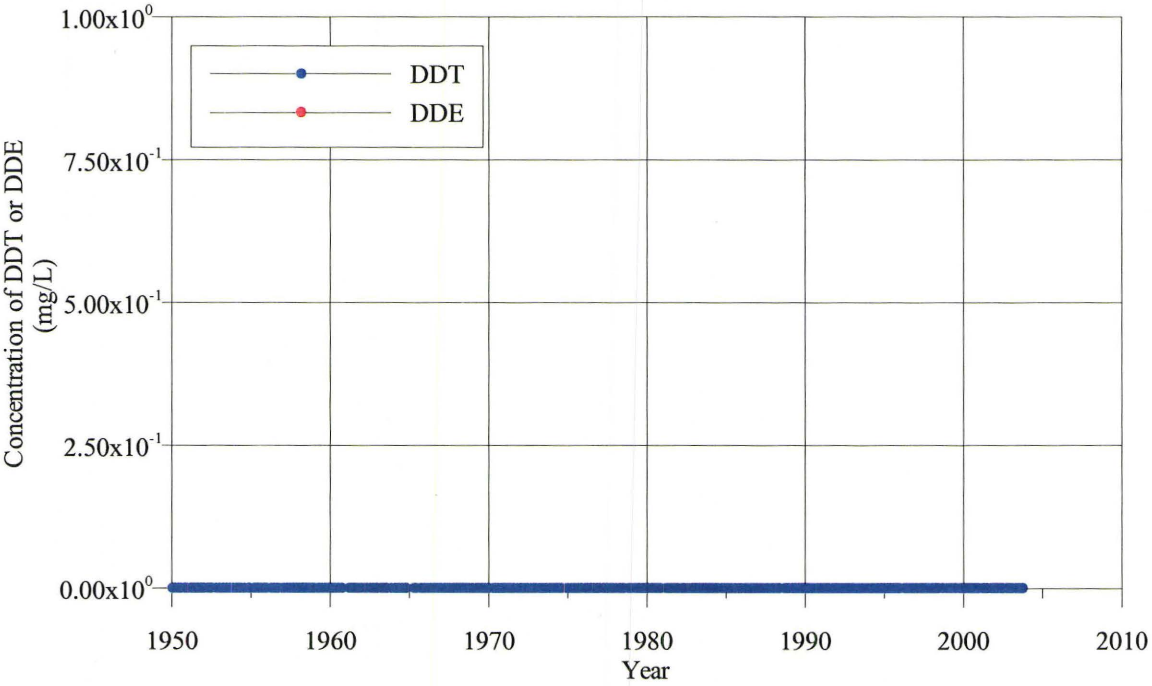

Figure 35. Solute breakthrough curves from 1950 to 2003 for simulation employing Pathway #2 and field measured organic carbon contents with depth at CHO.

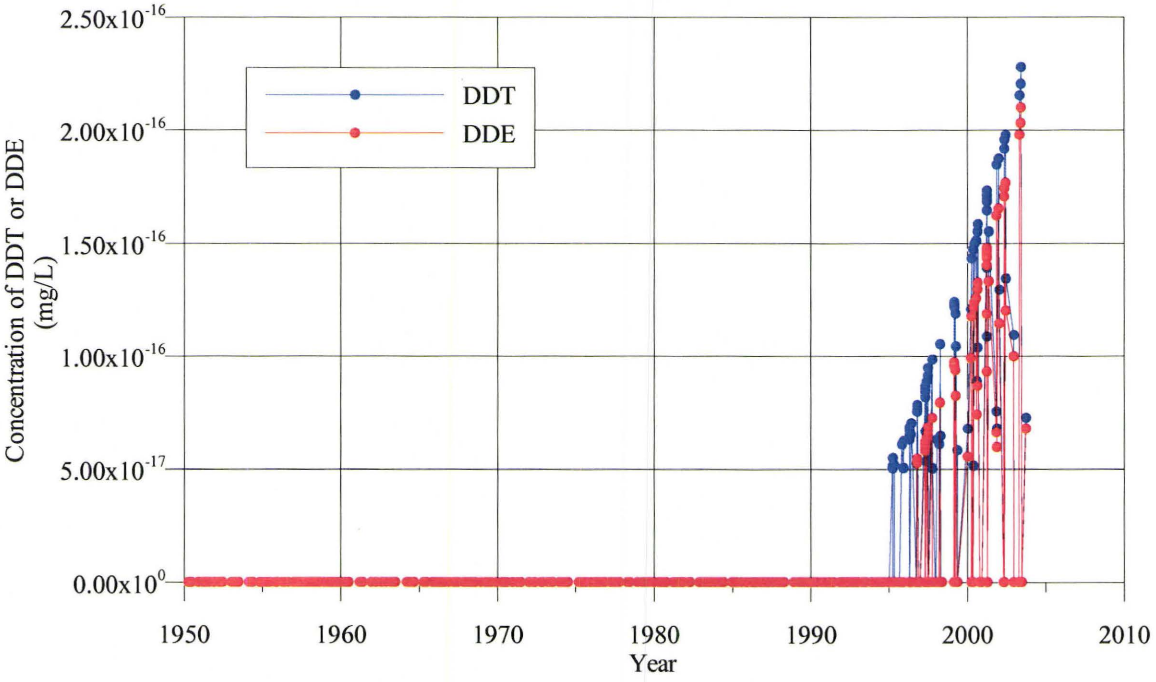

Figure 36. Solute breakthrough curves from 1950 to 2003 for simulation employing Pathway #2 and field measured organic carbon contents with depth at SHO.

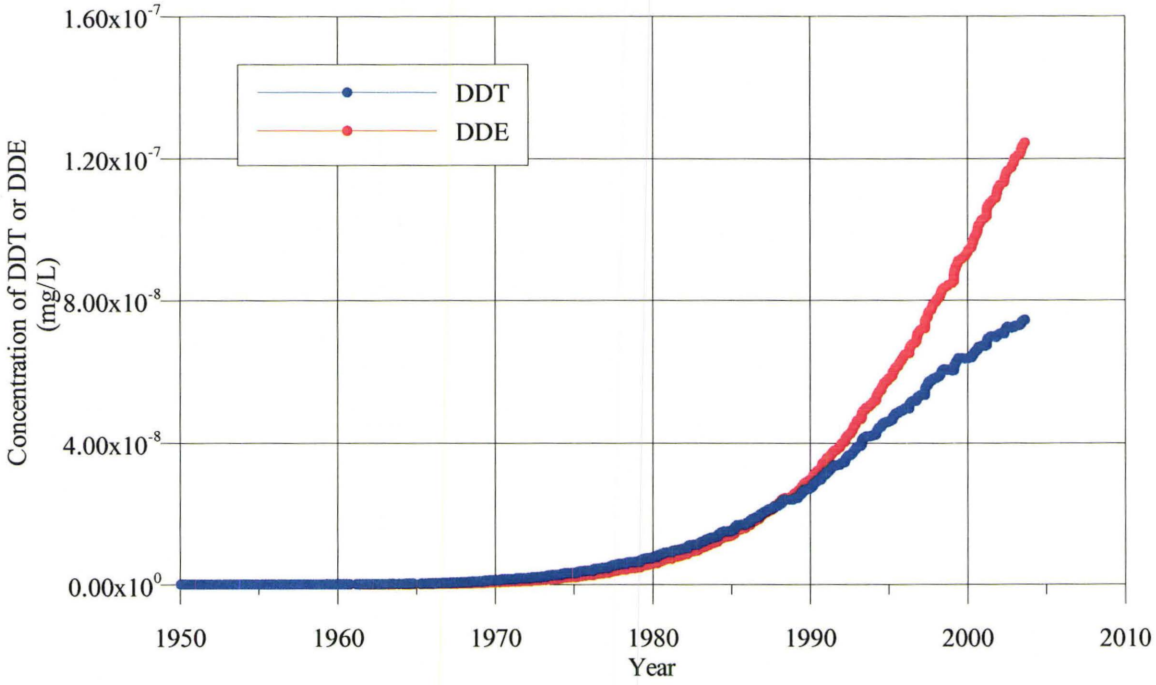

Figure 37. Solute breakthrough curves from 1950 to 2003 for simulation employing Pathway #2 and organic carbon contents reduced to zero below the Ah horizons (300 mm to the water table) at CHO

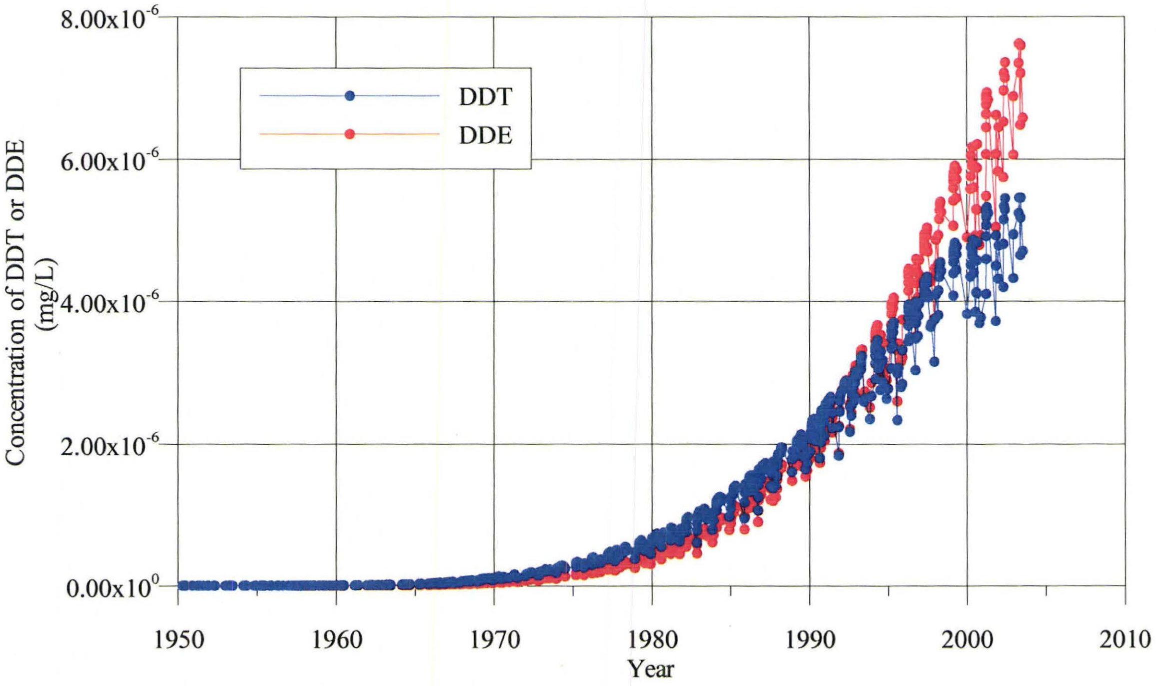

Figure 38. Solute breakthrough curves from 1950 to 2003 for simulation employing Pathway #2 and organic carbon contents reduced to zero below the Ah horizons (300 mm to the water table) at SHO.

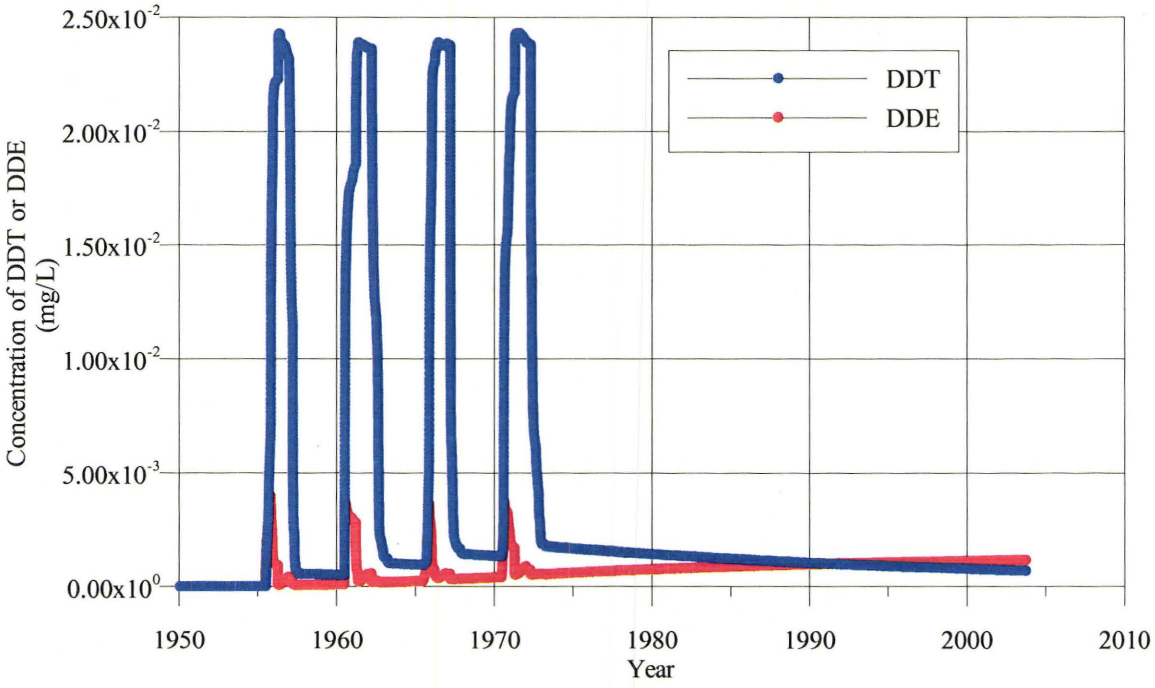

Figure 39. Solute breakthrough curves from 1950 to 2003 for simulation employing Pathway #2 where DDT was loaded below the Ah horizon in 1955, 1960, 1965 and 1970 at CHO and there was no organic carbon in the B or C horizon.

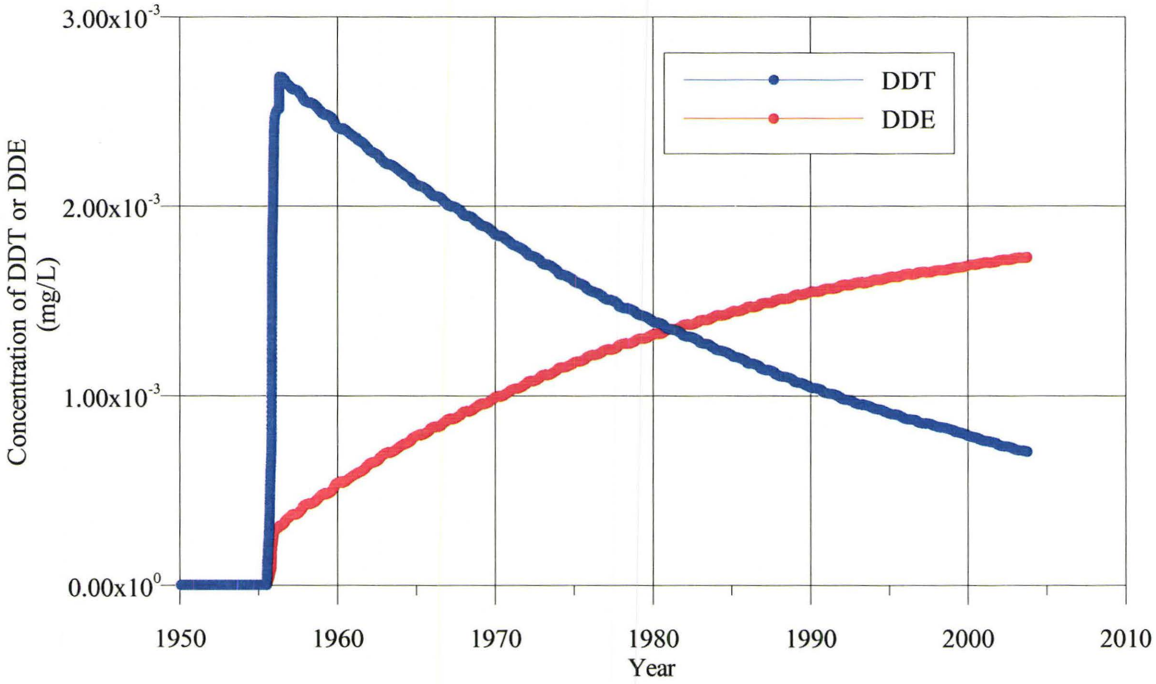

Figure 40. Solute breakthrough curves from 1950 to 2003 for simulation employing Pathway #2 where surficial soils at CHO were ploughed once in 1955 at CHO and there was no organic carbon in the B or C horizon.

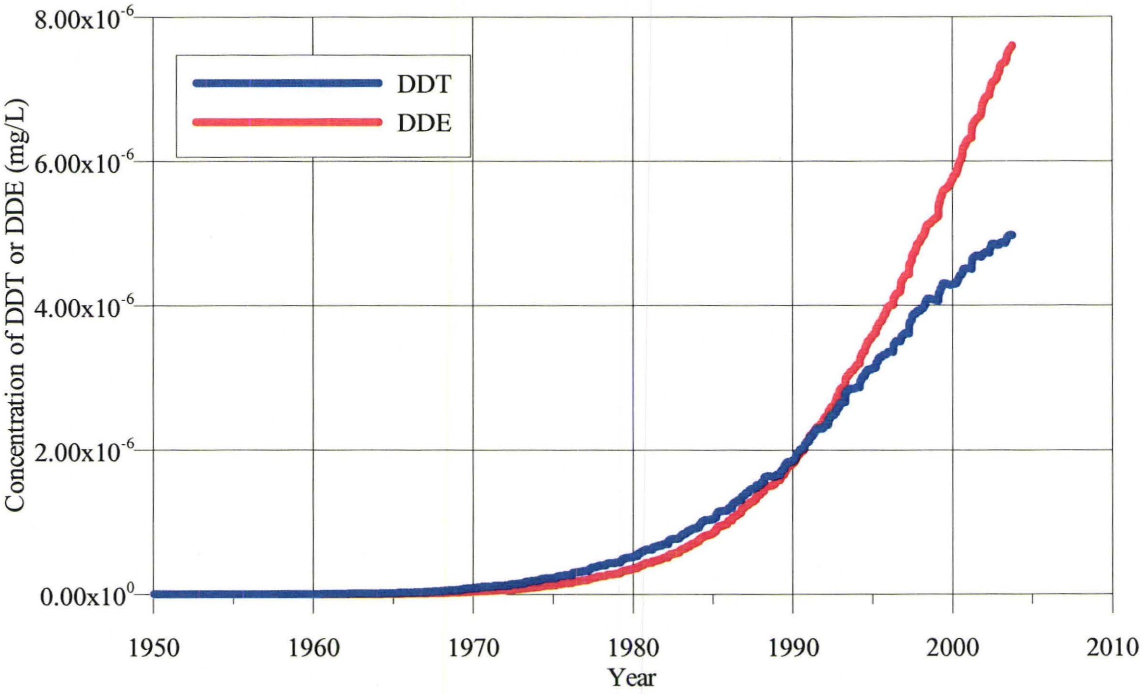

Figure 41. Solute breakthrough curves from 1950 to 2003 for simulations employing Pathway #2 where organic carbon content were reduced to zero below the Ah horizon (300 mm to the water table) and initial DDT loading was increased 10 fold at CHO.

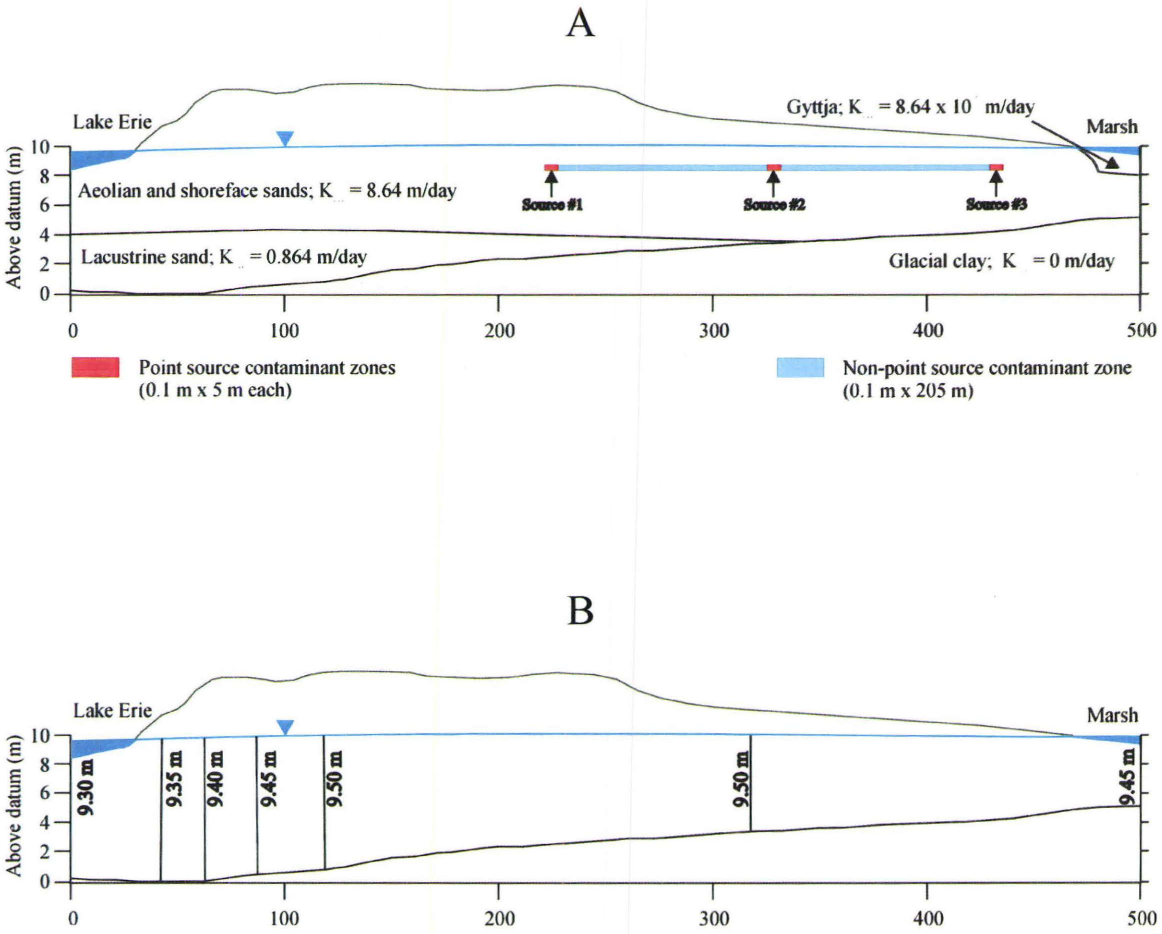

Figure 42. Two-dimensional cross-section at Camp Henry (modified from Crowe et al., 2004) including (a) conceptual model framework and DDT source zones employed in GW-WETLAND simulations of groundwater flow and solute transport and (b) hydraulic head distribution (June 1950).

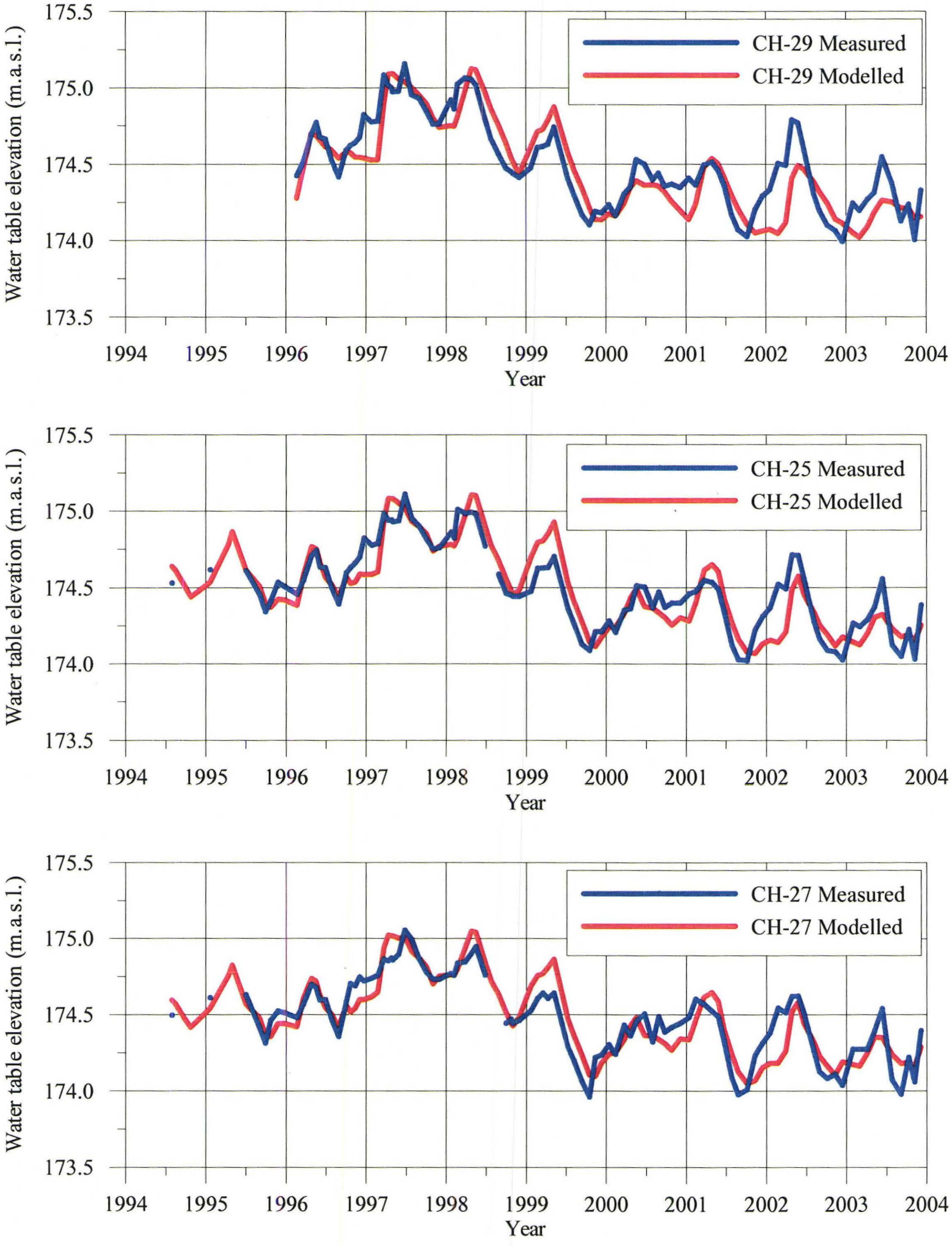

Figure 43. Comparison of simulated and field measured elevations of the water table at selected NWRI monitoring wells located along the Camp Henry Transect from 1994 to 2004.

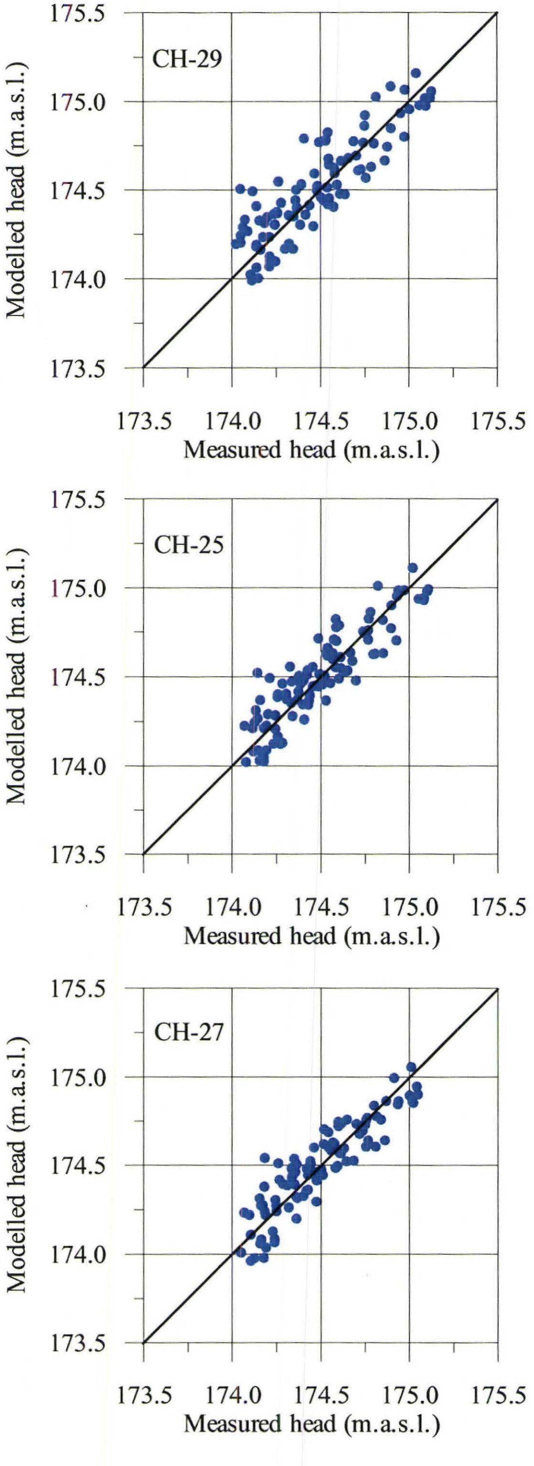

Figure 44. Comparison of simulated and modelled water table elevations at selected NWRI monitoring wells located along the Camp Henry Transect.

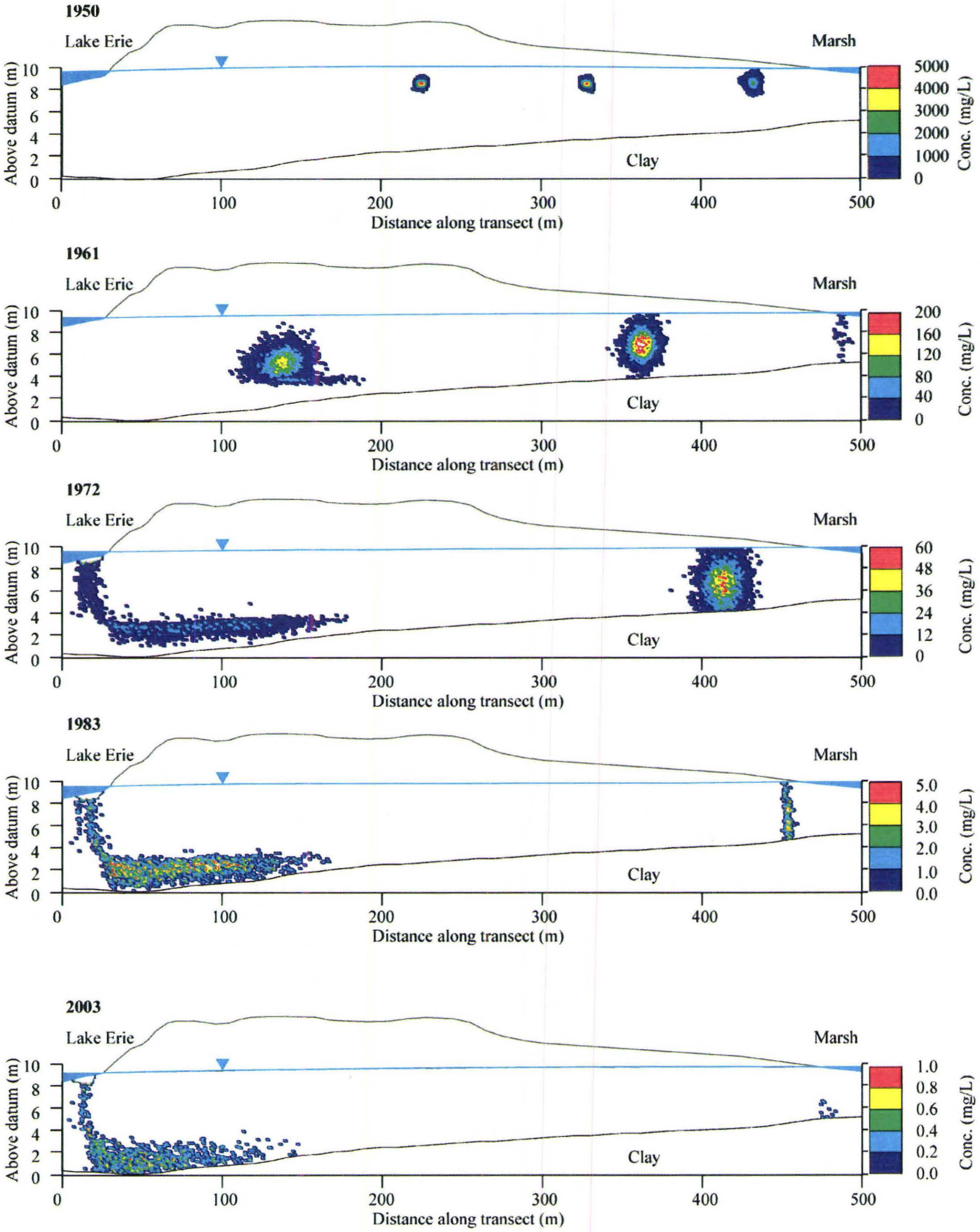

Figure 45. Distribution of Total DDT in the saturated zone throughout the Camp Henry transect from 1950 to 2003 based on initial high concentration, point source pulse loading at 225, 325 and 425 m in 1950.

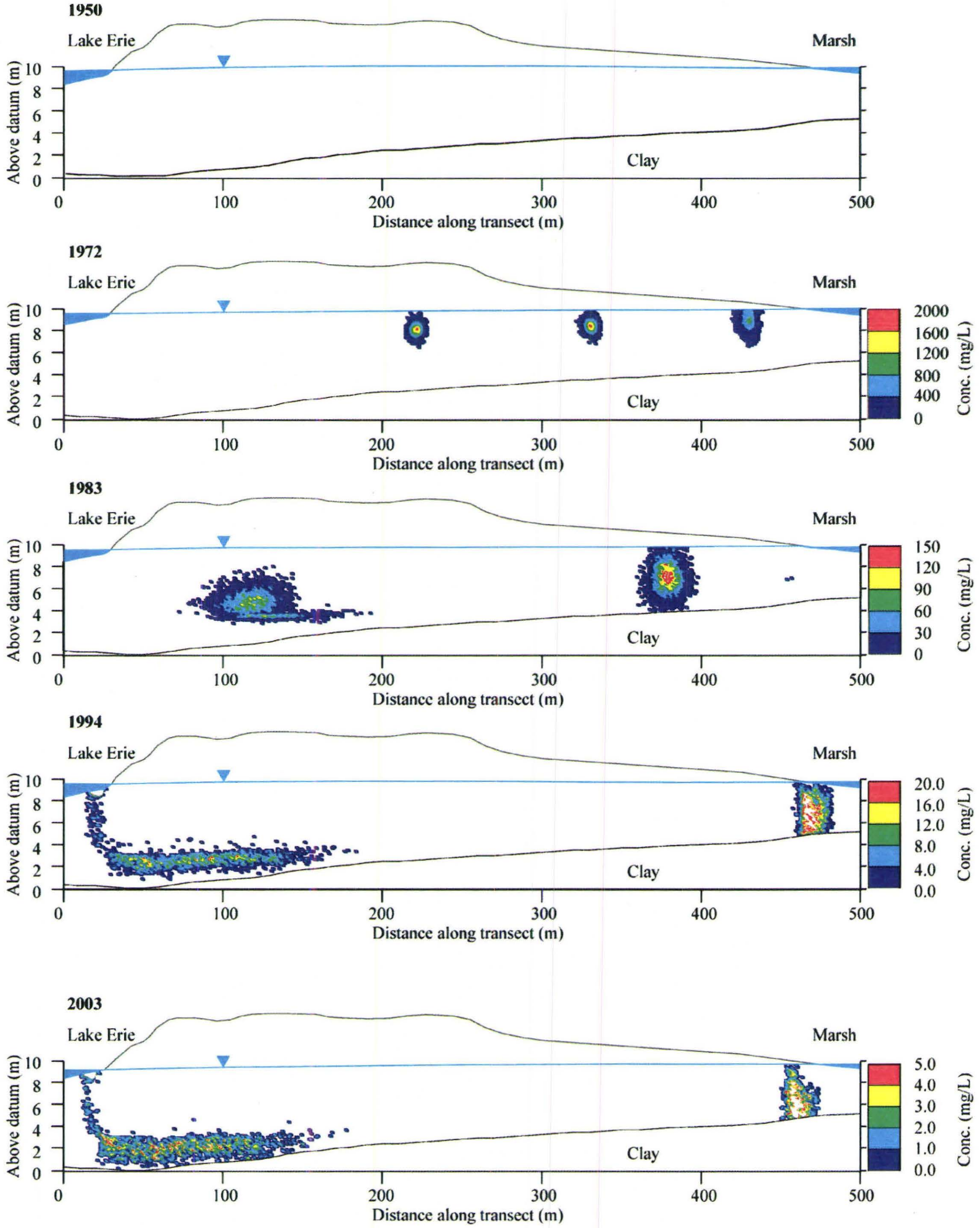

Figure 46. Distribution of Total DDT in the saturated zone throughout the Camp Henry transect from 1950 to 2003 based on initial high concentration, point source pulse loading at 225, 325 and 425 m in 1970.

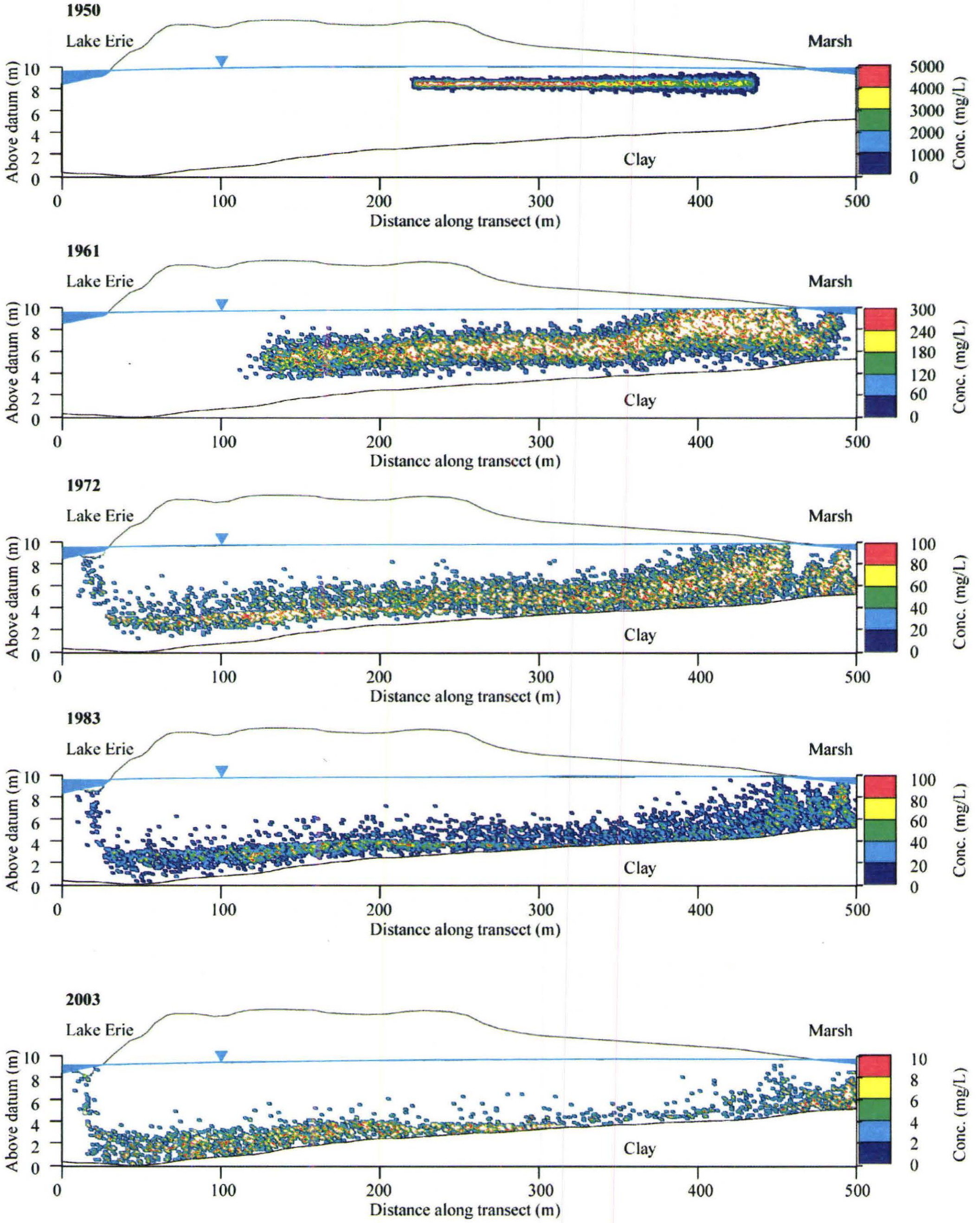

Figure 47. Distribution of Total DDT in the saturated zone throughout the Camp Henry transect from 1950 to 2003 based on initial high concentration, non-point source pulse loading from 225-430 m across the transect in 1950.

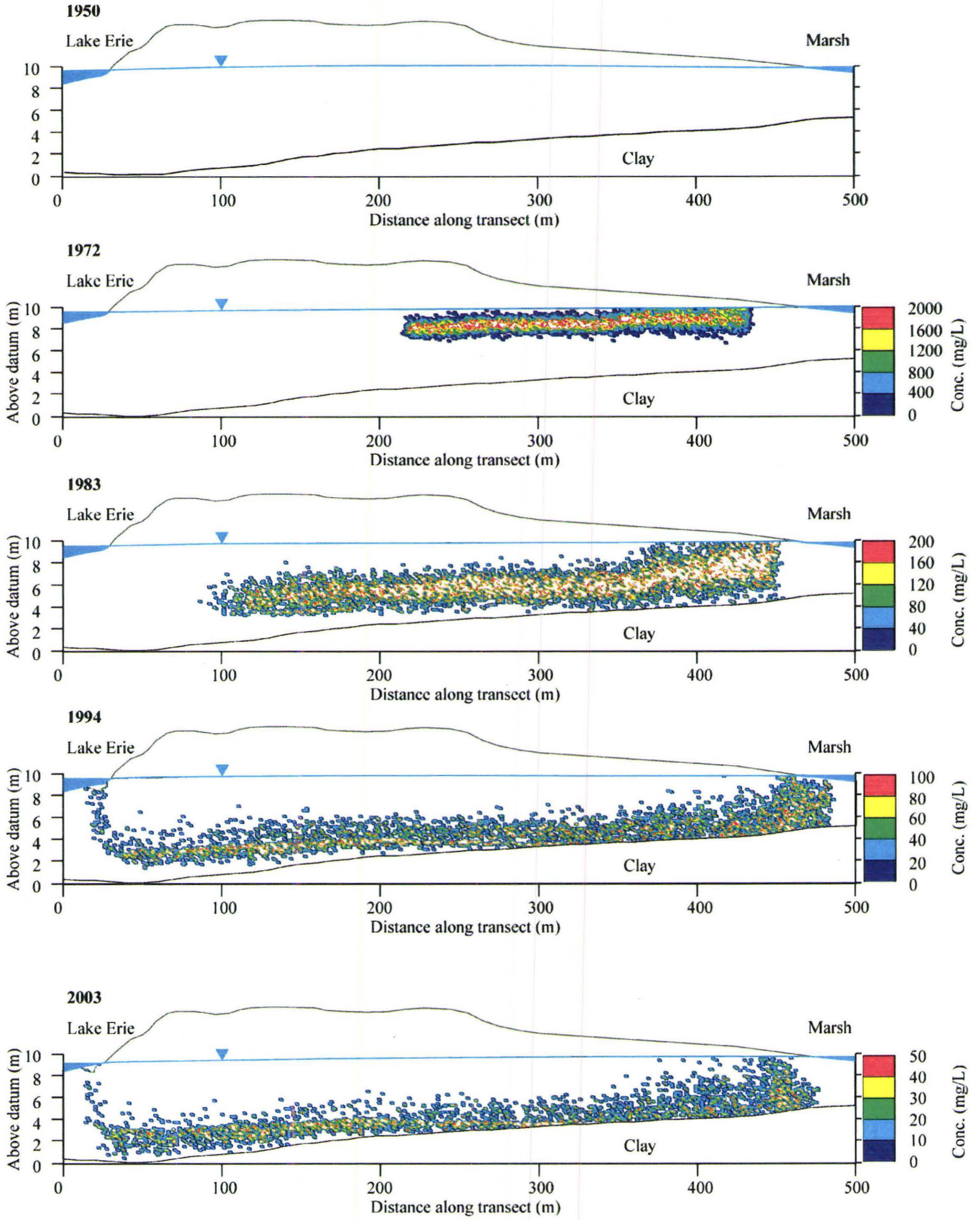

Figure 48. Distribution of Total DDT in the saturated zone throughout the Camp Henry transect from 1950 to 2003 based on initial high concentration, non-point source pulse loading from 225-430 m across the transect in 1970.

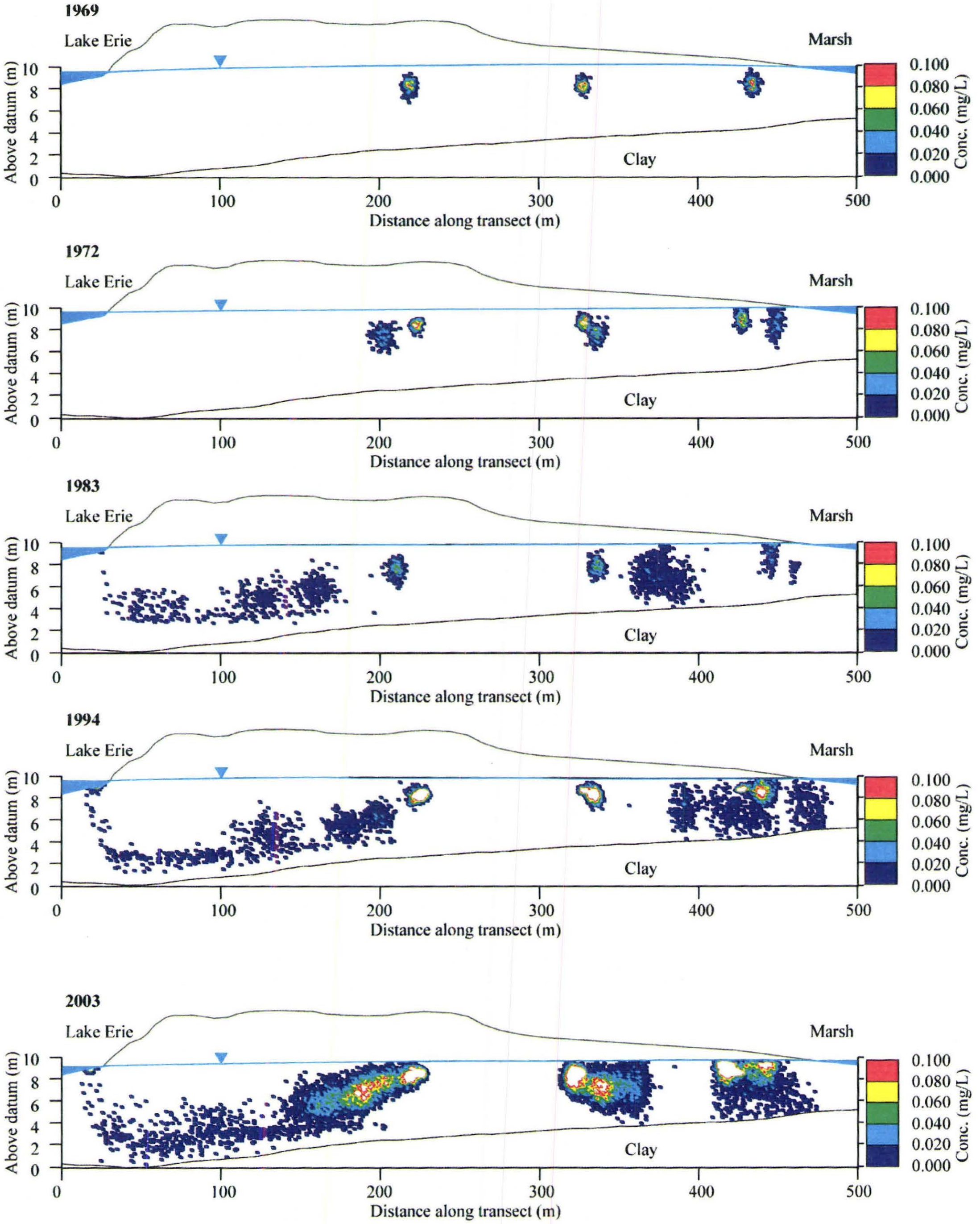

Figure 49. Distribution of Total DDT in the saturated zone throughout the Camp Henry transect from 1950 to 2003, based on long-term, slowly increasing point source loading at 225, 325 and 425 m in 1950.

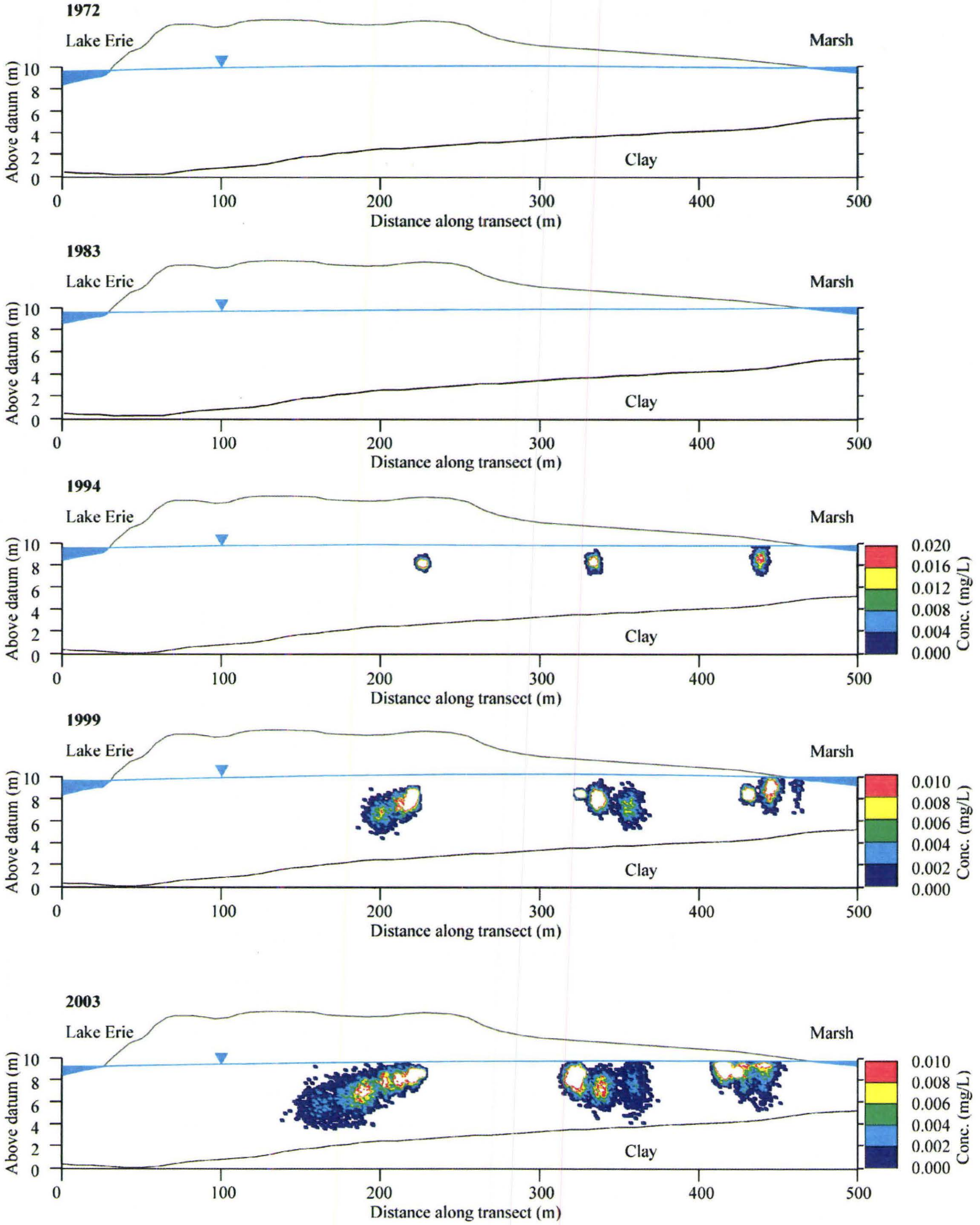

Figure 50. Distribution of Total DDT in the saturated zone throughout the Camp Henry transect from 1950 to 2003, based on long-term, slowly increasing point source loading at 225, 325 and 425 m in 1970.

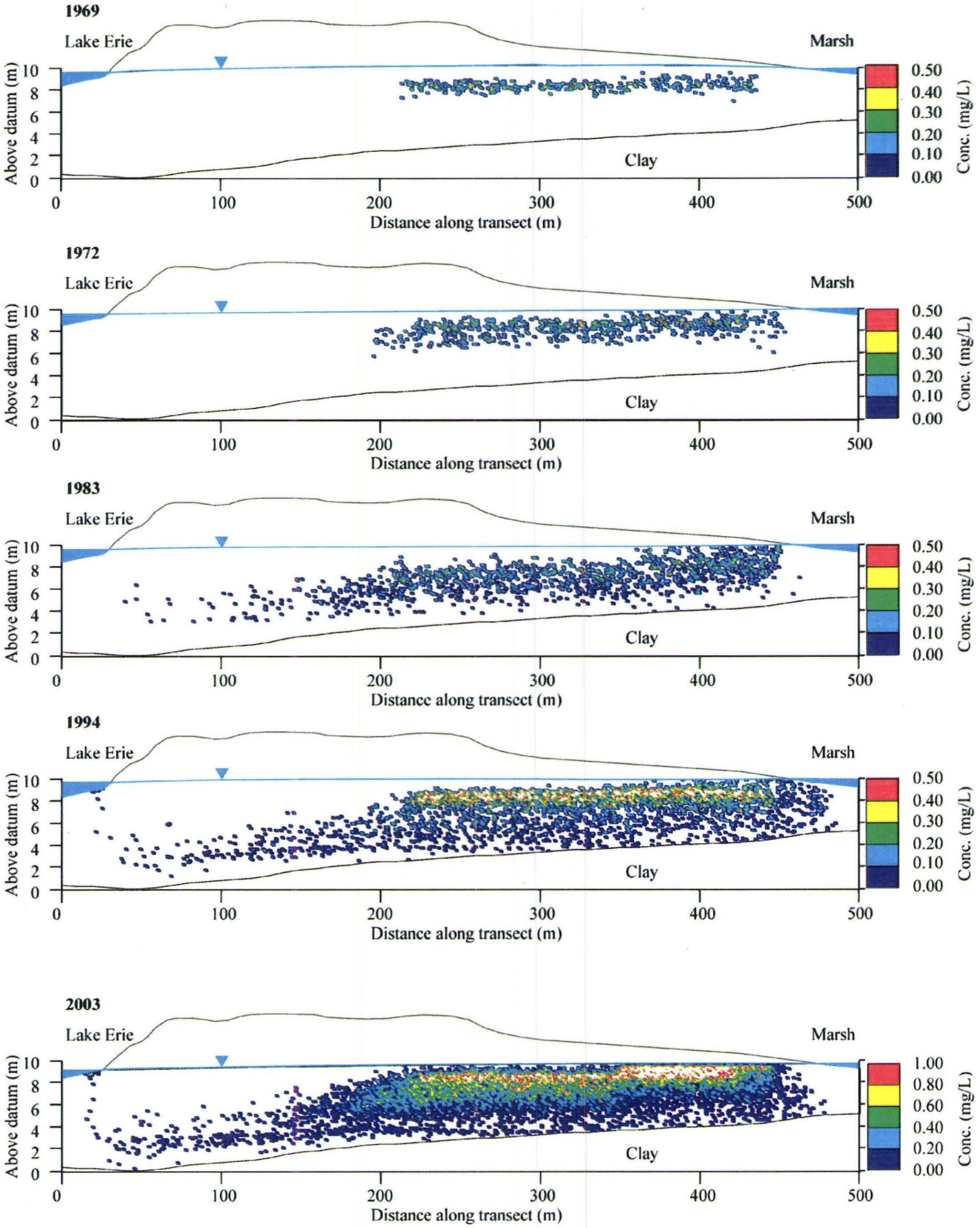

Figure 51. Distribution of Total DDT in the saturated zone throughout the Camp Henry transect from 1950 to 2003, based on long-term, slowly increasing non-point source loading from 225-430 m across the transect in 1950.

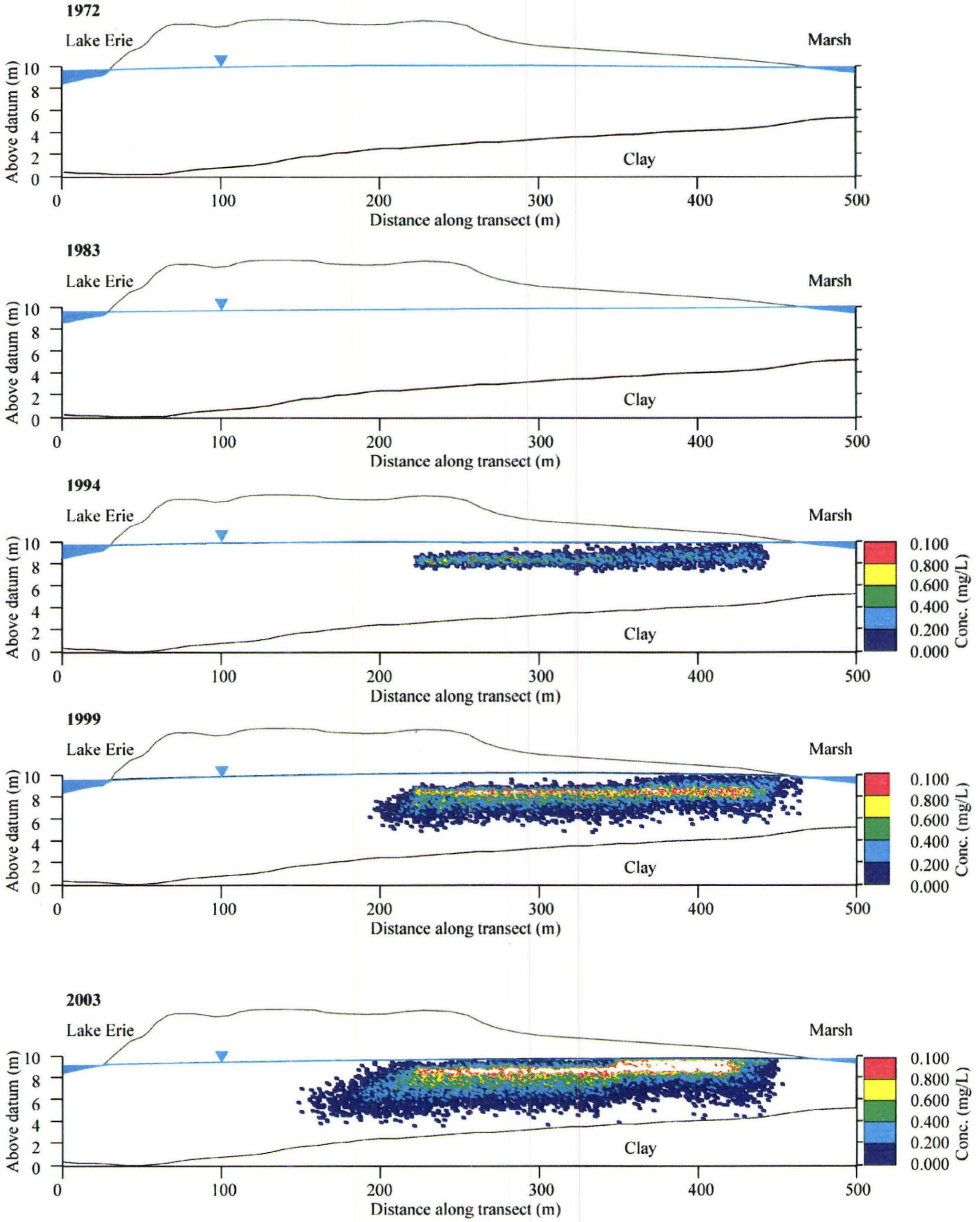

Figure 52. Distribution of Total DDT in the saturated zone throughout the Camp Henry transect from 1950 to 2003, based on long-term, slowly increasing non-point source loading from 225-430 m across the transect in 1970.

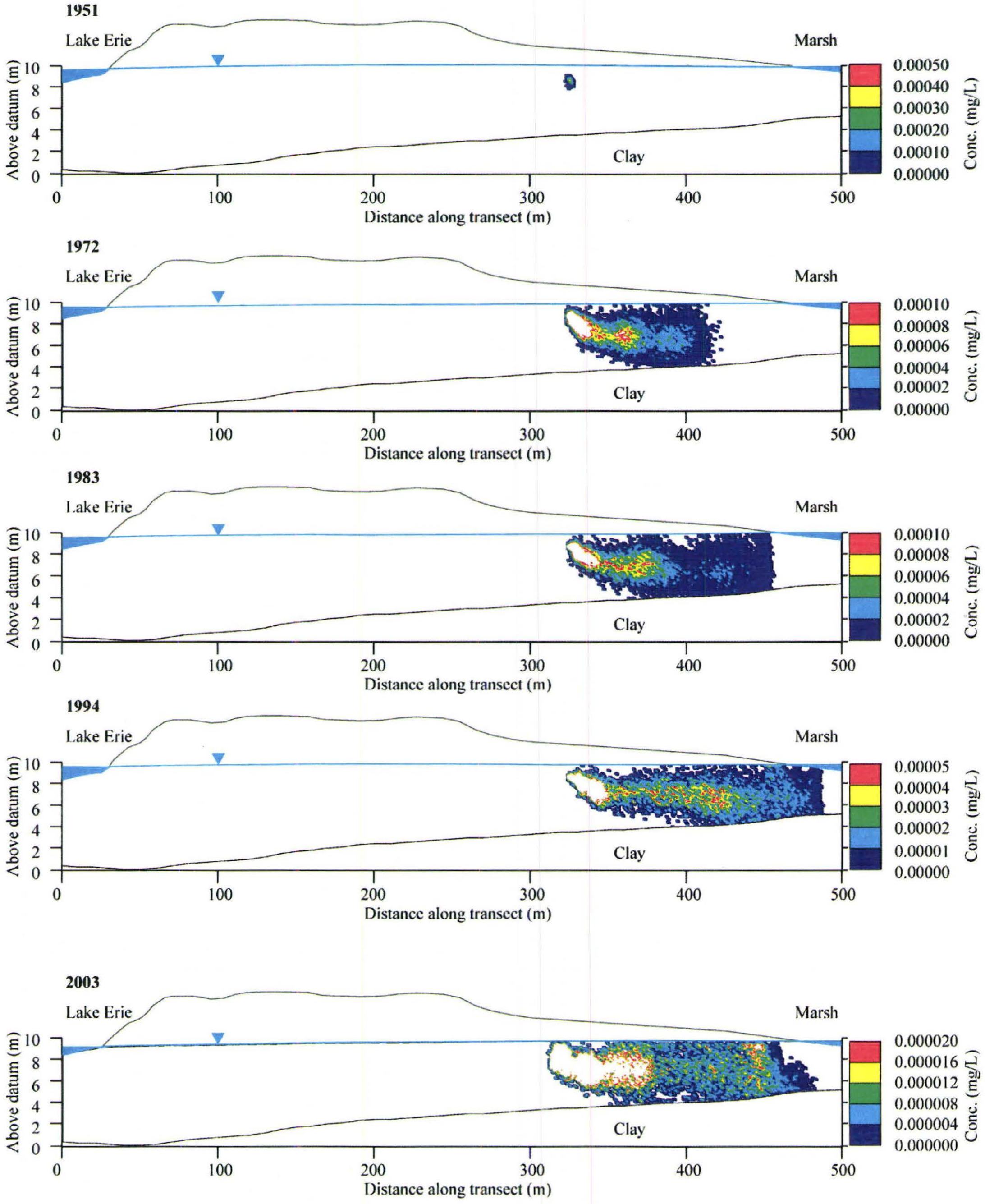

Figure 53. Distribution of Total DDT in the saturated zone throughout the Camp Henry transect from 1950 to 2003, based on long-term (1950-present) low concentration continuous point source loading at 225 m across the transect.

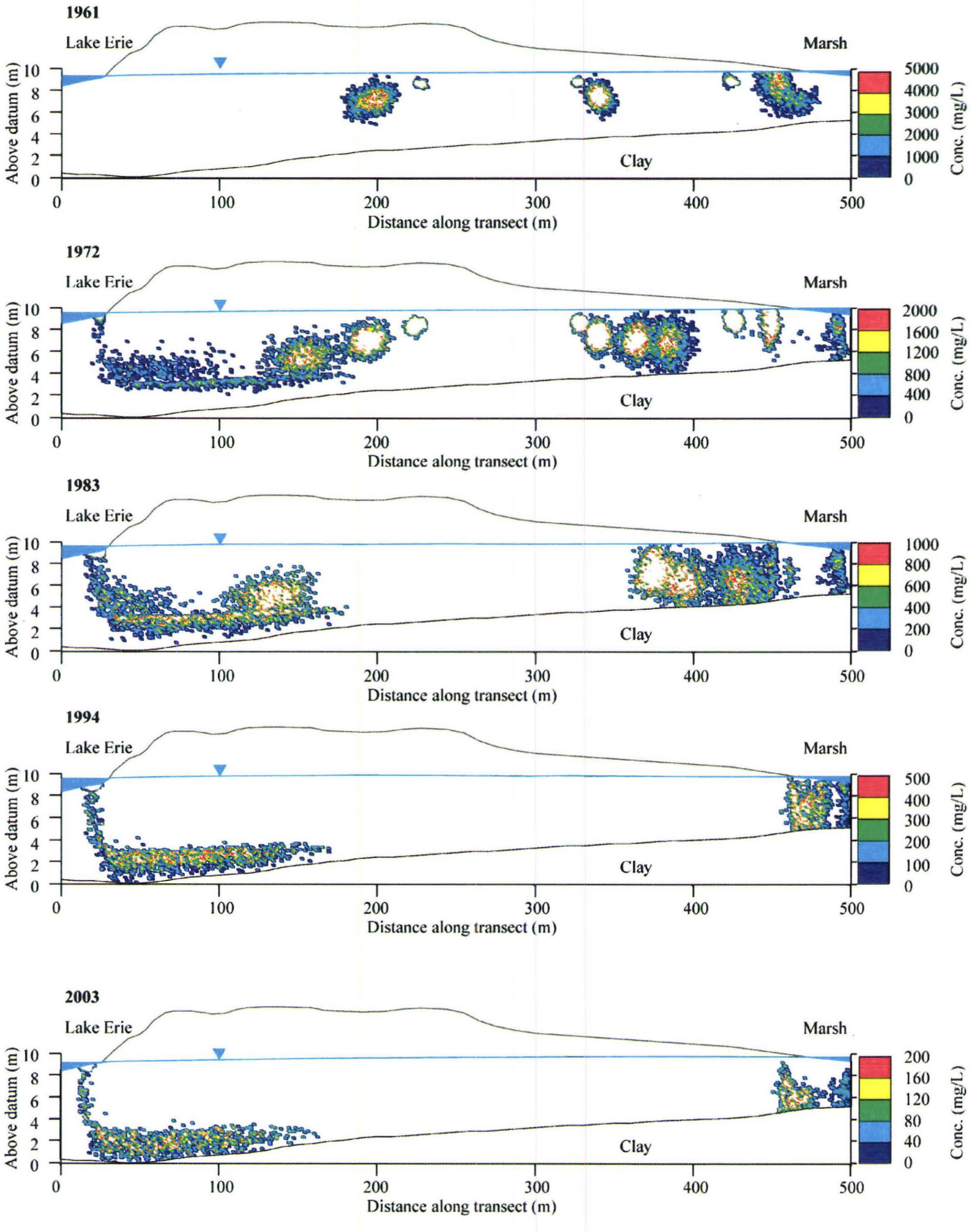

Figure 54. Distribution of Total DDT in the saturated zone throughout the Camp Henry transect from 1950 to 2003, based on point source loading at 225, 325 and 425 m after a series of four high concentration 2-year pulse loads in 1955, 1960, 1965 and 1970.

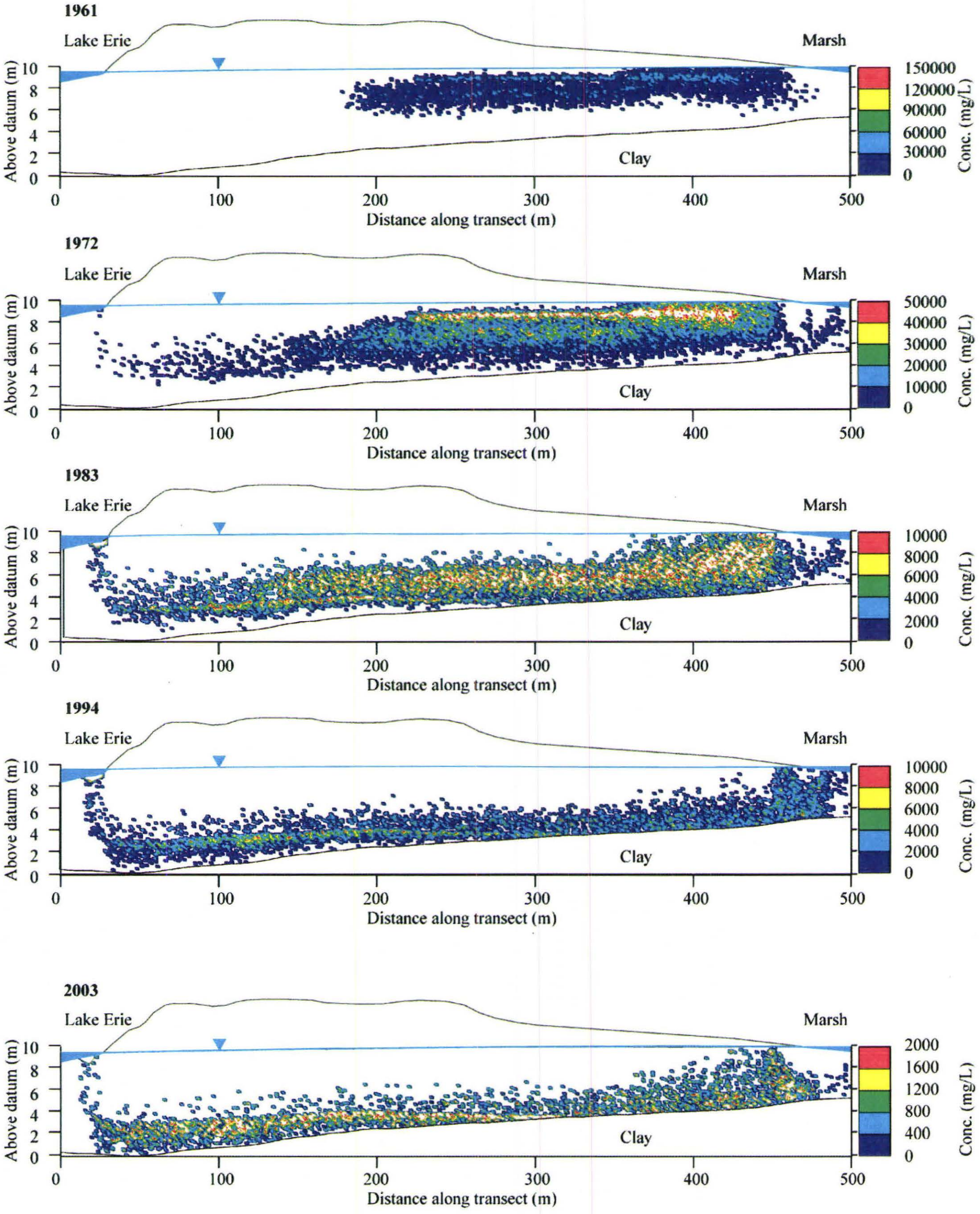

Figure 55. Distribution of Total DDT in the saturated zone throughout the Camp Henry transect from 1950 to 2003, based on non-point source loading from 225-430 m after a series of four high concentration 2-year pulse loads in 1955, 1960, 1965 and 1970.

CHAPTER 5: CONCLUSIONS AND RECOMMENDATIONS

PPNP is known for its abundant wildlife and natural environment. However, past agricultural activities within the Park have caused a variety of DDT problems. Although the application of DDT was discontinued over 30 years ago, high levels of DDT still exist within shallow soils and this contamination remains an issue for park managers today as it relates to drinking water, species mortality, and human health. The concentrations of DDE and DDD, the degradation products of DDT, are also high and of environmental concern. In order to assess these human health and environmental concerns, the objectives of this thesis focused on characterizing the distribution of DDT in shallow groundwater throughout the park and determining the primary factors controlling DDT fate and migration in the subsurface.

5.1 Conclusions

Field studies were undertaken to characterize the distribution of DDT within the shallow and deep soils and groundwater domain, and to assess possible relationships between DDT levels and degradation within the soil and groundwater. The results of field studies show that concentrations of Total DDT in the shallow soil are highly variable within former agricultural areas and range from 1,555 ng/g to 316,100 ng/g. Concentrations of DDT compounds within PPNP soil are often well above regulatory limits of 1.6 μg/g set forth by the OMOEE and CCME. DDT declines with depth by over 5 orders of magnitude in the uppermost 80 cm of the soil profile. Calculations of depth-weighted mass of DDT in the soil profile show that current amount of DDT in the former orchard soils are 22.2 kg/ha at Camp Henry Orchard, 33.9 kg/ha at Sleepy Hollow Orchard, and 7.5 kg/ha at Anders Orchard.

Concentrations of Total DDT in shallow groundwater are very low throughout former agricultural areas of PPNP, and range from 0.033 to 4.18 ng/L. No strong correlation exists between concentrations in soil and groundwater. Concentrations in groundwater were also poorly correlated to water table depth or ground surface elevation. The increased concentrations of DDT compounds in groundwater measured at CHO, SHO, and AO, between July 2002 and May 2003 show that concentrations vary over time. This suggests that large infiltration events may be an important mechanism promoting the flushing of DDT to groundwater.

Analysis of numerous field samples consistently shows that aerobic 1:1 transformation of DDT to DDE is the dominant transformation pathway throughout former agricultural areas. The relative proportions of DDT, DDE and DDD (34%, 62%, 4%, respectively) are consistent for soil and groundwater, indicating that there is no preferential degradation or leaching of any of these compounds. Degradation has proceeded further at AO than at SHO, which in turn has proceeded further than at CHO as indicated by relatively higher proportions of DDE and DDD than DDT with depth.

One-dimensional modelling of pesticide transport and fate (persistence, degradation, adsorption) from ground surface (the zone of high levels of DDT), through the unsaturated zone, to the water table was undertaken with LEACHMP to provide insight into the processes controlling the persistence and leaching of DDT within the unsaturated zone. Modelling using LEACHMP was able to match relative proportions of DDT with depth and concentrations throughout the soil profile well. Three potential transformation/degradation pathways were tested, with the best fits achieved for the transformation of DDT to DDE, and very little transformation of DDT to DDD or further degradation of DDE At CHO, the half-life for DDT is variable with depth, on the order of 30 years within surficial soils and approximately 9 years at depth based on singular applications of DDT in 1970 and 1950, respectively. Degradation of DDE to further compounds, and transformation of DDT to DDD are extremely slow ($t_{1/2}$ of 100 years and 450 years respectively), consistent with lower DDD concentrations seen in soil today.

Additional simulations at SHO have shown that transformation rates are variable within former agricultural areas with a uniform half-life of 14 years for the transformation of DDT to DDE fitting measured concentration profiles well.

Although water infiltrates through the soil at PPNP within a few days, the vertical migration of DDT compounds through the vadose zone under field conditions is very slow as a result of strong sorption and the presence of appreciable amounts of organic carbon in shallow soils. Under field conditions, LEACHMP was unable to predict concentrations measured in groundwater in May 2003. When organic carbon within the B and C horizons was eliminated, concentrations of DDT at the water table increased over time. This would imply that DDT does not adsorb according to an equilibrium adsorption model, as used in LEACHMP (rapid infiltration provides too little time for equilibrium adsorption), but DDT adsorbs according to a kinetic adsorption model.

Sensitivity analysis and scenario testing was conducted to address uncertainty in model parameters. The flow calibration was found to be most sensitive to the saturated hydraulic conductivity and the slope of the soil moisture characteristic curve, while it was relatively insensitive to meteorological conditions, the air entry value and the pore interaction parameter. The solute transport calibration was most sensitive to the organic carbon partition coefficient and percent organic carbon. Where the water table is shallower and organic carbon contents are lower and more uniform, as observed at SHO, more DDT will be flushed to groundwater. LEACHMP sensitivity analyses have shown that further attention should be devoted to better understanding sorption behaviour at PPNP. Thus, the primary factors controlling the leaching of DDT, DDE and DDD to groundwater at PPNP are (1) depth to the water table; (2) organic carbon content; and, (3) the organic carbon partition coefficient (K_{oc}). Because %OC is known to vary between 0.5% and 7.0% at PPNP, leaching of DDT is expected to vary between areas having different organic carbon contents.

There are no records of application loading dates, loading rates, and loading frequency of DDT at PPNP. However, LEACHMP simulations show DDT must have been applied over several years and probably well before 1970 in order to match soil concentrations and proportions of DDT:DDE:DDD seen today. The most likely way in which DDT is leaching to the water table, is through a very slow but continuous leaching of DDT from the Ah horizon, and given the slow movement of DDT through the soil profile due to adsorption and desorption, concentrations of dissolved DDT entering the groundwater will continuously increase for decades to come, should current meteorological and hydrological conditions continue.

Two-dimensional saturated zone modelling with the GW-WETLAND model was used to investigate the extent of DDT persistence and transport within the groundwater flow domain due to several possible DDT loading scenarios at the Camp Henry transect. Simulations show that if DDT reaches the water table, it rapidly disperses and moves both towards the marsh and Lake Erie, depending upon the position of the source zone relative to the groundwater flow divide. Simulations also show that DDT has and will continue to discharge into both the lake and the marsh. Groundwater recharge across water table pushes contaminated groundwater to base of aquifer where very high concentrations exist adjacent to base of aquifer but there is no contamination near the water table. DDT can become trapped within units having a lower hydraulic conductivity resulting in long retention times. Because degradation of DDT compounds proceeds slowly, the primary means for removal of mass from groundwater is via discharge to the marsh and Lake Erie.

The modelling shows that if DDT loading stops, concentrations in groundwater regime will decrease and DDT will eventually be flushed from the groundwater flow regime. However, if DDT loading continues, concentrations in groundwater will increase and DDT will not be flushed from the groundwater flow regime for a number of decades if current meteorological conditions persist. Much of the DDT that entered the saturated zone during 1950 to 1970 has already discharged to the marsh and Lake Erie. Simulations employing long-term continuous loading of small quantities (1 ng/L per day) of DDT to the saturated zone have shown that long-term loading is capable of distributing DDT throughout the aquifer from the lake to the marsh. Given the present low but increasing loading rates, simulations have shown that both DDT concentrations and the extent of aquifer contamination will continue to increase for many decades to come if current meteorological and hydrological conditions persist.

The findings presented here provide useful insight into the long-term persistence of the DDT throughout Canada and much of North America, where considerable amounts of DDT were applied to in the past. Even though the application of DDT in agricultural areas was banned decades ago, it remains in the soil environment and could be present at concentrations that can affect wildlife.

5.2 Recommendations

While this study provides a good indication of DDT degradation pathways and half-lives, a better understanding of the adsorption of DDT compounds on soil collected from PPNP would be beneficial to future field and modelling studies. Uncertainties exist relating to whether adsorption varies spatially and with depth, and whether sorption is kinetic and the partitioning relationship changes with time. Further laboratory experimentation aimed at determining the time and/or depth dependency of sorption within the various soil horizons at PPNP would also provide further insight into the processes controlling DDT migration to the water table.

Because the volumetric soil moisture profile was only measured on one date at CHO, additional insight into flow processes and transient changes in water content in the unsaturated zone could be availed if the volumetric water content profile was measured continuously over a long period of time in combination with evapotranspiration and precipitation at the field site. This would significantly contribute to the understanding of short-term flow phenomena and combined with weekly or monthly sampling of groundwater beneath the same location would provide considerable insight into the transient leaching behaviour of DDT.

LEACHMP simulations have shown that DDT leaching is sensitive to the transformation/degradation rates, further attention should be devoted to monitoring the long-term transformation of DDT to DDE. Further attention should also be given to sample collection procedures at PPNP due to the highly variable soil concentrations.

Verification of the two-dimensional transport of DDT could be provided by depth-profile sampling of groundwater along the Camp Henry transect. Sampling should be focused on the lacustrine sand, the base of the aeolian sand, and adjacent to the marsh, where elevated concentrations may still be present. Groundwater sampling over time would also provide infoirmation related to DDT transport and persistence within the saturated domain at PPNP. Groundwater sampling over time both above and below the water table at one location would provide significant insight into leaching behaviour, including adsorption/desorption mechanisms.

CHAPTER 6: REFERENCES

Ahlstrom, S.W., H.P. Foote, R.C. Arnette, C.R. Cole and R.J. Serne. 1977. *Multicomponent mass transport model: theory and numerical implementation (discrete-parcel-random-walk version).* Batelle P.N.L. Report 2127.

Aigner, E.J., A.D. Leone and R.L. Falconer. 1998. Concentrations and enantiomeric ratios of organochlorine pesticides in soils from the U.S. corn belt. *Environmental Science and Technology* 32: 1162-1168.

Aller, L., T. Bennet, J. Lehr and R. Petty. 1987. *DRASTIC: a standardized system for evaluating groundwater pollution potential using hydrogeologic settings*. U.S. EPA Report 600/2-85/018.

Anderson, M.P. and W.W. Woessner. 1992. *Applied Groundwater Modeling, Simulation of Flow and Advective Transport*. Academic Press.

Bailey, G.W. and J.L. White. 1964. Soil-Pesticide Relationships: Review of adsorption and desorption of organic pesticides by soil colloids with implications concerning pesticide bioactivity. *Journal of Agricultural Food Chemistry* 12: 324-332.

Badley, J. 2003. *Remediation of DDT Contaminated Soil: A field study.* Master of Science Thesis submitted to School of Graduate Studies, McMaster University.

Ball, W.P. and P.V. Roberts. 1991. Long-term sorption of halogenated organic chemicals by aquifer material. 1. Equilibrium. *Environmental Science and Technology* 25: 1223-1237.

Battin, J.G. and J.G. Nelson. 1978. *Mans's impact on Point Pelee National Park.* Toronto: National and Provincial Parks Association of Canada, 175 pp.

Boesten, J.J.T.I. and A.M.A. van der Linden. 1991. Modelling the influence of sorption and transformation on pesticide leaching and persistence. *Journal of Environmental Quality* 20: 425-435.

Bonazountas, M. and J. Wagner. 1984. *SESOIL: A Seasonal Soil Compartment Model.* Arthur D. Little, Inc., Cambridge, Massachusetts, prepared for the U.S. E.P.A., Office of Toxic Substances.

Boul, H.L., M.L. Garnham, D. Hucker and J. Aislabie. 1994. Influence of agricultural practices on the levels of DDT and its metabolites in soil. *Environmental Science and Technology* 28: 1397-1402.

Brady, NC and Weil, RR. 1999. *The Nature and Properties of Soils*, 12th ed. Prentice-Hall Inc., New Jersey, USA.

Brooke, D., I. Nielsen, J. de Bruijn and J. Hermens. 1990. An interlaboratory evaluation of the srir-flask method for the determination of octanol-water partition coefficients (Log P_{ow}): *Chemosphere* 21: 119-133.

Brown, C.D., U. Baer, P. Gunther, M. Trevisan, and A. Walker. 1996. Ring test with the models LEACHP, PRZM-2 and VARLEACH: Variability between model users in prediction of pesticide leaching using a standard data set. *Pesticide Science* 47: 249-258.

Brusseau, M.L., R.E. Jessup and S.C. Rao. 1991. Nonequilibrium sorption of organic chemicals: elucidation of rate-limiting processes. *Environmental Science and Technology* 25: 134-142.

Campbell, G.S., 1974. A simple method for determining unsaturated conductivity from moisture retention data. *Soil Science.* 117: 311-314.

Canadian Climate Normals, 2000, Environment Canada, http://www.msc.ec.gc.ca/climate/climate_normals/show_normals_e.cfm

Canadian Council of Resource and Environment Ministers (CCREM). 1987. *Canadian Water Quality Guidelines*. Task Force on Water Quality Guidelines. Ottawa.

Canadian Council of Resource and Environment Ministers (CCREM). 2002. *Canadian Water Quality Guidelines for the protection of aquatic life*. Winnipeg.

Carsel, F.R., L.A. Mulkey, M.M. Lorber and L.B. Baskin. 1985. The Pesticide Root Zone Model (PRZM): A procedure for evaluating pesticide leaching threats to groundwater. *Ecological Modelling* 30: 49-69.

Carter, C.W. and I.H. Suffet. 1982. Binding of DDT to dissolved humic materials. *Environmental Science and Technology* 16: 735-740.

Caux, P.Y., C. Bastien and A. Crowe. 1996. Fate and impact of pesticides applied to potato cultures: The Nicolet River basin. *Ecotoxicology and Environmental Safety* 33: 175-185.

Champion, D.F. and S.R. Olsen. 1971. Adsorption of DDT on solid particles. *Soil Science Society of America Proceedings* 35: 887-891.

Chiou, C.T., V.H. Freed, D.W. Schmedding and R.L. Kehnert. 1977. Partition coefficient and bioaccumulation of selected organic chemicals. *Environmental Science and Technology* 11: 475-478.

Chiou, C.T., D.W. Schmedding and J.H. Block. 1981. Correlation of water solubility with octanol-water partition coefficient. *Journal of Pharmaceutical Sciences* 70: 176-177.

Chiou, C.T., R.L. Malcolm, T.I. Brinton and D.E. Kile. 1986. Water solubility enhancement of some organic pollutants and pesticides by dissolved humic and fulvic acids. *Environmental Science and Technology* 20: 502-508.

Chiou, C.T., D.W. Schmedding and M. Manes. 1982. Partitioning of organic compounds in octanol-water systems. *Environmental Science and Technology* 16: 4-10.

Clemente, T.P. 1997. *RT3D – A modular computer code for simulating reactive multi-specis transport in 3-Dimensional groundwater aquifers*. Battelle Pacific Northwest Laboratory Research Report, PNNL-SA-28967.

Coakley, J.P. 1976. The formation and evolution of Point Pelee, western Lake Erie. *Canadian Journal of Earth Science* 13: 136-144.

Coakley, J.P., A.S. Crowe and P.A. Huddart. 1998. Subsurface sediment profiles below Point Pelee: indicators of postglacial evolution in western Lake Erie. *Canadian Journal of Earth Science* 35: 88-99.

Cooke, B.K. and A. Stringer. 1982. Distribution and breakdown of DDT in orchard soil. *Pesticide Science* 13: 545-551.

Corona-Cruz, A., G. Gold-Bouchot, M. Gutierrez-Rojas, O. Monroy-Hermosillo and E. Favela. 1999. Anaerobic-aerobic biodegradation of DDT (dichlorodiphenyltrichloroethane) in soils. *Bulletin of Environmental Contamination and Toxicology* 63: 219-225.

Cornelissen, G., K.A. Hassell, P.C.M. van Noort, R. Kraaij, P.J. van Ekeren, C. Dijkema, P.A. de Jager and H.A.J. Govers. 2000. Slow desorption of PCB's and chlorobenzenes from soils and sediments: relations with sorbent and sorbate characteristics. *Environmental Pollution* 108: 69-80.

Costa, J.L., R.E. Knighton, and L. Prunty. 1994. Model comparison of unsaturated steady-state solute transport in a field plot. *Soil Science Society of America Journal* 58: 1277-1287.

Coulston, F. 1989. The dilemma of DDT. *Chemtech.* pp. 660-661.

Crowe, A.S. 1999. Distribution and Persistence of DDT at Point Pelee National Park. In: *Proceedings of 3rd Annual Parks Research Forum – Ontario.* April 22-23, 1999, Guelph, Ontario, pp 379-387.

Crowe, Allan. Personal Communication, 2002. National Water Research Institute, Environment Canada.

Crowe, A.S. and C.J. Ptacek. 1995. Groundwater flow at a large freshwater coastal wetland: the Point Pelee marsh, Ontario, Canada. In: *Solutions '95 - Proceedings of the XXVI International Association of Hydrogeologists, June 4-10, 1995* (on CD).

Crowe, A.S. and S.G. Shikaze. 2004. Linkages between groundwater and coastal wetlands of the Laurentian Great Lakes. *Journal of Aquatic Ecosystem Health and Management* 7: 199-213.

Crowe, A.S., S.G. Shikaze and C.J. Ptacek. 2004. Numerical modelling of groundwater flow and contaminant transport to the Point Pelee marsh, Ontario, Canada. *Hydrological Processes* 18:293-314.

Crowe, A.S., S.G. Shikaze and J.E. Smith. 2000. *Hydrogeological Studies in Support of the Restoration of the Wainfleet Bog: Numerical Modelling*. Report submitted to the Niagara Peninsula Conservation Authority. National Water Research Institute Contribution 00-063, 86pp.

Crowe, A.S., S.G. Shikaze and J.E. Smith. 2002. Impact of a large quarry on the restoration of the water table at the Wainfleet Bog, Ontario, Canada. In: *Ground and Water: Theory to Practice. Proceedings of the 3rd Joint IAH-CNC/CGS Conference*, October 20 to 23, 2002, (D. Stolle, A.R. Piggott and J.J. Crowder, Eds.), Niagara Falls, Ontario, pp. 1365-1372.

Crowe, AS., J.E. Smith and S. Spencer. 2002. *DDT and Dieldrin Assessment and Monitoring Protocols for Point Pelee National Park.* NWRI Contribution No. 02-007. National Water Research Institute. 71 pp.

De Jong, R., W.D. Reynolds, S.R. Vieira and R.S. Clemente. 1994. *Prediciting pesticide migration through soils of the Great Lakes Basin.* Centre for Land and Biological Resources Research Contribution No. 94-70. 25 pp.

De Bruijn, J., F. Busser, W. Seinen and J. Hermens. 1989. Determination of octanol/water partition coefficients for hydrophobic organic chemicals with the "slow-stirring" method. *Environmental Toxicology and Chemistry* 8: 499-512.

Dimond, J.B. and R.B. Owen. 1995. Long-term residue of DDT compounds in forest soils in Maine. *Environmental Pollution* 92: 227-230.

Domenico, P.A. and F.W. Schwartz. 1998. *Physical and Chemical Hydrogeology, 2nd Edition.* John Wiley and Sons, Inc., New York, NY.

Edwards, C.A. 1970. *Persistent Pesticides in the Environment.* CRC Press, Cleveland, Ohio.

EHC 83. 1989. *DDT and its derivatives-Environmental aspects.* Environmental Health Criteria. International Program on Chemical Safety. World Health Organization, Geneva.

Elrick, DE, Reynolds, WD, Tan, KA. 1989. Hydraulic Conductivity measurements in the unsaturated zone using improved well analyses. *Ground water monitoring review* 9:3, 184-193.

Enfield, C.G., R.F. Carsel, S.Z. Cohen, T. Phan and D.M. Walters. 1982. Approximating pollutant transport to ground water. *Ground Water* 20: 711-722.

Environment Canada. 1997. *Toxic substance management policy.* DDT: Scientific justification, C97-980041-2.

EPA. 1986. *Environmental Protection Agency Superfund Public Health Evaluation Manual.* Office of Emergency and Remedial Response. EPA 540/1-86-060.

Farmer, W.J., W.F. Spencer, R.A. Shaphard and M.M. Cliath. 1974. Effect of flooding and organic matter applications of DDT metabolites in soil. *Journal of Environmental Quality* 3: 343-346.

Frank, R. 1981. Pesticides and PCB in the Grand and Saugenn River basins. *Journal of Great Lakes Research* 7:440-454.

Frank, R. and H.E. Braun. 1981. Residues from past uses of organochlorine insecticides and PCB in waters draining eleven agricultural watersheds in Southern Ontario, Canada, 1975-1977. *The Science of the Total Environment* 20: 255-276.

Frank, R., H.E. Braun, K. Ishida and P. Suda. 1976. Persisten organic and inorganic pesticide residues in orchard soils and vineyards of Southern Ontario. *Canadian Journal of Soil Science* 56: 463-484.

Frank, R., H.E. Braun, M. Van Hove Holdrinet, G.J. Sirons and B.D. Ripley. 1982. Agricultural and water quality in the Canadian Great Lakes Basin: V. Pesticide use in 11 agricultural watersheds and presence in stream water, 1975-1977. *Journal of Environmental Quality* 11: 497-505.

Frank, R., B.S. Clegg, B.D. Ripley and H.E. Braun. 1987b. Investigations of pesticide contaminations in rural wells, 1979-1984, Ontario, Canada. *Archives of Environmental Contamination and Toxicology* 16: 9-22.

Frank, R., K. Montgomery, H.E. Braun, A.H. Berst and K. Loftus. 1974. DDT and dieldrin in watersheds draining the tobacco belt of Southern Ontario. *Pesticides Monitoring Journal* 8: 184-201.

Frank, R., B.D. Ripley, H.E. Braun, B.S. Clegg, R. Johnston, T.J. Oneill. 1987a. Survey of farm wells for pesticides in Southern Ontario, Canada, 1981-1982, 1984. *Archives of Environmental Contamination and Toxicology* 16: 1-8.

Gevao, B., K.T. Semple and K.C. Jones. 2000. Bound pesticide residues in soils: a review. *Environmental Pollution* 108: 3-14.

Gillan, K.A., B.M. Haspieler, R.W. Russell, K. Adeli and G.D. Haffner. 1998. Ecotoxicological studies in amphibian populations of southern Ontario. *Journal of Great Lakes Research* 24: 45-54.

Goodrich, J.A., B.W. Lykins and R.M. Clark. 1991. Drinking water from agriculturally contaminated groundwater. *Journal of Environmental Quality* 20:707-717.

Goss, M.J., D.A.J. Barry and D.L.Rudolph. 1998. Contamination in Ontario farmstead domestic wells and its association with agriculture: 1. Results from drinking water wells. *Journal of Contaminant Hydrology* 32: 267-293.

Guenzi, W.D. and W.E. Beard. 1967. Movement and persistence of DDT and Lindane in soil columns. *Soil Science Society of America Proceedings* 31: 644-647.

Guenzi, W.D. and W.E. Beard. 1968. Anaerobic conversion of DDT to DDD and aerobic stability of DDT in soil. *Soil Science Society of America Proceedings* 32: 522-524.

Guenzi, W.D. and W.E. Beard. 1976. DDT degradation in flooded soil as related to temperature. *Journal of Environmental Quality* 5: 391-394.

Guo, L., R.J. Wagenet, J.L. Hutson, and C.W. Boast. 1997. Nonequilibrium transport of reactive solutes through layered soil profiles with depth-dependent adsorption. *Environmental Science and Technology* 31: 711-722.

Gustafson, D.I. 1989. Groundwater ubiquity score: a simple method for assessing pesticide leachability. *Environmental Toxicology and Chemistry* 8: 339-357.

Hallberg, G.R. 1989. Pesticide pollution of groundwater in the humid United States. *Agriculture Ecosystems and Environment* 26: 299-367

Harner, T., J.L. Wideman, L.M.M. Jantunen, T.F. Bidleman and W.J. Parkhurst. 1999. Residues of organochlorine pesticides in Alabama soils. *Environmental Pollution* 106: 323-332.

Harris, C.R. and J.R.W. Miles. 1975. Pesticide Residues in the Great Lakes Basin. *Residue Reviews* 57: 27-79.

Harris, C.R. and W.W. Sans. 1971. Insecticide residues in soils on 16 farms in southwester Ontario-1964, 1966, and 1969. *Pesticides Monitoring Journal* 5: 259-267.

Harvey, Geordon. Personal communication, 2003. Point Pelee National Park, Parks Canada.

Hassett, J.J., W.L. Banwart and R.A. Griffin. 1983. Correlation of compound properties with sorption characteristics of nonpolar compounds by soils and sediments - concepts and limitations. In: Francis, C.W., Auerbach, S.I., and Jacobs, V.A., eds. *Environmental and solid wastes—characterization, treatment and disposal*: Boston, Butterworths, p. 161–178.

Hebert, C.E., V. Glooschenko, G.D. Haffner and R. Lazar. 1993. Organic contaminants in snapping turtle (Chelydra serpentine) populations from southern Ontario, Canada. *Archives of Environmental Contamination and Toxicology* 24: 35-43.

Hileman, B. 1999. Paring of persistent pollutants progresses. *Chemical and Engineering News* 77: 25-26.

Howard, P and Meylan, W, eds. 1997. *Handbook of physical properties of organic chemicals*. Boca Raton, FL: CRC Press, Lewis Publishers, 3, 1849518, 723.

Huang, W., H. Yu and W.J. Weber. 1998. Hysteresis in the sorption and desorption of hydrophobic organic contaminants by soils and sediments. 1. A comparative analysis of experimental protocols. *Journal of Contaminant Hydrology* 31: 129-148.

Huddart, P.A., F.J. Longstaffe and A.S. Crowe. 1999. δD and δ^{18}O evidence for inputs to groundwater at a wetland coastal boundary in the southern Great Lakes region of Canada. *Journal of Hydrology* 214: 18-31.

Hutson, J.L. 2003. *LEACHM: Leaching Estimation and Chemistry Model, V. 4.0: Model Description and User's Guide*. School of Chemistry, Physics and Earth Sciences, Flinders University of South Australia, Adelaide, SA. 142 pp.

Hutson, J.L. and A. Cass. 1987. A retentivity function for use in soil-water simulation models. *Journal of Soil Science* 38: 105-113.

Hutson, J.L. and R.J. Wagenet. 1992. Simulating nitrogen dynamics in soils using a deterministic model. *Soil Use and Management* 1: 74-78.

Hutson, J.L., R.J. Wagenet and M.E. Niederhofer. 1997. *Leaching estimation and chemistry model: a process based model fo water and solute movement, transformations, plant uptake and chemical reactions in the unsaturated zone. Versions LEACHF and LEACHG (for simulating nitrogen and phosphorous transformations, cycling and transport)*. Research report R97-1, Department of Soil, Crop and Atmospheric Sciences, Cornell University, Ithica, New York, 138 pp.

Jarvis, N.J. 1995. Simulation of soil water dynamics and herbicide persistence in a silt loam soil using the MACRO model. *Ecological Modelling* 81: 97-109.

Jones, R.L. 1986. Field, laboratory, and modelling studies on the degradation and transport of aldicarb residues in soil and groundwater. In: Garner, W.Y. et al. (Eds.), *Evaluation of Pesticides in Ground Water*. ACS Syposium Series; 315, Salem, U.S.

Kan, A.T., G. Fu, M. Hunter, W. Chen, H. Ward and M.B. Tomson. 1998. Irreversible sorption on neutral hydrocarbons to sediments: experimental observations and model predictions. *Environmental Science and Technology* 32: 892-902.

Karickhoff, S.W. 1981. Semi-empirical estimation of sorption of hydrophobic pollutants on natural sediments and soils. *Chemosphere* 10: 833-846.

Karickhoff, S.W., D.S. Brown and T.A. Scott. 1979. Sorption of hydrophobic pollutants on natural sediments: *Water Research* 13: 241–248.

Klute, A., ed. 1986. *Methods of Soil Analysis: Part 1-Physical and Mineralogical Methods.* 2nd edition. Wisonsin, U.S.A. Soil Science Society of America, Inc.: American Society of Agronomy, Inc.

Kolpin, D.W., J.E. Barbash and R.J. Gilliom. 1998. Occurrence of pesticides in shallow groundwater of the United States: Initial results from the National Water-Quality Assessment Program. *Environmental Science and Technology* 32: 558-566.

Kolpin, D.W., J.E. Barbash and R.J. Gilliom. 2000. Pesticides in ground water of the United States, 1992-1996. *Groundwater* 38: 858-863.

Kolpin, D.W., E.M. Thurman and D.A. Goolsby. 1996. Occurrence of selected pesticides and their metabolites in near-surfact aquifers of the Midwestern United States. *Environmental Science and Technology* 30: 335-340.

Kuhr, R.J., A.C. Davis and J.B. Bourke. 1974. DDT residues in soil, water and fauna from New York apple orchards. *Pesticide Monitoring Journal* 7: 200-204.

Laskowski, D.A., C.A. Goring, P.J. McCall and R.L. Swann. 1982. Terrestrial environment. In: Conway, R.A. (Ed.) *Environmental Risk Analysis for Chemicals*. Van Nostrand Reinhold, New York.

Lewallen, M.J. 1971. Pesticide contamination of a shallow bored well in the southeastern coastal plains. *Groundwater* 9: 45-49.

Lichtenstein, E.P and K.R. Schulz. 1961. Effect of soil cultivation, soil surface, and water on the persistence of insecticidal residues in soils. *Journal of Economic Entomology* 54: 517-522.

Lichtenstein, E.P, T.W. Fuhreman and K.R. Schulz. 1971. Persistence and vertical distribution of DDT, lindane and aldrin residues 10 and 15 years after a single soil application. *Journal of Agricultural Food Chemistry* 19: 718-721.

Luthy, R.G., G.R. Aiken, M.L. Brusseau, S.D. Cunningham, P.W. Gschwend, J.J. Pignatello, M.Reinhard, S.J. Traina, W.J. Weber and J.C. Westall. 1997. Sequestration of hydrophobic organic contaminants by geosorbents. *Environmental Science and Technology* 31: 3341-3347.

Lyman, W.J., W.F. Reehl, and D.H. Rosenblatt. 1990. *Handbook of Chemical Property Estimation Methods*. American Chemical Society, Washington, DC.

Marenco, N. 2002. *The effect of subsurface hydrology on DDT degradation in soils at Point Pelee National Park, Ontario, Canada*. Master of Science Thesis submitted to the School of Graduate Studies, McMaster University.

McBride, M.S. and H.O. Pfannkuch. 1975. The distribution of seepage within lakebeds. U.S. Geological Survey, *Journal of Research* 3: 505-512.

McDonald, M.G. and A.W. Harbaugh. 1988. *A modular three-dimensional finite-difference groundwater flow model*. U.S. Geological Survey. Techniques of Water-Resources Investigations Book 6, Chapter A1, 586 pp.

McLaren, R.G. 1998. *GRIDBUILDER 5.21 User's Guide. A generator for 2-D triangular finite element meshes and mesh properties*. Institute for Groundwater Research, University of Waterloo, Waterloo, Ontario.

Meylan, W., P.H. Howard and R.S. Boethling. 1992. Molecular topology/fragment contribution method for predicting soil sorption coefficients. *Environmental Science and Technology* 26: 1560-1567.

Mitsch, W.J. and J.G. Gosselink. 2000. Wetlands. 3rd Edition. J. Wiley and Sons Inc. 920 pp.

Mutch, J.P., A.S. Crowe and O. Resler. 1993. *EXPRES: An expert system for assessing the fate of pesticides in the subsurface: User's Manual.* NWRI Contribution #93-201, National Water Research Institute, Burlington, ON. 137 pp.

Mutch, J.P., R.E. Jackson, M.W. Priddle and D.I. Bray. 1992. *The fate and simulation of aldicarb in the soil and groundwater of Prince Edward Island.* NWRI Contribution #92-194, National Water Research Institute, Burlington, ON. 81 pp.

Nash, R.G. and E.A. Woolson. 1967. Persistence of chlorinated hydrocarbon insecticides in soils. *Science* 157: 924-927.

National Laboratory for Environmental Testing (NLET). *2002-2003 Schedule of Services*. 2002. Burlington, Ontario: Environment Canada.

National Laboratory for Environmental Testing (NLET). *2003-2004 Schedule of Services*. 2003. Burlington, Ontario: Environment Canada.

O'Connor and Associated Environmental Inc. 2001. *Environmental Monitoring, Point Pelee National Park.* Reference No. KIN-0-00509, report prepared for Point Pelee National Park.

Oliver, B.G., M.M. Charlton and R.W. Durham. 1989. Distribution, redistribution and geochronology of PCB congeners and other chlorinated hydrocarbons in Lake Ontario sediments. *Environmental Science and Technology* 23: 200-208.

Olsen, R.L. and A. Davis. 1990. Predicting the fate and transport of organic compounds in groundwater, Part 1 and Part 2. *Hazardous Materials and Chemicals* July/August 1990: 39-64, 18-37.

OMOEE (Ontario Ministry of Environment and Energy). 1997. *Guideline for use at Contaminated Sites in Ontario*; Ontario Ministry of Environment publication PIBS 3161E01, revised February 1997.

OMAF (Ontario Ministry of Agriculture and Food). 1975. Publication 360, Fruit production recommendations (1973-1975), Ontario spray calendars (1867-1962).

Paramasivam, S., A.K. Alva, A Fares and K.S. Sajwan. 2002. Fate of nitrate and bromide in an unsaturated zone of a sandy soil under citrus production. *Journal of Environmental Quality* 31: 671-681.

Parr, J.F., G.H. Willis and S. Smith. 1970. Soil anaerobiosis: II. Effect of selected environments and energy sources on the degradation of DDT. *Soil Science* 110: 306-312.

Pennell, K.D., A.G. Hornsby, R.E. Jessup, and P.S.C. Rao. 1990. Evaluation of five simulations models for predicting aldicarb and bromide behaviour under filed conditions. *Water Resources Research* 26: 2679-2693.

Pignatello, J.M. and B. Xing. 1996. Mechanisms of slow sorption of organic chemicals to natural particles. *Environmental Science and Technology* 30: 1-11.

Pinder, G.F. and W.G. Gray. 1977. *Finite Element Simulation in Surface and Subsurface Hydrology*. Academic Press: San Diego.

Piwoni, M.D. and J.W. Keeley. 1990. *Basic concepts of contaminant sorption at hazardous waste sites*. EPA/540/4-90/053.

Point Pelee National Park Topographic Map Series: 1:3,000. 1987. Parks Canada, Point Pelee National Park.

Pontolillo, J., and R.P. Eganhouse. 2001. *The search for reliable aqueous solubility (S_w) and octanol-water partition coefficient (K_{ow}) data for hydrophobic organic compounds: DDT and DDE as a case study*. USGS Water-Resources Investigations Report 01-4201.

Prickett, T.A., T.G. Naymik and C.G. Lonquist. 1981. *A random-walk solute transport model for selected groundwater quality evaluations*. Illinois State Water Survey Bulletin 65, Champaign, Illinois.

Priddle, M.W., R.E. Jackson, A.S. Crowe, and J.P. Mutch. 1988. Aldicarb and nitrogen residues in a sandstone aquifer. In: *Proceeding of Agricultural Impacts on Ground Water, 191-210*. NWWA Conference, March 21-23, 1988, Des Moines, Iowa.

Ptacek, C. 1998. Geochemistry of a septic-system plume in a coastal barrier bar, Point Pelee, Ontario, Canada. *Journal of Contaminant Hydrology* 33: 293-312.

Ravi, V. and J.A. Johnson. 1992. *PESTAN: Pesticide Analytical Model, V. 4.0*. USEPA, Office of Research and Development, Center for Subsurface Modelling Support, Ada, Oklahoma. 35 pp.

Reid, B.J., K.C. Jones and K.T. Semple. 2000. Bioavailability of persistent organic pollutants in soils and sediments-a perspective on mechanisms, consequences and assessment. *Environmental Pollution* 108: 103-112.

Richards, N.R., A. Caldwell and F. Morwick. 1949. *Soil Survey of Essex County, Report No. 11 of the Ontario Soil Survey.* Ministry of Agriculture and Food, Guelph, Ontario, Canada.

Rieve, Dan. Personal Communication, 2003. Point Pelee National Park, Parks Canada

Ronen, D., B. Berkowitz, and M. Magaritz. 1989. The development and influence of gas bubbles in phreatic aquifers under natural flow conditions. *Transport Through Porous Media* 4: 295-306.

Roy, J. W., J.C. Hall, G.W. Parkin, C.Wagner-Riddle and B.S. Clegg. 2001. Seasonal leaching and biodegradation of dicamba in turfgrass. *Journal of Environmental Quality* 30: 1360-1370.

Rudolph, D.L., D.A.J. Barry and M.J. Goss. 1998. Contamination in Ontario farmstead domestic wells and its association with agriculture: 2. Results from multilevel monitoring well installations. *Journal of Contaminant Hydrology* 32: 295-311.

Russell, RW, K.A. Gillan and S.J. Haffner. 1997. Polychlorinated biphenyls and chlorinated pesticides southern Ontario, Canada, green frogs. *Environmental Toxicology and Chemistry* 16: 2258-2263.

Russell, RW and G.D. Haffner. 1997. *Contamination of soil, sediments, and biota with DDT and DDT metabolites at Point Pelee National Park.* Great Lakes Institute for Environmental Research, University of Windsor, Windsor Ontario, report prepared for Point Pelee National Park, 103 pp.

Russell, RW, S.J. Hecnar and G.D. Haffner. 1995. Organochlorine pesticide residues in southern Ontario spring peepers. *Environmental Toxicology and Chemistry* 14: 815-817.

Sabljic, A. 1984. Predictions of the nature and strength of soil sorption of organic pollutants by molecular topology. *Journal of Agricultural Food Chemistry* 32: 243-246.

Sayles, G.D., G. You, M. Wang and M. Kupferle. 1997. DDT, DDD and DDE dechlorination by zero-valent iron. *Environmental Science and Technology* 31: 3448-3454.

Schwartz, F.W. 1978. Application of probabilistic-deterministic modelling to problems of mass transport in groundwater systems. In *Third International Hydrology Symposium*, Ft Collins; pp. 281-296.

Schwarzenbach, R. and J. Westall. 1981. Transport of Nonpolar Organic Compounds from Surface Water to Groundwater: Laboratory Sorption Studies. *Environmental Science and Technology* 15: 1360-1367.

Shikaze, S.G. and A.S. Crowe. 1998. Impact of flooding and flood mitigation on groundwater quality. In *Proceedings of the Conference Groundwater in a Watershed Context*, December 2-4, 1998, Burlington, Ontario (published electronically on CD), pp. 389-396.

Shikaze, S.G. and A.S. Crowe. 1999. *User's Guide for GW-WETLAND: A Computer Program to Simulate Groundwater Flow, Particle Tracking, and Solute Transport in a Two-dimensional Cross Section with Transient Boundary Conditions and a Fluctuating Water Table.* National Water Research Institute Contribution 99-204, 65pp.

Shikaze, S.G. and A.S. Crowe. 2000. *Input Guide and Revisions for GW-WETLAND (version 1.1): A Computer Program to Simulate Groundwater-Wetland Interactions.* National Water Research Institute Contribution 00-065, 45pp.

Shikaze, S.G. and A.S. Crowe. 2001. *Input Guide and Revisions for GW-WETLAND (version 1.2): A Computer Program to Simulate Groundwater-Wetland Interactions.* National Water Research Institute Technical Note AEI-TN-01-001, 86pp.

Simunek, J., M. Sejna and M.Th. van Genuchten. 1999. *The HYDRUS-2D software package for simulating two-dimensional movement of water, heat, and multiple solutes in variably saturated media.* Version 2.0, IGWMC-TPS-53, International Ground Water Modeling Center, Colorado School of Mines, Golden, Colorado, 251 pp.

Sparks, D.L.. ed. 1996. *Methods of Soil Analysis: Part 3 – Chemical Methods.* Wisonsin, U.S.A. Soil Science Society of America, Inc.: American Society of Agronomy, Inc.

Spencer, W. F. and Cliath, M. M. 1975. Vaporization of chemicals (Book chapter). In: *Environmental Dynamics of Pesticides*. Plenum Press: New York.. pp. 61-78.

Spencer, W.F., G. Singh, C.D. Taylor, R.A. Lemert, M.M. Cliath and W.J. Farmer. 1996. DDT persistence and volatility as affected by management practices after 23 years. *Journal of Environmental Quality* 25: 815-821.

Tarrant, R.F., D.G. Moore, W.B. Bollen and B.R. Loper. 1972. DDT residues in forest floor and soil after aerial spraying, Oregon—1965-68. *Pesticides Monitoring Journal* 6: 65-72.

Taylor, A.W., D.E. Glotfelty, B.C. Turner, R.E. Silver, H.P. Freeman and A. Weiss. 1977. Volatilization of dieldrin and heptachlor residues from field vegetation. *Journal of Agricultural Food Chemistry* 25: 542-548.

Terasmae, J. 1970. *Report on stratigraphic drilling in Point Pelee National Park, Ontario.* Contract Report 68-200, National and Historic Parks Branch, Department of Indian and Northern Affairs.

Thornthwaite, C.W. 1948. An approach toward a rational classification of climate. *Geographic Review* 38: 55-94.

Trenhaile, A.S. and R. Dumala. 1978. The geomorphology and origin of Point Pelee, southwestern Ontario. *Canadian Journal of Earth Science* 15: 963-970.

Van den Hoop, M.A.G.T., P. Kreule and J.P.G. Loch. 1999. Sorption kinetics and transformation of DDT in sediment. *Water, Air, and Soil Pollution* 110: 57-66.

Villeneuve, J.P., O. Banton and P. Lafrance. 1990. A probabilistic approach for the groundwater vulnerability to contamination by pesticides: The VULPEST model. *Ecological Modelling* 51:47-58.

Villeneuve, J.P., O. Banton, P. Lafrance and P.G.C. Cambell. 1987. A new model for the evaluation of groundwater vulverability to non-point contamination by pesticides. pp. 1097-1109. In *Vulnerability of Soil and Groundwater to Pollutants*, W. van Duijvenbooden and H.G. van Waegeningh, eds. The Hague, Netherlands: TNO Committee on Hydro-logical Research, National Institute of Public Health and Hygiene.

Vink, J.P.M., B. Gottesburen, B. Diekkruger and S.E.A.T.M van der Zee. 1997. Simulation and model comparison of unsaturated movement of pesticides from a large clay lysimeter. *Ecological Modelling* 105: 113-127.

Wade, H.F., A.C. York, A.E. Morey, J.M. Padmore and K.M. Rudo. 1998. The impact of pesticide use on groundwater in North Carolina. *Journal of Environmental Quality* 27: 1018-1026.

Wagenet, R.J. 1986. Principles of modelling pesticide movement in the unsaturated zone. In: Garner, W.Y. et al. (Eds.), *Evaluation of Pesticides in Ground Water.* ACS Syposium Series; 315, Salem, U.S.

Wagenet, R.J. and J.L. Hutson. 1987. Predicting the fate of non-volatile pesticides in the unsaturated zone. *Journal of Environmental Quality* 15: 315-322.

Wagenet, R.J. and J.L. Hutson. 1989. LEACHM: A Finite Difference Model for Simulating Water, Salt and Pesticide Movement in the Plant Root Zone, Version 2.0. *Continuum* 2. New York State Water Resources Institute. Cornell University, Ithaca, N.Y.

Wagenet, R.J. and P.S.C. Rao. 1990. Modelling pesticide fate in soils. In: Cheng, H.H. et al. (eds.) *Pesticides in the soil environment-SSSA Book Series, no.2.*, Madison, U.S.

Wayland, J., J.R. Hayes Jr., J.R. Laws, eds. 1991. *DDT and its analogs.* Handbook of Pesticide Technology, Vol. 2. Classes of Pesticides. pp. 743-780.

Webber, M.D. 1994. *Industrial organic compounds in selected Canadian municipal sludges and agricultural soils.* Report prepared for Agriculture and Agri-Food Canada, Ottawa, Ont., October 1994. 100 pp.

Webber, M.D. and S.S. Singh. 1995. Contamination of Agricultural Soils - Chapter 9 in Soil Health. From http://sis.agr.gc.ca/cansis/publications/health/chapter09.html

Willis, G.H., L.L. McDowell, S. Smith, L.M. Southwick and E.R. Lemon. 1980. Toxaphene volatilization from a mature cotton canopy. *Agronomy Journal* 72: 627-631.

Willis, G.H., J.F. Parr and S. Smith. 1971. Volatilization of soil-applied DDT and DDD from flooded and nonflooded plots. *Pesticide Monitoring Journal* 4: 204-208.

Woodwell, G.M., P.P. Craig and H.A. Johnson. 1971. DDT in the biosphere: where does it go? *Science* 174: 1101-1107.

APPENDIX 1: DVD OF MODEL SIMULATIONS (SEE DVD IN BACK ENVELOPE)